Rates of Surface Change and Accretion in Coastal National Park Service Marshes in the Northeast U.S.

Trend Analyses for Northeast Coastal and Barrier Network, Northeast Temperate Network, and National Capital Region Network Parks

Andrew T. Tredennick, Mikey Tabak, John Lombardi, and Leigh Ann Starcevich

Western EcoSystems Technology, Inc.
Environmental & Statistical Consultants
1610 East Reynolds Street
Laramie, WY 82072
Phone: 307-275-5994
www.west-inc.com



Please cite this publication as:

Tredennick, A. T., M. Tabak, J. Lombardi, and L. Starcevich. 2023. Rates of surface change and accretion in coastal National Park Service marshes in the northeast U.S.: Trend analyses for the Northeast Coastal and Barrier Network, Northeast Temperate Network, and National Capital Region Network parks. Western EcoSystems Technology, Inc. Laramie, Wyoming.

Contents

Page

Figures v

Tables xxiii

Appendices xxix

Background 1

Materials and Methods 3

Data 3

Statistical Models 4

Posterior Analysis 7

The posterior analysis of the fitted models focused on model checking and computing quantities of interest for inference. 7

Model Checks 7

Inference from Models 7

Model Checks 9

General Trends 11

Trends across All Parks+- 11

Surface Elevation Table and Accretion Trends versus Sea Level Rise 11

Surface Elevation Table and Accretion Trends over Shorter Time Periods 14

Sampling Frequency 16

Comparison of Fenced and Non-Fenced Stations at Assateague Island National Seashore 17

References 19

Figures

Page

Figure 1. Example data sets for (A) accretion and (B) elevation at the Acadia National Park, Bass Harbor site 4

Figure 2. Mean estimated trends as a function of average latitude of each park 11

Figure 3. Fitted changepoint model for Watch Hill WH3 SET station 15

Figure 4. Trend estimate from the selected segment model for the Watch Hill WH3 SET station with two changepoints 16

Figure 5. Estimated trends at fenced and non-fenced stations at Assateague Island National Seashore 17

Figure A-1. Estimated accretion and elevation trends at the site level for Acadia National Park. 22

Figure A-2. Overall accretion and elevation trends for the Bass Harbor site at Acadia National Park 24

Figure A-3. Accretion and elevation trends at each station for the Bass Harbor site at Acadia National Park 24

Figure A-3. Overall accretion and elevation trends for the Maine Coast Heritage site at Acadia National Park 25

Figure A-5. Accretion and elevation trends at each station for the Maine Coast Heritage site at Acadia National Park 26

Figure A-6. Overall accretion and elevation trends for the Schoodic site at Acadia National Park 27

Figure A-7. Accretion and elevation trends at each station for the Schoodic site at Acadia National Park 27

Figure A-8. Overall accretion and elevation trends for the Thompson Island site at Acadia National Park 28

Figure A-9. Accretion and elevation trends at each station for the Thompson Island site at Acadia National Park 29

Figure A-10. Estimated accretion and elevation trends at the site level for Assateague Island National Seashore 29

Figure A-11. Overall accretion and elevation trends for the Marsh 5 site at Assateague Island National Seashore 31

Figure A-12. Accretion and elevation trends at each station for the Marsh 5 site at Assateague Island National Seashore 31

Figure A-13. Overall accretion and elevation trends for the Marsh 6 site at Assateague Island National Seashore..... 32

Figure A-14. Accretion and elevation trends at each station for the Marsh 6 site at Assateague Island National Seashore 33

Figure A-15. Overall accretion and elevation trends for the Marsh 8 site at Assateague Island National Seashore..... 34

Figure A-16. Accretion and elevation trends at each station for the Marsh 8 site at Assateague Island National Seashore 34

Figure A-17. Overall accretion and elevation trends for the Marsh 11 site at Assateague Island National Seashore..... 35

Figure A-18. Accretion and elevation trends at each station for the Marsh 11 site at Assateague Island National Seashore. 36

Figure A-19. Overall accretion and elevation trends for the exclosure stations at Assateague Island National Seashore 37

Figure A-20. Accretion and elevation trends at each station for the exclosure stations at Assateague Island National Seashore. 37

Figure A-21. Overall accretion and elevation trends for the non-exclosure stations at Assateague Island National Seashore 39

Figure A-22. Accretion and elevation trends at each station for the non-exclosure stations at Assateague Island National Seashore..... 39

Figure A-23. Estimated accretion and elevation trends at the site level for Boston Harbor Islands National Recreation Area. 40

Figure A-24. Overall accretion and elevation trends for the Calf Island site at Boston Harbor Islands National Recreation Area 41

Figure A-25. Accretion and elevation trends at each station for the Calf Island site at Boston Harbor Islands National Recreation Area..... 42

Figure A-26. Overall accretion and elevation trends for the Peddocks Island site at Boston Harbor Islands National Recreation Area..... 43

Figure A-27. Accretion and elevation trends at each station for the Peddocks Island site at Boston Harbor Islands National Recreation Area..... 43

Figure A-28. Overall accretion and elevation trends for the Thompson Island site at Boston Harbor Islands National Recreation Area..... 44

Figure A-29. Accretion and elevation trends at each station for the Thompson Island site at Boston Harbor Islands National Recreation Area 45

Figure A-30. Estimated accretion and elevation trends at the site level for Cape Cod National Seashore. 45

Figure A-31. Overall accretion and elevation trends for the Blackfish Creek site at Cape Cod National Seashore 47

Figure A-32. Accretion and elevation trends at each station for the Blackfish Creek site at Cape Cod National Seashore 48

Figure A-33. Overall accretion and elevation trends for the Hatches Harbor HH1 site at Cape Cod National Seashore 49

Figure A-34. Accretion and elevation trends at each station for the Hatches Harbor HH1-HH6 (Behind Dike) site at Cape Cod National Seashore 49

Figure A-35. Overall accretion and elevation trends for the Hatches Harbor HH2 site at Cape Cod National Seashore 50

Figure A-36. Accretion and elevation trends at each station for the Hatches Harbor HH2 site at Cape Cod National Seashore 51

Figure A-37. Overall accretion and elevation trends for the Hatches Harbor H1 site at Cape Cod National Seashore 52

Figure A-38. Accretion and elevation trends at each station for the Hatches Harbor H1 site at Cape Cod National Seashore 52

Figure A-39. Overall accretion and elevation trends for the Hatches Harbor H2 site at Cape Cod National Seashore 53

Figure A-40. Accretion and elevation trends at each station for the Hatches Harbor H2 site at Cape Cod National Seashore. 54

Figure A-41. Overall accretion and elevation trends for the Herring River G site at Cape Cod National Seashore 55

Figure A-42. Accretion and elevation trends at each station for the Herring River G site at Cape Cod National Seashore 55

Figure A-43. Overall accretion and elevation trends for the Herring River GUT site at Cape Cod National Seashore 56

Figure A-44. Accretion and elevation trends at each station for the Herring River GUT site at Cape Cod National Seashore 57

Figure A-45. Overall accretion and elevation trends for the Herring River High Toss site at Cape Cod National Seashore 58

Figure A-46. Accretion and elevation trends at each station for the Herring River High Toss site at Cape Cod National Seashore....58

Figure A-48. Accretion and elevation trends at each station for the Herring River Phrag site at Cape Cod National Seashore....60

Figure A-49. Overall accretion and elevation trends for the Nauset Marsh N site at Cape Cod National Seashore....61

Figure A-50. Accretion and elevation trends at each station for the Nauset Marsh N site at Cape Cod National Seashore....61

Figure A-51. Overall accretion and elevation trends for the Nauset Marsh Old N site at Cape Cod National Seashore....62

Figure A-52. Accretion and elevation trends at each station for the Nauset Marsh OldN site at Cape Cod National Seashore....63

Figure A-53. Estimated accretion and elevation trends at the site level for Colonial National Historical Park....63

Figure A-54. Overall accretion and elevation trends for the Marsh 5 site at Colonial National Historical Park....65

Figure A-55. Accretion and elevation trends at each station for the Marsh 5 site at Colonial National Historical Park....65

Figure A-56. Overall accretion and elevation trends for the Marsh 13 site at Colonial National Historical Park....66

Figure A-57. Accretion and elevation trends at each station for the Marsh 13 site at Colonial National Historical Park....67

Figure A-58. Overall accretion and elevation trends for the Marsh 19 site at Colonial National Historical Park....68

Figure A-59. Accretion and elevation trends at each station for the Marsh 19 site at Colonial National Historical Park....68

Figure A-60. Overall accretion and elevation trends for the Marsh 30 site at Colonial National Historical Park....69

Figure A-61. Accretion and elevation trends at each station for the Marsh 30 site at Colonial National Historical Park....70

Figure A-62. Estimated accretion and elevation trends at the site level for Fire Island National Seashore....70

Figure A-63. Overall accretion and elevation trends for the Great Gun site at Fire Island National Seashore....72

Figure A-64. Accretion and elevation trends at each station for the Great Gun site at Fire Island National Seashore....72

Figure A-65. Overall accretion and elevation trends for the Hospital Point site at Fire Island National Seashore....73

Figure A-66. Accretion and elevation trends at each station for the Hospital Point site at Fire Island National Seashore....74

Figure A-67. Overall accretion and elevation trends for the Watch Hill site at Fire Island National Seashore....75

Figure A-68. Accretion and elevation trends at each station for the Watch Hill site at Fire Island National Seashore....75

Figure A-69. Estimated accretion and elevation trends at the site level for Gateway National Recreation Area....76

Figure A-70. Overall accretion and elevation trends for the Big Egg Control site at Gateway National Recreation Area....78

Figure A-71. Accretion and elevation trends at each station for the Big Egg Control site at Gateway National Recreation Area....78

Figure A-72. Overall accretion and elevation trends for the Big Egg Spray site at Gateway National Recreation Area....79

Figure A-73. Accretion and elevation trends at each station for the Big Egg Spray site at Gateway National Recreation Area....80

Figure A-74. Overall accretion and elevation trends for the Black Bank site at Gateway National Recreation Area....81

Figure A-75. Accretion and elevation trends at each station for the Black Bank site at Gateway National Recreation Area....81

Figure A-76. Overall accretion and elevation trends for the Elders East site at Gateway National Recreation Area....82

Figure A-77. Accretion and elevation trends at each station for the Elders East site at Gateway National Recreation Area....83

Figure A-78. Overall accretion and elevation trends for the Elders East NF site at Gateway National Recreation Area....84

Figure A-79. Accretion and elevation trends at each station for the Elders East NF site at Gateway National Recreation Area....84

Figure A-80. Overall accretion and elevation trends for the Elders East Shallow site at Gateway National Recreation Area....85

Figure A-81. Accretion and elevation trends at each station for the Elders East Shallow site at Gateway National Recreation Area 86

Figure A-82. Overall accretion and elevation trends for the JOCO site at Gateway National Recreation Area 87

Figure A-83. Accretion and elevation trends at each station for the JOCO site at Gateway National Recreation Area 87

Figure A-84. Overall accretion and elevation trends for the JOCO REF site at Gateway National Recreation Area 88

Figure A-85. Accretion and elevation trends at each station for the JOCO REF site at Gateway National Recreation Area 89

Figure A-86. Overall accretion and elevation trends for the JOCO REF Shallow site at Gateway National Recreation Area 90

Figure A-87. Accretion and elevation trends at each station for the JOCO REF Shallow site at Gateway National Recreation Area 90

Figure A-88. Overall accretion and elevation trends for the Sandy Hook site at Gateway National Recreation Area 91

Figure A-89. Accretion and elevation trends at each station for the Sandy Hook site at Gateway National Recreation Area 92

Figure A-90. Estimated accretion and elevation trends at the site level for George Washington Memorial Parkway 92

Figure A-91. Overall accretion and elevation trends for the Dyke Marsh Creek site at George Washington Memorial Parkway 94

Figure A-92. Accretion and elevation trends at each station for the Dyke Marsh Creek site at George Washington Memorial Parkway 94

Figure A-93. Overall accretion and elevation trends for the Dyke Marsh Interior site at George Washington Memorial Parkway 95

Figure A-94. Accretion and elevation trends at each station for the Dyke Marsh Interior site at George Washington Memorial Parkway. 96

Figure A-95. Overall accretion and elevation trends for the Dyke Marsh River site at George Washington Memorial Parkway 97

Figure A-96. Accretion and elevation trends at each station for the Dyke Marsh River site at George Washington Memorial Parkway 97

Figure A-97. Estimated accretion and elevation trends at the site level for National Capital Parks-East 98

Figure A-98. Overall accretion and elevation trends for the Kenilworth Marsh site at National Capital Parks-East 99

Figure A-99. Accretion and elevation trends at each station for the Kenilworth Marsh site at National Capital Parks-East 100

Figure A-100. Overall accretion and elevation trends for the Kingman Lake site at National Capital Parks-East 101

Figure A-101. Accretion and elevation trends at each station for the Kingman Lake site at National Capital Parks-East 101

Figure C-1. Elevation data over time at the three Watch Hill SETs, Fire Island National Seashore 110

Figure C-2. Fitted elevation trends from the hierarchical Bayesian generalized linear mixed effects model 113

Figure C-3. Posterior distribution of first derivatives of the fitted trends over time. 115

Figure D-1. Elevation data over time at Watch Hill, Fire Island National Seashore. 118

Figure D-2. Density (right column) and trace (left column) plots for model fit_cp.The lower row shows an example of a coefficient with moderately poor convergence 121

Figure D-3. Density (right column) and trace (left column) plots for model fit_ncp. Both coefficients show convergence. 124

Figure D-4. Fitted changepoint model for Watch Hill WH3 SET station, arm ‘A.’ The horizontal line shows the estimated changepoint data from the model. 126

Figure D-5. Model with two breakpoints showing a better representation of the data. The changepoint dates are 2011-10-06 and 2013-06-12. 128

Figure E-1. Elevation trend estimates by season for each station at the Bass Harbor site, Acadia National Park. 136

Figure E-2. Elevation trend estimates by season for each station at the Maine Coast Heritage site, Acadia National Park. 136

Figure E-3. Elevation trend estimates by season for each station at the Schoodic site, Acadia National Park. 136

Figure E-4. Elevation trend estimates by season for each station at the Thompson Island site, Acadia National Park. 137

Figure E-5. Elevation trend estimates by season for each station at the Marsh 5 site, Assateague Island National Seashore. 137

Figure E-6. Elevation trend estimates by season for each station at the Marsh 6 site, Assateague Island National Seashore. 137

Figure E-7. Elevation trend estimates by season for each station at the Marsh 8 site, Assateague Island National Seashore. 138

Figure E-8. Elevation trend estimates by season for each station at the Marsh 11 site, Assateague Island National Seashore. 138

Figure E-9. Elevation trend estimates by season for each station at the Marsh Exclosure site, Assateague Island National Seashore. 138

Figure E-10. Elevation trend estimates by season for each station at the Marsh non-Exclosure (Marsh 5 and 6) sites, Assateague Island National Seashore. 139

Figure E-11. Elevation trend estimates by season for each station at the Calf Island site, Boston Harbor Islands Recreation Area. 139

Figure E-12. Elevation trend estimates by season for each station at the Peddocks Island site, Boston Harbor Islands Recreation Area. 139

Figure E-13. Elevation trend estimates by season for each station at the Thompson Island site, Boston Harbor Islands Recreation Area. 140

Figure E-14. Elevation trend estimates by season for each station at the Blackfish Creek site, Cape Cod National Seashore. 140

Figure E-15. Elevation trend estimates by season for each station at the Hatches Harbor HH1 site, Cape Cod National Seashore. 140

Figure E-16. Elevation trend estimates by season for each station at the Hatches Harbor HH2 site, Cape Cod National Seashore. 141

Figure E-17. Elevation trend estimates by season for each station at the Hatches Harbor H1 site, Cape Cod National Seashore. 141

Figure E-18. Elevation trend estimates by season for each station at the Hatches Harbor H2 site, Cape Cod National Seashore. 141

Figure E-19. Elevation trend estimates by season for each station at the Herring River G site, Cape Cod National Seashore. 142

Figure E-20. Elevation trend estimates by season for each station at the Herring River GUT site, Cape Cod National Seashore. 142

Figure E-21. Elevation trend estimates by season for each station at the Herring River High Toss site, Cape Cod National Seashore. 142

Figure E-22. Elevation trend estimates by season for each station at the Herring River Phrag site, Cape Cod National Seashore. 143

Figure E-23. Elevation trend estimates by season for each station at the Nauset Marsh N site, Cape Cod National Seashore. 143

Figure E-24. Elevation trend estimates by season for each station at the Nauset Marsh Old N site, Cape Cod National Seashore. 143

Figure E-25. Elevation trend estimates by season for each station at the Marsh 5 site, Colonial National Historical Park. 144

Figure E-26. Elevation trend estimates by season for each station at the Marsh 13 site, Colonial National Historical Park. 144

Figure E-27. Elevation trend estimates by season for each station at the Marsh 19 site, Colonial National Historical Park. 144

Figure E-28. Elevation trend estimates by season for each station at the Marsh 30 site, Colonial National Historical Park. 145

Figure E-29. Elevation trend estimates by season for each station at the Great Gun site, Fire Island National Seashore. 145

Figure E-30. Elevation trend estimates by season for each station at the Hospital Point site, Fire Island National Seashore 145

Figure E-31. Elevation trend estimates by season for each station at the Watch Hill site, Fire Island National Seashore. 146

Figure E-32. Elevation trend estimates by season for each station at the Big Egg Control site, Gateway National Recreation Area. 146

Figure E-33. Elevation trend estimates by season for each station at the Big Egg Spray site, Gateway National Recreation Area. 146

Figure E-34. Elevation trend estimates by season for each station at the Black Bank site, Gateway National Recreation Area 147

Figure E-35. Elevation trend estimates by season for each station at the Elders East site, Gateway National Recreation Area 147

Figure E-36. Elevation trend estimates by season for each station at the Elders East NF site, Gateway National Recreation Area. 147

Figure E-37. Elevation trend estimates by season for each station at the Elders East Shallow site, Gateway National Recreation Area. 148

Figure E-38. Elevation trend estimates by season for each station at the JOCO site, Gateway National Recreation Area 148

Figure E-39. Elevation trend estimates by season for each station at the JOCO REF site, Gateway National Recreation Area 148

Figure E-40. Elevation trend estimates by season for each station at the JOCO REF Shallow site, Gateway National Recreation Area. 149

Figure E-41. Elevation trend estimates by season for each station at the Sandy Hook site, Gateway National Recreation Area 149

Figure E-42. Elevation trend estimates by season for each station at the Dyke Marsh Creek site, George Washington Memorial Parkway. 149

Figure E-43. Elevation trend estimates by season for each station at the Dyke Marsh Interior site, George Washington Memorial Parkway. 150

Figure E-44. Elevation trend estimates by season for each station at the Dyke Marsh River site, George Washington Memorial Parkway. 150

Figure E.45. Elevation trend estimates by season for each station at the Kenilworth Marsh River site, National Capital Parks-East 150

Figure E.46. Elevation trend estimates by season for each station at the Kingman Lake site, National Capital Parks-East 151

Figure E-47. Overall elevation trend estimates by season for the Bass Harbor site, Acadia National Park 151

Figure E-48. Overall elevation trend estimates by season for the Maine Coast Heritage site, Acadia National Park 152

Figure E-49. Overall elevation trend estimates by season for the Schoodic site, Acadia National Park 152

Figure E-50. Overall elevation trend estimates by season for the Thompson Island site, Acadia National Park 152

Figure E-51. Overall elevation trend estimates by season for the Marsh 5 site, Assateague Island National Seashore 153

Figure E-52. Overall elevation trend estimates by season for the Marsh 6 site, Assateague Island National Seashore 153

Figure E-53. Overall elevation trend estimates by season for the Marsh 8 site, Assateague Island National Seashore 153

Figure E-54. Overall elevation trend estimates by season for the Marsh 11 site, Assateague Island National Seashore 154

Figure E-55. Overall elevation trend estimates by season for the Marsh Exclosure site, Assateague Island National Seashore 154

Figure E-56. Overall elevation trend estimates by season for the Marsh non-Exclosure site, Assateague Island National Seashore. 154

Figure E-57. Overall elevation trend estimates by season for the Calf Island site, Boston Harbor Islands Recreation Area 155

Figure E-58. Overall elevation trend estimates by season for the Peddocks Island site, Boston Harbor Islands Recreation Area 155

Figure E-59. Overall elevation trend estimates by season for the Thompson Island site, Boston Harbor Islands Recreation Area 155

Figure E-60. Overall elevation trend estimates by season for the Blackfish Creek site, Cape Cod National Seashore 156

Figure E-61. Overall elevation trend estimates by season for the Hatches Harbor HH1 site, Cape Cod National Seashore 156

Figure E-62. Overall elevation trend estimates by season for the Hatches Harbor HH2 site, Cape Cod National Seashore 156

Figure E-63. Overall elevation trend estimates by season for the Hatches Harbor H1 site, Cape Cod National Seashore 157

Figure E-64. Overall elevation trend estimates by season for the Hatches Harbor H2 site, Cape Cod National Seashore 157

Figure E-65. Overall elevation trend estimates by season for the Herring River G site, Cape Cod National Seashore 157

Figure E-66. Overall elevation trend estimates by season for the Herring River GUT site, Cape Cod National Seashore 158

Figure E-67. Overall elevation trend estimates by season for the Herring River High Toss site, Cape Cod National Seashore 158

Figure E-68. Overall elevation trend estimates by season for the Herring River Phrag site, Cape Cod National Seashore. 158

Figure E-69. Overall elevation trend estimates by season for the Nauset Marsh N site, Cape Cod National Seashore 159

Figure E-70. Overall elevation trend estimates by season for the Nauset Marsh OldN site, Cape Cod National Seashore 159

Figure E-71. Overall elevation trend estimates by season for the Marsh 5 site, Colonial National Historical Park. 159

Figure E-72. Overall elevation trend estimates by season for the Marsh 13 site, Colonial National Historical Park 160

Figure E-73. Overall elevation trend estimates by season for the Marsh 19 site, Colonial National Historical Park 160

Figure E-74. Overall elevation trend estimates by season for the Marsh 30 site, Colonial National Historical Park. 160

Figure E-75. Overall elevation trend estimates by season for the Great Gun site, Fire Island National Seashore 161

Figure E-76. Overall elevation trend estimates by season for the Hospital Point site, Fire Island National Seashore 161

Figure E-77. Overall elevation trend estimates by season for the Watch Hill site, Fire Island National Seashore 161

Figure E-78. Overall elevation trend estimates by season for the Big Egg Control site, Gateway National Recreation Area 162

Figure E-79. Overall elevation trend estimates by season for the Big Egg Spray site, Gateway National Recreation Area 162

Figure E-80. Overall elevation trend estimates by season for the Black Bank site, Gateway National Recreation Area 162

Figure E-81. Overall elevation trend estimates by season for the Elders East site, Gateway National Recreation Area 163

Figure E-82. Overall elevation trend estimates by season for the Elders East NF site, Gateway National Recreation Area 163

Figure E-83. Overall elevation trend estimates by season for the Elders East Shallow site, Gateway National Recreation Area 163

Figure E-84. Overall elevation trend estimates by season for the JOCO site, Gateway National Recreation Area. 164

Figure E-85. Overall elevation trend estimates by season for the JOCO REF site, Gateway National Recreation Area 164

Figure E-86. Overall elevation trend estimates by season for the JOCO REF Shallow site, Gateway National Recreation Area 164

Figure E-87. Overall elevation trend estimates by season for the Sandy Hook site, Gateway National Recreation Area 165

Figure E-88. Overall elevation trend estimates by season for the Dyke Marsh Creek site, George Washington Memorial Parkway 165

Figure E-89. Overall elevation trend estimates by season for the Dyke Marsh Interior site, George Washington Memorial Parkway. 165

Figure E-90. Overall elevation trend estimates by season for the Dyke Marsh River site, George Washington Memorial Parkway 166

Figure E-91. Overall elevation trend estimates by season for the Kenilworth Marsh River site, National Capital Parks-East.....166

Figure E-92. Overall elevation trend estimates by season for the Kingman Lake site, National Capital Parks-East.....166

Figure E-93. Accretion trend estimates by season for each station at the Bass Harbor site, Acadia National Park.....167

Figure E-94. Accretion trend estimates by season for each station at the Maine Coast Heritage site, Acadia National Park.....167

Figure E-95. Accretion trend estimates by season for each station at the Schoodic site, Acadia National Park.....168

Figure E-96. Accretion trend estimates by season for each station at the Thompson Island site, Acadia National Park.....168

Figure E-97. Accretion trend estimates by season for each station at the Marsh 5 site, Assateague Island National Seashore.....168

Figure E-98. Accretion trend estimates by season for each station at the Marsh 6 site, Assateague Island National Seashore.....169

Figure E-99. Accretion trend estimates by season for each station at the Marsh 8 site, Assateague Island National Seashore.....169

Figure E-100. Accretion trend estimates by season for each station at the Marsh 11 site, Assateague Island National Seashore.....169

Figure E-101. Accretion trend estimates by season for each station at the Marsh Exclosure site, Assateague Island National Seashore.....170

Figure E-102. Accretion trend estimates by season for each station at the Marsh non-Exclosure sites, Assateague Island National Seashore.....170

Figure E-103. Accretion trend estimates by season for each station at the Calf Island site, Boston Harbor Islands Recreation Area.....170

Figure E-104. Accretion trend estimates by season for each station at the Peddocks Island site, Boston Harbor Islands Recreation Area.....171

Figure E-105. Accretion trend estimates by season for each station at the Thompson Island site, Boston Harbor Islands Recreation Area.....171

Figure E-106. Accretion trend estimates by season for each station at the Blackfish Creek site, Cape Cod National Seashore.....171

Figure E-107. Accretion trend estimates by season for each station at the Hatches Harbor HH1 site, Cape Cod National Seashore.....172

Figure E-108. Accretion trend estimates by season for each station at the Hatches Harbor HH2 site, Cape Cod National Seashore. 172

Figure E-109. Accretion trend estimates by season for each station at the Hatches Harbor H1 site, Cape Cod National Seashore. 172

Figure E-110. Accretion trend estimates by season for each station at the Hatches Harbor H2 site, Cape Cod National Seashore. 173

Figure E-111. Accretion trend estimates by season for each station at the Herring River GUT site, Cape Cod National Seashore. 173

Figure E-112. Accretion trend estimates by season for each station at the Herring River High Toss site, Cape Cod National Seashore. 173

Figure E-113. Accretion trend estimates by season for each station at the Herring River Phrag site, Cape Cod National Seashore. 174

Figure E-114. Accretion trend estimates by season for each station at the Nauset Marsh N site, Cape Cod National Seashore. 174

Figure E-115. Accretion trend estimates by season for each station at the Nauset Marsh OldN site, Cape Cod National Seashore. 174

Figure E-116. Accretion trend estimates by season for each station at the Marsh 5 site, Colonial National Historical Park. 175

Figure E-117. Accretion trend estimates by season for each station at the Marsh 13 site, Colonial National Historical Park. 175

Figure E-118. Accretion trend estimates by season for each station at the Marsh 19 site, Colonial National Historical Park. 175

Figure E-119. Accretion trend estimates by season for each station at the Marsh 30 site, Colonial National Historical Park. 176

Figure E-120. Accretion trend estimates by season for each station at the Great Gun site, Fire Island National Seashore. 176

Figure E-121. Accretion trend estimates by season for each station at the Hospital Point site, Fire Island National Seashore. 176

Figure E-122. Accretion trend estimates by season for each station at the Watch Hill site, Fire Island National Seashore. 177

Figure E-123. Accretion trend estimates by season for each station at the Big Egg Control site, Gateway National Recreation Area. 177

Figure E-124. Accretion trend estimates by season for each station at the Big Egg Spray site, Gateway National Recreation Area. 177

Figure E-125. Accretion trend estimates by season for each station at the Black Bank site, Gateway National Recreation Area. 178

Figure E-126. Accretion trend estimates by season for each station at the Elders East site, Gateway National Recreation Area..... 178

Figure E-127. Accretion trend estimates by season for each station at the JOCO site, Gateway National Recreation Area..... 178

Figure E-128. Accretion trend estimates by season for each station at the JOCO REF site, Gateway National Recreation Area. 179

Figure E-129. Accretion trend estimates by season for each station at the JOCO REF Shallow site, Gateway National Recreation Area. 179

Figure E-130. Accretion trend estimates by season for each station at the Dyke Marsh Creek site, George Washington Memorial Parkway..... 179

Figure E-131. Accretion trend estimates by season for each station at the Dyke Marsh Interior site, George Washington Memorial Parkway. 180

Figure E-132. Accretion trend estimates by season for each station at the Dyke Marsh River site, George Washington Memorial Parkway. 180

Figure E.133. Accretion trend estimates by season for each station at the Kenilworth Marsh River site, National Capital Parks-East..... 180

Figure E.134. Accretion trend estimates by season for each station at the Kingman Lake site, National Capital Parks-East..... 181

Figure E-135. Overall accretion trend estimates by season for the Bass Harbor site, Acadia National Park 181

Figure E-136. Overall accretion trend estimates by season for the Maine Coast Heritage site, Acadia National Park..... 182

Figure E-137. Overall accretion trend estimates by season for the Schoodic site, Acadia National Park 182

Figure E-138. Overall accretion trend estimates by season for the Thompson Island site, Acadia National Park 182

Figure E-139. Overall accretion trend estimates by season for the Marsh 5 site, Assateague Island National Seashore 183

Figure E-140. Overall accretion trend estimates by season for the Marsh 6 site, Assateague Island National Seashore 183

Figure E-141. Overall accretion trend estimates by season for the Marsh 8 site, Assateague Island National Seashore 183

Figure E-142. Overall accretion trend estimates by season for the Marsh 11 site, Assateague Island National Seashore 184

Figure E-143. Overall accretion trend estimates by season for the Marsh Exclosure site, Assateague Island National Seashore. 184

Figure E-144. Overall accretion trend estimates by season for the Marsh non-Exclosure site, Assateague Island National Seashore. 184

Figure E-145. Overall accretion trend estimates by season for the Calf Island site, Boston Harbor Islands Recreation Area 185

Figure E-146. Overall accretion trend estimates by season for the Peddocks Island site, Boston Harbor Islands Recreation Area 185

Figure E-147. Overall accretion trend estimates by season for the Thompson Island site, Boston Harbor Islands Recreation Area 185

Figure E-148. Overall accretion trend estimates by season for the Blackfish Creek site, Cape Cod National Seashore 186

Figure E-149. Overall accretion trend estimates by season for the Hatches Harbor HH1 site, Cape Cod National Seashore 186

Figure E-150. Overall accretion trend estimates by season for the Hatches Harbor HH2 site, Cape Cod National Seashore 186

Figure E-151. Overall accretion trend estimates by season for the Hatches Harbor H1 site, Cape Cod National Seashore 187

Figure E-152. Overall accretion trend estimates by season for the Hatches Harbor H2 site, Cape Cod National Seashore. 187

Figure E-153. Overall accretion trend estimates by season for the Herring River GUT site, Cape Cod National Seashore. 187

Figure E-154. Overall accretion trend estimates by season for the Herring River High Toss site, Cape Cod National Seashore 188

Figure E-155. Overall accretion trend estimates by season for the Herring River Phrag site, Cape Cod National Seashore. 188

Figure E-156. Overall accretion trend estimates by season for the Nauset Marsh N site, Cape Cod National Seashore 188

Figure E-157. Overall accretion trend estimates by season for the Nauset Marsh OldN site, Cape Cod National Seashore. 189

Figure E-158. Overall accretion trend estimates by season for the Marsh 5 site, Colonial National Historical Park. 189

Figure E-159. Overall accretion trend estimates by season for the Marsh 13 site, Colonial National Historical Park.....189

Figure E-160. Overall accretion trend estimates by season for the Marsh 19 site, Colonial National Historical Park.....190

Figure E-161. Overall accretion trend estimates by season for the Marsh 30 site, Colonial National Historical Park.....190

Figure E-162. Overall accretion trend estimates by season for the Great Gun site, Fire Island National Seashore.....190

Figure E-163. Overall accretion trend estimates by season for the Hospital Point site, Fire Island National Seashore. 191

Figure E-164. Overall accretion trend estimates by season for the Watch Hill site, Fire Island National Seashore.....191

Figure E-165. Overall accretion trend estimates by season for the Big Egg Control site, Gateway National Recreation Area.....191

Figure E-166. Overall accretion trend estimates by season for the Big Egg Spray site, Gateway National Recreation Area.....192

Figure E-167. Overall accretion trend estimates by season for the Black Bank site, Gateway National Recreation Area.....192

Figure E-168. Overall accretion trend estimates by season for the Elders East site, Gateway National Recreation Area.....192

Figure E-169. Overall accretion trend estimates by season for the JOCO site, Gateway National Recreation Area.....193

Figure E-170. Overall accretion trend estimates by season for the JOCO REF site, Gateway National Recreation Area.....193

Figure E-171. Overall accretion trend estimates by season for the Sandy Hook site, Gateway National Recreation Area.....193

Figure E-172. Overall accretion trend estimates by season for the Dyke Marsh Creek site, George Washington Memorial Parkway 194

Figure E-173. Overall accretion trend estimates by season for the Dyke Marsh Interior site, George Washington Memorial Parkway 194

Figure E-174. Overall accretion trend estimates by season for the Dyke Marsh River site, George Washington Memorial Parkway.....194

Figure E-175. Overall accretion trend estimates by season for the Kenilworth Marsh River site, National Capital Parks-East.....195

Figure E-176. Overall accretion trend estimates by season for the Kingman Lake site, National Capital Parks-East 195

Tables

Page

Table 1. Summary of sample sizes for each park....3

Table 2. Prior distributions used in the analysis....6

Table 3. Groupings of sites into categories based on whether the estimated accretion trend was above, not different, or below the rate of sea level rise....12

Table 4. Groupings of sites into categories based on whether the estimated elevation trend was above, not different, or below the rate of sea level rise....13

Table A-1. Sea level rise rate (mm/yr) estimates for each site and the source of the sea level data. The NOAA ID is the tide gauge station number. 21

Table A-2. Posterior trends (mean and 95% Bayesian credible interval) and the posterior probabilities that the trends in elevation or accretion are greater than 0 [Pr(trend > 0)], that the trend is greater than the upper bound of sea level rise [Pr(trend > slr)], and that the trend is less than the lower bound of sea level rise [Pr(trend < slr)] at each site in Acadia National Park 23

Table A-3. Estimated rates of elevation and accretion trends at Bass Harbor in Acadia National Park. 23

Table A-4. Estimated rates of elevation and accretion trends at Maine Coast Heritage in Acadia National Park 25

Table A-5. Estimated rates of elevation and accretion trends at Schoodic in Acadia National Park. 26

Table A-6. Estimated rates of elevation and accretion trends at Thompson Island in Acadia National Park 28

Table A-7. Posterior trends (mean and 95% Bayesian credible interval) and the posterior probabilities that the trends in elevation or accretion are greater than 0 [Pr(trend > 0)], that the trend is greater than the upper bound of sea level rise [Pr(trend > slr)], and that the trend is less than the lower bound of sea level rise [Pr(trend < slr)] at each site in Assateague Island National Seashore. 30

Table A-8. Estimated rates of elevation and accretion trends at Marsh 5 in Assateague Island National Seashore....30

Table A-9. Estimated rates of elevation and accretion trends at Marsh 6 in Assateague Island National Seashore....32

Table A-10. Estimated rates of elevation and accretion trends at Marsh 8 in Assateague Island National Seashore....33

Table A-11. Estimated rates of elevation and accretion trends at Marsh 11 in Assateague Island National Seashore....35

Table A-12. Estimated rates of elevation and accretion trends at the exclosure stations (fenced) in Assateague Island National Seashore....36

Table A-13. Estimated rates of elevation and accretion trends at the non-exclosure stations (not fenced) in Assateague Island National Seashore....38

Table A-14. Posterior trends (mean and 95% Bayesian credible interval) and the posterior probabilities that the trends in elevation or accretion are greater than 0 [Pr(trend > 0)], that the trend is greater than the upper bound of sea level rise [Pr(trend > slr)], and that the trend is less than the lower bound of sea level rise [Pr(trend < slr)] at each site in Boston Harbor Islands National Recreation Area....40

Table A-15. Estimated rates of elevation and accretion trends at Calf Island in Boston Harbor Islands National Recreation Area. 41

Table A-16. Estimated rates of elevation and accretion trends at Peddocks Island in Boston Harbor Islands National Recreation Area. 42

Table A-17. Estimated rates of elevation and accretion trends at Thompson Island in Boston Harbor Islands National Recreation Area. 44

Table A-18. Posterior trends (mean and 95% Bayesian credible interval) and the posterior probabilities that the trends in elevation or accretion are greater than 0 [Pr(trend > 0)], that the trend is greater than the upper bound of sea level rise [Pr(trend > slr)], and that the trend is less than the lower bound of sea level rise [Pr(trend < slr)] at each site in Cape Cod National Seashore....46

Table A-19. Estimated rates of elevation and accretion trends at Blackfish Creek in Cape Cod National Seashore....47

Table A-20. Estimated rates of elevation and accretion trends at Hatches Harbor HH1 in Cape Cod National Seashore....48

Table A-21. Estimated rates of elevation and accretion trends at Hatches Harbor HH2 in Cape Cod National Seashore....50

Table A-22. Estimated rates of elevation and accretion trends at Hatches Harbor H1 in Cape Cod National Seashore....51

Table A-23. Estimated rates of elevation and accretion trends at Hatches Harbor H2 in Cape Cod National Seashore....53

Table A-24. Estimated rates of elevation and accretion trends at Herring River G in Cape Cod National Seashore....54

Table A-25. Estimated rates of elevation and accretion trends at Herring River GUT in Cape Cod National Seashore.....56

Table A-26. Estimated rates of elevation and accretion trends at Herring River High Toss in Cape Cod National Seashore. 57

Table A-27. Estimated rates of elevation and accretion trends at Herring River Phrag in Cape Cod National Seashore.....59

Table A-28. Estimated rates of elevation and accretion trends at Nauset Marsh N in Cape Cod National Seashore.....60

Table A-29. Estimated rates of elevation and accretion trends at Nauset Marsh Old N in Cape Cod National Seashore.....62

Table A-30. Posterior trends (mean and 95% Bayesian credible interval) and the posterior probabilities that the trends in elevation or accretion are greater than 0 [Pr(trend > 0)], that the trend is greater than the upper bound of sea level rise [Pr(trend > slr)], and that the trend is less than the lower bound of sea level rise [Pr(trend < slr)] at each site in Colonial National Historical Park.....64

Table A-31. Estimated rates of elevation and accretion trends at Marsh 5 in Colonial National Historical Park.....64

Table A-32. Estimated rates of elevation and accretion trends at Marsh 13 in Colonial National Historical Park.....66

Table A-33. Estimated rates of elevation and accretion trends at Marsh 19 in Colonial National Historical Park.....67

Table A-34. Estimated rates of elevation and accretion trends at Marsh 30 in Colonial National Historical Park.....69

Table A-35. Posterior trends (mean and 95% Bayesian credible interval) and the posterior probabilities that the trends in elevation or accretion are greater than 0 [Pr(trend > 0)], that the trend is greater than the upper bound of sea level rise [Pr(trend > slr)], and that the trend is less than the lower bound of sea level rise [Pr(trend < slr)] at each site in Fire Island National Seashore 71

Table A-36. Estimated rates of elevation and accretion trends at Great Gun in Fire Island National Seashore. 71

Table A-37. Estimated rates of elevation and accretion trends at Hospital Point in Fire Island National Seashore.....73

Table A-38. Estimated rates of elevation and accretion trends at Watch Hill in Fire Island National Seashore 74

Table A-39. Posterior trends (mean and 95% Bayesian credible interval) and the posterior probabilities that the trends in elevation or accretion are greater than 0 [Pr(trend > 0)], that the trend is greater than the upper bound of sea level rise [Pr(trend > slr)], and that the trend is less than the lower bound of sea level rise [Pr(trend < slr)] at each site in Gateway National Recreation Area.....77

Table A-40. Estimated rates of elevation and accretion trends at Big Egg Control in Gateway National Recreation Area.....77

Table A-41. Estimated rates of elevation and accretion trends at Big Egg Spray in Gateway National Recreation Area.....79

Table A-42. Estimated rates of elevation and accretion trends at Black Bank in Gateway National Recreation Area.....80

Table A-43. Estimated rates of elevation and accretion trends at Elders East in Gateway National Recreation Area.....82

Table A-44. Estimated rates of elevation and accretion trends at Elders East NF in Gateway National Recreation Area.....83

Table A-45. Estimated rates of elevation and accretion trends at Elders East Shallow in Gateway National Recreation Area.....85

Table A-46. Estimated rates of elevation and accretion trends at JOCO in Gateway National Recreation Area.....86

Table A-47. Estimated rates of elevation and accretion trends at JOCO REF in Gateway National Recreation Area.....88

Table A-48. Estimated rates of elevation and accretion trends at JOCO REF Shallow in Gateway National Recreation Area.....89

Table A-49. Estimated rates of elevation and accretion trends at Sandy Hook in Gateway National Recreation Area.....91

Table A-50. Posterior trends (mean and 95% Bayesian credible interval) and the posterior probabilities that the trends in elevation or accretion are greater than 0 [Pr(trend > 0)], that the trend is greater than the upper bound of sea level rise [Pr(trend > slr)], and that the trend is less than the lower bound of sea level rise [Pr(trend < slr)] at each site in George Washington Memorial Parkway.....93

Table A-51. Estimated rates of elevation and accretion trends at Dyke Marsh Creek in George Washington Memorial Parkway.....93

Table A-52. Estimated rates of elevation and accretion trends at Dyke Marsh Interior in George Washington Memorial Parkway.....95

Table A-53. Estimated rates of elevation and accretion trends at Dyke Marsh River in George Washington Memorial Parkway 96

Table A-54. Posterior trends (mean and 95% Bayesian credible interval) and the posterior probabilities that the trends in elevation or accretion are greater than 0 [Pr(trend > 0)], that the trend is greater than the upper bound of sea level rise [Pr(trend > slr)], and that the trend is less than the lower bound of sea level rise [Pr(trend < slr)] at each site in National Capital Parks-East 98

Table A-55. Estimated rates of elevation and accretion trends at Kenilworth Marsh in National Capital Parks-East. 99

Table A-56. Estimated rates of elevation and accretion trends at Kingman Lake in National Capital Parks-East. 100

Table C-1. Elevation trend estimates from the hierarchical Bayesian generalized additive model, computed from estimates of the first derivatives. 116

Table C-2. Elevation trend estimates from the hierarchical Bayesian generalized linear mixed-effects model from the main report. 116

Table E-1. SET stations for which the median elevation trend estimate of one season did not fall within the 95% CI of the estimate for the other season. 132

Table D-2. Sites for which the median elevation trend estimate of one season did not fall within the 95% CI of the estimate for the other season 133

Table D-3. SET stations for which the median accretion trend estimate of one season did not fall within the 95% CI of the estimate for the other season. 134

Table D-4. Sites for which the median accretion trend estimate of one season did not fall within the 95% CI of the estimate for the other season 135

Appendices

Page

Appendix A. Site- and station-level trends 21

Appendix B: Details of model selection and data aggregation 103

Appendix C: Example of fitting hierarchical Bayesian generalized additive model for trend estimates 109

Appendix D: Example of fitting a Bayesian piece-wise linear regression to detect changepoints in trends over time 117

Appendix E: Seasonal analysis of elevation and accretion 131

Background

The National Park Service Inventory and Monitoring (I&M) Division maintains the Vital Signs Program in which indicators of park health are monitored to understand park condition and trends in important, and often iconic, park resources. Wetland elevation change was selected as a Vital Sign for the Northeast Coastal and Barrier Network (NCBN), the National Capital Region Network (NCRN), and the Northeast Temperate Network (NETN) so the resilience of wetland communities may be monitored in response to potential effects of climate change. Data on marsh elevation and vertical accretion have been collected at nine parks in NCBN, NCRN, and NETN beginning as early as 1998. Each park contains tidal marshes where sediment elevation change is monitored with surface elevation tables (SETs) and sediment accretion is measured with marker horizons obtained from applied artificial soil layers (Lynch et al. 2015).

The elevation data measured using the SET method are collected at marsh sites within a park. Within these sites, sampling stations were established at randomly chosen locations. A SET benchmark (or *SET mark*) was installed at each station. The elevation of the SET mark is assumed to be stable over time so the changes measured using this method are an indicator of the movement of the marsh surface. At the time of data collection, the portable SET instrument (arm) is attached to the SET mark. The SET instrument uses nine pins to measure marsh elevation relative to the SET mark. The arm is positioned in up to eight fixed directions and these directions do not vary among data collection events. Therefore, SET data at a given site are spatially nested within each park, site, station, and arm position. Each SET instrument measures an area of about 1.5 square meters (16 square feet).

Marker horizons are established at each sampling station by placing an artificial layer, such as white feldspar clay, on a wetland surface so that sediment deposited above the layer can be measured. Accretion rates, measured in millimeters of deposition per year, are determined from a plug or core obtained from the marker horizon during data collection events. These measurements typically represent accumulation rather than erosion since measuring the amount of missing sediment relative to a marker is difficult if the horizon has also eroded. The goal of this project is to analyze SET and horizon data to:

1. Estimate rates of elevation change and accretion for all sites and stations within the 9 parks,
2. Estimate and compare trends in those rates over time, and
3. Provide guidance based on those results on sampling and analysis frequency.

In this report, SET and marker data are analyzed using a hierarchical Bayesian approach reflecting the data collection structure.

Materials and Methods

Data

The data come from nine national parks in the northeastern United States (Table 1). Monitoring was conducted for 8 to 22 years at the sites within each park. At each sampling station within a site, a SET benchmark and marker horizons were established, and measurements were taken twice per year, on average.

Table 1. Summary of sample sizes for each park. Note that the "Years Sampled" indicates the time span across which at least some sampling occurred at a surface elevation table (SET) station within the park. The time span does not necessarily indicate all SET stations were sampled throughout the entire period.

Park	Number of Sites	Years Sampled	Number of Stations	Total Observations
Acadia National Park (ACAD)	4	2011 – 2019	12	7,344
Assateague Island National Seashore (ASIS)	6	2009 – 2019	16	21,888
Boston Harbor Islands National Recreation Area (BOHA)	3	2010 – 2019	10	6,516
Cape Cod National Seashore (CACO)	9	1998 – 2019	40	33,840
Colonial National Historical Park (COLO)	4	2012 – 2019	12	6,588
Fire Island National Seashore (FIIS)	3	2002 - 2019	9	11,412
Gateway National Recreation Area (GATE)	10	2002 – 2019	30	27,585
George Washington Memorial Parkway (GWMP)	3	2006 – 2019	10	8,136
National Capital Parks-East (NACE)	2	2002 – 2019	10	10,260

Minimal data processing was required before modeling. We ensured all response variables were in the same units across all sites (millimeters [mm] for both elevation and accretion depth). All observations were indexed by park, site, SET station, arm (for elevation data) or horizon (for accretion data), and year. For the elevation data, pin-level observations were averaged within arms and the arm-level averages were used for modeling (see Appendix A). For the accretion data, observation replicates were averaged within each marker horizon and the marker horizon-level averages were used for modeling (see Appendix A). Example data sets for elevation and accretion are plotted in Figure 1. Figure 1 shows the raw data used as model inputs.

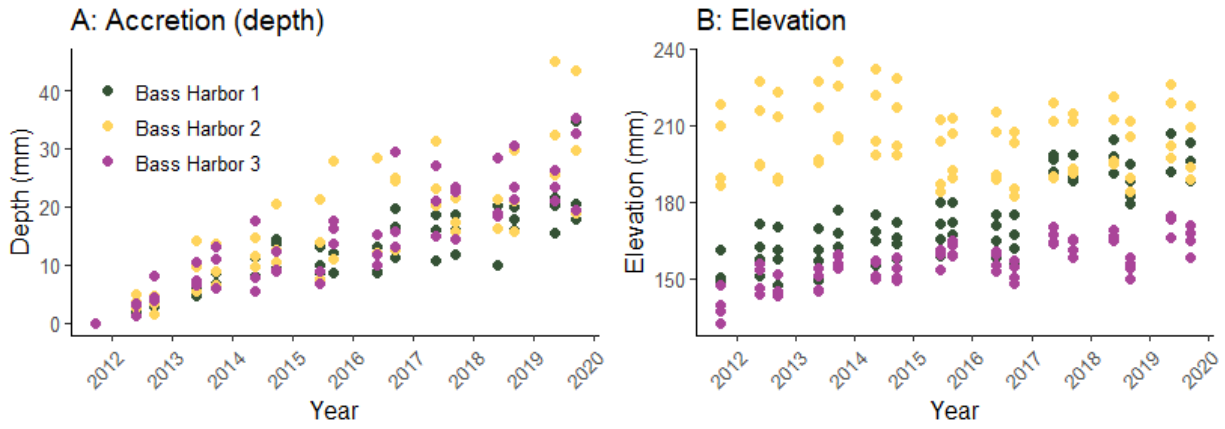


Figure 1. Example data sets for (A) accretion and (B) elevation at the Acadia National Park, Bass Harbor site. Colors represent the data from different surface elevation table (SET) stations at the site.

Statistical Models

We fit hierarchical Bayesian models (generalized linear mixed effects models [GLMMs]) to estimate the trends in elevation and accretion over time at each site. The temporal window used for model fitting included the full record of observations for most stations. For both elevation and accretion models, the only predictor was year. Year was defined as the number of years (in units of days) since monitoring began for each site:

$$(\text{observation date} - \text{first observation date})/365.25.$$

In general, there were two observations per year for each arm within SET within site.

The models included a nested random effects structure for the intercept and the slope (effect of year, i.e., trend). In what follows, "set" refers to the SET station within a site, "arm" refers to an arm of a SET station for the elevation data, and "horizon" refers to the measurement horizon for accretion data. For elevation, the model for an individual site was:

$$\underset{}{\text{elevation}_{ijt}} = \underbrace{\beta_0 + \beta_1 \text{year}_t}_{\text{site effects}} + \underbrace{\mu_{0i} + \mu_{1i}\text{year}_t}_{\text{SET effects}} + \underbrace{\mu_{0j(i)} + \mu_{1j(i)}\text{year}_t}_{\text{arm within SET effects}} + \underbrace{\varepsilon_{ijt}}_{\text{resids.}}$$

where i indexes set, j indexes arm, t indexes year, and the notation $j(i)$ reads: "arm j associated with set i." β terms are the site-level effects: β_0 is the intercept and β_1 is the site-level trend in units of $\text{mm}^{-\text{yr}}$. The μ terms represent random effects associated with the intercept (subscript 0) or slope (subscript 1). Residual variation (ε) is modeled as normally distributed error around 0: $\varepsilon \overset{\text{iid}}{\sim} \text{normal}(0, \sigma)$.

For accretion, the model for an individual site was:

$$\underset{}{\text{accretion}_{ijt}} = \underbrace{\beta_0 + \beta_1 \text{year}_t}_{\text{site effects}} + \underbrace{\mu_{0i} + \mu_{1i}\text{year}_t}_{\text{SET effects}} + \underbrace{\mu_{0j(i)} + \mu_{1j(i)}\text{year}_t}_{\text{horizon within SET effects}} + \underbrace{\varepsilon_{ijt}}_{\text{resids.}}$$

where i indexes set, j indexes horizon, t indexes year, and the notation $j(i)$ reads: "horizon j associated with set i." β terms are the site-level effects: β_0 is the intercept and β_1 is the site-level trend in units of $\text{mm}^{-\text{yr}}$. The μ terms represent random effects associated with the intercept (subscript 0) or slope (subscript 1). Residual variation (ε) is modeled as normally distributed error around 0: $\varepsilon \overset{\text{iid}}{\sim} \text{normal}(0, \sigma)$.

Adding additional hierarchy at the upper level (e.g., sites within parks) is possible. But doing so would dilute the trend signal because "partial pooling" results in group-level estimates being pulled toward the population mean (Gelman and Hill 2006). Too much pooling results in lost signals at the group levels. Therefore, we chose to constrain the hierarchy to "arm-within-set" and model each site independently.

Additional hierarchy at the lower level is also possible, by extending the random effects to account for variation among pins-within-arm-within-set. Initial model exploration (using the lme4 R package) suggested that including the "pins-within-arms" level of random effects was not necessary because fits for many sites were "singular" (about 50% of site models had singular fits, and more had convergence problems). Singular fits mean that the standard deviation among pins was estimated to be approximately zero. If there is little variation among groups, as suggested by exploratory model fits, then there is little reason to include that level of random effects. Including a random effect with virtually zero among-group variation does not impact estimates at the upper groups, nor does excluding that level of random effect impact the upper level estimates. Including the lowest level of nested-ness does significantly increase computation time, however. We chose to limit the random effects structure to "arm-within-set" because: i) there was little evidence of among-pin variation and ii) including the "pin-within-arm" level would have dramatically increased computation time, for no statistical gain. Models were fit independently for each site.

We fit the models using the brms package (Bürkner et al. 2020) in R (Core Team}} 2020). The brms code the for the elevation model is:

```
brm(
  data = df,
  family = gaussian,
  formula = elevation ~ 1 + year +  # site level
            (1 + year | set) +      # set level
            (1 + year | set:arm)    # arm-within-set level
)
```

where ***df*** is an appropriate data frame. Similarly, the **brms** code for the accretion model is:

```
brm(
  data = df,
  family = gaussian,
  formula = accretion ~ 1 + year +    # site level
            (1 + year | set) +        # set level
```

```
            (1 + year | set:horizon)  # horizon-within-set level
)
```

Note that we assumed the response variables (elevation or accretion) were normally (Gaussian) distributed. The assumption of normality is justified because both elevation and accretion can take negative and positive values since they are relative to sea level. The assumption is also justified because we are analyzing mean values. We used a mixture of informative and vague prior distributions (Table 2). For the site-level intercept, we used the prior Normal(a, s), where a is the minimum observed elevation or depth for the data being fit and s is the standard deviation across all observed elevations or depths. This choice of prior works well for these data since nearly all trends were increasing or stable, meaning the intercept will be close the average minimum observation. However, the prior is diffuse enough around the mean to accommodate an intercept for a decreasing trend, too. We made sure the prior was appropriately diffuse by defining the standard deviation using all observed elevations or depths, rather than just the standard deviation of the minimum values.

Table 2. Prior distributions used in the analysis.

Parameter family	Prior distribution
Population intercept	Normal(a, s)
Population year effect	Normal(0, 2)
Group standard deviations	Cauchy(0, 2)
Group/parameter correlations	LKJCorr(2)

The **brms** package relies on the computational machinery of Stan (Development Team}} 2020, Guo et al. 2020) to fit the models via Hamiltonian Monte Carlo (HMC). We used the default **brms** priors for all unknown parameters. We launched three parallel HMC chains, each sampling for 1000 iterations after a warm-up phase of 3000 iterations (4000 iterations total per chain). Note that HMC requires many fewer iterations than Markov Chain Monte Carlo (MCMC) methods used by other software packages (e.g., WinBUGS or JAGS). HMC is a very efficient sampler, meaning fewer iterations are required to approximate the posterior distributions of all parameters. For context, the default settings in Stan are 1000 warmup iterations and 1000 sampling iterations.

We developed a custom R package, **ncbset**, that includes the formatted data and functions for data processing, model fitting, and posterior analysis, which is described next. Note that the R package is not meant to be a generalizable piece of software. Rather, it is a convenient way to ensure a reproducible analysis across all the sites by defining wrapper functions that are applied to each site in the exact same way. For future use, we recommend either: a) carefully processing the data such that it matches the format of the data currently stored with the package, or b) copying code from the relevant functions (e.g., `FitElevGLMM`) and making adjustments as needed. We also recommend investigating the use of Generalized Additive Mixed-Effects Models (GAMMs) in the future (see Appendix C for discussion and caveats related to GAMMs).

The following modeling software/package versions were used: **brms** version 2.15.0; **rstan** version 2.19.3; **stanHeaders** version 2.21.0.7; R version 4.0.4.

Posterior Analysis

The posterior analysis of the fitted models focused on model checking and computing quantities of interest for inference.

Model Checks

For model checking, we performed posterior predictive checks to ensure the fitted models could generate data distributions that conform to the observations (Hobbs and Hooten 2015, Conn et al. 2018). We evaluated the normality assumption using QQ plots. The evaluation of residuals with QQ plots and the posterior predictive distributions also indicated cases in which more flexible models (e.g., generalized additive models) might be necessary. Last, we ensured all scale reduction factors were less than 1.1, indicating that the posterior distributions had converged (Gelman and Rubin 1992, Gelman and Hill 2006). The model checks allow us to evaluate whether the fitted models are capable of generating data similar to the observations. This provides a check on the assumption of linear trends and indicates situations where a more flexible model (e.g., Generalized Additive Model) might be more suitable.

Inference from Models

For inference, we compared and summarized the posterior distributions of key quantities. First, we summarized the year effect (trend over time) as the mean of the posterior distribution and associated 85% and 95% Bayesian confidence interval (bounded by the 0.025, 0.075, 0.925, and 0.975 quantiles of the posterior distribution). This was done for the "global trend" (β_1) at each site and the trend at each sampling station within a site ($\beta_1 + \mu_{1i}$). The global trend is the population level estimate, which, by definition, must be variable enough to capture all the variation of the set and arm level trends. Because its posterior distribution is so wide, we also computed an "overall" site-level trend estimate as the average of the n set-level posterior distributions: ${\beta_1}' = (\sum_{i=1}^{n} \beta_1 + \mu_{1i})/n$ for each iteration in the posterior distribution (yielding a posterior distribution for β_1'). Throughout this report, we refer to "global" as the estimated population level trend (β_1) and "overall" as the average trend across sets (β_1).

We calculated several posterior probabilities to test specific hypotheses. We tested each hypothesis at the set level, the overall level, and the global level for each site. First, we calculated the posterior probability that the trend was greater than 0 (a one-tailed probability). Second, we calculated the posterior probability that the trend was greater than the upper 95% confidence bound on the estimate of sea level rise. Third, we calculated the posterior probability that the trend at each set station was less than the lower 95% confidence bound on the estimate of sea level rise. Trends in sea level rise used available historical data (the entire record of data) from the NOAA stations associated with each site and were estimated using the `lm` function in R (see Appendix A for details).

Model Checks

Model checking results can be found in *Wetland Elevation and Accretion Trend Analyses: Posterior Predicted Model Checks* (Tredennick et al. 2021). The document shows:

1. The site and SET station-level estimates (also presented in this document),

2. Comparisons between the data and the mean trend lines estimated from the model at the site level, and

3. Posterior predictive checks
    - Distributions of model simulations on top of the true observations
    - Comparisons between model simulations and true observations
    - QQ plots
    - Residual plots.

The comparisons between model-simulated values and the true observations indicate when a more flexible model is needed. For example, the posterior predictive checks for FIIS: Watch Hill indicate the model is not capable of reproducing the observed data distribution and the residual plots tell a similar story (Tredennick et al. 2021). This is because the WH3 station shows a nonlinear trend. Visual inspection of these diagnostics can guide choices on more flexible models (see Appendix B on Generalized Additive Models). Most models passed visual checks, indicating that the linear mixed effects model is an adequate representation of the observations. This is true even in cases where a more flexible model might provide a slightly better fit. Therefore, most results can be "trusted" because they do not violate the assumptions of the model.

General Trends

Here we present a few general trends, looking at the mean trend estimates across parks related to location (latitude) and local sea level rise trends. Only natural tidal sites and those that have records longer than 5 years were used to assess general trends, resulting in 68 trend estimates.

Trends across All Parks+-

Estimated rates of accretion and elevation change were mostly positive across all parks (Figure 2). The probability of a trend greater than zero was below 90% only for 5 elevation trend estimates. The probability that the trend was greater than zero was above 90% for all accretion trend estimates. Accretion and elevation trends decreased as latitude increased (i.e., trends increased from north to south), but the relationship was only significant for accretion ($p = 0.02$ for accretion; $p = 0.18$ for elevation).

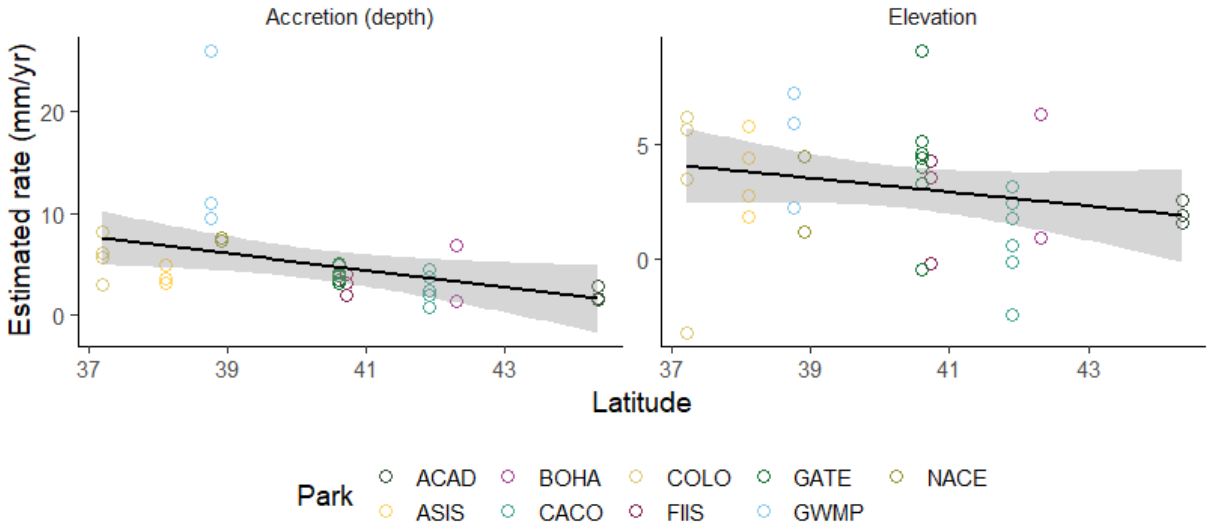


Figure 2. Mean estimated trends as a function of average latitude of each park. Each point is the posterior mean of the overall estimate for a site within a park. Points are colored by park. The fitted line shows a simple linear model fit (+/- standard error) to mean estimates.

Surface Elevation Table and Accretion Trends versus Sea Level Rise

We evaluated whether accretion and elevational trends were less than, not different, or above the rate of sea level rise based on the following thresholds:

- $Pr(\text{trend} < \text{SLR}) \geq 0.95$ = "Below SLR"
- $Pr(\text{trend} < \text{SLR}) < 0.95$ AND $Pr(\text{trend} > \text{SLR}) < 0.95$ = "Not different"
- $Pr(\text{trend} > \text{SLR}) \geq 0.95$ = "Above SLR."

Recall that "Pr(trend > SLR)" reads, "the probability that the estimated trend is greater than the rate of sea level rise."

Across the 33 sites, 12 sites had accretion trends that were less than the sea level rise rate, 12 sites had accretion trends that were not different than the sea level rise rate, and 9 sites had accretion trends that were greater than the sea level rise rate. The category to which each site belongs is reported in Table 3.

Table 3. Groupings of sites into categories based on whether the estimated accretion trend was above, not different, or below the rate of sea level rise.

Park*	Below SLR	Not Different	Above SLR
ACAD	Maine Coast Heritage	Bass Harbor	–
ACAD	Thompson Island	–	–
ASIS	Marsh 11	–	–
ASIS	Marsh 5	–	–
ASIS	Marsh 6	–	–
ASIS	Marsh 8	–	–
BOHA	Peddocks Island	–	Thompson Island
CACO	Hatches Harbor HH2	Hatches Harbor H1	Nauset Marsh OldN
CACO	–	Herring River GUT	–
CACO	–	Nauset Marsh N	–
COLO	Marsh 5	Marsh 13	–
COLO	–	Marsh 19	–
COLO	–	Marsh 30	–
FIIS	Great Gun	Watch Hill	–
FIIS	Hospital Point	–	–
GATE	Big Egg Control	Big Egg Spray	Black Bank
GATE	–	–	Elders East
GATE	–	JOCO	–
GATE	–	JOCO REF	–
GATE	–	Sandy Hook	–
GWMP	–	–	Dyke Marsh Creek
GWMP	–	–	Dyke Marsh Interior
GWMP	–	–	Dyke Marsh River
NACE	–	–	Kenilworth Marsh
NACE	–	–	Kingman Lake

*Park abbreviations: ASIS - Assateague Island National Seashore, BOHA - Boston Harbor Islands National Recreation Area, CACO - Cape Cod National Seashore, COLO - Colonial National Historical Park, FIIS - Fire Island National Seashore, GATE - Gateway National Recreation Area, GWMP - George Washington Memorial Parkway, NACE - National Capital Parks-East.

Across the 33 sites, 18 sites had elevation trends that were less than the sea level rise rate, 9 sites had elevation trends that were not different than the sea level rise rate, and 8 sites had elevation trends that were greater than the sea level rise rate. The category to which each site belongs is reported in Table 4.

Table 4. Groupings of sites into categories based on whether the estimated elevation trend was above, not different, or below the rate of sea level rise.

Park*	Below SLR	Not Different	Above SLR
ACAD	Thompson Island	Bass Harbor	–
ACAD	–	Maine Coast Heritage	–
ASIS	Marsh 11	Marsh 8	–
ASIS	Marsh 5	–	–
ASIS	Marsh 6	–	–
BOHA	Peddocks Island	–	Thompson Island
CACO	Hatches Harbor HH2	–	–
CACO	Hatches Harbor H1	–	–
CACO	Herring River G	–	–
CACO	Herring River GUT	–	–
CACO	Nauset Marsh N	–	–
CACO	Nauset Marsh OldN	–	–
COLO	Marsh 13	Marsh 30	Marsh 19
COLO	Marsh 5	–	–
FIIS	Great Gun	Watch Hill	–
FIIS	Hospital Point	–	–
GATE	Big Egg Control	Big Egg Spray	Elders East NF
GATE	–	–	JOCO
GATE	–	–	JOCO REF
GATE	–	Black Bank	–
GATE	–	Elders East	–
GATE	–	Sandy Hook	–
GATE	–	–	–
GATE	–	–	–
GWMP	Dyke Marsh Creek	–	Dyke Marsh Interior
GWMP	–	–	Dyke Marsh River
NACE	Kingman Lake	–	Kenilworth Marsh

*Park abbreviations: ASIS - Assateague Island National Seashore, BOHA - Boston Harbor Islands National Recreation Area, CACO - Cape Cod National Seashore, COLO - Colonial National Historical Park, FIIS - Fire Island National Seashore, GATE - Gateway National Recreation Area, GWMP - George Washington Memorial Parkway, NACE - National Capital Parks-East.

The probability that the trend is less than the rate of sea level rise was not related to latitude ($p = 0.51$ for accretion; $p = 0.47$ for elevation). To test whether the probability of the estimated trend was related to the magnitude of sea level rise, we fitted a Binomial Generalized Linear Model. First, we subsetted the data to just the probabilities that were either 0 or 1. We did so because most probabilities were either 0 or 1 and it is difficult to model proportions that also include true 0s and 1s. Second, we fit a Binomial GLM (or logistic model) to the elevation and accretion trend estimates independently, using the mean estimate of sea level rise as a predictor. Whether the probability for elevation was 0 or 1 was not related to the magnitude of sea level rise ($p = 0.6$). Whether the probability for accretion was 0 or 1 was positively related to the magnitude of sea level rise ($p =$

0.09). However, the p-value is marginal (less than 0.1 but greater than 0.5) and the results are mainly influenced by the high sea level rise rate at ASIS. Therefore, we conclude that the magnitude of sea level rise is not an important predictor of whether the accretion trend is keeping up with sea level rise or not.

The only generality related to sea level rise is that the estimated trends were either certainly keeping up with sea level rise or certainly not keeping up with sea level rise. This is demonstrated by evaluating the probability that the estimated trend is less than the lower 95% confidence interval bound of the sea level trend. Most probabilities were either zero (no probability that the estimated trend is less than sea level rise trend) or one (100% probability that the estimated trend is less than sea level rise trend; Figure 3). Moreover, about half of all estimated trends were either certainly lower than or certainly at least equal to the sea level rise trend (Figure 3). In other words, there was no clear signal that park trends are generally keeping up with sea level rise or not. The probabilities were not related to latitude ($p = 0.44$ for accretion; $p = 0.69$ for elevation).

To test whether the probability of the estimated trend was related to the magnitude of sea level rise, we fitted a Binomial Generalized Linear Model (GLM). First, we subsetted the data to just the probabilities that were either zero or one. We did so because most probabilities were either zero or one and it is difficult to model proportions that also include true zeros and ones. Second, we fit a Binomial GLM (or logistic model) to the elevation and accretion trend estimates independently, using the mean estimate of sea level rise as a predictor. Whether the probability for elevation was zero or one was not related to the magnitude of sea level rise ($p = 0.35$). Whether the probability for accretion was zero or one was positively related to the magnitude of sea level rise ($p = 0.06$). However, the p-value is marginal (less than 0.1 but greater than 0.5) and the results are mainly influenced by the higher sea level rise rate at ASIS. Therefore, we conclude that the magnitude of sea level rise is not an important predictor of whether the accretion trend is keeping up with sea level rise or not.

Surface Elevation Table and Accretion Trends over Shorter Time Periods

There are several sites at which the SET or accretion trends exhibit abrupt changes from one linear trend to another. This means we might expect different trends during different time periods. We used piece-wise linear regression to test a method for automatically detecting a changepoint in the Watch Hill SET elevation data (Appendix D). We used the Watch Hill data because a changepoint is visually apparent around 2013-2014, presumably due to Hurricane Sandy. As described in more detail in Appendix D, we fit a piece-wise linear regression (or changepoint) model to the data using brms to remain consistent with the core analysis. We fit the model to a single station within Watch Hill because the full random effects model was not necessary to test the method. We used a Bayesian model selection criterion ("loo," see Appendix D) to compare the changepoint model and a non-changepoint model.

The model selection criterion showed that the changepoint model was a better fit to the data. The changepoint model estimated a changepoint at September 18, 2006, with two estimated trends on either side of that date (Figure 3). The median slope before the changepoint is 1.86 mm/year. After the changepoint, the median slope is 5.77 mm/year. Interestingly, the changepoint estimated by the

model is far from the date we expected a priori based on local, extreme weather events. This is an important reminder that the best statistical model might not always agree with the underlying process we expect.

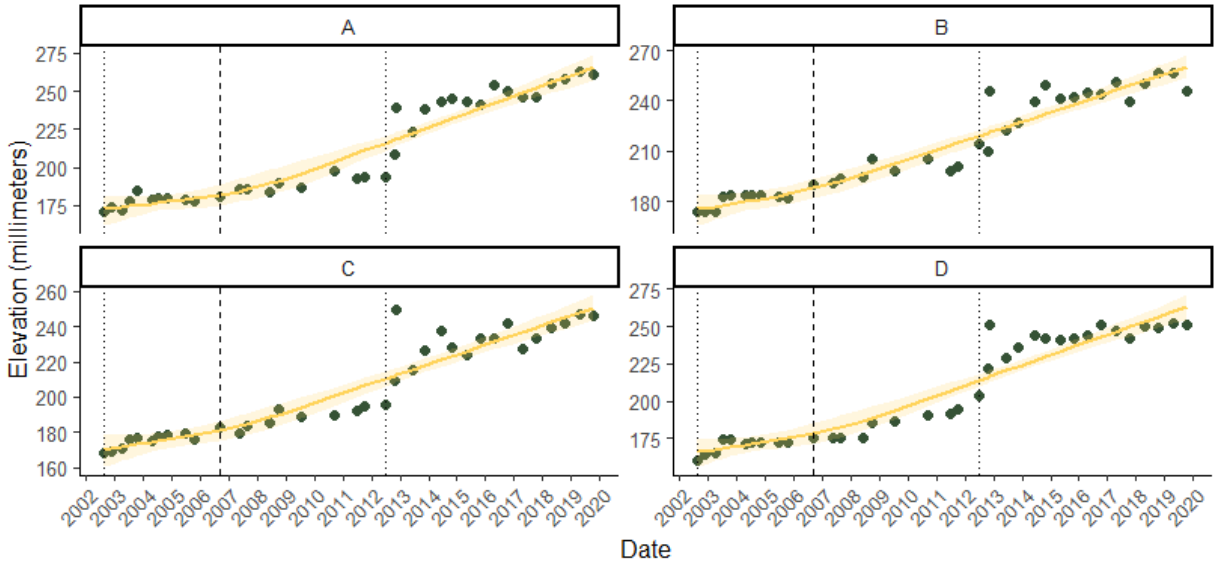


Figure 3. Fitted changepoint model for Watch Hill WH3 SET station. Model fits for each arm direction are shown in different panels. The horizontal line shows the estimated overall changepoint date from the model (dashed lines bound the 95% Bayesian credible interval). The line shows the mean of the posterior fit and the shaded region shows the 95% Bayesian credible interval.

The changepoint model was successful, but it did not lead to inference based on the process we were actually interested in. Moreover, the changepoint model did not appear to fit the data particularly well. Therefore, we also explored a simpler changepoint modeling framework using the R package segmented (Muggeo 2008). Note that we were unable to fit a random effects model with segmented. As discussed in detail in Appendix D, we were able to fit several models with different numbers of changepoints (i.e., more than just one) and select the best model. The best model included two changepoints (2011-10-06 and 2013-06-12) and provided a much better fit to the data. The model with two changepoints provides a better fit because the change in trend was not abrupt over just a single year. Rather there are three clear trends: trend before 2011-10-06 = 2.72 mm/yr (95% CI = 2.02, 3.43); trend after 2011-10-06 and before 2013-06-12 = 21.03 mm/yr (95% CI = 14.56, 27.5); trend after 2013-06-12 = 2.88 mm/yr (95% CI = 1.67, 4.08).

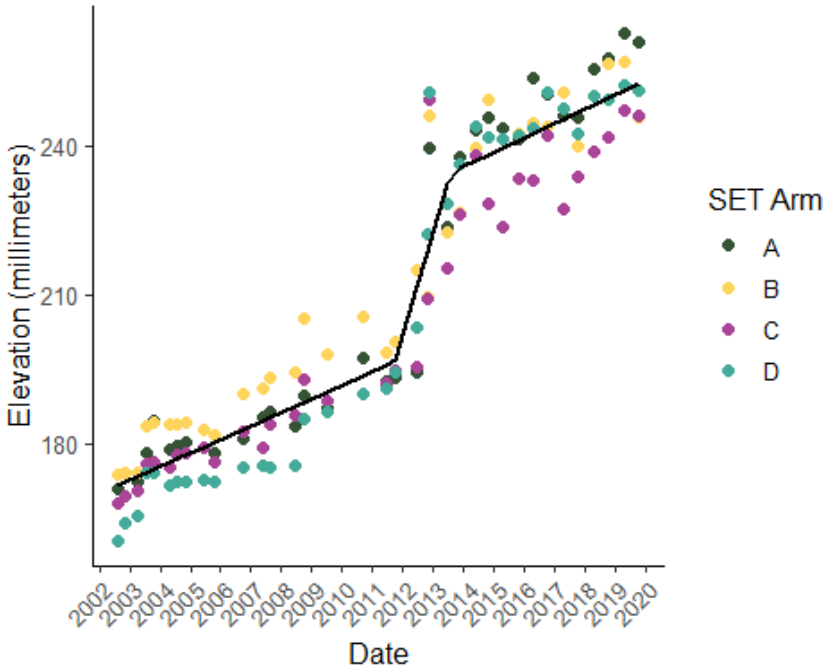


Figure 4. Trend estimate from the selected segment model for the Watch Hill WH3 SET station with two changepoints.

These conclusions lead us to the following recommendations:

1. If the goal is to best portray the trend over time when the trend is potentially nonlinear, we suggest using Generalized Additive Mixed-Effects Models (GAMMs; Appendix C).
2. If the goal is to identify changepoints to model shorter time periods, we suggest using the **segmented** package (or another appropriate R package) to fit several models with different numbers of change-points and then fitting the segmented data separately using the general **brms** methods provided.
3. If the goal is to best portray the trend over time *and* identify changepoints in a Bayesian random effects framework, we suggest working with a qualified statistician (either at NPS or elsewhere) to design the statistical model and implement in an appropriate Bayesian modeling computer language (or a custom MCMC algorithm).

Sampling Frequency

Each SET station or marker (for accretion) is typically sampled twice per year: once in the spring and once in the fall. We fit "spring" models and "fall" models using the same methods as above to test whether the trend estimates vary depending on the season during which data were collected. The statistical methods were exactly the same as detailed above, we simply subsetted the data to spring for the "spring" models and fall for the "fall" models. We then compared the overall posterior estimates (mean of $\beta_1+\mu_1i$ across all i SET stations within a site) for the full (both seasons), spring, and fall models. Appendix E provides more details and full results.

In general, across all sites and parks, we found that the trend estimates did not differ based on the data included. The vast majority of parks, sites, and sets had trend estimate credible intervals that overlapped with the model that was fit to their respective entire data set. Two sites had overall elevation trend estimate confidence intervals that did not overlap; 16 sites had median estimates for one season that did not overlap with the 95% BCI of the other season. Two sites had overall accretion trend estimate confidence intervals that did not overlap; 8 sites had median estimates for one season that did not overlap with the 95% BCI of the other season. Plots of all model estimates and confidence intervals are provided in Appendix E. Based on overlapping confidence intervals, our conclusion is that SET and marker stations could be sampled once per year, assuming seasonal variation in the past is representative of seasonal variation in the future. However, the fact that there are several sites and stations with seasonal median estimates that do not overlap the 95% CI of the other season (see Appendix E for details) indicates some bias may be introduced into the estimate if the stations are sampled once per year. Unfortunately, results were too idiosyncratic for us to confidently recommend sampling in one season over the other.

Comparison of Fenced and Non-Fenced Stations at Assateague Island National Seashore

At Assateague Island National Seashore, one station at each of the four sites was fenced to keep horses out. We grouped these four fenced stations into a "site" and modeled elevation and accretion trends as described for all other sites. We also grouped all the non-fenced stations into a single site (*n* = 12) to model elevation and accretion trends. There was no difference in the accretion trends between fenced and non-fenced stations (Figure 5; 95% Bayesian credible intervals broadly overlap). However, a difference between the fenced and non-fenced elevation trends was detected. The elevation trend at the fenced stations was higher than the trend at the non-fenced stations (Figure 5; 95% Bayesian credible intervals do not overlap).

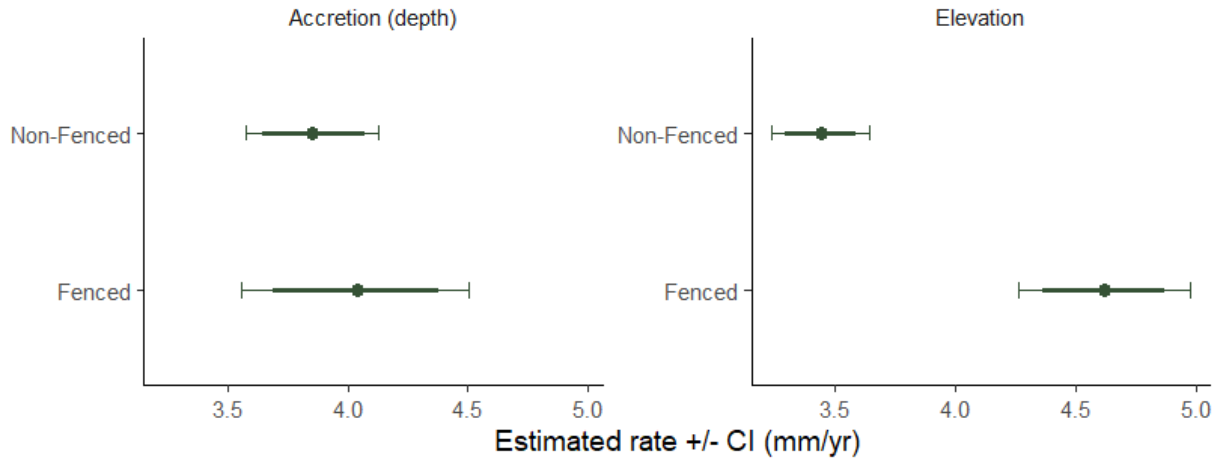


Figure 5. Estimated trends at fenced and non-fenced stations at Assateague Island National Seashore. Points are the mean trend estimates; thick error bars are the 85% Bayesian credible intervals; thin error bars are the 95% Bayesian credible intervals..

References

Bürkner, P.-C., J. Gabry, and S. Weber. 2020. brms: Bayesian Regression Models using 'Stan'. November 2020.

Conn, P. B., D. S. Johnson, P. J. Williams, S. R. Melin, and M. B. Hooten. 2018. A Guide to Bayesian Model Checking for Ecologists. Ecological Monographs 88:526–542.

R Core Team. 2020. R: A Language and Environment for Statistical Computing. R Foundation for Statistical Computing.

Sten Development Team. 2020. Stan Modeling Language Users Guide and Reference Manual, 2.12.2.

Gelman, A., and J. Hill. 2006. Data Analysis Using Regression and Multilevel/Hierarchical Models. Cambridge University Press.

Gelman, A., and D. B. Rubin. 1992. Inference from Iterative Simulation Using Multiple Sequences. Statistical Science 7:457–472.

Guo, J., J. Gabry, B. Goodrich, S. Weber, D. Lee, K. Sakrejda, and M. Martin. 2020. RStan: R Interface to Stan. July 2020.

Hobbs, N. T., and M. B. Hooten. 2015. Bayesian Models: A Statistical Primer for Ecologists. Princeton University Press.

Lynch, J. C., P. Hensel, and D. R. Cahoon. 2015. The Surface Elevation Table and Marker Horizon Technique: A Protocol for Monitoring Wetland Elevation Dynamics. Natural Resource Report NPS/NCBN/NRR—2015/1078. National Park Service, Fort Collins, Colorado.

Muggeo, V. M. R. 2008. Segmented: An R Package to Fit Regression Models with Broken-Line Relationships.

Tredennick A.T., M. Tabak, J. Lombardi , L. Starcevich. 2021. Wetland Elevation and Accretion Trend Analyses: Posterior Predicted Model Checks. Western EcoSystems Technology, Inc. Laramie, Wyoming. Available internally at: https://irma.nps.gov/DataStore/Reference/Profile/2296709 (Accessed 29 December 2022).

Appendix A. Site- and station-level trends

Andrew T. Tredennick, Western EcoSystems Technology, Inc.
Mikey Tabak, Western EcoSystems Technology, Inc.
John Lombardi, Western EcoSystems Technology, Inc.
Leigh Ann Starcevich, Western EcoSystems Technology, Inc.
2021-11-08

Trend Estimates and Fits

Here we present the trend estimates, fits, and associated posterior probabilities for each site within a park. We also present the SET-station level estimates. All results can be queried from the provided Excel spreadsheet with data, trend estimates, and fitted trends. Trend estimates are compared to local rates of sea level rise (SLR). SLR was estimated by fitting a linear model to the fully record of available data from each NOAA tide gauge station associated with each park and/or site (Table A.1).

Table A-1. Sea level rise rate (mm/yr) estimates for each site and the source of the sea level data. The NOAA ID is the tide gauge station number.

Park*	Site	Sea level rise rate (mm/yr)	Location	NOAA ID
ACAD	Bass Harbor	2.29 (2.16 – 2.42)	Bar Harbor, ME	8413320
ACAD	Maine Coast Heritage	2.29 (2.16 – 2.42)	Bar Harbor, ME	8413320
ACAD	Schoodic	2.29 (2.16 – 2.42)	Bar Harbor, ME	8413320
ACAD	Thompson Island	2.29 (2.16 – 2.42)	Bar Harbor, ME	8413320
ASIS	Marsh 5	6.1 (5.62 – 6.57)	Ocean City, MD	8570283
ASIS	Marsh 6	6.1 (5.62 – 6.57)	Ocean City, MD	8570283
ASIS	Marsh 8	6.1 (5.62 – 6.57)	Ocean City, MD	8570283
ASIS	Marsh 11	6.1 (5.62 – 6.57)	Ocean City, MD	8570283
ASIS	Marsh Exclosures	6.1 (5.62 – 6.57)	Ocean City, MD	8570283
ASIS	Marsh non-Exclosures	6.1 (5.62 – 6.57)	Ocean City, MD	8570283
BOHA	Calf Island	2.88 (2.78 – 2.98)	Boston, MA	8443970
BOHA	Peddocks Island	2.88 (2.78 – 2.98)	Boston, MA	8443970
BOHA	Thompson Island	2.88 (2.78 – 2.98)	Boston, MA	8443970
CACO	Blackfish Creek	2.88 (2.78 – 2.98)	Boston, MA	8443970
CACO	Hatches Harbor HH1	2.88 (2.78 – 2.98)	Boston, MA	8443970
CACO	Hatches Harbor HH2	2.88 (2.78 – 2.98)	Boston, MA	8443970
CACO	Hatches Harbor H1	2.88 (2.78 – 2.98)	Boston, MA	8443970
CACO	Hatches Harbor H2	2.88 (2.78 – 2.98)	Boston, MA	8443970
CACO	Herring River G	2.88 (2.78 – 2.98)	Boston, MA	8443970
CACO	Herring River GUT	2.88 (2.78 – 2.98)	Boston, MA	8443970
CACO	Herring River High Toss	2.88 (2.78 – 2.98)	Boston, MA	8443970
CACO	Herring River Phrag	2.88 (2.78 – 2.98)	Boston, MA	8443970
CACO	Nauset Marsh RSET	3.84 (3.62 – 4.06)	Nantucket, MA	8449130
CACO	Nauset Marsh OLD SET	3.84 (3.62 – 4.06)	Nantucket, MA	8449130
COLO	Marsh 5	4.73 (4.59 – 4.88)	Norfolk, VA	8638610
COLO	Marsh 13	4.73 (4.59 – 4.88)	Norfolk, VA	8638610

Park*	Site	Sea level rise rate (mm/yr)	Location	NOAA ID
COLO	Marsh 19	4.73 (4.59 – 4.88)	Norfolk, VA	8638610
COLO	Marsh 30	4.73 (4.59 – 4.88)	Norfolk, VA	8638610
FIIS	Great Gun	4.16 (4.02 – 4.3)	Sandy Hook, NJ	8531680
FIIS	Hospital Point	4.16 (4.02 – 4.3)	Sandy Hook, NJ	8531680
FIIS	Watch Hill	4.16 (4.02 – 4.3)	Sandy Hook, NJ	8531680
GATE	Big Egg Control	4.16 (4.02 – 4.3)	Sandy Hook, NJ	8531680
GATE	Big Egg Spray	4.16 (4.02 – 4.3)	Sandy Hook, NJ	8531680
GATE	Black Bank	4.16 (4.02 – 4.3)	Sandy Hook, NJ	8531680
GATE	Elders East	4.16 (4.02 – 4.3)	Sandy Hook, NJ	8531680
GATE	Elders East NF	4.16 (4.02 – 4.3)	Sandy Hook, NJ	8531680
GATE	Elders East Shallow	4.16 (4.02 – 4.3)	Sandy Hook, NJ	8531680
GATE	JOCO	4.16 (4.02 – 4.3)	Sandy Hook, NJ	8531680
GATE	JOCO REF	4.16 (4.02 – 4.3)	Sandy Hook, NJ	8531680
GATE	JOCO REF Shallow	4.16 (4.02 – 4.3)	Sandy Hook, NJ	8531680
GATE	Sandy Hook	4.16 (4.02 – 4.3)	Sandy Hook, NJ	8531680
GWMP	Dyke Marsh Creek	3.42 (3.24 – 3.6)	Washington, DC	8594900
GWMP	Dyke Marsh Interior	3.42 (3.24 – 3.6)	Washington, DC	8594900
GWMP	Dyke Marsh River	3.42 (3.24 – 3.6)	Washington, DC	8594900
NACE	Kenilworth Marsh	3.42 (3.24 – 3.6)	Washington, DC	8594900
NACE	Kingman Lake	3.42 (3.24 – 3.6)	Washington, DC	8594900

*Park abbreviations: ASIS - Assateague Island National Seashore, BOHA - Boston Harbor Islands National Recreation Area, CACO - Cape Cod National Seashore, COLO - Colonial National Historical Park, FIIS - Fire Island National Seashore, GATE - Gateway National Recreation Area, GWMP - George Washington Memorial Parkway, NACE - National Capital Parks-East.

Acadia National Park

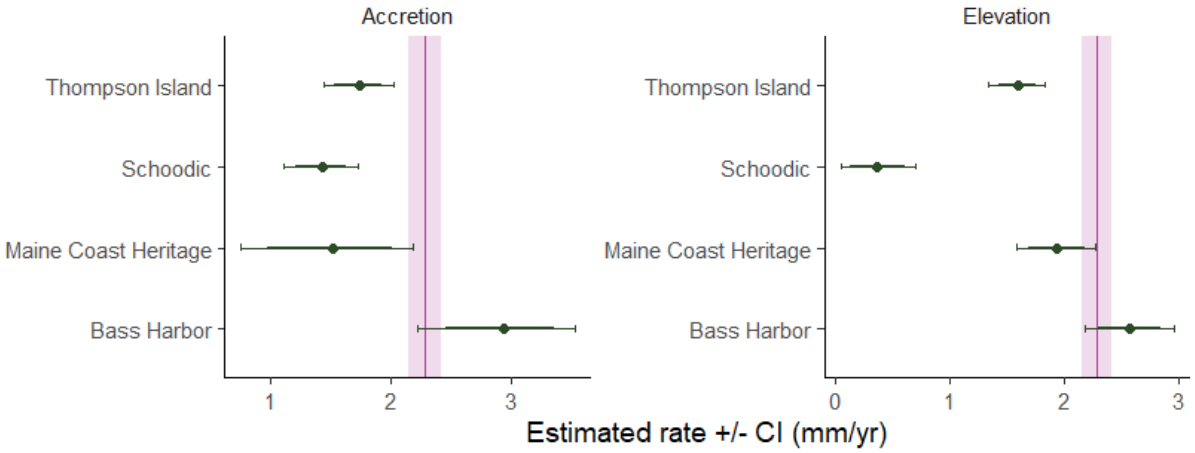


Figure A-1. Estimated accretion and elevation trends at the site level for Acadia National Park. The estimates are averages of the posteriors of the set-level trend estimates. The point shows the mean of the posterior; the thick error bars show the 85% Bayesian credible interval; the thin error bars show the 95% Bayesian credible interval. The vertical pink line shows the mean estimate of sea level rise and the pink rectangle bounds the 95% confidence interval.

Table A-2. Posterior trends (mean and 95% Bayesian credible interval) and the posterior probabilities that the trends in elevation or accretion are greater than 0 [Pr(trend > 0)], that the trend is greater than the upper bound of sea level rise [Pr(trend > slr)], and that the trend is less than the lower bound of sea level rise [Pr(trend < slr)] at each site in Acadia National Park. The final column [Pr(trend_i < trend_j)] is the probability that the trend specified in the row (either elevation or accretion) is less than the other estimated trend (either accretion or elevation) at the same site..

Site	Response	Trend estimate (mm/yr)	Pr(trend > 0)	Pr(trend > slr)	Pr(trend < slr)	Pr(trend_i < trend_j)
Bass Harbor	Accretion	2.93 (2.22 – 3.5)	1.00	0.94	0.02	0.15
Maine Coast Heritage	Accretion	1.52 (0.72 – 2.21)	1.00	0.01	0.96	0.85
Schoodic	Accretion	1.43 (1.13 – 1.72)	1.00	0.00	1.00	0.00
Thompson Island	Accretion	1.75 (1.48 – 2.02)	1.00	0.00	1.00	0.18
Bass Harbor	Elevation	2.56 (2.18 – 2.92)	1.00	0.79	0.02	0.85
Maine Coast Heritage	Elevation	1.93 (1.56 – 2.29)	1.00	0.01	0.90	0.15
Schoodic	Elevation	0.37 (0.05 – 0.69)	0.99	0.00	1.00	1.00
Thompson Island	Elevation	1.59 (1.34 – 1.81)	1.00	0.00	1.00	0.82

Bass Harbor

Table A-3. Estimated rates of elevation and accretion trends at Bass Harbor in Acadia National Park. Values in parentheses are the 95% Bayesian credible intervals. Pr(trend > 0) columns report the posterior probability that the estimated trend is greater than zero.

SET	Response	Trend estimate (mm/yr)	Pr(trend > 0)	Pr(trend > slr)	Pr(trend < slr)
Bass Harbor 1	Accretion	2.7 (1.78 – 3.49)	0.46	0.01	0.99
Bass Harbor 2	Accretion	3.1 (2.21 – 3.96)	0.78	0.03	0.96
Bass Harbor 3	Accretion	2.97 (2.14 – 3.76)	0.66	0.02	0.97
Bass Harbor 1	Elevation	5.59 (4.91 – 6.25)	1.00	0.91	0.06
Bass Harbor 2	Elevation	-0.64 (-1.29 – 0.02)	0.07	0.00	1.00
Bass Harbor 3	Elevation	2.72 (2.08 – 3.36)	0.83	0.18	0.77
Overall	**Accretion**	**2.93 (2.22 – 3.5)**	**1.00**	**0.94**	**0.02**
Overall	**Elevation**	**2.56 (2.18 – 2.92)**	**1.00**	**0.79**	**0.02**

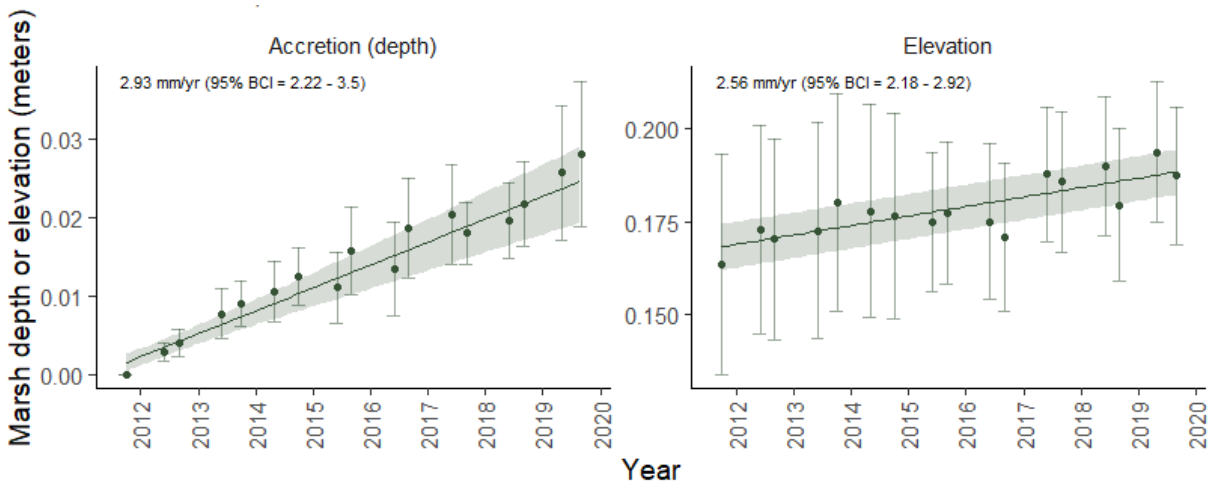


Figure A-2. Overall accretion and elevation trends for the Bass Harbor site at Acadia National Park. Solid line shows the mean of the posterior fitted trend; shaded region around the line bounds the 95% Bayesian credible interval of the fitted trend. These trend lines were computed using the mean of the intercept posteriors across SETs within the site and the mean of the slope posteriors across SETs within a site. Data are shown as means (points) plus and minus the standard deviation (error bars) across all observation locations within the site. Observations were grouped by month for aggregating.

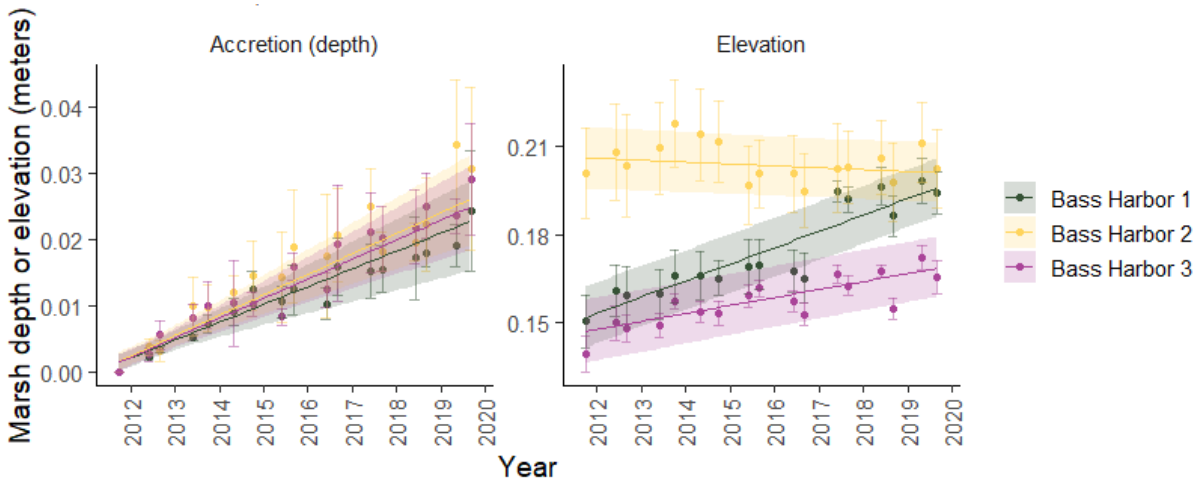


Figure A-3. Accretion and elevation trends at each station for the Bass Harbor site at Acadia National Park. Solid line shows the mean of the posterior fitted trend; shaded region around the line bounds the 95% Bayesian credible interval of the fitted trend. Data are shown as means (points) plus and minus the standard deviation (error bars) across all observation locations within the station. Observations were grouped by month for aggregating.

Maine Coast Heritage

Table A-4. Estimated rates of elevation and accretion trends at Maine Coast Heritage in Acadia National Park. Values in parentheses are the 95% Bayesian credible intervals. Pr(trend > 0) columns report the posterior probability that the estimated trend is greater than zero.

SET	Response	Trend estimate (mm/yr)	Pr(trend > 0)	Pr(trend > slr)	Pr(trend < slr)
MCHT 1	Accretion	1.79 (0.78 – 2.9)	0.76	0.01	0.98
MCHT 2	Accretion	1.53 (0.52 – 2.45)	0.58	0.00	1.00
MCHT 3	Accretion	1.24 (0.13 – 2.18)	0.36	0.00	1.00
MCHT 1	Elevation	2.13 (1.58 – 2.71)	0.74	0.01	0.98
MCHT 2	Elevation	2.82 (2.15 – 3.42)	0.96	0.04	0.92
MCHT 3	Elevation	0.84 (0.2 – 1.51)	0.08	0.00	1.00
Overall	**Accretion**	**1.52 (0.72 – 2.21)**	**1.00**	**0.01**	**0.96**
Overall	**Elevation**	**1.93 (1.56 – 2.29)**	**1.00**	**0.01**	**0.90**

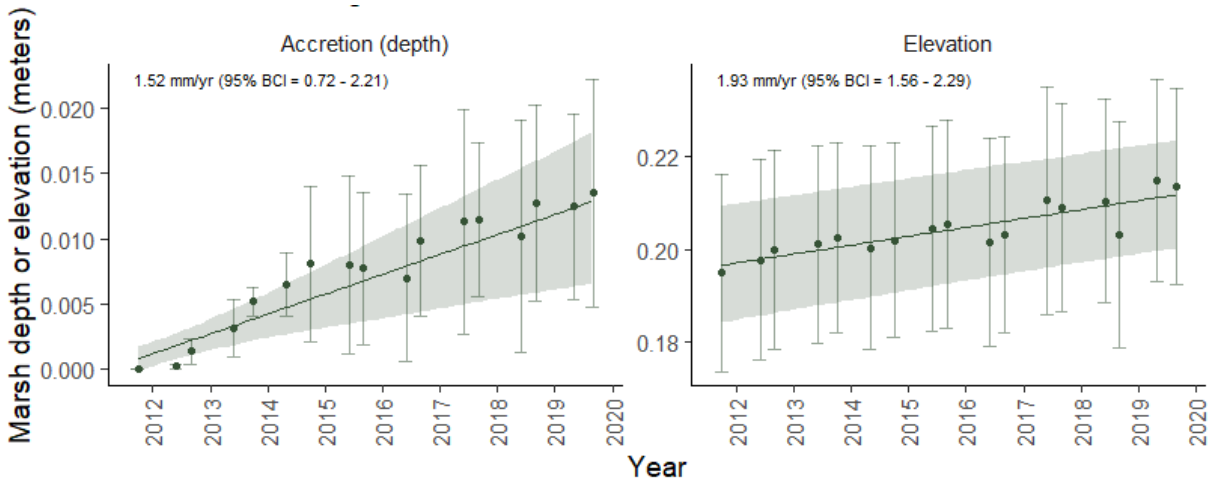


Figure A-3. Overall accretion and elevation trends for the Maine Coast Heritage site at Acadia National Park. Solid line shows the mean of the posterior fitted trend; shaded region around the line bounds the 95% Bayesian credible interval of the fitted trend. These trend lines were computed using the mean of the intercept posteriors across SETs within the site and the mean of the slope posteriors across SETs within a site. Data are shown as means (points) plus and minus the standard deviation (error bars) across all observation locations within the site. Observations were grouped by month for aggregating.

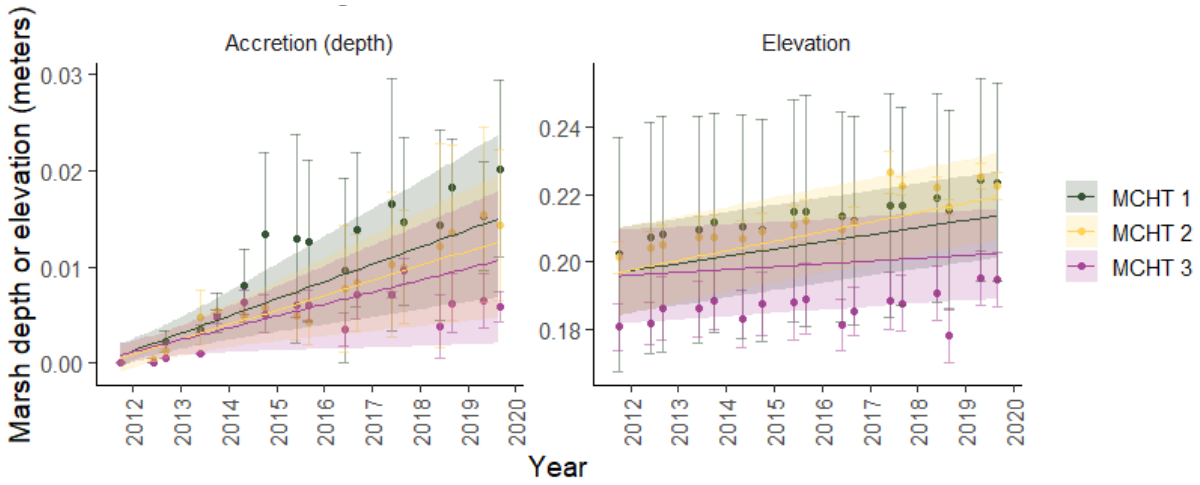


Figure A-5. Accretion and elevation trends at each station for the Maine Coast Heritage site at Acadia National Park. Solid line shows the mean of the posterior fitted trend; shaded region around the line bounds the 95% Bayesian credible interval of the fitted trend. Data are shown as means (points) plus and minus the standard deviation (error bars) across all observation locations within the station. Observations were grouped by month for aggregating.

Schoodic

Table A-5. Estimated rates of elevation and accretion trends at Schoodic in Acadia National Park. Values in parentheses are the 95% Bayesian credible intervals. Pr(trend > 0) columns report the posterior probability that the estimated trend is greater than zero.

SET	Response	Trend estimate (mm/yr)	Pr(trend > 0)	Pr(trend > slr)	Pr(trend < slr)
Schoodic 1	Accretion	1.12 (0.67 – 1.62)	0.24	0.00	1.00
Schoodic 2	Accretion	1.85 (1.29 – 2.31)	0.92	0.01	0.99
Schoodic 3	Accretion	1.33 (0.9 – 1.73)	0.45	0.00	1.00
Schoodic 1	Elevation	0.33 (-0.09 – 0.76)	0.45	0.00	1.00
Schoodic 2	Elevation	0.31 (-0.13 – 0.73)	0.42	0.00	1.00
Schoodic 3	Elevation	0.45 (0.05 – 0.92)	0.64	0.00	1.00
Overall	**Accretion**	**1.43 (1.13 – 1.72)**	**1.00**	**0.00**	**1.00**
Overall	**Elevation**	**0.37 (0.05 – 0.69)**	**0.99**	**0.00**	**1.00**

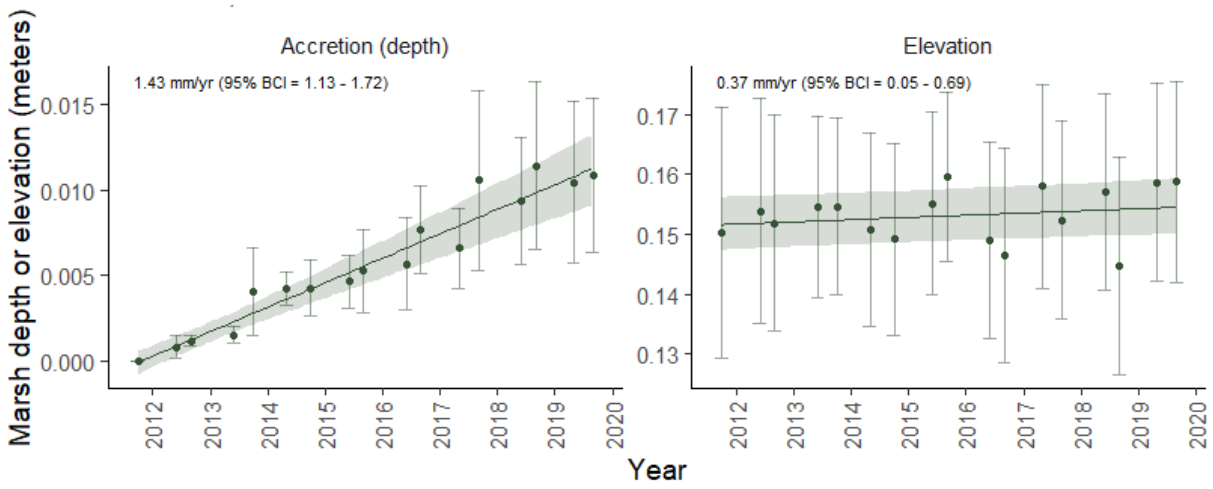


Figure A-6. Overall accretion and elevation trends for the Schoodic site at Acadia National Park. Solid line shows the mean of the posterior fitted trend; shaded region around the line bounds the 95% Bayesian credible interval of the fitted trend. These trend lines were computed using the mean of the intercept posteriors across SETs within the site and the mean of the slope posteriors across SETs within a site. Data are shown as means (points) plus and minus the standard deviation (error bars) across all observation locations within the site. Observations were grouped by month for aggregating.

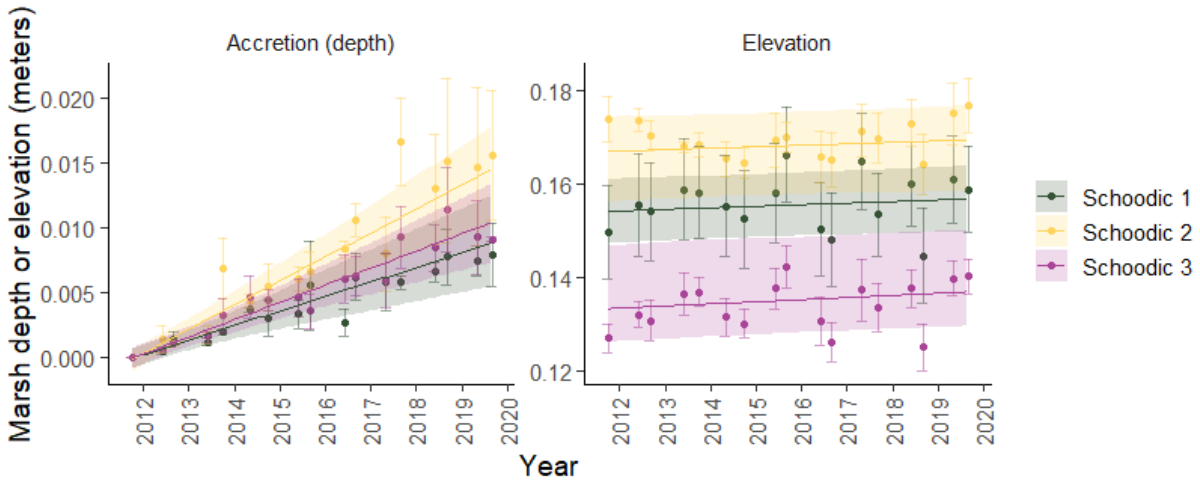


Figure A-7. Accretion and elevation trends at each station for the Schoodic site at Acadia National Park. Solid line shows the mean of the posterior fitted trend; shaded region around the line bounds the 95% Bayesian credible interval of the fitted trend. Data are shown as means (points) plus and minus the standard deviation (error bars) across all observation locations within the station. Observations were grouped by month for aggregating.

Thompson Island

Table A-6. Estimated rates of elevation and accretion trends at Thompson Island in Acadia National Park. Values in parentheses are the 95% Bayesian credible intervals. Pr(trend > 0) columns report the posterior probability that the estimated trend is greater than zero.

SET	Response	Trend estimate (mm/yr)	Pr(trend > 0)	Pr(trend > slr)	Pr(trend < slr)
Thompson 1	Accretion	1.74 (1.34 – 2.18)	0.57	0	1.00
Thompson 2	Accretion	1.48 (1.02 – 1.93)	0.24	0	1.00
Thompson 3	Accretion	2.02 (1.54 – 2.52)	0.87	0	1.00
Thompson 1	Elevation	1.82 (1.39 – 2.2)	0.78	0	1.00
Thompson 2	Elevation	1.96 (1.51 – 2.33)	0.87	0	0.99
Thompson 3	Elevation	0.98 (0.58 – 1.54)	0.10	0	1.00
Overall	**Accretion**	**1.75 (1.48 – 2.02)**	**1.00**	**0**	**1.00**
Overall	**Elevation**	**1.59 (1.34 – 1.81)**	**1.00**	**0**	**1.00**

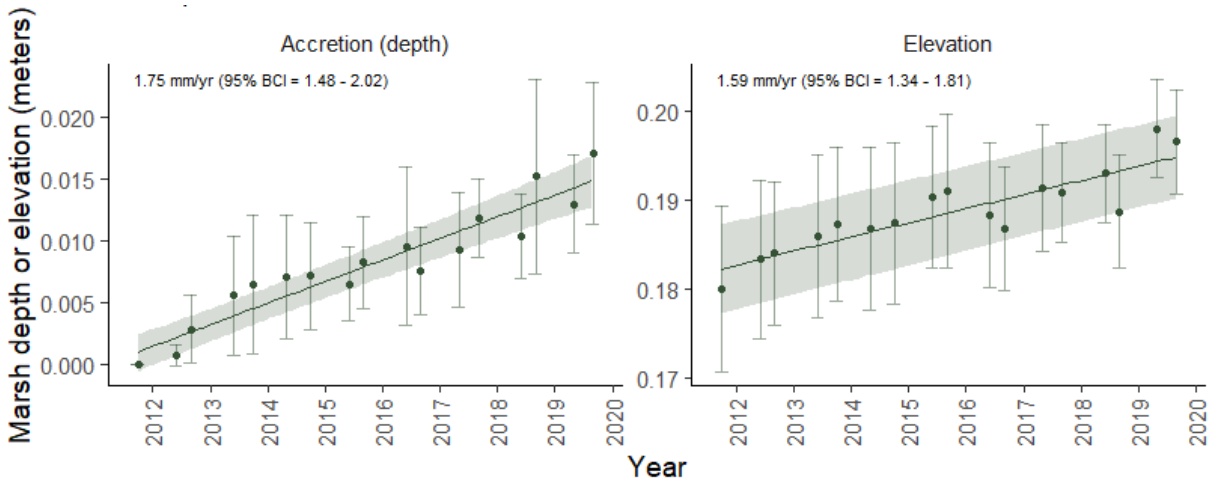


Figure A-8. Overall accretion and elevation trends for the Thompson Island site at Acadia National Park. Solid line shows the mean of the posterior fitted trend; shaded region around the line bounds the 95% Bayesian credible interval of the fitted trend. These trend lines were computed using the mean of the intercept posteriors across SETs within the site and the mean of the slope posteriors across SETs within a site. Data are shown as means (points) plus and minus the standard deviation (error bars) across all observation locations within the site. Observations were grouped by month for aggregating.

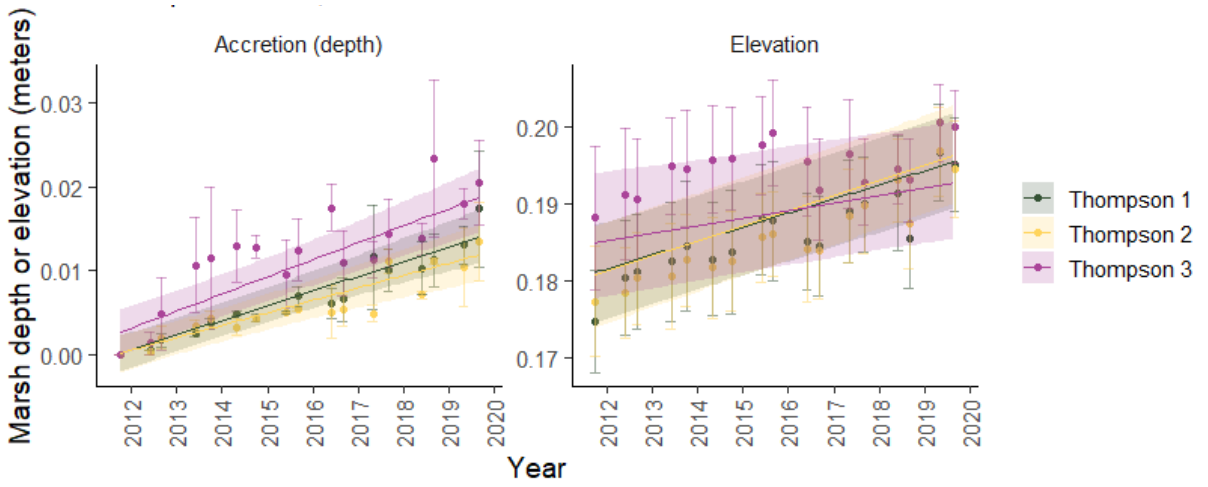


Figure A-9. Accretion and elevation trends at each station for the Thompson Island site at Acadia National Park. Solid line shows the mean of the posterior fitted trend; shaded region around the line bounds the 95% Bayesian credible interval of the fitted trend. Data are shown as means (points) plus and minus the standard deviation (error bars) across all observation locations within the station. Observations were grouped by month for aggregating.

Assateague Island National Seashore

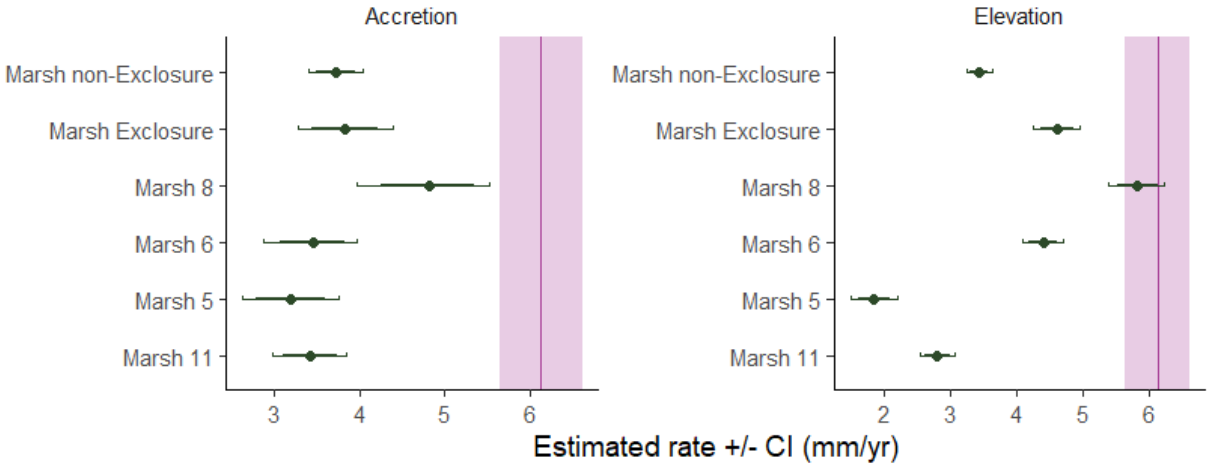


Figure A-10. Estimated accretion and elevation trends at the site level for Assateague Island National Seashore. The estimates are averages of the posteriors of the set-level trend estimates. The point shows the mean of the posterior; the thick error bars show the 85% Bayesian credible interval; the thin error bars show the 95% Bayesian credible interval. The vertical pink line shows the mean estimate of sea level rise and the pink rectangle bounds the 95% confidence interval.

Table A-7. Posterior trends (mean and 95% Bayesian credible interval) and the posterior probabilities that the trends in elevation or accretion are greater than 0 [Pr(trend > 0)], that the trend is greater than the upper bound of sea level rise [Pr(trend > slr)], and that the trend is less than the lower bound of sea level rise [Pr(trend < slr)] at each site in Assateague Island National Seashore. The final column [Pr(trend_i < trend_j)] is the probability that the trend specified in the row (either elevation or accretion) is less than the other estimated trend (either accretion or elevation) at the same site.

Site	Response	Trend estimate (mm/yr)	Pr(trend > 0)	Pr(trend > slr)	Pr(trend < slr)	Pr(trend_i < trend_j)
Marsh 11	Accretion	3.66 (3.26 – 4.05)	1	0	1.00	0.00
Marsh 5	Accretion	3.23 (2.74 – 3.69)	1	0	1.00	0.00
Marsh 6	Accretion	3.61 (3.10 – 4.07)	1	0	1.00	1.00
Marsh 8	Accretion	4.97 (4.24 – 5.56)	1	0	0.98	0.99
Marsh Exclosure	Accretion	4.04 (3.56 – 4.50)	1	0	1.00	0.98
Marsh non-Exclosure	Accretion	3.86 (3.57 – 4.13)	1	0	1.00	0.01
Marsh 11	Elevation	2.80 (2.54 – 3.06)	1	0	1.00	1.00
Marsh 5	Elevation	1.86 (1.49 – 2.19)	1	0	1.00	1.00
Marsh 6	Elevation	4.40 (4.10 – 4.70)	1	0	1.00	0.00
Marsh 8	Elevation	5.83 (5.42 – 6.22)	1	0	0.15	0.01
Marsh Exclosure	Elevation	4.62 (4.26 – 4.98)	1	0	1.00	0.02

Marsh 5

Table A-8. Estimated rates of elevation and accretion trends at Marsh 5 in Assateague Island National Seashore. Values in parentheses are the 95% Bayesian credible intervals. Pr(trend > 0) columns report the posterior probability that the estimated trend is greater than zero.

SET	Response	Trend estimate (mm/yr)	Pr(trend > 0)	Pr(trend > slr)	Pr(trend < slr)
M5-1	Accretion	2.84 (2.08 – 3.53)	0.29	0	1
M5-2	Accretion	3.22 (2.59 – 3.83)	0.67	0	1
M5-3	Accretion	3.26 (2.6 – 3.88)	0.70	0	1
M5-4	Accretion	3.61 (2.84 – 4.39)	0.90	0	1
M5-1	Elevation	1.07 (0.4 – 1.76)	0.21	0	1
M5-2	Elevation	2.62 (1.9 – 3.27)	0.92	0	1
M5-3	Elevation	3.25 (2.44 – 3.88)	0.98	0	1
M5-4	Elevation	0.49 (-0.26 – 1.32)	0.07	0	1
Overall	**Accretion**	**3.23 (2.74 – 3.69)**	**1.00**	**0**	**1**
Overall	**Elevation**	**1.86 (1.49 – 2.19)**	**1.00**	**0**	**1**

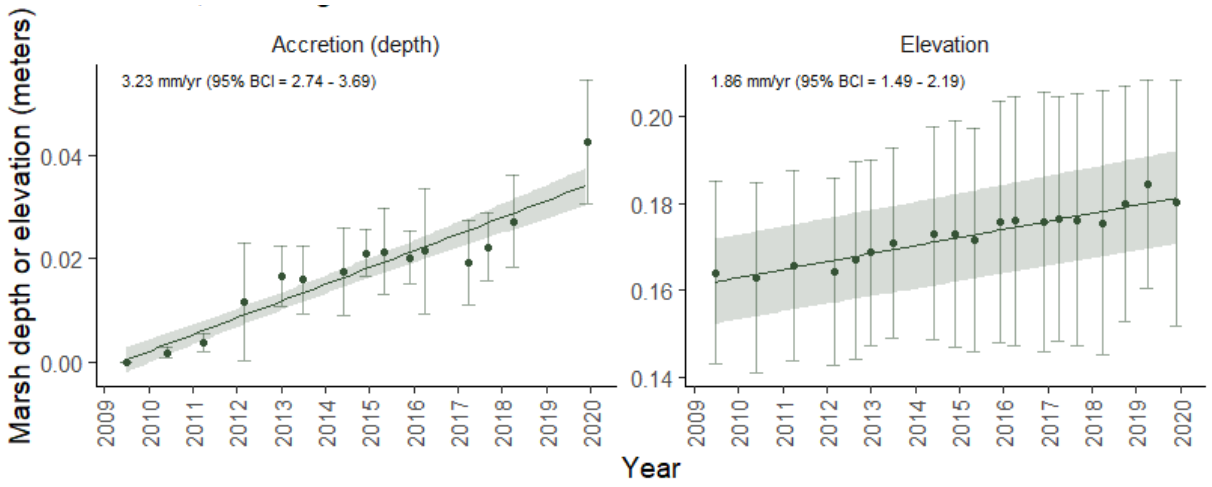


Figure A-11. Overall accretion and elevation trends for the Marsh 5 site at Assateague Island National Seashore. Solid line shows the mean of the posterior fitted trend; shaded region around the line bounds the 95% Bayesian credible interval of the fitted trend. These trend lines were computed using the mean of the intercept posteriors across SETs within the site and the mean of the slope posteriors across SETs within a site. Data are shown as means (points) plus and minus the standard deviation (error bars) across all observation locations within the site. Observations were grouped by month for aggregating.

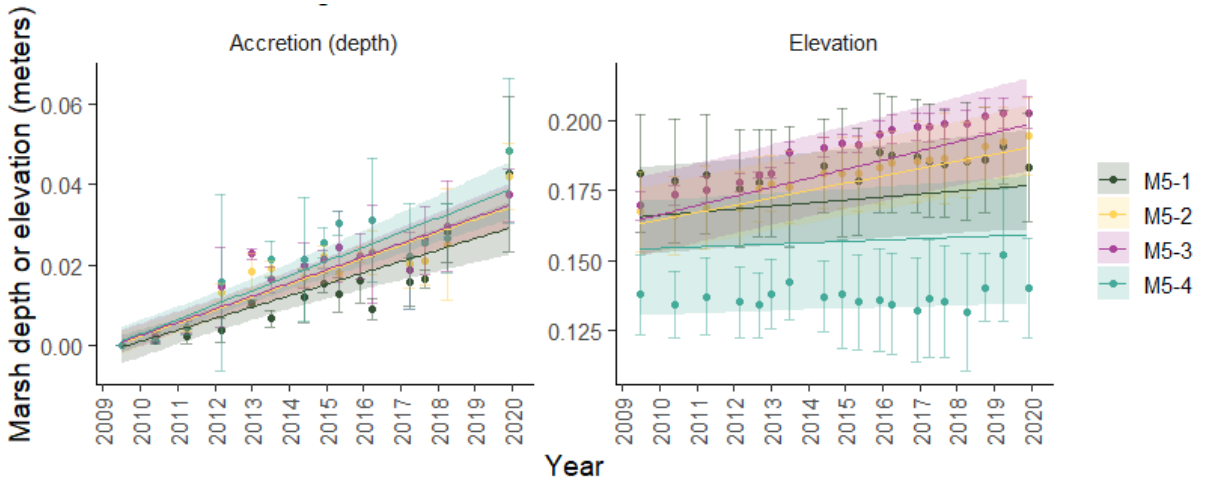


Figure A-12. Accretion and elevation trends at each station for the Marsh 5 site at Assateague Island National Seashore. Solid line shows the mean of the posterior fitted trend; shaded region around the line bounds the 95% Bayesian credible interval of the fitted trend. Data are shown as means (points) plus and minus the standard deviation (error bars) across all observation locations within the station. Observations were grouped by month for aggregating.

Marsh 6

Table A-9. Estimated rates of elevation and accretion trends at Marsh 6 in Assateague Island National Seashore. Values in parentheses are the 95% Bayesian credible intervals. Pr(trend > 0) columns report the posterior probability that the estimated trend is greater than zero.

SET	Response	Trend estimate (mm/yr)	Pr(trend > 0)	Pr(trend > slr)	Pr(trend < slr)
M6-1	Accretion	4.21 (3.29 – 5.01)	0.98	0.00	0.99
M6-2	Accretion	4.2 (3.28 – 4.98)	0.98	0.00	0.99
M6-3	Accretion	2.62 (1.79 – 3.47)	0.50	0.00	1.00
M6-4	Accretion	3.41 (2.6 – 4.19)	0.83	0.00	1.00
M6-1	Elevation	5.36 (4.77 – 5.95)	0.98	0.01	0.99
M6-2	Elevation	5.8 (5.18 – 6.38)	1.00	0.01	0.98
M6-3	Elevation	2.62 (2.02 – 3.22)	0.11	0.00	1.00
M6-4	Elevation	3.84 (3.26 – 4.43)	0.49	0.00	1.00
Overall	**Accretion**	**3.61 (3.1 – 4.07)**	**1.00**	**0.00**	**1.00**
Overall	**Elevation**	**4.4 (4.1 – 4.7)**	**1.00**	**0.00**	**1.00**

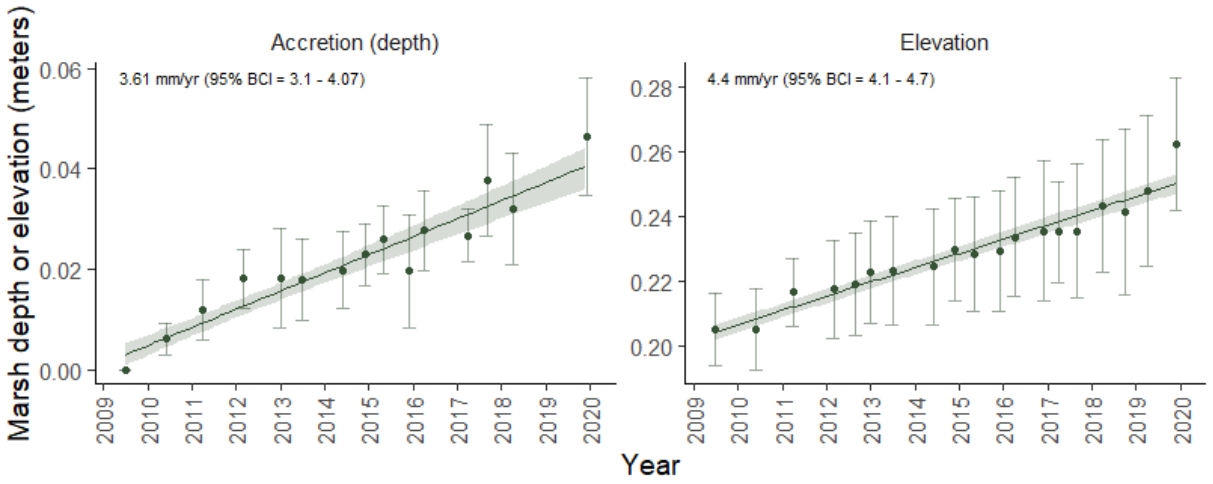


Figure A-13. Overall accretion and elevation trends for the Marsh 6 site at Assateague Island National Seashore. Solid line shows the mean of the posterior fitted trend; shaded region around the line bounds the 95% Bayesian credible interval of the fitted trend. These trend lines were computed using the mean of the intercept posteriors across SETs within the site and the mean of the slope posteriors across SETs within a site. Data are shown as means (points) plus and minus the standard deviation (error bars) across all observation locations within the site. Observations were grouped by month for aggregating.

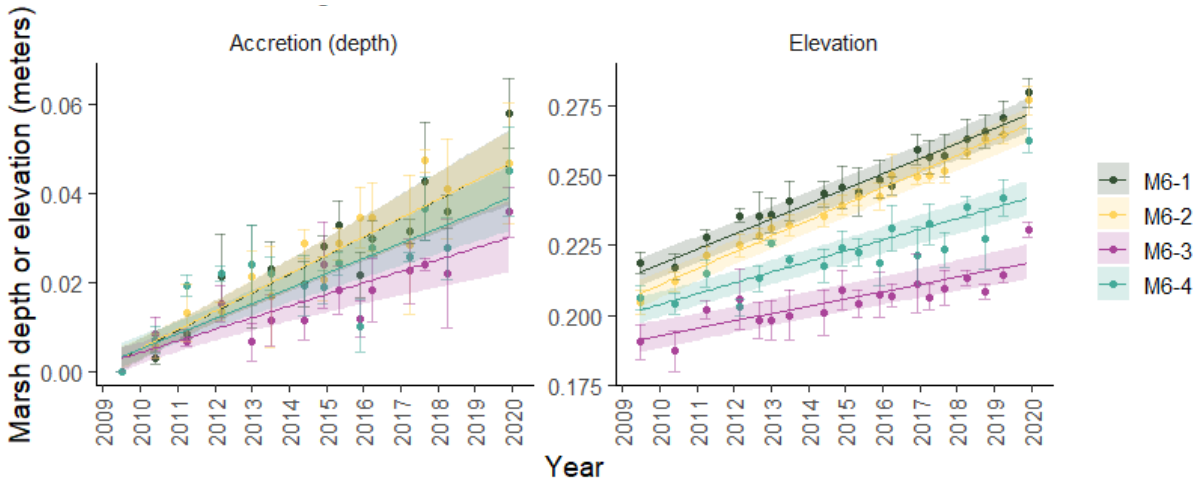


Figure A-14. Accretion and elevation trends at each station for the Marsh 6 site at Assateague Island National Seashore. Solid line shows the mean of the posterior fitted trend; shaded region around the line bounds the 95% Bayesian credible interval of the fitted trend. Data are shown as means (points) plus and minus the standard deviation (error bars) across all observation locations within the station. Observations were grouped by month for aggregating.

Marsh 8

Table A-10. Estimated rates of elevation and accretion trends at Marsh 8 in Assateague Island National Seashore. Values in parentheses are the 95% Bayesian credible intervals. Pr(trend > 0) columns report the posterior probability that the estimated trend is greater than zero.

SET	Response	Trend estimate (mm/yr)	Pr(trend > 0)	Pr(trend > slr)	Pr(trend < slr)
M8-1	Accretion	5.12 (4.07 – 6.13)	0.96	0.02	0.91
M8-2	Accretion	5.16 (4.14 – 6.16)	0.97	0.02	0.91
M8-3	Accretion	4.13 (3.08 – 5.15)	0.87	0.00	0.98
M8-4	Accretion	5.47 (4.29 – 6.47)	0.98	0.04	0.88
M8-1	Elevation	5.55 (4.85 – 6.18)	0.32	0.00	1.00
M8-2	Elevation	6.2 (5.49 – 6.98)	0.88	0.00	1.00
M8-3	Elevation	5.51 (4.75 – 6.15)	0.29	0.00	1.00
M8-4	Elevation	6.06 (5.43 – 6.78)	0.83	0.00	1.00
Overall	**Accretion**	**4.97 (4.24 – 5.56)**	**1.00**	**0.00**	**0.98**
Overall	**Elevation**	**5.83 (5.42 – 6.22)**	**1.00**	**0.00**	**0.15**

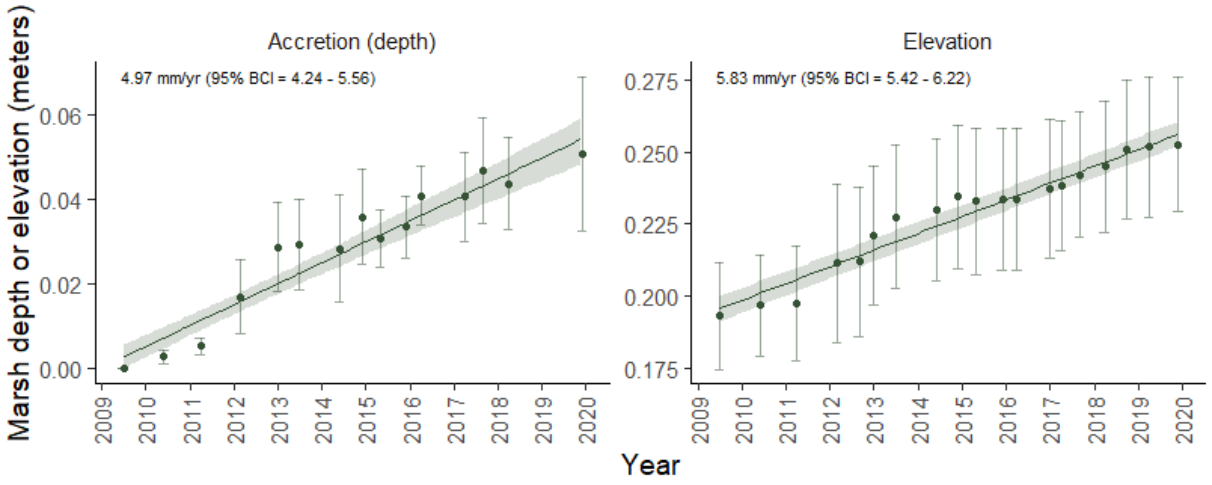


Figure A-15. Overall accretion and elevation trends for the Marsh 8 site at Assateague Island National Seashore. Solid line shows the mean of the posterior fitted trend; shaded region around the line bounds the 95% Bayesian credible interval of the fitted trend. These trend lines were computed using the mean of the intercept posteriors across SETs within the site and the mean of the slope posteriors across SETs within a site. Data are shown as means (points) plus and minus the standard deviation (error bars) across all observation locations within the site. Observations were grouped by month for aggregating.

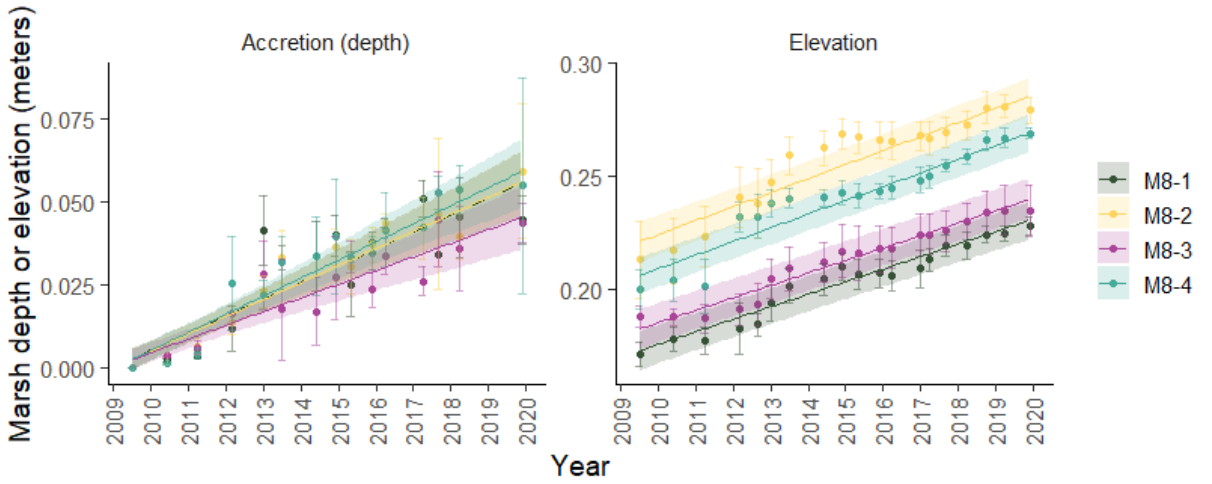


Figure A-16. Accretion and elevation trends at each station for the Marsh 8 site at Assateague Island National Seashore. Solid line shows the mean of the posterior fitted trend; shaded region around the line bounds the 95% Bayesian credible interval of the fitted trend. Data are shown as means (points) plus and minus the standard deviation (error bars) across all observation locations within the station. Observations were grouped by month for aggregating.

Marsh 11

Table A-11. Estimated rates of elevation and accretion trends at Marsh 11 in Assateague Island National Seashore. Values in parentheses are the 95% Bayesian confidence intervals. Pr(trend > 0) columns report the posterior probability that the estimated trend is greater than zero.

SET	Response	Trend estimate (mm/yr)	Pr(trend > 0)	Pr(trend > slr)	Pr(trend < slr)
M11-1	Accretion	2.76 (2.11 – 3.4)	0.55	0.00	1.00
M11-2	Accretion	3.62 (3.01 – 4.21)	0.91	0.00	1.00
M11-3	Accretion	4.41 (3.71 – 5.02)	0.99	0.00	0.99
M11-4	Accretion	3.87 (3.27 – 4.47)	0.97	0.00	1.00
M11-1	Elevation	-0.1 (-0.64 – 0.46)	0.06	0.00	1.00
M11-2	Elevation	3.44 (2.92 – 3.99)	0.92	0.00	1.00
M11-3	Elevation	5.71 (5.17 – 6.22)	1.00	0.03	0.91
M11-4	Elevation	2.15 (1.63 – 2.7)	0.56	0.00	1.00
Overall	**Accretion**	**3.66 (3.26 – 4.05)**	**1.00**	**0.00**	**1.00**
Overall	**Elevation**	**2.8 (2.54 – 3.06)**	**1.00**	**0.00**	**1.00**

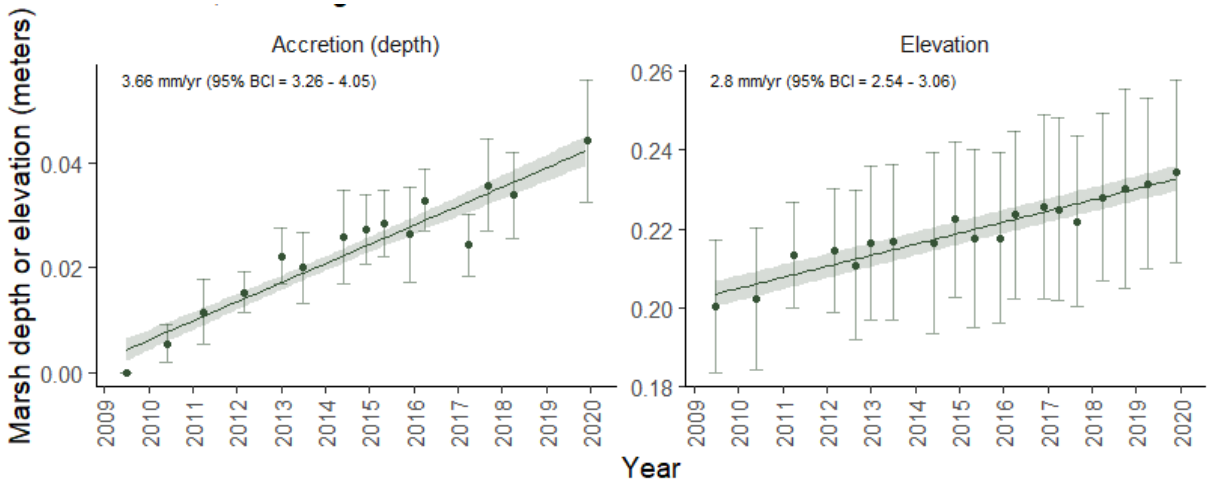


Figure A-17. Overall accretion and elevation trends for the Marsh 11 site at Assateague Island National Seashore. Solid line shows the mean of the posterior fitted trend; shaded region around the line bounds the 95% Bayesian credible interval of the fitted trend. These trend lines were computed using the mean of the intercept posteriors across SETs within the site and the mean of the slope posteriors across SETs within a site. Data are shown as means (points) plus and minus the standard deviation (error bars) across all observation locations within the site. Observations were grouped by month for aggregating.

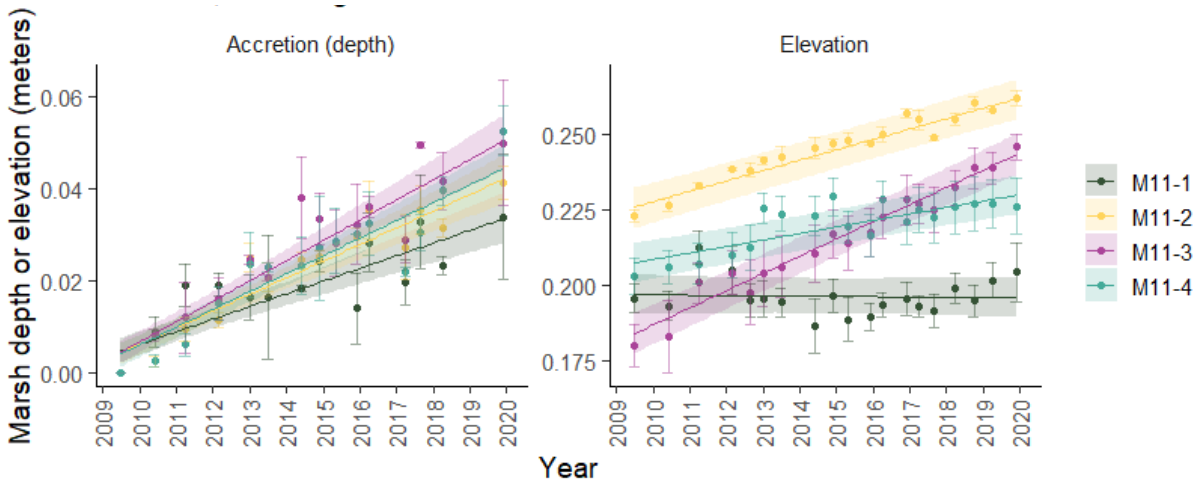


Figure A-18. Accretion and elevation trends at each station for the Marsh 11 site at Assateague Island National Seashore. Solid line shows the mean of the posterior fitted trend; shaded region around the line bounds the 95% Bayesian credible interval of the fitted trend. Data are shown as means (points) plus and minus the standard deviation (error bars) across all observation locations within the station. Observations were grouped by month for aggregating.

Marsh Exclosures

Table A-12. Estimated rates of elevation and accretion trends at the exclosure stations (fenced) in Assateague Island National Seashore. Values in parentheses are the 95% Bayesian credible intervals. Pr(trend > 0) columns report the posterior probability that the estimated trend is greater than zero.

SET	Response	Trend estimate (mm/yr)	Pr(trend > 0)	Pr(trend > slr)	Pr(trend < slr)
M11-3	Accretion	4.54 (3.81 – 5.25)	1.00	0.00	0.96
M5-2	Accretion	2.88 (2.16 – 3.61)	0.82	0.00	1.00
M6-4	Accretion	3.35 (2.58 – 4.09)	0.91	0.00	0.99
M8-4	Accretion	5.39 (4.57 – 6.13)	1.00	0.03	0.89
M11-3	Elevation	5.65 (4.9 – 6.34)	0.98	0.00	0.98
M5-2	Elevation	2.69 (1.97 – 3.44)	0.17	0.00	1.00
M6-4	Elevation	3.92 (3.22 – 4.64)	0.53	0.00	1.00
M8-4	Elevation	6.22 (5.54 – 6.94)	1.00	0.01	0.97
Overall	**Accretion**	**4.04 (3.56 – 4.5)**	**1.00**	**0.00**	**1.00**
Overall	**Elevation**	**4.62 (4.26 – 4.98)**	**1.00**	**0.00**	**1.00**

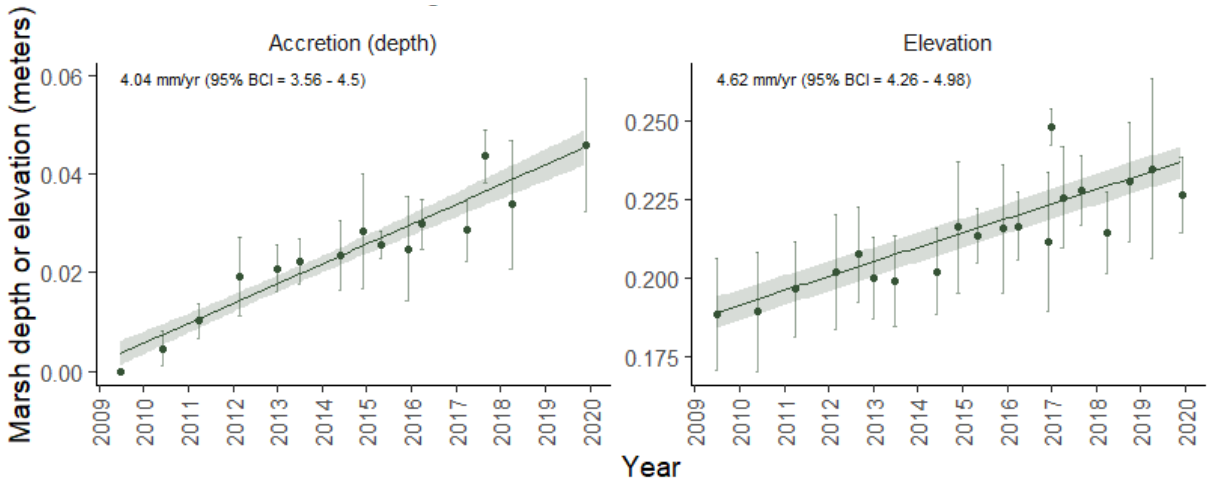


Figure A-19. Overall accretion and elevation trends for the exclosure stations at Assateague Island National Seashore. Solid line shows the mean of the posterior fitted trend; shaded region around the line bounds the 95% Bayesian credible interval of the fitted trend. These trend lines were computed using the mean of the intercept posteriors across SETs within the site and the mean of the slope posteriors across SETs within a site. Data are shown as means (points) plus and minus the standard deviation (error bars) across all observation locations within the site. Observations were grouped by month for aggregating.

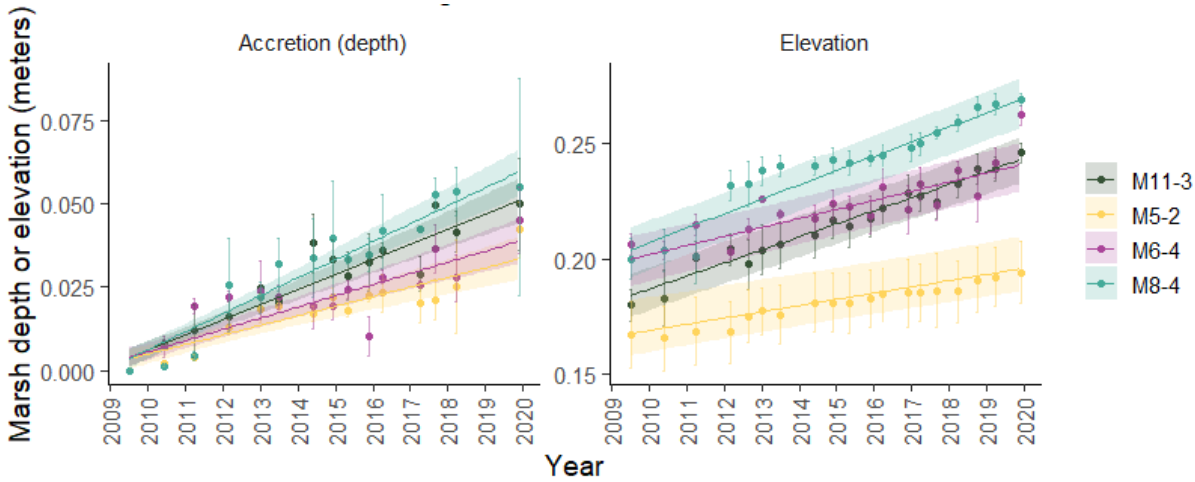


Figure A-20. Accretion and elevation trends at each station for the exclosure stations at Assateague Island National Seashore. Solid line shows the mean of the posterior fitted trend; shaded region around the line bounds the 95% Bayesian credible interval of the fitted trend. Data are shown as means (points) plus and minus the standard deviation (error bars) across all observation locations within the station. Observations were grouped by month for aggregating.

Marsh non-Exclosure

Table A-13. Estimated rates of elevation and accretion trends at the non-exclosure stations (not fenced) in Assateague Island National Seashore. Values in parentheses are the 95% Bayesian credible intervals. Pr(trend > 0) columns report the posterior probability that the estimated trend is greater than zero.

SET	Response	Trend estimate (mm/yr)	Pr(trend > 0)	Pr(trend > slr)	Pr(trend < slr)
M11-1	Accretion	3.13 (2.43 – 3.87)	0.14	0	1
M11-2	Accretion	3.89 (3.18 – 4.57)	0.74	0	1
M11-4	Accretion	4.1 (3.43 – 4.77)	0.88	0	1
M5-1	Accretion	2.53 (1.76 – 3.32)	0.01	0	1
M5-3	Accretion	3.21 (2.51 – 3.88)	0.16	0	1
M5-4	Accretion	3.71 (3.02 – 4.4)	0.58	0	1
M6-1	Accretion	4.36 (3.63 – 5.05)	0.96	0	1
M6-2	Accretion	4.35 (3.64 – 5.06)	0.96	0	1
M6-3	Accretion	2.8 (2.06 – 3.53)	0.03	0	1
M8-1	Accretion	5.02 (4.24 – 5.77)	1.00	0	1
M8-2	Accretion	5.06 (4.29 – 5.78)	1.00	0	1
M8-3	Accretion	4.09 (3.41 – 4.75)	0.88	0	1
M11-1	Elevation	-0.01 (-0.66 – 0.66)	0.00	0	1
M11-2	Elevation	3.47 (2.81 – 4.12)	0.71	0	1
M11-4	Elevation	2.2 (1.55 – 2.9)	0.11	0	1
M5-1	Elevation	1.06 (0.42 – 1.73)	0.01	0	1
M5-3	Elevation	3.34 (2.67 – 4.04)	0.65	0	1
M5-4	Elevation	0.37 (-0.29 – 1.02)	0.00	0	1
M6-1	Elevation	5.33 (4.67 – 6)	1.00	0	1
M6-2	Elevation	5.86 (5.17 – 6.49)	1.00	0	1
M6-3	Elevation	2.64 (1.96 – 3.29)	0.27	0	1
M8-1	Elevation	5.39 (4.74 – 6.06)	1.00	0	1
M8-2	Elevation	6.38 (5.71 – 7.05)	1.00	0	1
M8-3	Elevation	5.24 (4.58 – 5.89)	1.00	0	1
Overall	**Accretion**	**3.86 (3.57 – 4.13)**	**1.00**	**0**	**1**
Overall	**Elevation**	**3.44 (3.24 – 3.64)**	**1.00**	**0**	**1**

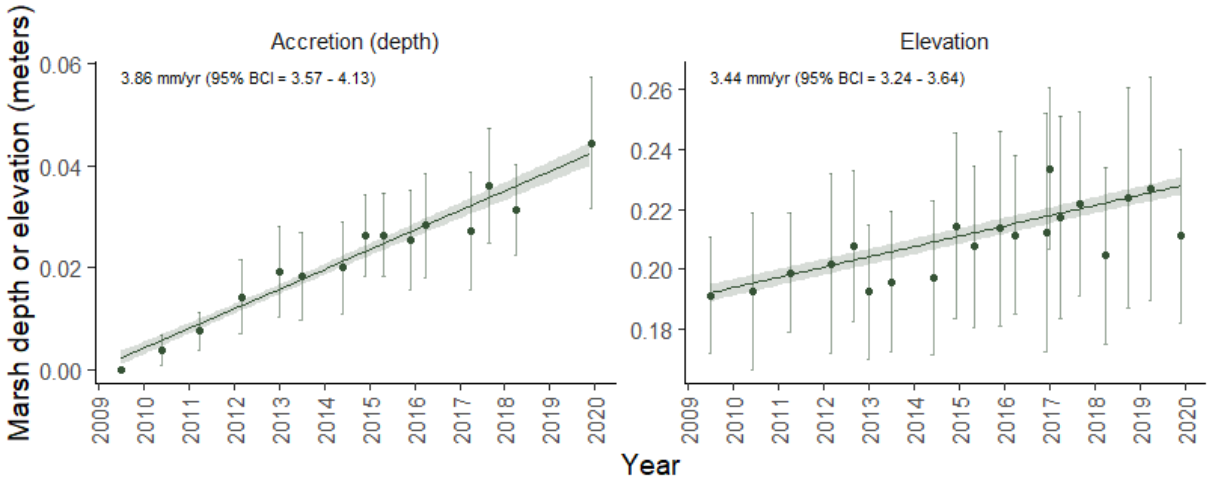


Figure A-21. Overall accretion and elevation trends for the non-exclosure stations at Assateague Island National Seashore. Solid line shows the mean of the posterior fitted trend; shaded region around the line bounds the 95% Bayesian credible interval of the fitted trend. These trend lines were computed using the mean of the intercept posteriors across SETs within the site and the mean of the slope posteriors across SETs within a site. Data are shown as means (points) plus and minus the standard deviation (error bars) across all observation locations within the site. Observations were grouped by month for aggregating.

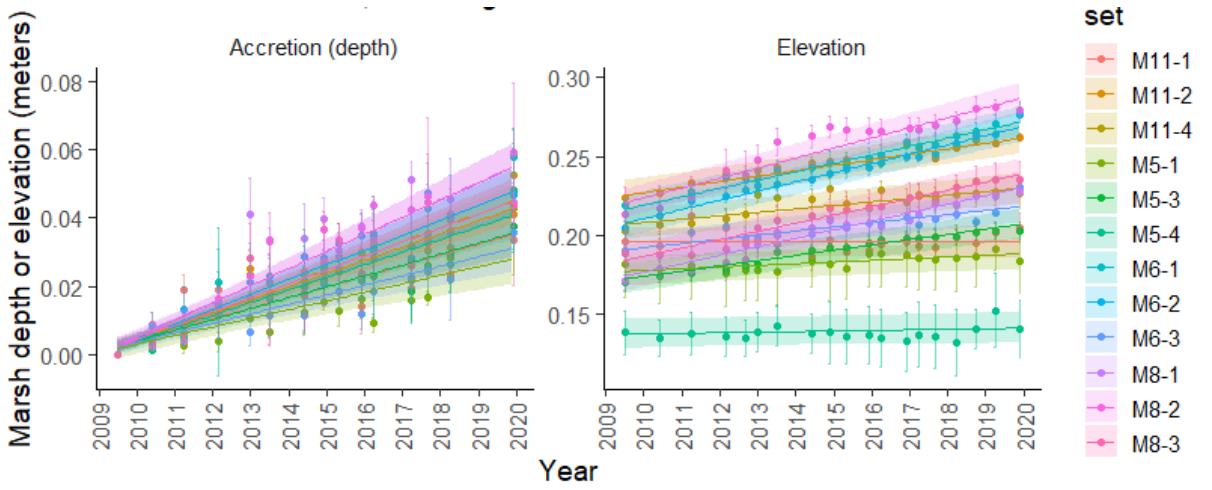


Figure A-22. Accretion and elevation trends at each station for the non-exclosure stations at Assateague Island National Seashore. Solid line shows the mean of the posterior fitted trend; shaded region around the line bounds the 95% Bayesian credible interval of the fitted trend. Data are shown as means (points) plus and minus the standard deviation (error bars) across all observation locations within the station. Observations were grouped by month for aggregating.

Boston Harbor Islands National Recreation Area

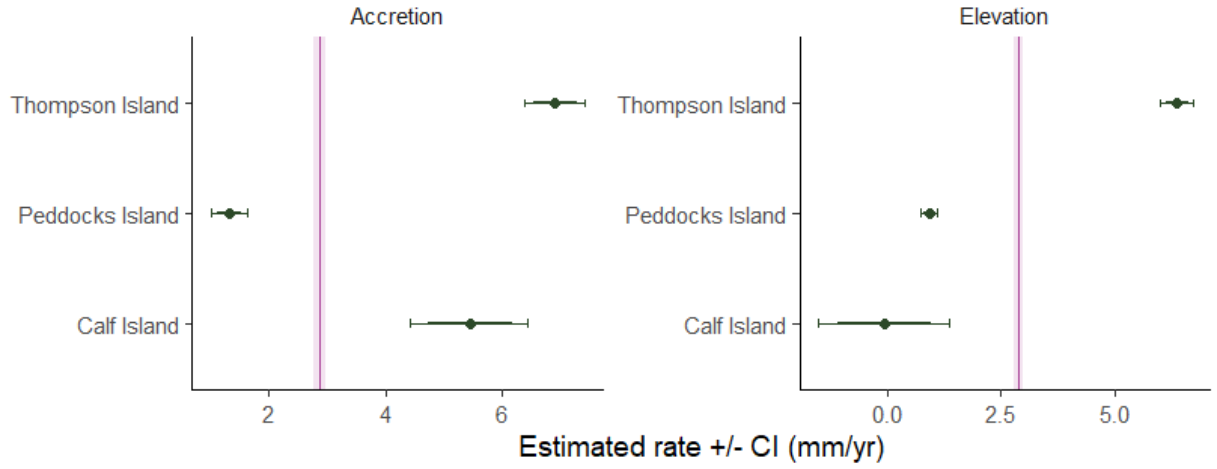


Figure A-23. Estimated accretion and elevation trends at the site level for Boston Harbor Islands National Recreation Area. The estimates are averages of the posteriors of the set-level trend estimates. The point shows the mean of the posterior; the thick error bars show the 85% Bayesian credible interval; the thin error bars show the 95% Bayesian credible interval. The vertical pink line shows the mean estimate of sea level rise and the pink rectangle bounds the 95% confidence interval.

Table A-14. Posterior trends (mean and 95% Bayesian credible interval) and the posterior probabilities that the trends in elevation or accretion are greater than 0 [Pr(trend > 0)], that the trend is greater than the upper bound of sea level rise [Pr(trend > slr)], and that the trend is less than the lower bound of sea level rise [Pr(trend < slr)] at each site in Boston Harbor Islands National Recreation Area. The final column [Pr(trend_i < trend_j)] is the probability that the trend specified in the row (either elevation or accretion) is less than the other estimated trend (either accretion or elevation) at the same site.

Site	Response	Trend estimate (mm/yr)	Pr(trend > 0)	Pr(trend > slr)	Pr(trend < slr)	Pr(trend_i < trend_j)
Calf Island	Accretion	5.44 (4.28 – 6.44)	1.00	1	0	0.00
Peddocks Island	Accretion	1.33 (1.02 – 1.62)	1.00	0	1	0.02
Thompson Island	Accretion	6.92 (6.39 – 7.45)	1.00	1	0	0.04
Calf Island	Elevation	-0.04 (-1.41 – 1.35)	0.48	0	1	1.00
Peddocks Island	Elevation	0.92 (0.73 – 1.11)	1.00	0	1	0.98
Thompson Island	Elevation	6.37 (6.01 – 6.71)	1.00	1	0	0.96

Calf Island

Table A-15. Estimated rates of elevation and accretion trends at Calf Island in Boston Harbor Islands National Recreation Area. Values in parentheses are the 95% Bayesian credible intervals. Pr(trend > 0) columns report the posterior probability that the estimated trend is greater than zero.

SET	Response	Trend estimate (mm/yr)	Pr(trend > 0)	Pr(trend > slr)	Pr(trend < slr)
Calf 1	Accretion	4.95 (3.14 – 6.74)	0.83	0.34	0.64
Calf 2	Accretion	4.87 (3.75 – 6.02)	0.83	0.32	0.66
Calf 3	Accretion	6.51 (4.66 – 7.99)	0.98	0.59	0.38
Calf 1	Elevation	-5.35 (-8.25 – -2.06)	0.01	0.00	1.00
Calf 2	Elevation	4.03 (1.51 – 6.32)	0.98	0.72	0.25
Calf 3	Elevation	1.19 (-1.17 – 3.3)	0.75	0.16	0.81
Overall	**Accretion**	**5.44 (4.28 – 6.44)**	**1.00**	**1.00**	**0.00**
Overall	**Elevation**	**-0.04 (-1.41 – 1.35)**	**0.48**	**0.00**	**1.00**

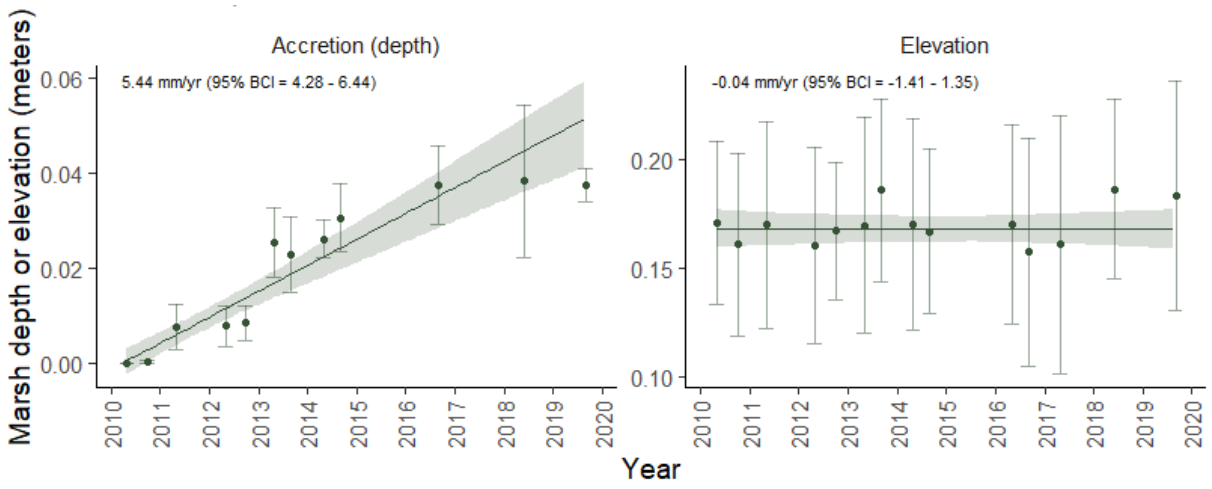


Figure A-24. Overall accretion and elevation trends for the Calf Island site at Boston Harbor Islands National Recreation Area. Solid line shows the mean of the posterior fitted trend; shaded region around the line bounds the 95% Bayesian credible interval of the fitted trend. These trend lines were computed using the mean of the intercept posteriors across SETs within the site and the mean of the slope posteriors across SETs within a site. Data are shown as means (points) plus and minus the standard deviation (error bars) across all observation locations within the site. Observations were grouped by month for aggregating.

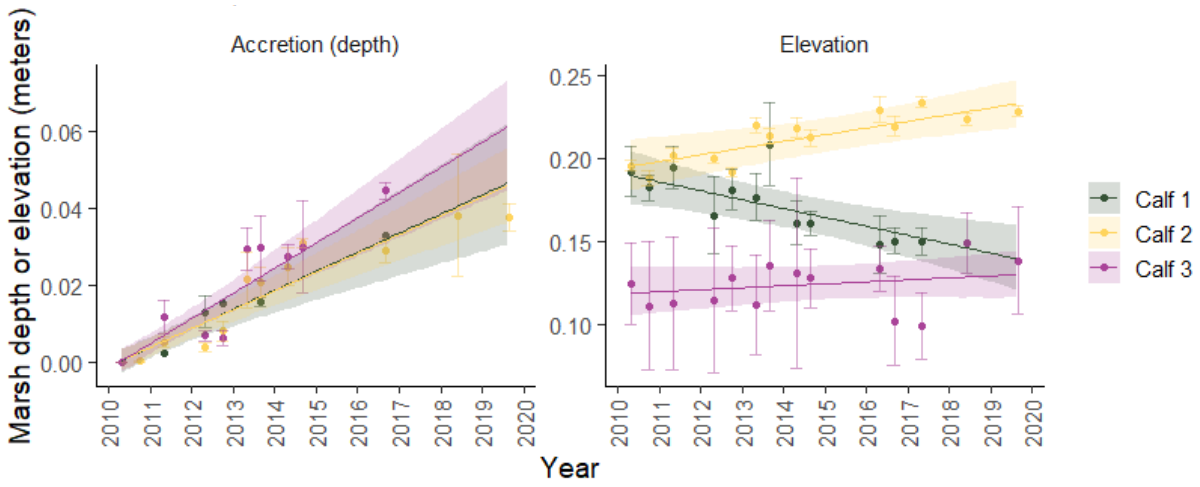


Figure A-25. Accretion and elevation trends at each station for the Calf Island site at Boston Harbor Islands National Recreation Area. Solid line shows the mean of the posterior fitted trend; shaded region around the line bounds the 95% Bayesian credible interval of the fitted trend. Data are shown as means (points) plus and minus the standard deviation (error bars) across all observation locations within the station. Observations were grouped by month for aggregating.

Peddocks Island

Table A-16. Estimated rates of elevation and accretion trends at Peddocks Island in Boston Harbor Islands National Recreation Area. Values in parentheses are the 95% Bayesian credible intervals. Pr(trend > 0) columns report the posterior probability that the estimated trend is greater than zero.

SET	Response	Trend estimate (mm/yr)	Pr(trend > 0)	Pr(trend > slr)	Pr(trend < slr)
Peddocks 1	Accretion	1.61 (1.09 – 2.12)	0.87	0.00	1.00
Peddocks 2	Accretion	1.38 (0.96 – 1.83)	0.66	0.00	1.00
Peddocks 3	Accretion	1 (0.49 – 1.52)	0.23	0.00	1.00
Peddocks 1	Elevation	1.22 (0.86 – 1.53)	0.75	0.01	0.99
Peddocks 2	Elevation	1.75 (1.41 – 2.04)	0.92	0.01	0.98
Peddocks 3	Elevation	-0.2 (-0.5 – 0.16)	0.08	0.00	1.00
Overall	**Accretion**	**1.33 (1.02 – 1.62)**	**1.00**	**0.00**	**1.00**
Overall	**Elevation**	**0.92 (0.73 – 1.11)**	**1.00**	**0.00**	**1.00**

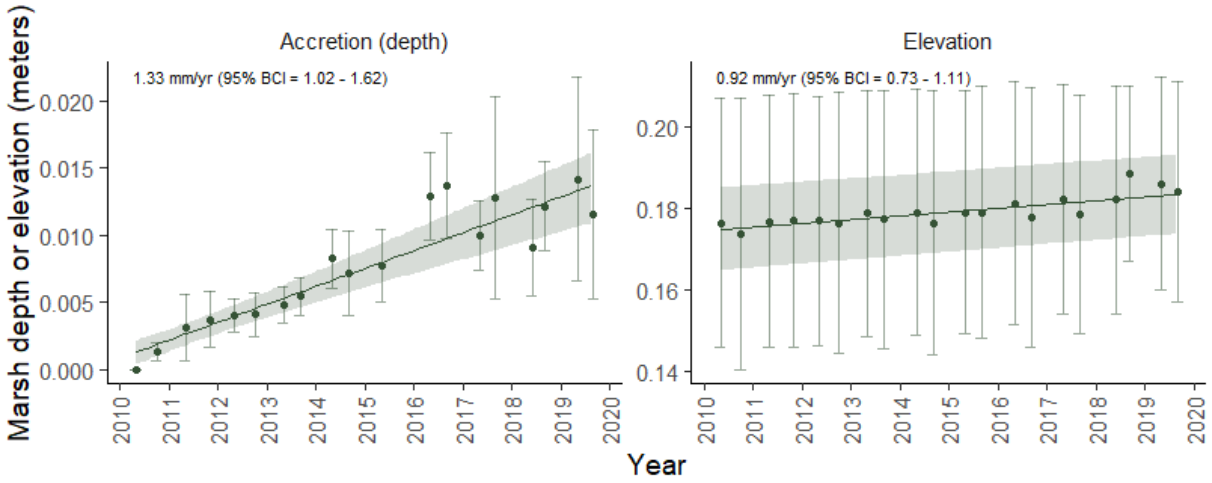


Figure A-26. Overall accretion and elevation trends for the Peddocks Island site at Boston Harbor Islands National Recreation Area. Solid line shows the mean of the posterior fitted trend; shaded region around the line bounds the 95% Bayesian credible interval of the fitted trend. These trend lines were computed using the mean of the intercept posteriors across SETs within the site and the mean of the slope posteriors across SETs within a site. Data are shown as means (points) plus and minus the standard deviation (error bars) across all observation locations within the site. Observations were grouped by month for aggregating.

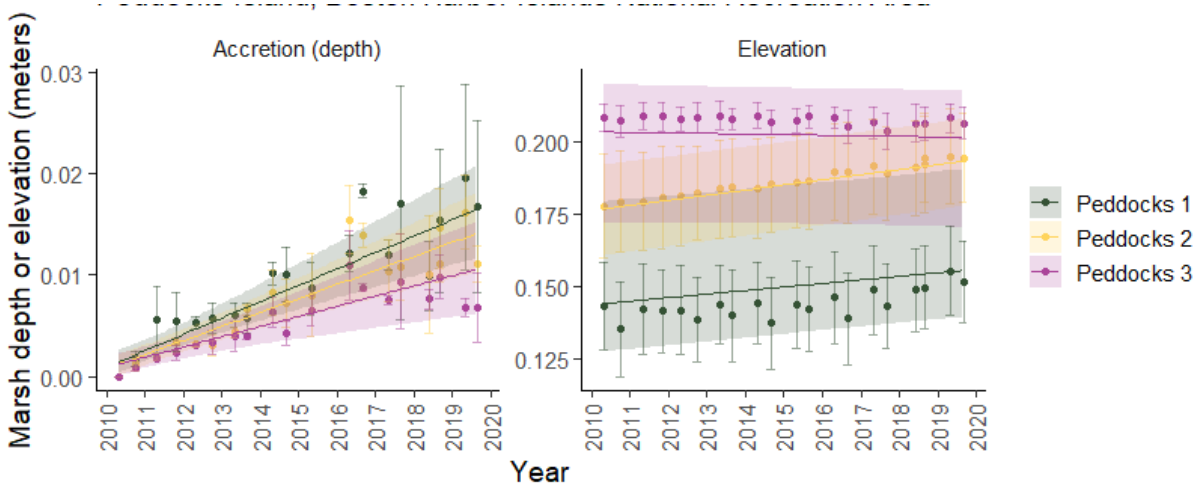


Figure A-27. Accretion and elevation trends at each station for the Peddocks Island site at Boston Harbor Islands National Recreation Area. Solid line shows the mean of the posterior fitted trend; shaded region around the line bounds the 95% Bayesian credible interval of the fitted trend. Data are shown as means (points) plus and minus the standard deviation (error bars) across all observation locations within the station. Observations were grouped by month for aggregating.

Thompson Island

Table A-17. Estimated rates of elevation and accretion trends at Thompson Island in Boston Harbor Islands National Recreation Area. Values in parentheses are the 95% Bayesian credible intervals. Pr(trend > 0) columns report the posterior probability that the estimated trend is greater than zero.

SET	Response	Trend estimate (mm/yr)	Pr(trend > 0)	Pr(trend > slr)	Pr(trend < slr)
Thompson 1	Accretion	5.93 (5.12 – 6.67)	0.99	0.78	0.18
Thompson 2	Accretion	7.11 (6.39 – 7.83)	1.00	0.92	0.07
Thompson 3	Accretion	5.77 (5.15 – 6.42)	0.99	0.76	0.21
Thompson 4	Accretion	8.88 (7.53 – 10.2)	1.00	0.99	0.01
Thompson 1	Elevation	4.4 (3.67 – 5.15)	0.34	0.05	0.94
Thompson 2	Elevation	6.47 (5.79 – 7.21)	0.92	0.21	0.77
Thompson 3	Elevation	6.69 (6 – 7.36)	0.96	0.23	0.74
Thompson 4	Elevation	7.92 (7.17 – 8.57)	1.00	0.47	0.48
Overall	**Accretion**	**6.92 (6.39 – 7.45)**	**1.00**	**1.00**	**0.00**
Overall	**Elevation**	**6.37 (6.01 – 6.71)**	**1.00**	**1.00**	**0.00**

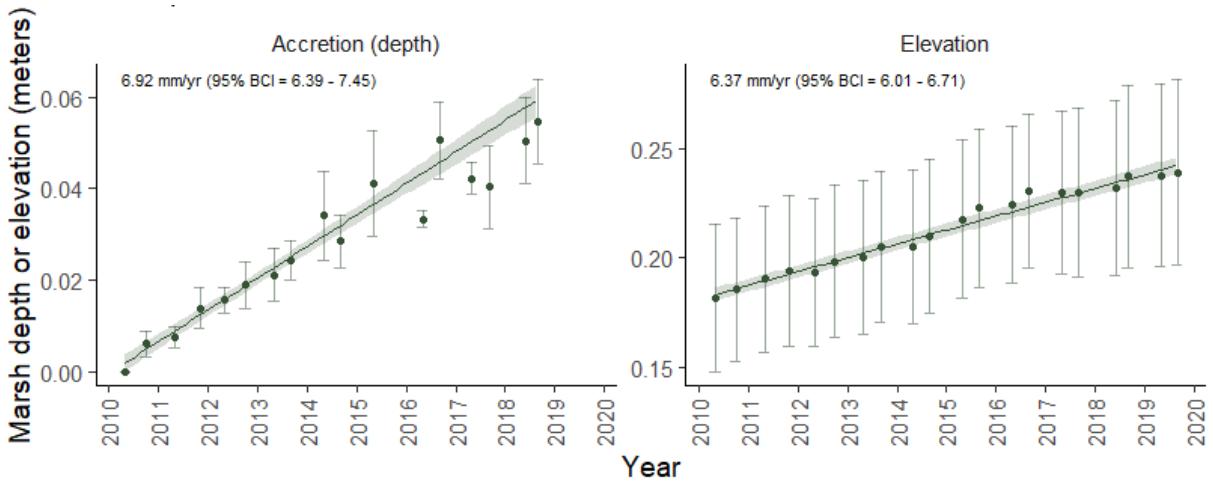


Figure A-28. Overall accretion and elevation trends for the Thompson Island site at Boston Harbor Islands National Recreation Area. Solid line shows the mean of the posterior fitted trend; shaded region around the line bounds the 95% Bayesian credible interval of the fitted trend. These trend lines were computed using the mean of the intercept posteriors across SETs within the site and the mean of the slope posteriors across SETs within a site. Data are shown as means (points) plus and minus the standard deviation (error bars) across all observation locations within the site. Observations were grouped by month for aggregating.

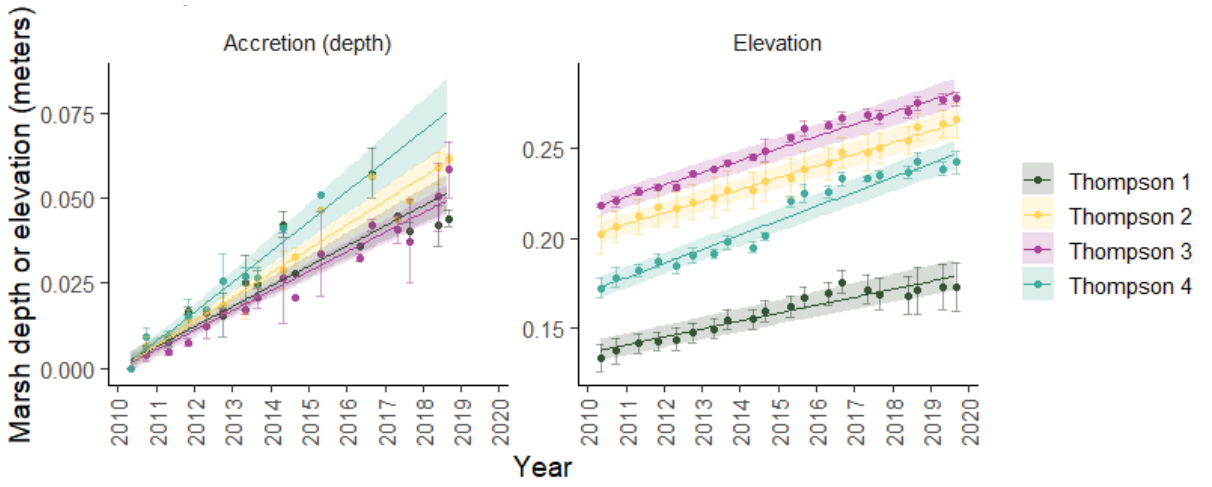


Figure A-29. Accretion and elevation trends at each station for the Thompson Island site at Boston Harbor Islands National Recreation Area. Solid line shows the mean of the posterior fitted trend; shaded region around the line bounds the 95% Bayesian credible interval of the fitted trend. Data are shown as means (points) plus and minus the standard deviation (error bars) across all observation locations within the station. Observations were grouped by month for aggregating.

Cape Cod National Seashore

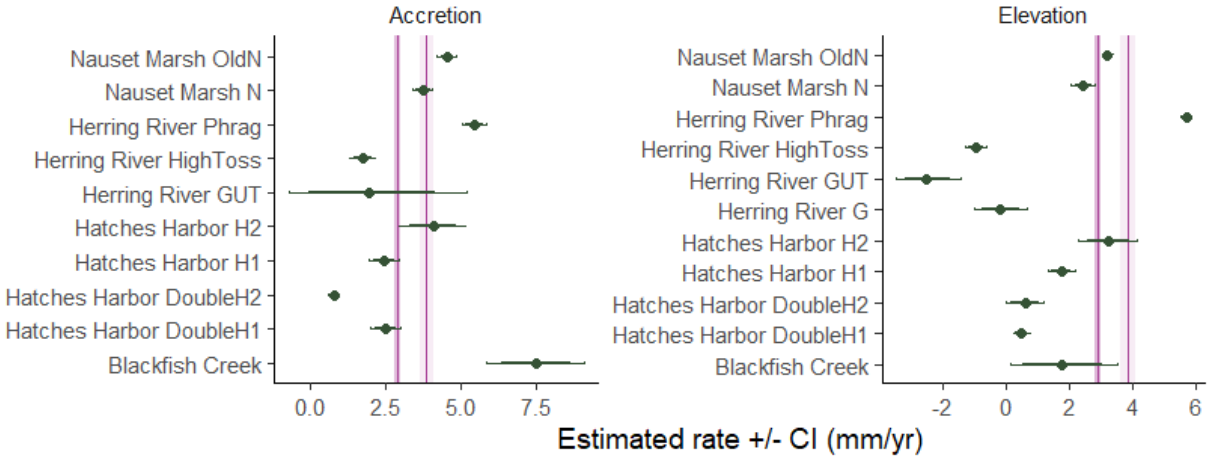


Figure A-30. Estimated accretion and elevation trends at the site level for Cape Cod National Seashore. The estimates are averages of the posteriors of the set-level trend estimates. The point shows the mean of the posterior; the thick error bars show the 85% Bayesian credible interval; the thin error bars show the 95% Bayesian credible interval. The vertical pink line shows the mean estimate of sea level rise and the pink rectangle bounds the 95% confidence interval. There are two estimates for sea level rise because the Nauset sites reference a different NOAA station than the other sites; the higher estimate is for the Nauset sites.

Table A-18. Posterior trends (mean and 95% Bayesian credible interval) and the posterior probabilities that the trends in elevation or accretion are greater than 0 [Pr(trend > 0)], that the trend is greater than the upper bound of sea level rise [Pr(trend > slr)], and that the trend is less than the lower bound of sea level rise [Pr(trend < slr)] at each site in Cape Cod National Seashore. The final column [Pr(trend_i < trend_j)] is the probability that the trend specified in the row (either elevation or accretion) is less than the other estimated trend (either accretion or elevation) at the same site.

Site	Response	Trend estimate (mm/yr)	Pr(trend > 0)	Pr(trend > slr)	Pr(trend < slr)	Pr(trend_i < trend_j)
Blackfish Creek	Accretion	7.47 (5.83 – 9.08)	1.00	1.00	0.00	0.00
Hatches Harbor HH1-6	Accretion	2.48 (1.97 – 2.96)	1.00	0.02	0.89	0.00
Hatches Harbor HH7-9	Accretion	0.78 (0.6 – 0.95)	1.00	0.00	1.00	0.29
Hatches Harbor H1-3	Accretion	2.43 (1.94 – 2.94)	1.00	0.02	0.92	0.02
Hatches Harbor H4-6	Accretion	4.08 (2.95 – 5.13)	1.00	0.97	0.01	0.12
Herring River GUT	Accretion	1.93 (-0.71 – 5.18)	0.92	0.21	0.76	0.00
Herring River High Toss	Accretion	1.76 (1.29 – 2.15)	1.00	0.00	1.00	0.00
Herring River Phrag	Accretion	5.41 (5.01 – 5.82)	1.00	1.00	0.00	0.90
Nauset Marsh N1-N3	Accretion	3.72 (3.37 – 4.06)	1.00	0.02	0.28	0.00
Nauset Marsh OldSET	Accretion	4.53 (4.2 – 4.84)	1.00	0.99	0.00	0.00
Blackfish Creek	Elevation	1.76 (0.13 – 3.49)	0.98	0.09	0.88	1.00
Hatches Harbor HH1-6	Elevation	0.49 (0.22 – 0.75)	1.00	0.00	1.00	1.00
Hatches Harbor HH7-9	Elevation	0.6 (-0.01 – 1.2)	0.97	0.00	1.00	0.71
Hatches Harbor H1-3	Elevation	1.75 (1.3 – 2.18)	1.00	0.00	1.00	0.98
Hatches Harbor H4-6	Elevation	3.23 (2.27 – 4.14)	1.00	0.72	0.15	0.88
Herring River G1-G3	Elevation	-0.17 (-1 – 0.68)	0.33	0.00	1.00	NA
Herring River OldSET	Elevation	-2.5 (-3.46 – -1.43)	0.00	0.00	1.00	1.00
Herring River High Toss	Elevation	-0.96 (-1.3 – -0.62)	0.00	0.00	1.00	1.00
Herring River Phrag	Elevation	5.69 (5.52 – 5.86)	1.00	1.00	0.00	0.10
Nauset Marsh N1-N3	Elevation	2.43 (2.05 – 2.82)	1.00	0.00	1.00	1.00
Nauset Marsh OldSET	Elevation	3.2 (3.03 – 3.37)	1.00	0.00	1.00	1.00

Blackfish Creek

Table A-19. Estimated rates of elevation and accretion trends at Blackfish Creek in Cape Cod National Seashore. Values in parentheses are the 95% Bayesian credible intervals. Pr(trend > 0) columns report the posterior probability that the estimated trend is greater than zero.

SET	Response	Trend estimate (mm/yr)	Pr(trend > 0)	Pr(trend > slr)	Pr(trend < slr)
BF1	Accretion	4.54 (2.07 – 6.94)	0.83	0.35	0.62
BF2	Accretion	15.11 (12.48 – 17.5)	1.00	1.00	0.00
BF3	Accretion	3.58 (-0.37 – 7.58)	0.67	0.25	0.73
BF4	Accretion	8.42 (6.12 – 10.73)	1.00	0.92	0.07
BF5	Accretion	1.42 (-2.35 – 5.26)	0.35	0.07	0.92
BF6	Accretion	11.75 (8.98 – 14.5)	1.00	1.00	0.00
BF1	Elevation	1.68 (-0.52 – 3.71)	0.53	0.01	0.99
BF2	Elevation	1.78 (-0.27 – 3.93)	0.56	0.01	0.98
BF3	Elevation	1.45 (-1.14 – 3.47)	0.44	0.00	1.00
BF4	Elevation	2.07 (0.11 – 4.73)	0.65	0.04	0.95
BF5	Elevation	1.64 (-0.49 – 3.72)	0.51	0.01	0.99
BF6	Elevation	1.93 (-0.08 – 4.28)	0.59	0.02	0.97
Overall	**Accretion**	**7.47 (5.83 – 9.08)**	**1.00**	**1.00**	**0.00**
Overall	**Elevation**	**1.76 (0.13 – 3.49)**	**0.98**	**0.09**	**0.88**

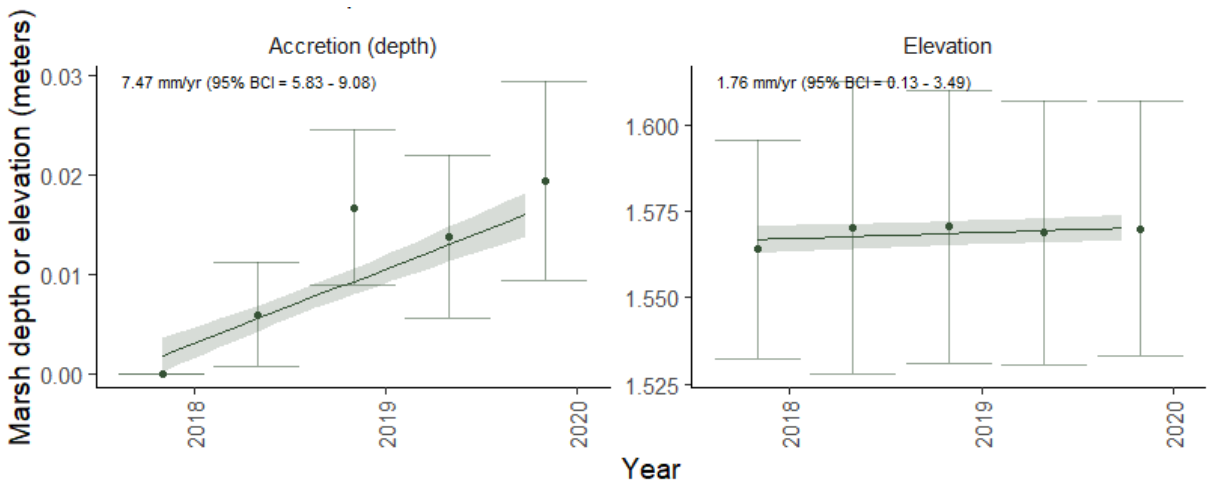


Figure A-31. Overall accretion and elevation trends for the Blackfish Creek site at Cape Cod National Seashore. Solid line shows the mean of the posterior fitted trend; shaded region around the line bounds the 95% Bayesian credible interval of the fitted trend. These trend lines were computed using the mean of the intercept posteriors across SETs within the site and the mean of the slope posteriors across SETs within a site. Data are shown as means (points) plus and minus the standard deviation (error bars) across all observation locations within the site. Observations were grouped by month for aggregating.

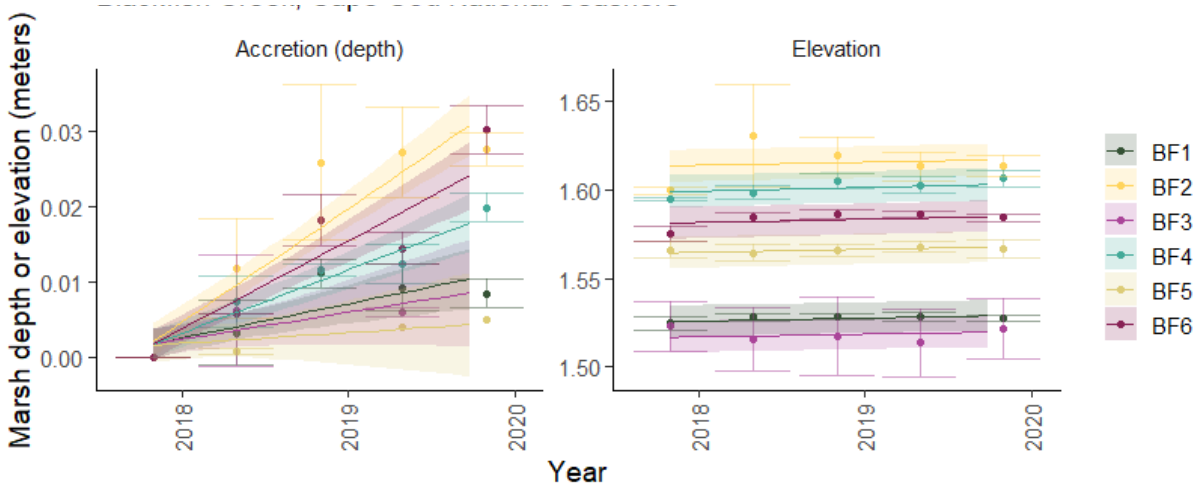


Figure A-32. Accretion and elevation trends at each station for the Blackfish Creek site at Cape Cod National Seashore. Solid line shows the mean of the posterior fitted trend; shaded region around the line bounds the 95% Bayesian credible interval of the fitted trend. Data are shown as means (points) plus and minus the standard deviation (error bars) across all observation locations within the station. Observations were grouped by month for aggregating.

Hatches Harbor: HH1 (Behind Dike)

Table A-20. Estimated rates of elevation and accretion trends at Hatches Harbor HH1 in Cape Cod National Seashore. Values in parentheses are the 95% Bayesian credible intervals. Pr(trend > 0) columns report the posterior probability that the estimated trend is greater than zero.

SET	Response	Trend estimate (mm/yr)	Pr(trend > 0)	Pr(trend > slr)	Pr(trend < slr)
HH1	Accretion	2.86 (1.87 – 3.84)	0.91	0.03	0.97
HH2	Accretion	3.99 (2.54 – 5.1)	0.99	0.20	0.75
HH3	Accretion	1.59 (0.57 – 2.67)	0.30	0.00	1.00
HH4	Accretion	2.07 (1.14 – 2.98)	0.56	0.01	0.99
HH5	Accretion	2.45 (1.57 – 3.33)	0.79	0.01	0.98
HH6	Accretion	1.92 (0.59 – 3.09)	0.48	0.00	1.00
HH1	Elevation	1.65 (0.98 – 2.3)	0.97	0.02	0.97
HH2	Elevation	3.16 (2.48 – 3.83)	1.00	0.39	0.50
HH3	Elevation	-0.09 (-0.75 – 0.58)	0.26	0.00	1.00
HH4	Elevation	-0.54 (-1.19 – 0.12)	0.12	0.00	1.00
HH5	Elevation	0.2 (-0.44 – 0.85)	0.41	0.00	1.00
HH6	Elevation	-1.46 (-2.11 – -0.79)	0.01	0.00	1.00
Overall	**Accretion**	**2.48 (1.97 – 2.96)**	**1.00**	**0.02**	**0.89**
Overall	**Elevation**	**0.49 (0.22 – 0.75)**	**1.00**	**0.00**	**1.00**

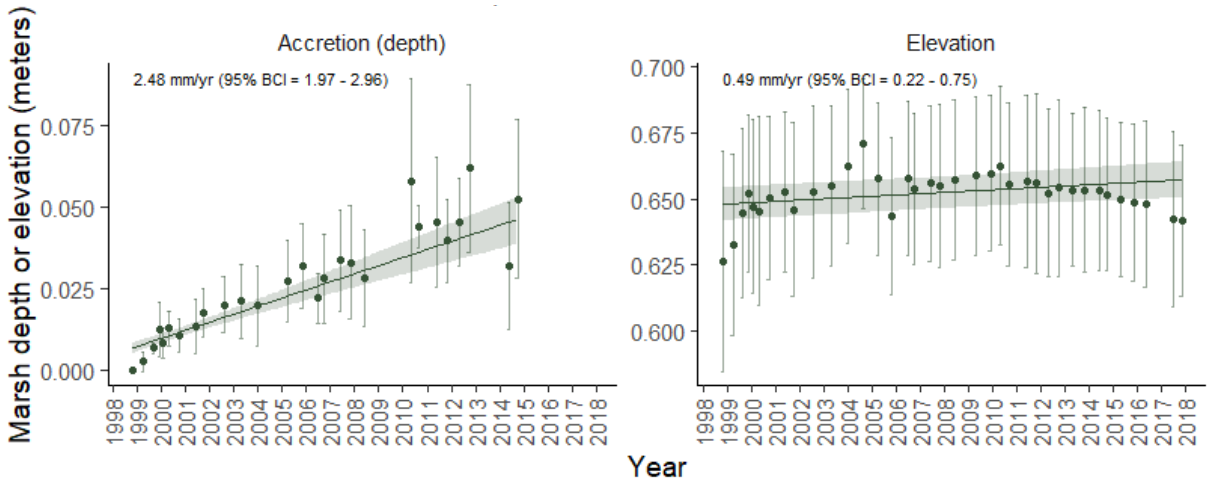


Figure A-33. Overall accretion and elevation trends for the Hatches Harbor HH1 site at Cape Cod National Seashore. Solid line shows the mean of the posterior fitted trend; shaded region around the line bounds the 95% Bayesian credible interval of the fitted trend. These trend lines were computed using the mean of the intercept posteriors across SETs within the site and the mean of the slope posteriors across SETs within a site. Data are shown as means (points) plus and minus the standard deviation (error bars) across all observation locations within the site. Observations were grouped by month for aggregating.

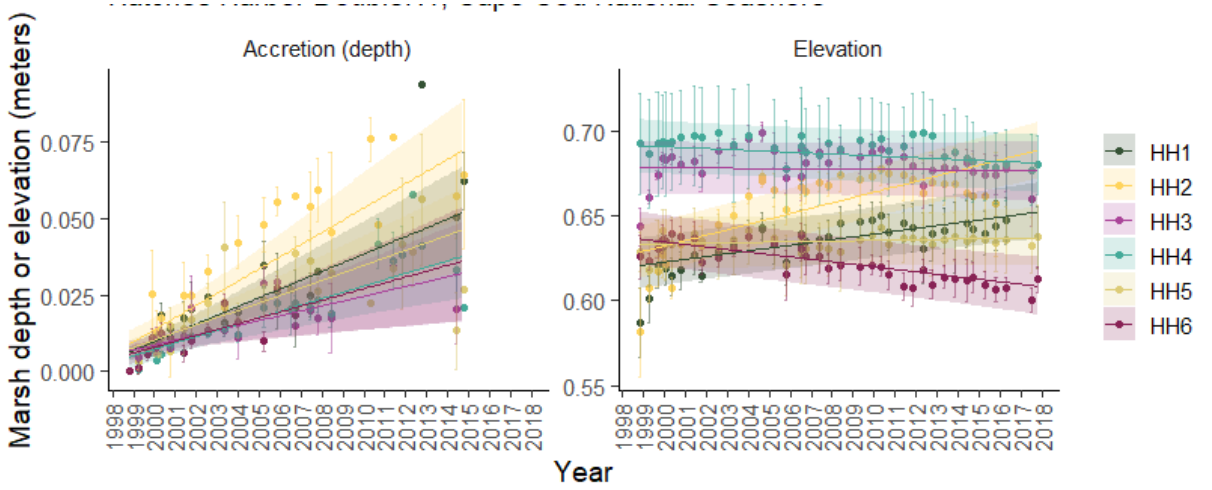


Figure A-34. Accretion and elevation trends at each station for the Hatches Harbor HH1-HH6 (Behind Dike) site at Cape Cod National Seashore. Solid line shows the mean of the posterior fitted trend; shaded region around the line bounds the 95% Bayesian credible interval of the fitted trend. Data are shown as means (points) plus and minus the standard deviation (error bars) across all observation locations within the station. Observations were grouped by month for aggregating.

Hatches Harbor: HH2(Outside Dike)

Table A-21. Estimated rates of elevation and accretion trends at Hatches Harbor HH2 in Cape Cod National Seashore. Values in parentheses are the 95% Bayesian credible intervals. Pr(trend > 0) columns report the posterior probability that the estimated trend is greater than zero.

SET	Response	Trend estimate (mm/yr)	Pr(trend > 0)	Pr(trend > slr)	Pr(trend < slr)
HH7	Accretion	0.81 (0.6 – 1.02)	0.68	0.00	1.00
HH8	Accretion	0.72 (0.41 – 0.97)	0.42	0.00	1.00
HH9	Accretion	0.8 (0.6 – 1)	0.62	0.00	1.00
HH7	Elevation	-0.67 (-1.38 – 0.2)	0.12	0.00	1.00
HH8	Elevation	2.06 (0.48 – 3.53)	0.97	0.14	0.83
HH9	Elevation	0.41 (-0.36 – 1.19)	0.56	0.01	0.99
Overall	**Accretion**	**0.78 (0.6 – 0.95)**	**1.00**	**0.00**	**1.00**
Overall	**Elevation**	**0.6 (-0.01 – 1.2)**	**0.97**	**0.00**	**1.00**

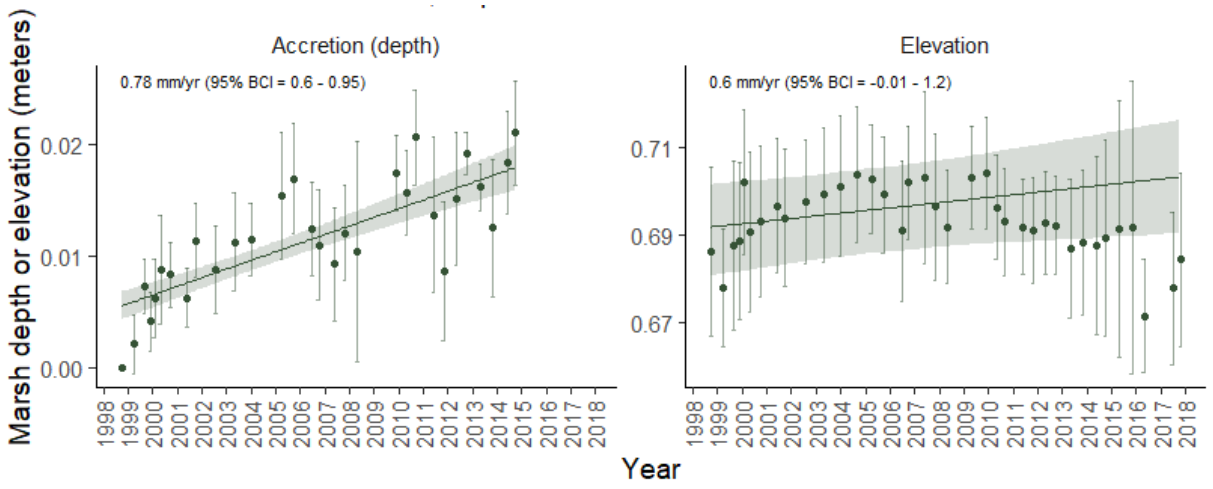


Figure A-35. Overall accretion and elevation trends for the Hatches Harbor HH2 site at Cape Cod National Seashore. Solid line shows the mean of the posterior fitted trend; shaded region around the line bounds the 95% Bayesian credible interval of the fitted trend. These trend lines were computed using the mean of the intercept posteriors across SETs within the site and the mean of the slope posteriors across SETs within a site. Data are shown as means (points) plus and minus the standard deviation (error bars) across all observation locations within the site. Observations were grouped by month for aggregating.

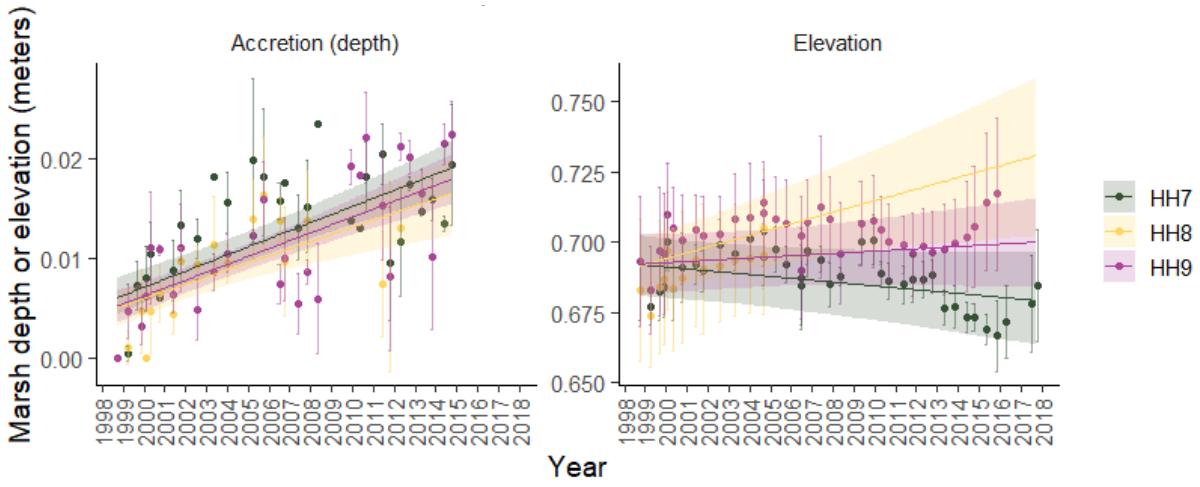


Figure A-36. Accretion and elevation trends at each station for the Hatches Harbor HH2 site at Cape Cod National Seashore. Solid line shows the mean of the posterior fitted trend; shaded region around the line bounds the 95% Bayesian credible interval of the fitted trend. Data are shown as means (points) plus and minus the standard deviation (error bars) across all observation locations within the station. Observations were grouped by month for aggregating.

Hatches Harbor H1(Outside Dike)

Table A-22. Estimated rates of elevation and accretion trends at Hatches Harbor H1 in Cape Cod National Seashore. Values in parentheses are the 95% Bayesian credible intervals. Pr(trend > 0) columns report the posterior probability that the estimated trend is greater than zero.

SET	Response	Trend estimate (mm/yr)	Pr(trend > 0)	Pr(trend > slr)	Pr(trend < slr)
H1	Accretion	2.59 (1.98 – 3.17)	0.77	0.00	1.00
H2	Accretion	2.45 (1.81 – 3.12)	0.60	0.00	1.00
H3	Accretion	2.25 (1.61 – 2.85)	0.32	0.00	1.00
H1	Elevation	0.88 (0.09 – 1.91)	0.21	0.00	1.00
H2	Elevation	2.25 (1.45 – 2.96)	0.86	0.02	0.97
H3	Elevation	2.11 (1.38 – 2.85)	0.81	0.02	0.98
Overall	**Accretion**	**2.43 (1.94 – 2.94)**	**1.00**	**0.02**	**0.92**
Overall	**Elevation**	**1.75 (1.3 – 2.18)**	**1.00**	**0.00**	**1.00**

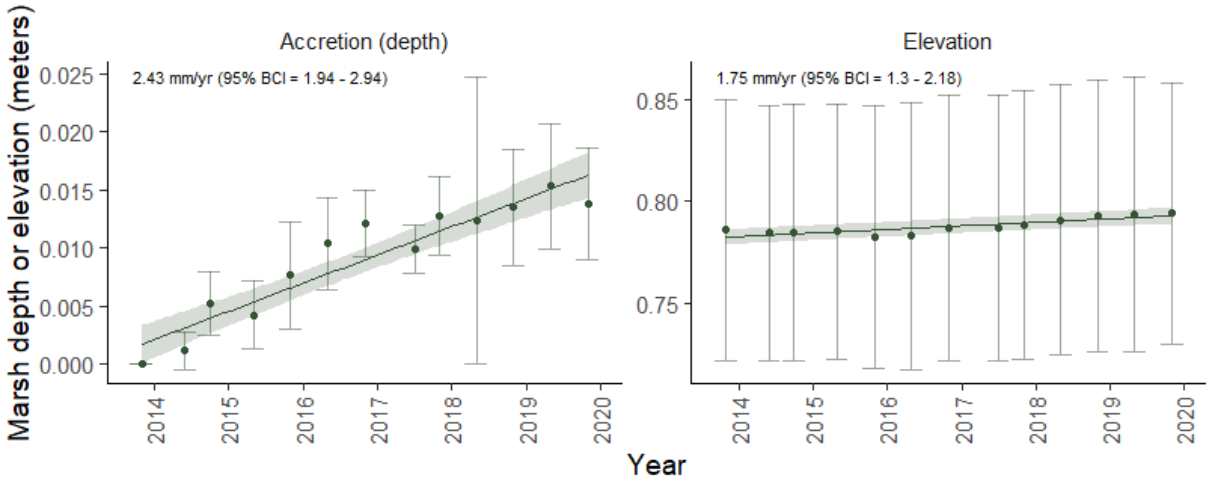


Figure A-37. Overall accretion and elevation trends for the Hatches Harbor H1 site at Cape Cod National Seashore. Solid line shows the mean of the posterior fitted trend; shaded region around the line bounds the 95% Bayesian credible interval of the fitted trend. These trend lines were computed using the mean of the intercept posteriors across SETs within the site and the mean of the slope posteriors across SETs within a site. Data are shown as means (points) plus and minus the standard deviation (error bars) across all observation locations within the site. Observations were grouped by month for aggregating.

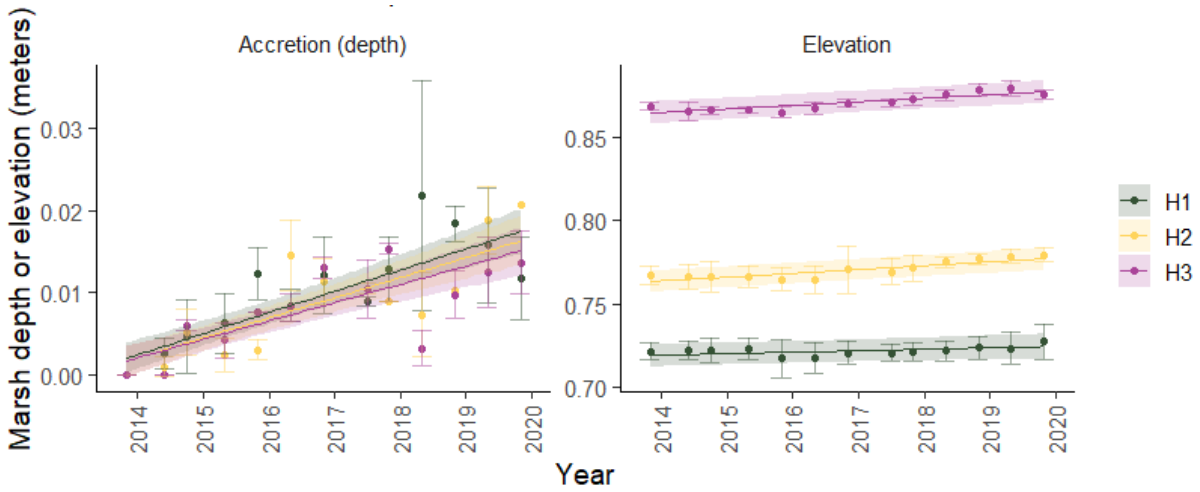


Figure A-38. Accretion and elevation trends at each station for the Hatches Harbor H1 site at Cape Cod National Seashore. Solid line shows the mean of the posterior fitted trend; shaded region around the line bounds the 95% Bayesian credible interval of the fitted trend. Data are shown as means (points) plus and minus the standard deviation (error bars) across all observation locations within the station. Observations were grouped by month for aggregating.

Hatches Harbor H2 (Behind Dike)

Table A-23. Estimated rates of elevation and accretion trends at Hatches Harbor H2 in Cape Cod National Seashore. Values in parentheses are the 95% Bayesian credible intervals. Pr(trend > 0) columns report the posterior probability that the estimated trend is greater than zero.

SET	Response	Trend estimate (mm/yr)	Pr(trend > 0)	Pr(trend > slr)	Pr(trend < slr)
H4	Accretion	4.19 (2.95 – 5.54)	0.68	0.02	0.98
H5	Accretion	4.02 (2.58 – 5.22)	0.56	0.01	0.99
H6	Accretion	4.04 (2.76 – 5.21)	0.57	0.01	0.99
H4	Elevation	4.14 (2.44 – 5.88)	0.89	0.17	0.81
H5	Elevation	2.54 (1 – 3.93)	0.43	0.02	0.98
H6	Elevation	3.02 (1.7 – 4.26)	0.61	0.04	0.95
Overall	**Accretion**	**4.08 (2.95 – 5.13)**	**1.00**	**0.97**	**0.01**
Overall	**Elevation**	**3.23 (2.27 – 4.14)**	**1.00**	**0.72**	**0.15**

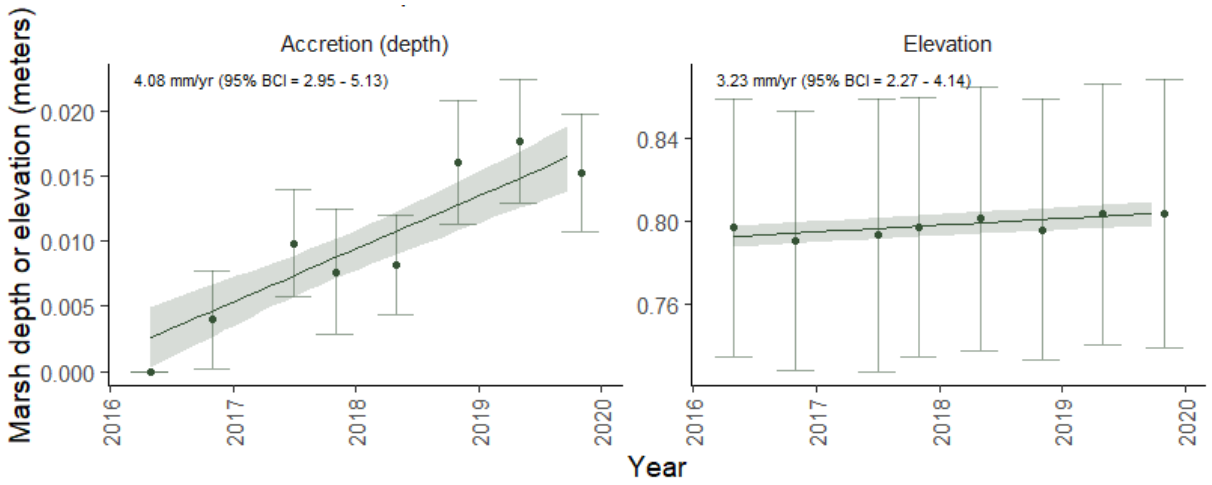


Figure A-39. Overall accretion and elevation trends for the Hatches Harbor H2 site at Cape Cod National Seashore. Solid line shows the mean of the posterior fitted trend; shaded region around the line bounds the 95% Bayesian credible interval of the fitted trend. These trend lines were computed using the mean of the intercept posteriors across SETs within the site and the mean of the slope posteriors across SETs within a site. Data are shown as means (points) plus and minus the standard deviation (error bars) across all observation locations within the site. Observations were grouped by month for aggregating.

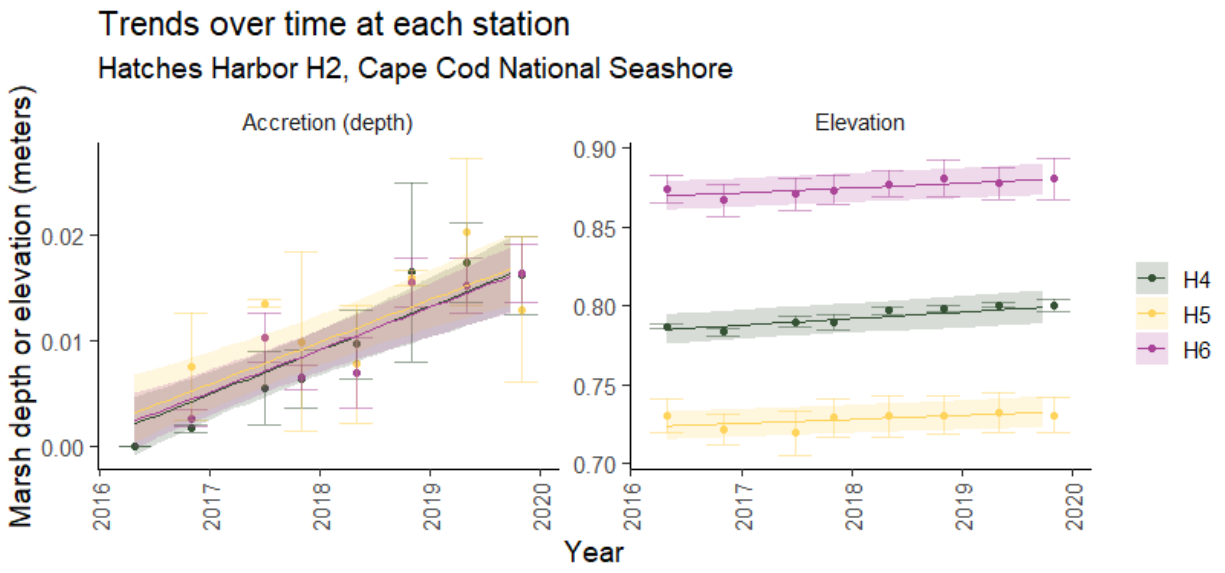


Figure A-40. Accretion and elevation trends at each station for the Hatches Harbor H2 site at Cape Cod National Seashore. Solid line shows the mean of the posterior fitted trend; shaded region around the line bounds the 95% Bayesian credible interval of the fitted trend. Data are shown as means (points) plus and minus the standard deviation (error bars) across all observation locations within the station. Observations were grouped by month for aggregating.

Herring River G (Outside Dike)

Table A-24. Estimated rates of elevation and accretion trends at Herring River G in Cape Cod National Seashore. Values in parentheses are the 95% Bayesian credible intervals. Pr(trend > 0) columns report the posterior probability that the estimated trend is greater than zero.

SET	Response	Trend estimate (mm/yr)	Pr(trend > 0)	Pr(trend > slr)	Pr(trend < slr)
G1	Elevation	-0.94 (-2.27 – 0.51)	0.25	0.01	0.99
G2	Elevation	-1.77 (-3.15 – -0.16)	0.10	0.00	1.00
G3	Elevation	2.2 (0.11 – 3.68)	0.95	0.31	0.65
Overall	**Elevation**	**-0.17 (-1 – 0.68)**	**0.33**	**0.00**	**1.00**

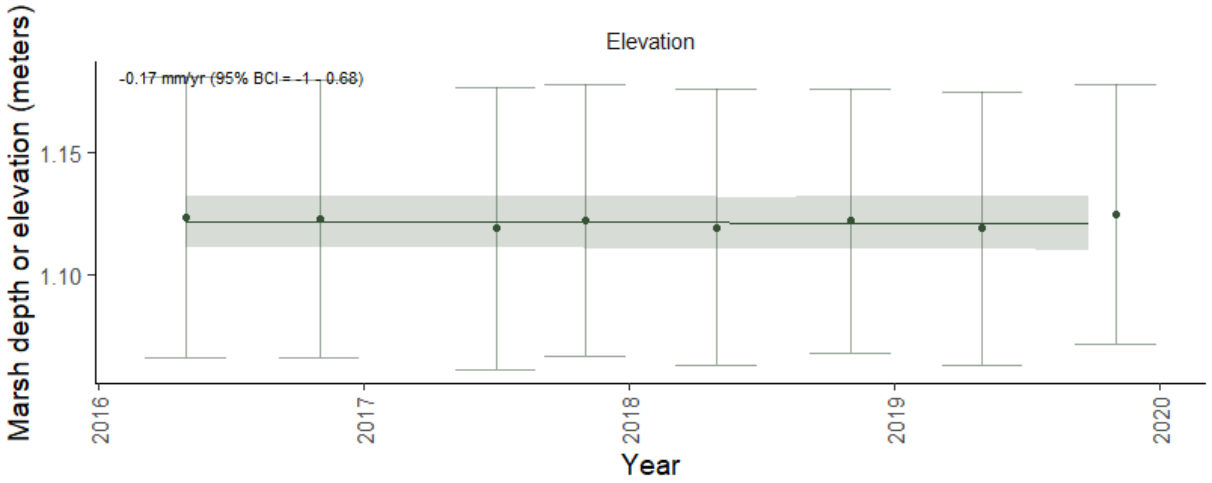


Figure A-41. Overall accretion and elevation trends for the Herring River G site at Cape Cod National Seashore. Solid line shows the mean of the posterior fitted trend; shaded region around the line bounds the 95% Bayesian credible interval of the fitted trend. These trend lines were computed using the mean of the intercept posteriors across SETs within the site and the mean of the slope posteriors across SETs within a site. Data are shown as means (points) plus and minus the standard deviation (error bars) across all observation locations within the site. Observations were grouped by month for aggregating.

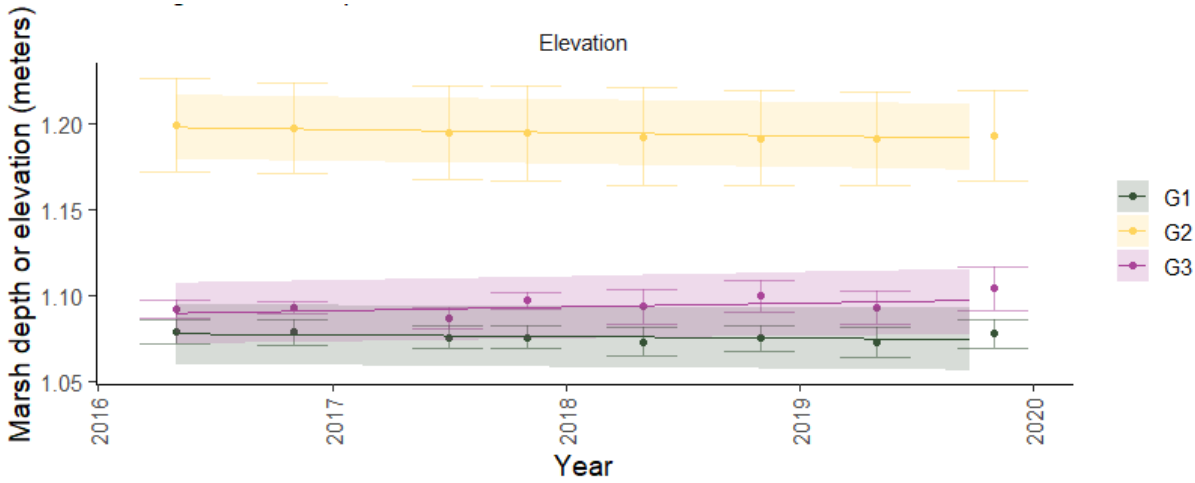


Figure A-42. Accretion and elevation trends at each station for the Herring River G site at Cape Cod National Seashore. Solid line shows the mean of the posterior fitted trend; shaded region around the line bounds the 95% Bayesian credible interval of the fitted trend. Data are shown as means (points) plus and minus the standard deviation (error bars) across all observation locations within the station. Observations were grouped by month for aggregating.

Herring River GUT (Outside Dike)

Table A-25. Estimated rates of elevation and accretion trends at Herring River GUT in Cape Cod National Seashore. Values in parentheses are the 95% Bayesian credible intervals. Pr(trend > 0) columns report the posterior probability that the estimated trend is greater than zero.

SET	Response	Trend estimate (mm/yr)	Pr(trend > 0)	Pr(trend > slr)	Pr(trend < slr)
GUT1	Accretion	2.17 (-0.9 – 7.31)	0.63	0.07	0.92
GUT2	Accretion	1.54 (-0.99 – 4.12)	0.47	0.01	0.99
GUT3	Accretion	2.07 (-1 – 6.48)	0.61	0.06	0.94
GUT1	Elevation	-5.01 (-6.67 – -2.53)	0.02	0.00	1.00
GUT2	Elevation	-2.54 (-4.18 – -0.95)	0.22	0.00	1.00
GUT3	Elevation	0.05 (-2.13 – 1.73)	0.82	0.16	0.81
Overall	**Accretion**	**1.93 (-0.71 –-5.18)**	**0.92**	**0.21**	**0.76**
Overall	**Elevation**	**-2.5 (-3.46 – -1.43)**	**0.00**	**0.00**	**1.00**

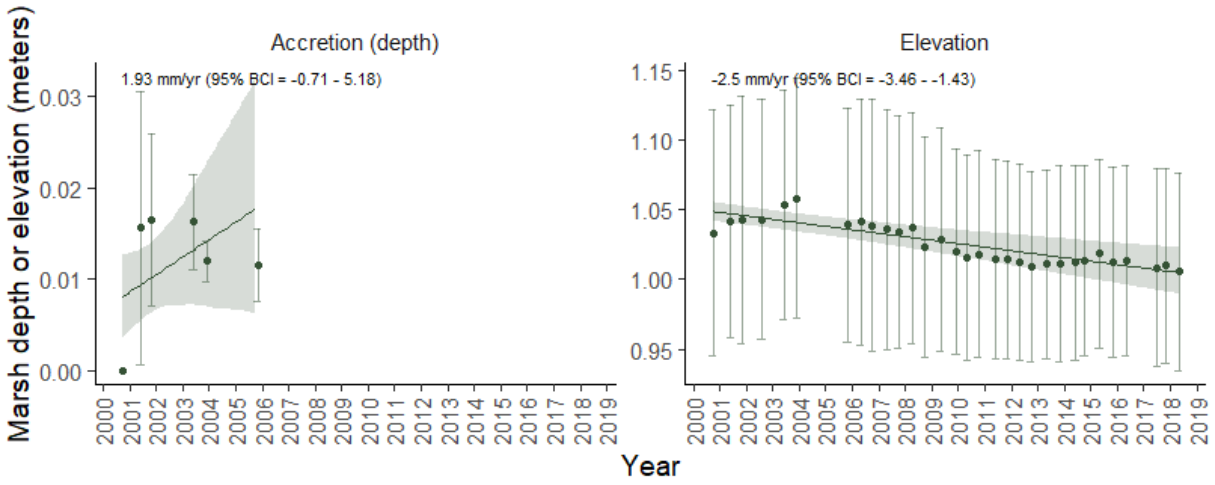


Figure A-43. Overall accretion and elevation trends for the Herring River GUT site at Cape Cod National Seashore. Solid line shows the mean of the posterior fitted trend; shaded region around the line bounds the 95% Bayesian credible interval of the fitted trend. These trend lines were computed using the mean of the intercept posteriors across SETs within the site and the mean of the slope posteriors across SETs within a site. Data are shown as means (points) plus and minus the standard deviation (error bars) across all observation locations within the site. Observations were grouped by month for aggregating.

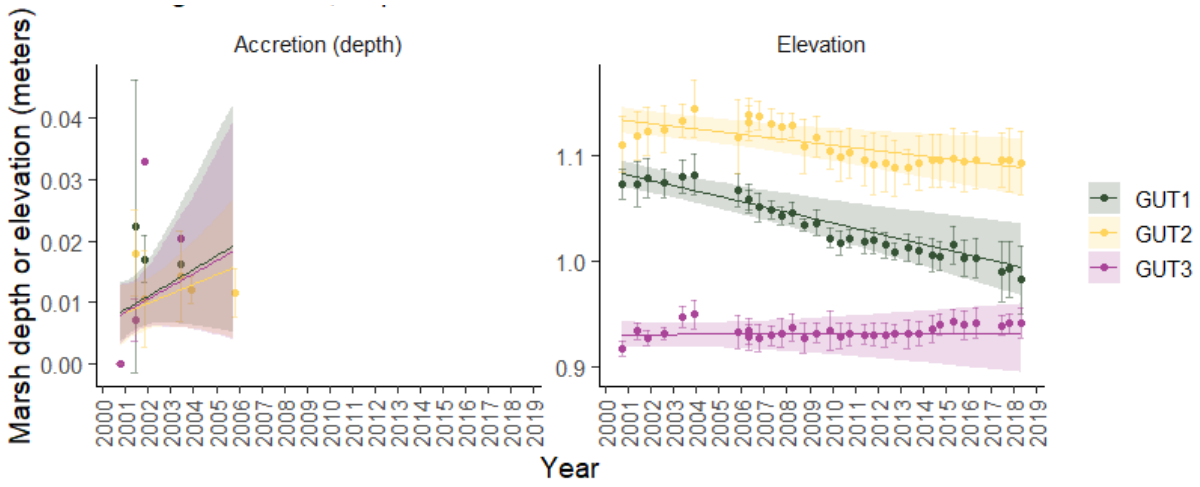


Figure A-44. Accretion and elevation trends at each station for the Herring River GUT site at Cape Cod National Seashore. Solid line shows the mean of the posterior fitted trend; shaded region around the line bounds the 95% Bayesian credible interval of the fitted trend. Data are shown as means (points) plus and minus the standard deviation (error bars) across all observation locations within the station. Observations were grouped by month for aggregating.

Herring River High Toss (Behind Dike)

Table A-26. Estimated rates of elevation and accretion trends at Herring River High Toss in Cape Cod National Seashore. Values in parentheses are the 95% Bayesian credible intervals. Pr(trend > 0) columns report the posterior probability that the estimated trend is greater than zero.

SET	Response	Trend estimate (mm/yr)	Pr(trend > 0)	Pr(trend > slr)	Pr(trend < slr)
HighToss1	Accretion	1.81 (1.29 – 2.29)	0.70	0	1
HighToss2	Accretion	1.69 (1.02 – 2.21)	0.55	0	1
HighToss3	Accretion	1.77 (1.25 – 2.28)	0.65	0	1
HighToss1	Elevation	-0.84 (-1.29 – -0.38)	0.69	0	1
HighToss2	Elevation	-1.08 (-1.56 – -0.66)	0.29	0	1
HighToss3	Elevation	-0.96 (-1.42 – -0.52)	0.50	0	1
Overall	**Accretion**	**1.76 (1.29 – 2.15)**	**1.00**	**0**	**1**
Overall	**Elevation**	**-0.96 (-1.3 – -0.62)**	**0.00**	**0**	**1**

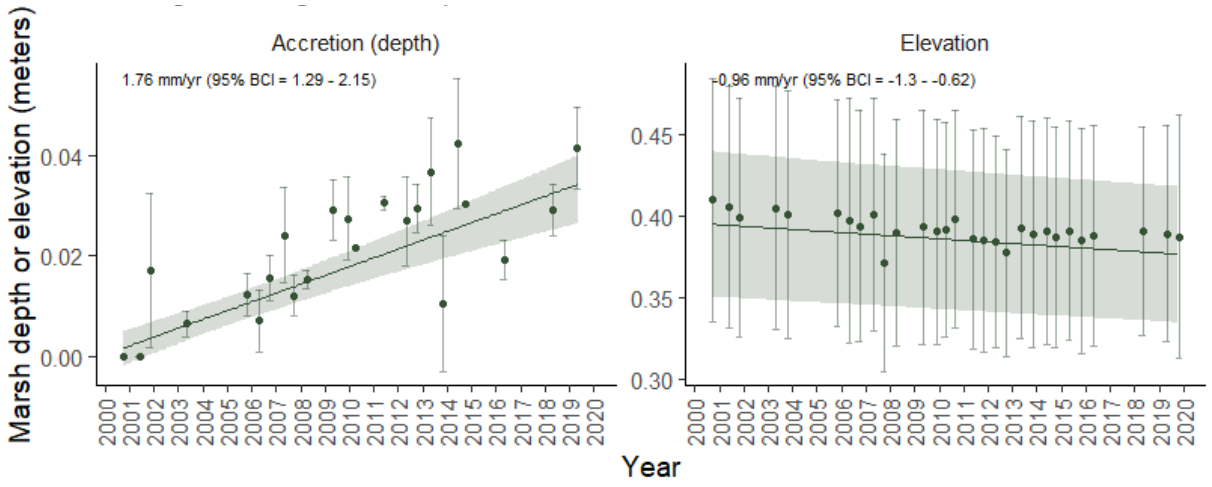


Figure A-45. Overall accretion and elevation trends for the Herring River High Toss site at Cape Cod National Seashore. Solid line shows the mean of the posterior fitted trend; shaded region around the line bounds the 95% Bayesian credible interval of the fitted trend. These trend lines were computed using the mean of the intercept posteriors across SETs within the site and the mean of the slope posteriors across SETs within a site. Data are shown as means (points) plus and minus the standard deviation (error bars) across all observation locations within the site. Observations were grouped by month for aggregating.

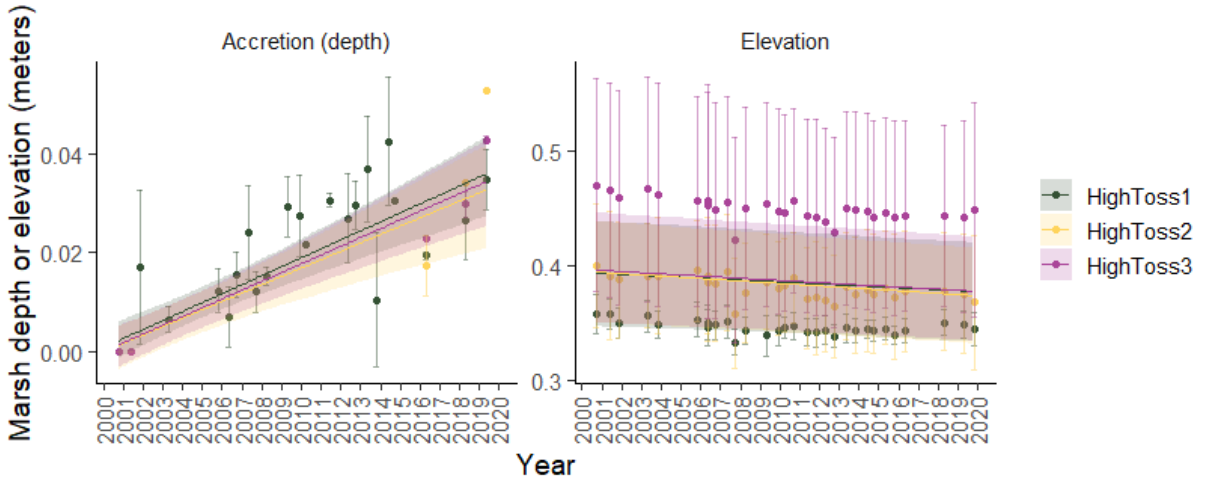


Figure A-46. Accretion and elevation trends at each station for the Herring River High Toss site at Cape Cod National Seashore. Solid line shows the mean of the posterior fitted trend; shaded region around the line bounds the 95% Bayesian credible interval of the fitted trend. Data are shown as means (points) plus and minus the standard deviation (error bars) across all observation locations within the station. Observations were grouped by month for aggregating.

Herring River Phrag (Behind Dike)

Table A-27. Estimated rates of elevation and accretion trends at Herring River Phrag in Cape Cod National Seashore. Values in parentheses are the 95% Bayesian credible intervals. Pr(trend > 0) columns report the posterior probability that the estimated trend is greater than zero.

SET	Response	Trend estimate (mm/yr)	Pr(trend > 0)	Pr(trend > slr)	Pr(trend < slr)
Phrag1	Accretion	5.4 (4.88 – 5.96)	1.00	0.98	0.01
Phrag2	Accretion	5.78 (5.26 – 6.31)	1.00	0.99	0.00
Phrag3	Accretion	5.04 (4.48 – 5.6)	1.00	0.94	0.03
Phrag1	Elevation	5.14 (4.85 – 5.42)	0.29	0.01	0.98
Phrag2	Elevation	6.3 (6.01 – 6.59)	0.99	0.04	0.96
Phrag3	Elevation	5.64 (5.34 – 5.9)	0.70	0.02	0.98
Overall	**Accretion**	**5.41 (5.01 – 5.82)**	**1.00**	**1.00**	**0.00**
Overall	**Elevation**	**5.69 (5.52 – 5.86)**	**1.00**	**1.00**	**0.00**

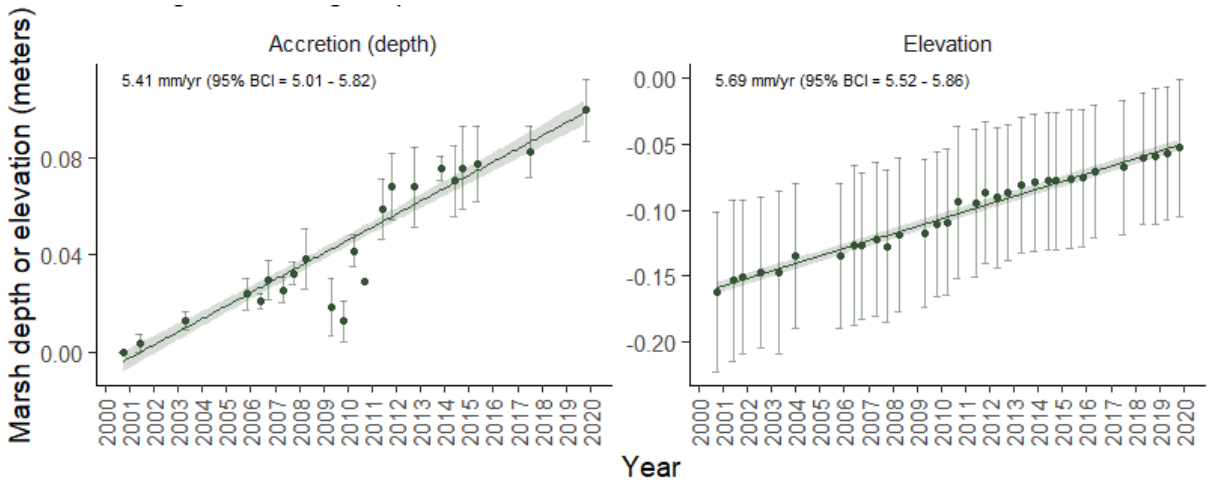


Figure A-47. Overall accretion and elevation trends for the Herring River Phrag site at Cape Cod National Seashore. Solid line shows the mean of the posterior fitted trend; shaded region around the line bounds the 95% Bayesian credible interval of the fitted trend. These trend lines were computed using the mean of the intercept posteriors across SETs within the site and the mean of the slope posteriors across SETs within a site. Data are shown as means (points) plus and minus the standard deviation (error bars) across all observation locations within the site. Observations were grouped by month for aggregating.

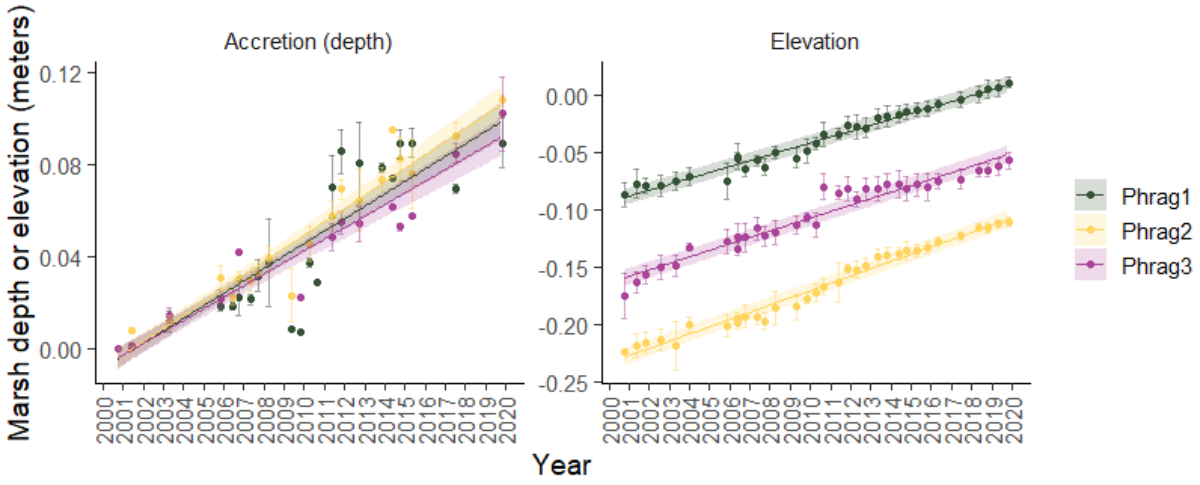


Figure A-48. Accretion and elevation trends at each station for the Herring River Phrag site at Cape Cod National Seashore. Solid line shows the mean of the posterior fitted trend; shaded region around the line bounds the 95% Bayesian credible interval of the fitted trend. Data are shown as means (points) plus and minus the standard deviation (error bars) across all observation locations within the station. Observations were grouped by month for aggregating.

Nauset Marsh N

Table A-28. Estimated rates of elevation and accretion trends at Nauset Marsh N in Cape Cod National Seashore. Values in parentheses are the 95% Bayesian credible intervals. Pr(trend > 0) columns report the posterior probability that the estimated trend is greater than zero.

SET	Response	Trend estimate (mm/yr)	Pr(trend > 0)	Pr(trend > slr)	Pr(trend < slr)
N1	Accretion	4.63 (4.09 – 5.16)	0.99	0.04	0.94
N2	Accretion	3.29 (2.81 – 3.76)	0.53	0.01	0.98
N3	Accretion	3.25 (2.77 – 3.74)	0.51	0.01	0.99
N1	Elevation	2.95 (2.29 – 3.58)	0.86	0.01	0.98
N2	Elevation	2.83 (2.19 – 3.44)	0.83	0.01	0.98
N3	Elevation	1.52 (0.89 – 2.32)	0.19	0.00	1.00
Overall	**Accretion**	**3.72 (3.37 – 4.06)**	**1.00**	**0.02**	**0.28**
Overall	**Elevation**	**2.43 (2.05 – 2.82)**	**1.00**	**0.00**	**1.00**

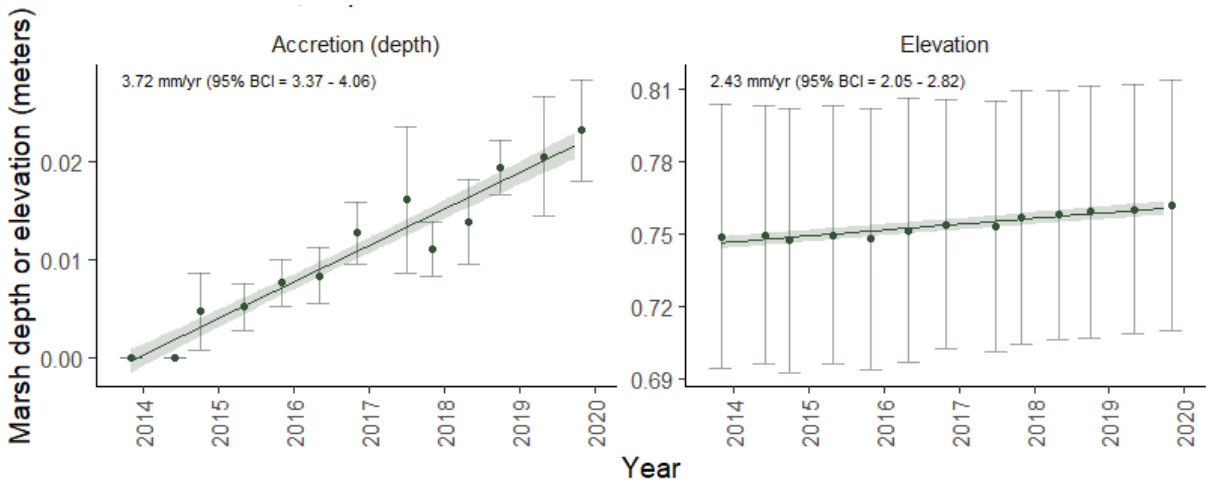


Figure A-49. Overall accretion and elevation trends for the Nauset Marsh N site at Cape Cod National Seashore. Solid line shows the mean of the posterior fitted trend; shaded region around the line bounds the 95% Bayesian credible interval of the fitted trend. These trend lines were computed using the mean of the intercept posteriors across SETs within the site and the mean of the slope posteriors across SETs within a site. Data are shown as means (points) plus and minus the standard deviation (error bars) across all observation locations within the site. Observations were grouped by month for aggregating.

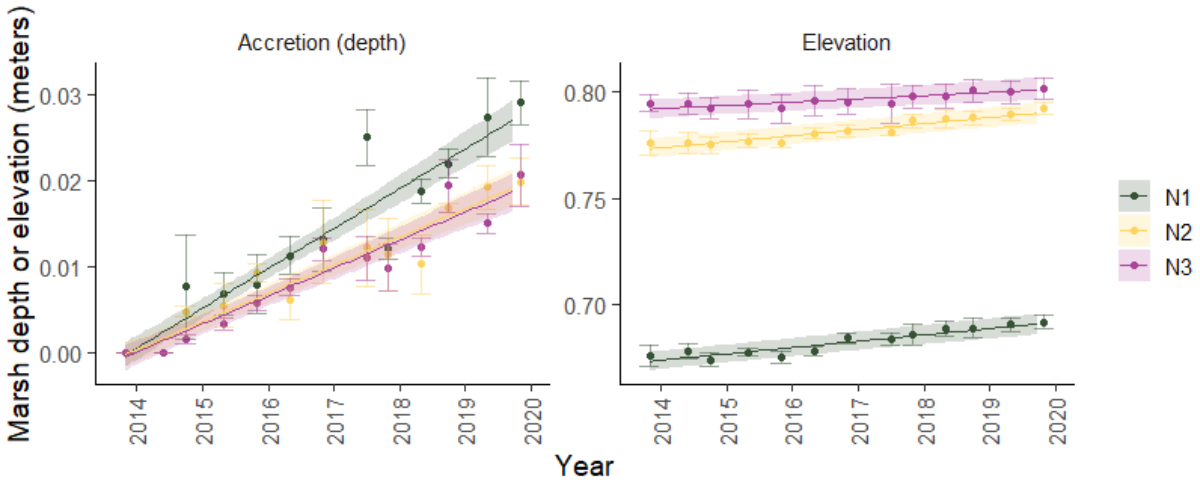


Figure A-50. Accretion and elevation trends at each station for the Nauset Marsh N site at Cape Cod National Seashore. Solid line shows the mean of the posterior fitted trend; shaded region around the line bounds the 95% Bayesian credible interval of the fitted trend. Data are shown as means (points) plus and minus the standard deviation (error bars) across all observation locations within the station. Observations were grouped by month for aggregating.

Nauset Marsh Old N

Table A-29. Estimated rates of elevation and accretion trends at Nauset Marsh Old N in Cape Cod National Seashore. Values in parentheses are the 95% Bayesian credible intervals. Pr(trend > 0) columns report the posterior probability that the estimated trend is greater than zero.

SET	Response	Trend estimate (mm/yr)	Pr(trend > 0)	Pr(trend > slr)	Pr(trend < slr)
Old N1	Accretion	4.62 (3.99 – 5.18)	1.00	0.27	0.55
Old N2	Accretion	4 (3.44 – 4.56)	1.00	0.10	0.79
Old N3	Accretion	4.67 (4.09 – 5.22)	1.00	0.28	0.53
Old N4	Accretion	4.84 (4.24 – 5.47)	1.00	0.35	0.47
Old N1	Elevation	3.28 (2.96 – 3.59)	0.71	0.00	1.00
Old N2	Elevation	2.22 (1.89 – 2.57)	0.12	0.00	1.00
Old N3	Elevation	3.71 (3.35 – 4.06)	0.94	0.00	0.99
Old N4	Elevation	3.59 (3.25 – 3.91)	0.89	0.00	0.99
Overall	**Accretion**	**4.53 (4.2 – 4.84)**	**1.00**	**0.99**	**0.00**
Overall	**Elevation**	**3.2 (3.03 – 3.37)**	**1.00**	**0.00**	**1.00**

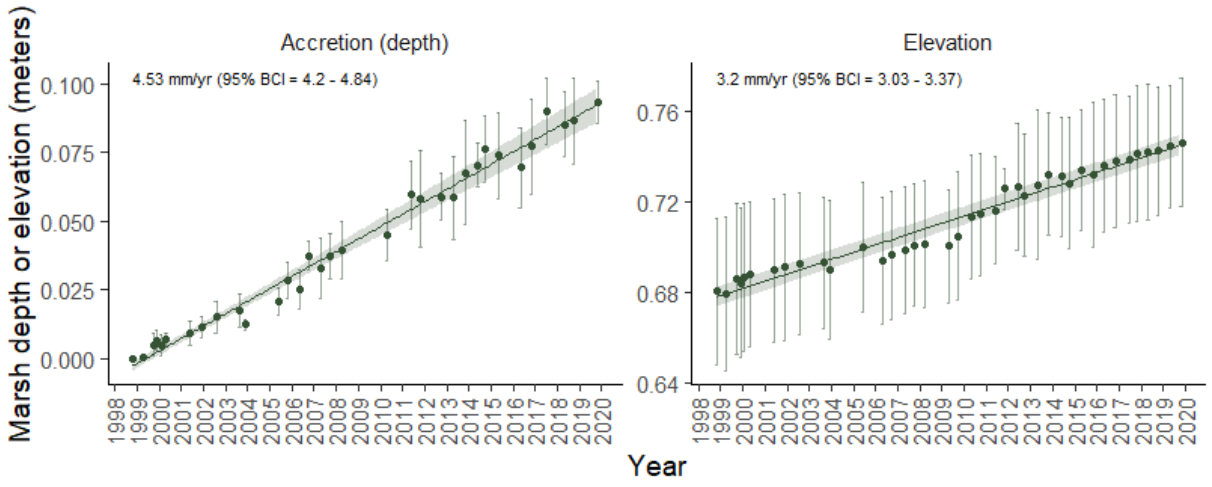


Figure A-51. Overall accretion and elevation trends for the Nauset Marsh Old N site at Cape Cod National Seashore. Solid line shows the mean of the posterior fitted trend; shaded region around the line bounds the 95% Bayesian credible interval of the fitted trend. These trend lines were computed using the mean of the intercept posteriors across SETs within the site and the mean of the slope posteriors across SETs within a site. Data are shown as means (points) plus and minus the standard deviation (error bars) across all observation locations within the site. Observations were grouped by month for aggregating.

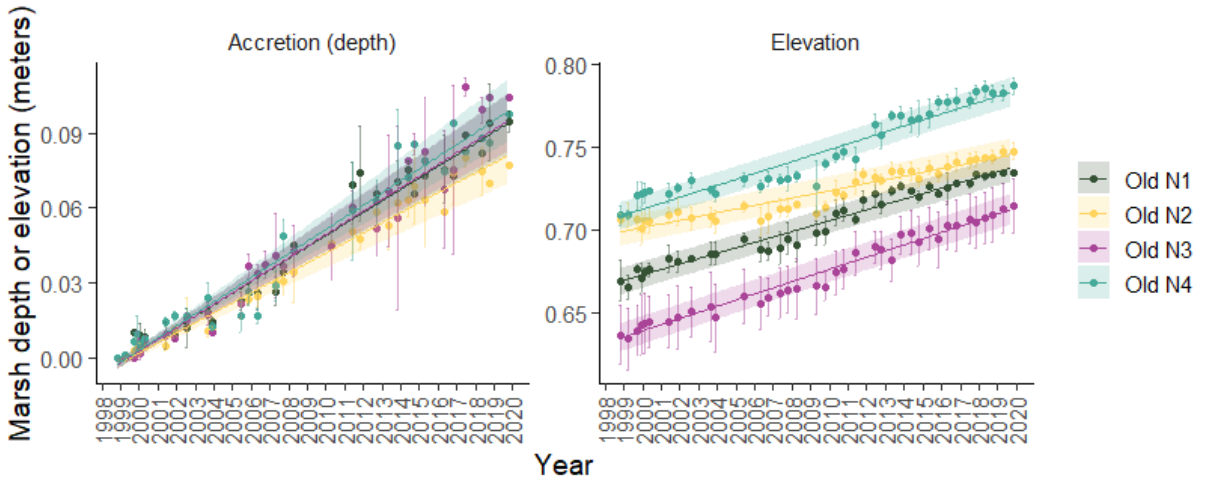


Figure A-52. Accretion and elevation trends at each station for the Nauset Marsh OldN site at Cape Cod National Seashore. Solid line shows the mean of the posterior fitted trend; shaded region around the line bounds the 95% Bayesian credible interval of the fitted trend. Data are shown as means (points) plus and minus the standard deviation (error bars) across all observation locations within the station. Observations were grouped by month for aggregating.

Colonial National Historical Park

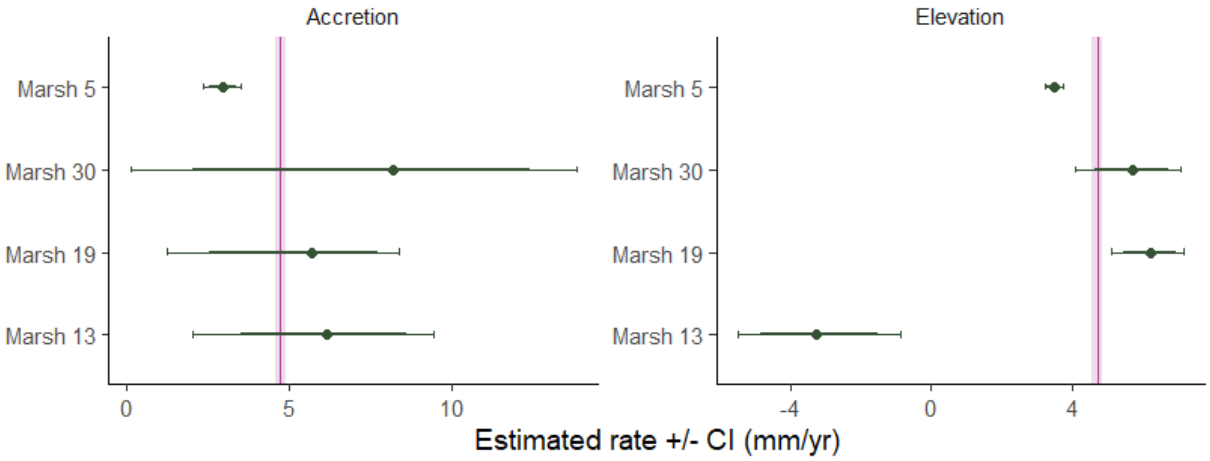


Figure A-53. Estimated accretion and elevation trends at the site level for Colonial National Historical Park. The estimates are averages of the posteriors of the set-level trend estimates. The point shows the mean of the posterior; the thick error bars show the 85% Bayesian credible interval; the thin error bars show the 95% Bayesian credible interval. The vertical pink line shows the mean estimate of sea level rise and the pink rectangle bounds the 95% confidence interval.

Table A-30. Posterior trends (mean and 95% Bayesian credible interval) and the posterior probabilities that the trends in elevation or accretion are greater than 0 [Pr(trend > 0)], that the trend is greater than the upper bound of sea level rise [Pr(trend > slr)], and that the trend is less than the lower bound of sea level rise [Pr(trend < slr)] at each site in Colonial National Historical Park. The final column [Pr(trend_i < trend_j)] is the probability that the trend specified in the row (either elevation or accretion) is less than the other estimated trend (either accretion or elevation) at the same site.

Site	Response	Trend estimate (mm/yr)	Pr(trend > 0)	Pr(trend > slr)	Pr(trend < slr)	Pr(trend_i < trend_j)
Marsh 13	Accretion	6.14 (2 – 9.43)	0.99	0.78	0.17	0.00
Marsh 19	Accretion	5.68 (1.26 – 8.38)	0.99	0.74	0.23	0.55
Marsh 30	Accretion	8.2 (0.12 – 13.84)	0.98	0.81	0.18	0.22
Marsh 5	Accretion	2.95 (2.35 – 3.51)	1.00	0.00	1.00	0.96
Marsh 13	Elevation	-3.25 (-5.48 – -0.86)	0.00	0.00	1.00	1.00
Marsh 19	Elevation	6.25 (5.15 – 7.21)	1.00	0.99	0.00	0.45
Marsh 30	Elevation	5.73 (4.1 – 7.12)	1.00	0.88	0.07	0.78
Marsh 5	Elevation	3.49 (3.24 – 3.75)	1.00	0.00	1.00	0.04

Marsh 5

Table A-31. Estimated rates of elevation and accretion trends at Marsh 5 in Colonial National Historical Park. Values in parentheses are the 95% Bayesian credible intervals. Pr(trend > 0) columns report the posterior probability that the estimated trend is greater than zero.

SET	Response	Trend estimate (mm/yr)	Pr(trend > 0)	Pr(trend > slr)	Pr(trend < slr)
M5 Pipe 1	Accretion	3.17 (2.39 – 3.93)	0.80	0.00	1.00
M5 Pipe 2	Accretion	3.07 (2.32 – 3.8)	0.76	0.00	1.00
M5 Pipe 3	Accretion	2.6 (1.7 – 3.42)	0.37	0.00	1.00
M5 Pipe 1	Elevation	4.37 (3.94 – 4.79)	0.96	0.03	0.96
M5 Pipe 2	Elevation	4.95 (4.54 – 5.39)	0.99	0.05	0.93
M5 Pipe 3	Elevation	1.16 (0.74 – 1.57)	0.14	0.00	1.00
Overall	**Accretion**	**2.95 (2.35 – 3.51)**	**1.00**	**0.00**	**1.00**
Overall	**Elevation**	**3.49 (3.24 – 3.75)**	**1.00**	**0.00**	**1.00**

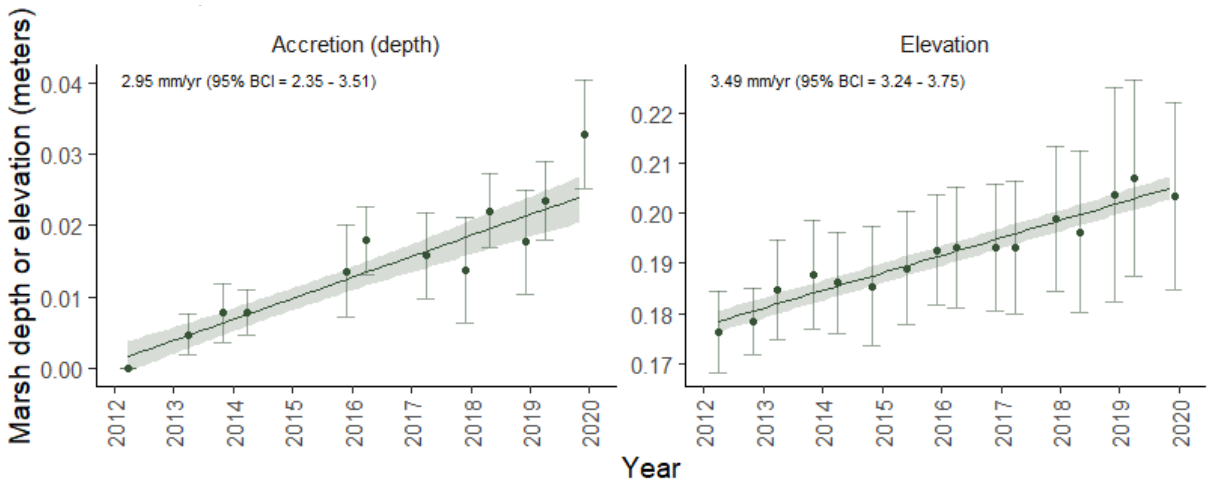


Figure A-54. Overall accretion and elevation trends for the Marsh 5 site at Colonial National Historical Park. Solid line shows the mean of the posterior fitted trend; shaded region around the line bounds the 95% Bayesian credible interval of the fitted trend. These trend lines were computed using the mean of the intercept posteriors across SETs within the site and the mean of the slope posteriors across SETs within a site. Data are shown as means (points) plus and minus the standard deviation (error bars) across all observation locations within the site. Observations were grouped by month for aggregating.

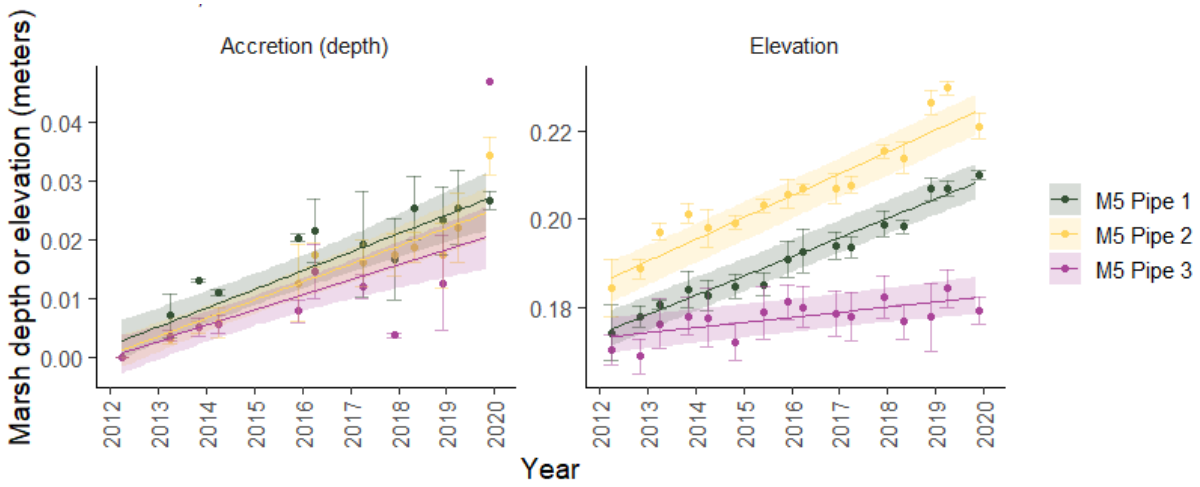


Figure A-55. Accretion and elevation trends at each station for the Marsh 5 site at Colonial National Historical Park. Solid line shows the mean of the posterior fitted trend; shaded region around the line bounds the 95% Bayesian credible interval of the fitted trend. Data are shown as means (points) plus and minus the standard deviation (error bars) across all observation locations within the station. Observations were grouped by month for aggregating.

Marsh 13

Table A-32. Estimated rates of elevation and accretion trends at Marsh 13 in Colonial National Historical Park. Values in parentheses are the 95% Bayesian credible intervals. Pr(trend > 0) columns report the posterior probability that the estimated trend is greater than zero.

SET	Response	Trend estimate (mm/yr)	Pr(trend > 0)	Pr(trend > slr)	Pr(trend < slr)
M13 Pipe 1	Accretion	7.18 (1.77 – 11.85)	0.92	0.60	0.38
M13 Pipe 2	Accretion	6.47 (1.96 – 9.88)	0.93	0.54	0.42
M13 Pipe 3	Accretion	4.78 (0.31 – 9.5)	0.84	0.30	0.67
M13 Pipe 1	Elevation	-3.42 (–6.56 – -0.66)	0.38	0.00	1.00
M13 Pipe 2	Elevation	-3.1 (-5.61 – -0.38)	0.48	0.00	1.00
M13 Pipe 3	Elevation	-3.23 (-5.78 – -0.66)	0.43	0.00	1.00
Overall	**Accretion**	**6.14 (2 – 9.43)**	**0.99**	**0.78**	**0.17**
Overall	**Elevation**	**-3.25 (-5.48 – -0.86)**	**0.00**	**0.00**	**1.00**

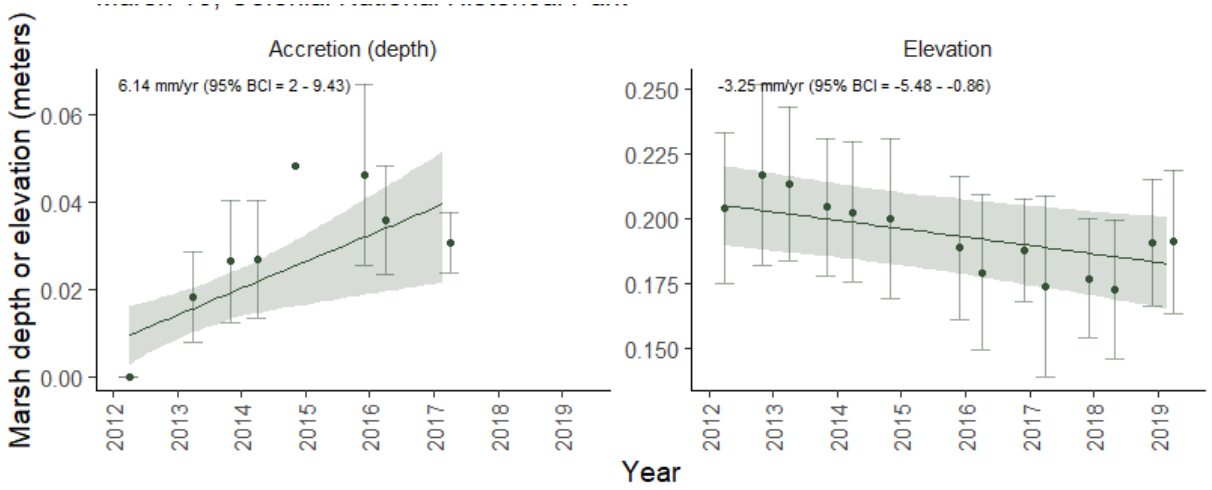


Figure A-56. Overall accretion and elevation trends for the Marsh 13 site at Colonial National Historical Park. Solid line shows the mean of the posterior fitted trend; shaded region around the line bounds the 95% Bayesian credible interval of the fitted trend. These trend lines were computed using the mean of the intercept posteriors across SETs within the site and the mean of the slope posteriors across SETs within a site. Data are shown as means (points) plus and minus the standard deviation (error bars) across all observation locations within the site. Observations were grouped by month for aggregating.

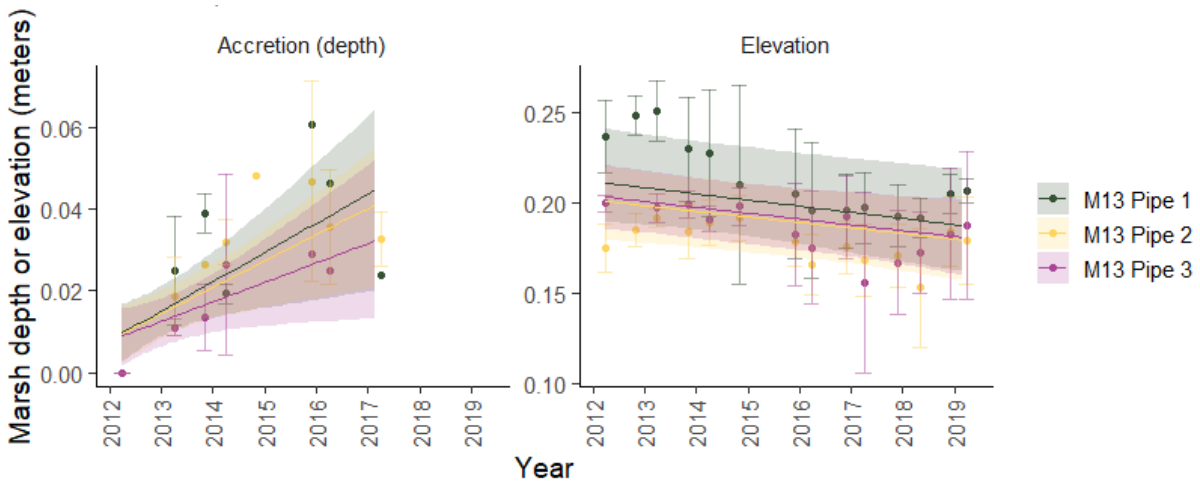


Figure A-57. Accretion and elevation trends at each station for the Marsh 13 site at Colonial National Historical Park. Solid line shows the mean of the posterior fitted trend; shaded region around the line bounds the 95% Bayesian credible interval of the fitted trend. Data are shown as means (points) plus and minus the standard deviation (error bars) across all observation locations within the station. Observations were grouped by month for aggregating.

Marsh 19

Table A-33. Estimated rates of elevation and accretion trends at Marsh 19 in Colonial National Historical Park. Values in parentheses are the 95% Bayesian credible intervals. Pr(trend > 0) columns report the posterior probability that the estimated trend is greater than zero.

SET	Response	Trend estimate (mm/yr)	Pr(trend > 0)	Pr(trend > slr)	Pr(trend < slr)
M19 Pipe 1	Accretion	5.29 (0.66 – 9.38)	0.91	0.40	0.56
M19 Pipe 2	Accretion	7.07 (0.97 – 11.2)	0.93	0.64	0.33
M19 Pipe 3	Accretion	4.69 (0.67 – 8.14)	0.89	0.31	0.65
M19 Pipe 1	Elevation	6.75 (5.27 – 8.19)	0.89	0.10	0.88
M19 Pipe 2	Elevation	5.41 (3.92 – 6.76)	0.50	0.03	0.96
M19 Pipe 3	Elevation	6.58 (5.1 – 7.98)	0.88	0.08	0.90
Overall	**Accretion**	**5.68 (1.26 – 8.38)**	**0.99**	**0.74**	**0.23**
Overall	**Elevation**	**6.25 (5.15 – 7.21)**	**1.00**	**0.99**	**0.00**

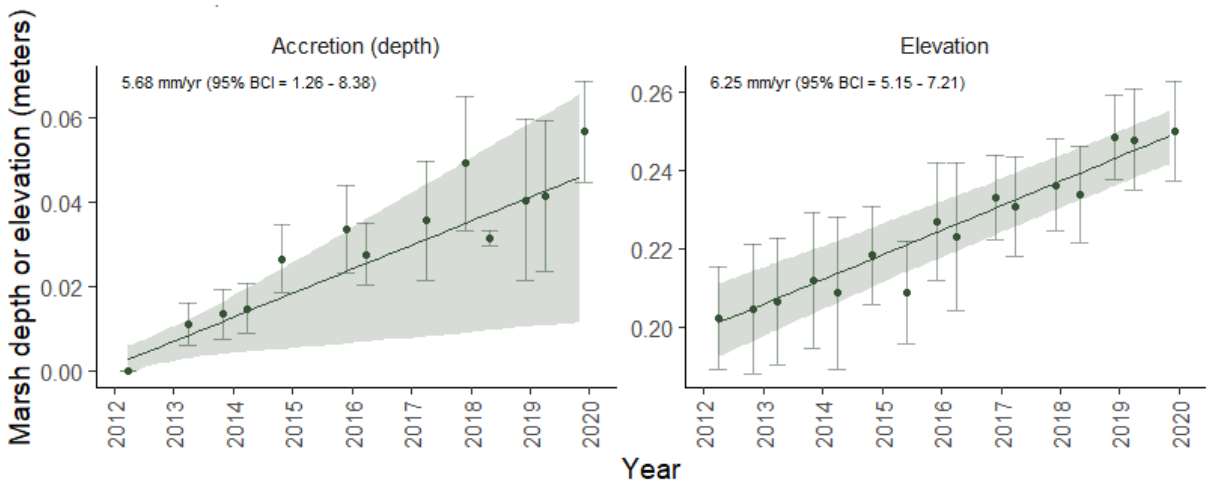


Figure A-58. Overall accretion and elevation trends for the Marsh 19 site at Colonial National Historical Park. Solid line shows the mean of the posterior fitted trend; shaded region around the line bounds the 95% Bayesian credible interval of the fitted trend. These trend lines were computed using the mean of the intercept posteriors across SETs within the site and the mean of the slope posteriors across SETs within a site. Data are shown as means (points) plus and minus the standard deviation (error bars) across all observation locations within the site. Observations were grouped by month for aggregating.

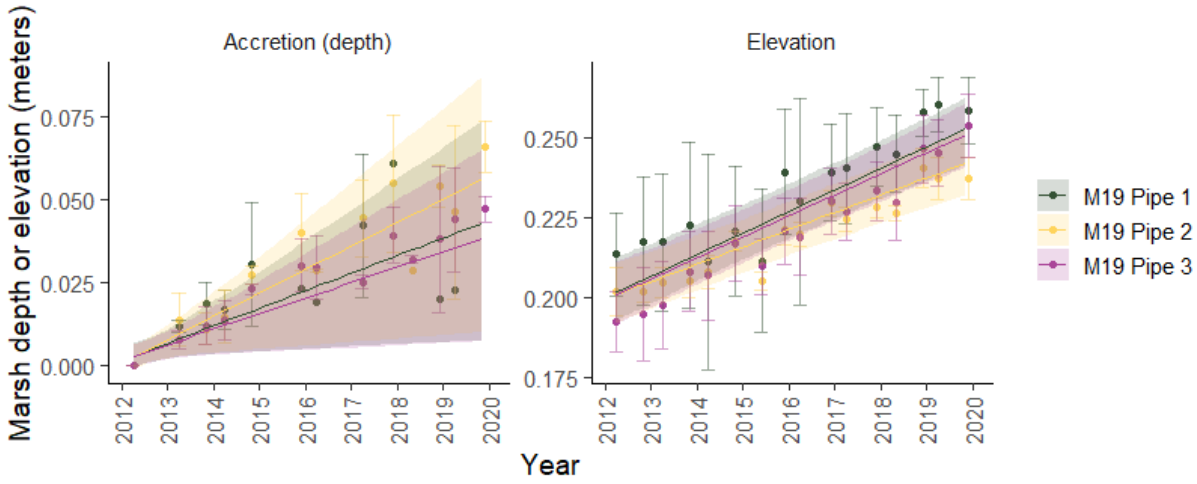


Figure A-59. Accretion and elevation trends at each station for the Marsh 19 site at Colonial National Historical Park. Solid line shows the mean of the posterior fitted trend; shaded region around the line bounds the 95% Bayesian credible interval of the fitted trend. Data are shown as means (points) plus and minus the standard deviation (error bars) across all observation locations within the station. Observations were grouped by month for aggregating.

Marsh 30

Table A-34. Estimated rates of elevation and accretion trends at Marsh 30 in Colonial National Historical Park. Values in parentheses are the 95% Bayesian credible intervals. Pr(trend > 0) columns report the posterior probability that the estimated trend is greater than zero.

SET	Response	Trend estimate (mm/yr)	Pr(trend > 0)	Pr(trend > slr)	Pr(trend < slr)
M30 Pipe 1	Accretion	9.42 (-0.24 – 15.88)	0.92	0.77	0.23
M30 Pipe 2	Accretion	8.54 (0.22 – 15.58)	0.93	0.73	0.26
M30 Pipe 3	Accretion	6.64 (-1.1 – 15.65)	0.87	0.54	0.44
M30 Pipe 1	Elevation	4.45 (2.4 – 6.47)	0.55	0.03	0.96
M30 Pipe 2	Elevation	7.08 (4.27 – 9.5)	0.92	0.27	0.70
M30 Pipe 3	Elevation	5.66 (3.62 – 7.54)	0.81	0.11	0.88
Overall	**Accretion**	**8.2 (0.12 – 13.84)**	**0.98**	**0.81**	**0.18**
Overall	**Elevation**	**5.73 (4.1 – 7.12)**	**1.00**	**0.88**	**0.07**

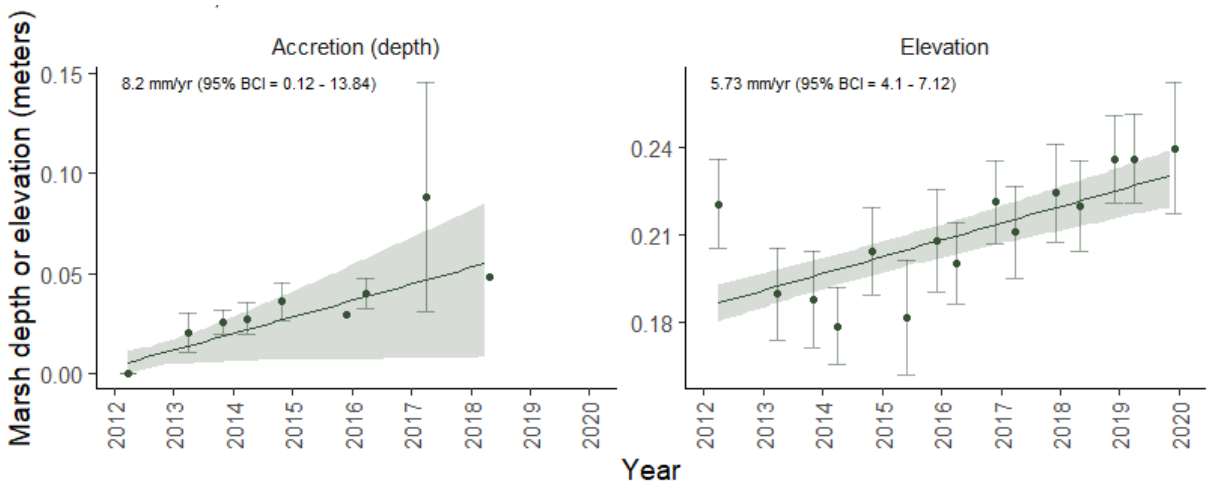


Figure A-60. Overall accretion and elevation trends for the Marsh 30 site at Colonial National Historical Park. Solid line shows the mean of the posterior fitted trend; shaded region around the line bounds the 95% Bayesian credible interval of the fitted trend. These trend lines were computed using the mean of the intercept posteriors across SETs within the site and the mean of the slope posteriors across SETs within a site. Data are shown as means (points) plus and minus the standard deviation (error bars) across all observation locations within the site. Observations were grouped by month for aggregating.

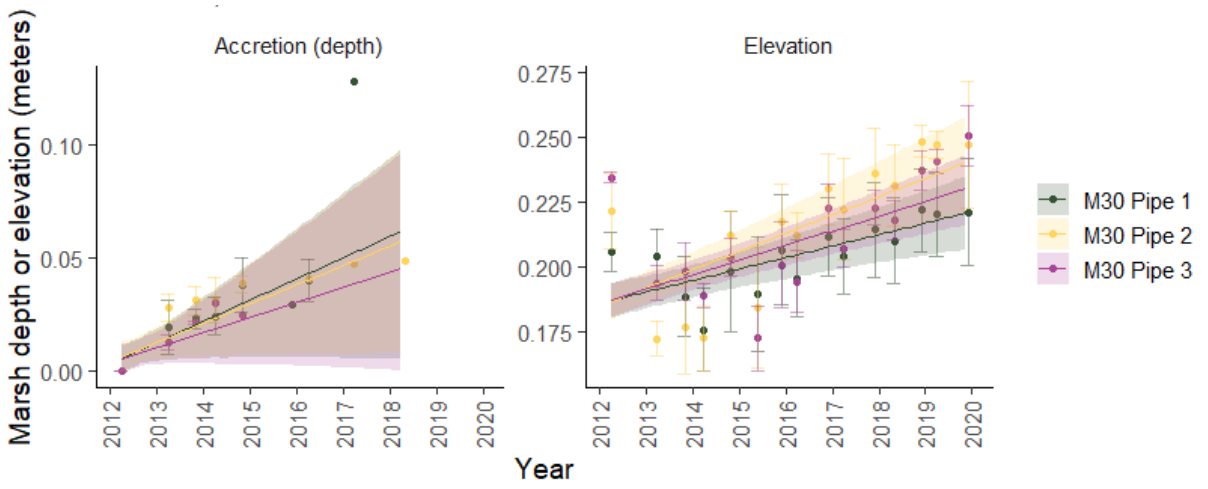


Figure A-61. Accretion and elevation trends at each station for the Marsh 30 site at Colonial National Historical Park. Solid line shows the mean of the posterior fitted trend; shaded region around the line bounds the 95% Bayesian credible interval of the fitted trend. Data are shown as means (points) plus and minus the standard deviation (error bars) across all observation locations within the station. Observations were grouped by month for aggregating.

Fire Island National Seashore

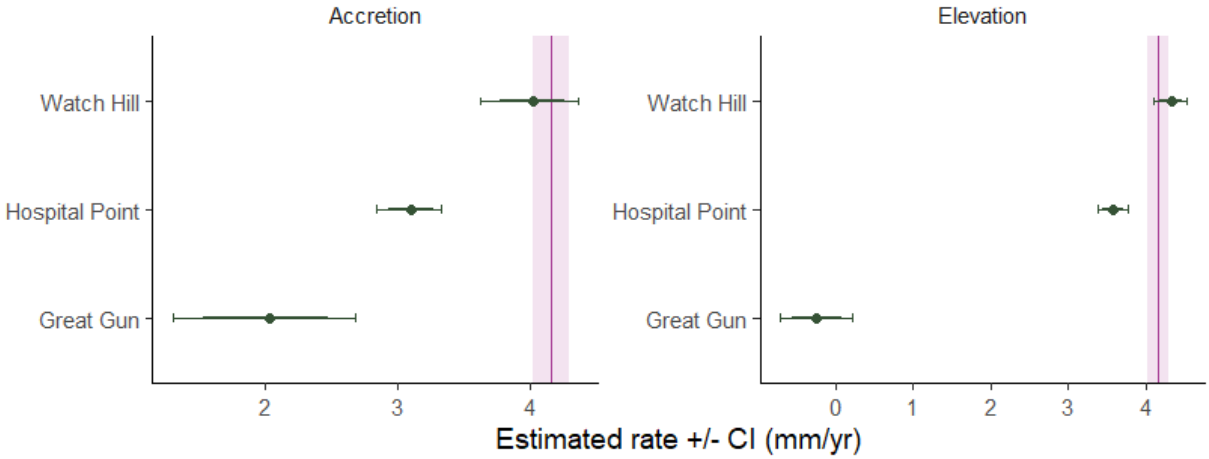


Figure A-62. Estimated accretion and elevation trends at the site level for Fire Island National Seashore. The estimates are averages of the posteriors of the set-level trend estimates. The point shows the mean of the posterior; the thick error bars show the 85% Bayesian credible interval; the thin error bars show the 95% Bayesian credible interval. The vertical pink line shows the mean estimate of sea level rise and the pink rectangle bounds the 95% confidence interval.

Table A-35. Posterior trends (mean and 95% Bayesian credible interval) and the posterior probabilities that the trends in elevation or accretion are greater than 0 [Pr(trend > 0)], that the trend is greater than the upper bound of sea level rise [Pr(trend > slr)], and that the trend is less than the lower bound of sea level rise [Pr(trend < slr)] at each site in Fire Island National Seashore. The final column [Pr(trend_i < trend_j)] is the probability that the trend specified in the row (either elevation or accretion) is less than the other estimated trend (either accretion or elevation) at the same site.

Site	Response	Trend estimate (mm/yr)	Pr(trend > 0)	Pr(trend > slr)	Pr(trend < slr)	Pr(trend_i < trend_j)
Great Gun	Accretion	2.04 (1.31 – 2.68)	1.00	0.00	1.00	0.00
Hospital Point	Accretion	3.1 (2.84 – 3.33)	1.00	0.00	1.00	1.00
Watch Hill	Accretion	4.02 (3.63 – 4.36)	1.00	0.05	0.48	0.94
Great Gun	Elevation	-0.25 (-0.71 – 0.21)	0.14	0.00	1.00	1.00
Hospital Point	Elevation	3.58 (3.39 – 3.77)	1.00	0.00	1.00	0.00
Watch Hill	Elevation	4.33 (4.1 – 4.52)	1.00	0.62	0.00	0.06

Great Gun

Table A-36. Estimated rates of elevation and accretion trends at Great Gun in Fire Island National Seashore. Values in parentheses are the 95% Bayesian credible intervals. Pr(trend > 0) columns report the posterior probability that the estimated trend is greater than zero.

SET	Response	Trend estimate (mm/yr)	Pr(trend > 0)	Pr(trend > slr)	Pr(trend < slr)
GG1	Accretion	2.11 (1.16 – 3.04)	0.71	0.00	1.00
GG2	Accretion	1.82 (0.9 – 2.59)	0.49	0.00	1.00
GG3	Accretion	2.19 (1.27 – 3.06)	0.76	0.00	1.00
GG1	Elevation	-3.23 (-4.15 – -2.16)	0.01	0.00	1.00
GG2	Elevation	-0.45 (-1.34 – 0.4)	0.40	0.00	1.00
GG3	Elevation	2.94 (2.04 – 3.7)	0.99	0.16	0.78
Overall	**Accretion**	**2.04 (1.31 – 2.68)**	**1.00**	**0.00**	**1.00**
Overall	**Elevation**	**-0.25 (-0.71 – 0.21)**	**0.14**	**0.00**	**1.00**

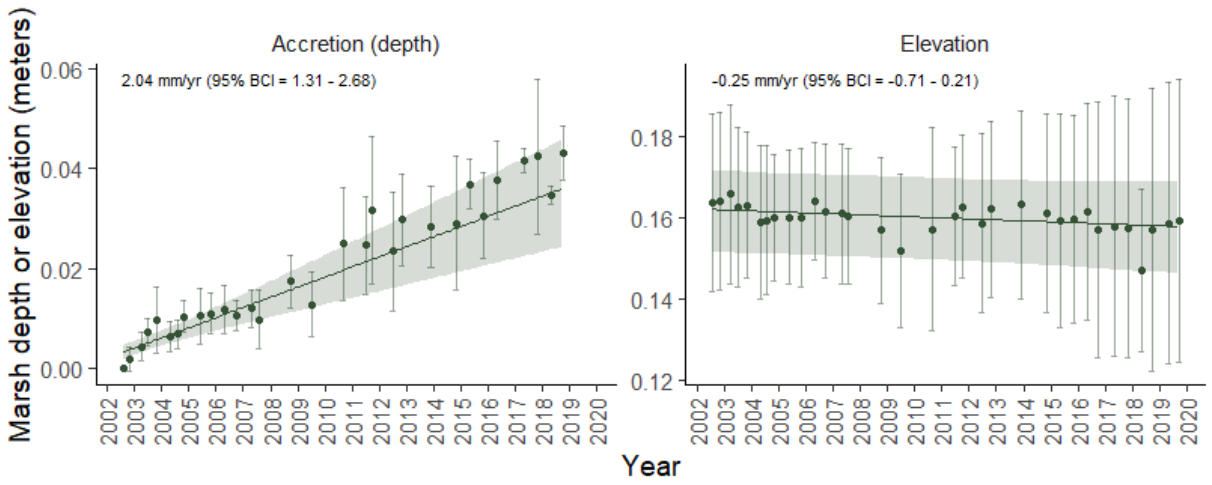


Figure A-63. Overall accretion and elevation trends for the Great Gun site at Fire Island National Seashore. Solid line shows the mean of the posterior fitted trend; shaded region around the line bounds the 95% Bayesian credible interval of the fitted trend. These trend lines were computed using the mean of the intercept posteriors across SETs within the site and the mean of the slope posteriors across SETs within a site. Data are shown as means (points) plus and minus the standard deviation (error bars) across all observation locations within the site. Observations were grouped by month for aggregating.

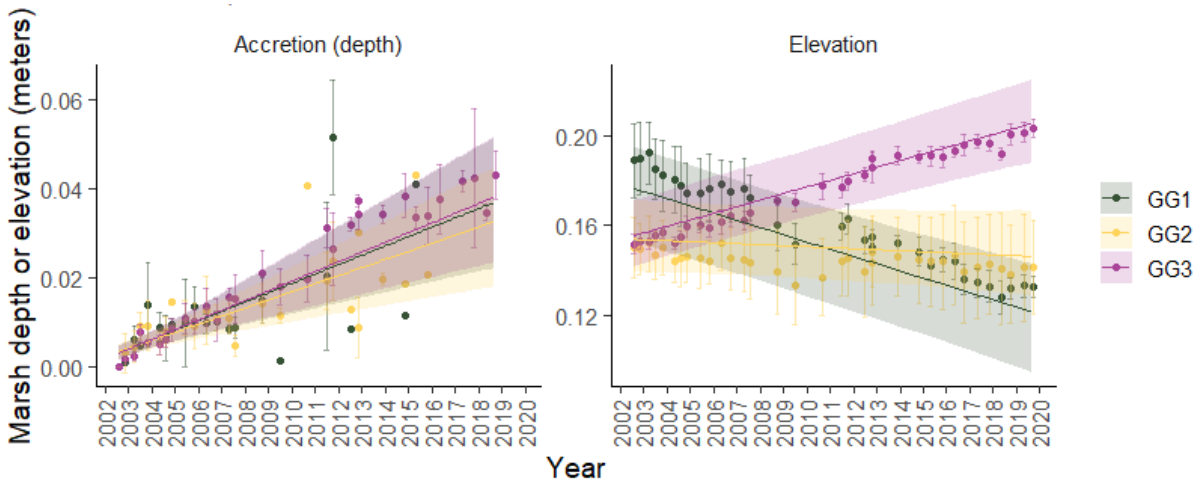


Figure A-64. Accretion and elevation trends at each station for the Great Gun site at Fire Island National Seashore. Solid line shows the mean of the posterior fitted trend; shaded region around the line bounds the 95% Bayesian credible interval of the fitted trend. Data are shown as means (points) plus and minus the standard deviation (error bars) across all observation locations within the station. Observations were grouped by month for aggregating.

Hospital Point

Table A-37. Estimated rates of elevation and accretion trends at Hospital Point in Fire Island National Seashore. Values in parentheses are the 95% Bayesian credible intervals. Pr(trend > 0) columns report the posterior probability that the estimated trend is greater than zero.

SET	Response	Trend estimate (mm/yr)	Pr(trend > 0)	Pr(trend > slr)	Pr(trend < slr)
HP1	Accretion	2.67 (2.26 – 3.06)	0.95	0.01	0.98
HP2	Accretion	3.07 (2.68 – 3.46)	0.98	0.03	0.95
HP3	Accretion	3.58 (3.11 – 3.96)	1.00	0.09	0.86
HP1	Elevation	3.57 (3.3 – 3.84)	0.57	0.00	1.00
HP2	Elevation	3.25 (2.89 – 3.59)	0.18	0.00	1.00
HP3	Elevation	3.92 (3.58 – 4.31)	0.92	0.00	1.00
Overall	**Accretion**	**3.1 (2.84 – 3.33)**	**1.00**	**0.00**	**1.00**
Overall	**Elevation**	**3.58 (3.39 – 3.77)**	**1.00**	**0.00**	**1.00**

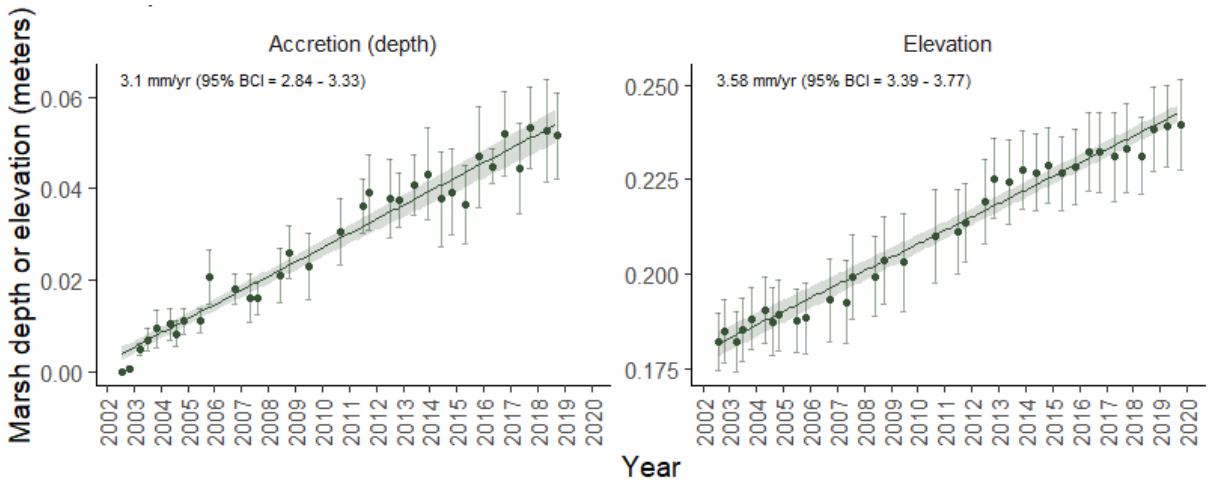


Figure A-65. Overall accretion and elevation trends for the Hospital Point site at Fire Island National Seashore. Solid line shows the mean of the posterior fitted trend; shaded region around the line bounds the 95% Bayesian credible interval of the fitted trend. These trend lines were computed using the mean of the intercept posteriors across SETs within the site and the mean of the slope posteriors across SETs within a site. Data are shown as means (points) plus and minus the standard deviation (error bars) across all observation locations within the site. Observations were grouped by month for aggregating.

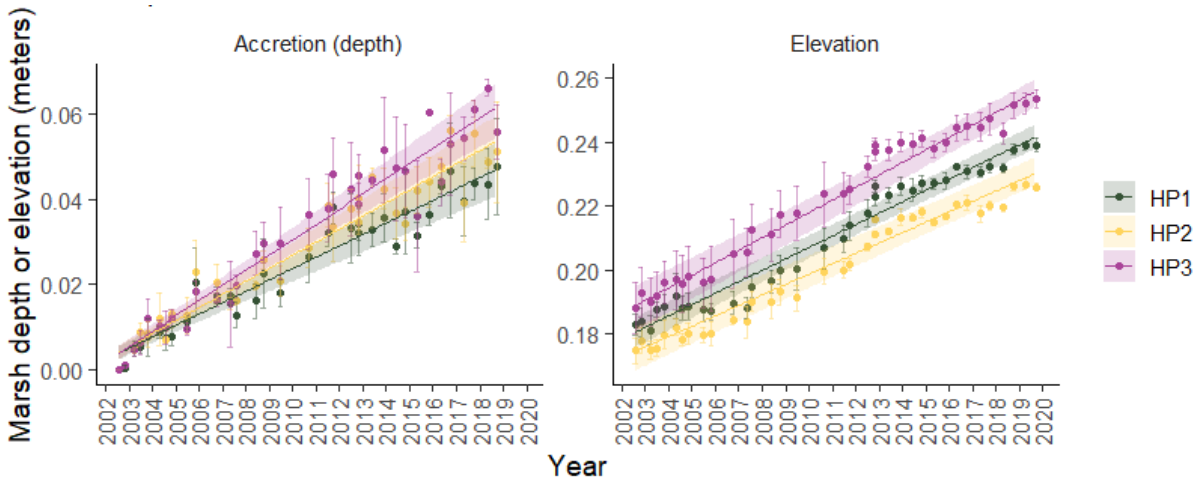


Figure A-66. Accretion and elevation trends at each station for the Hospital Point site at Fire Island National Seashore. Solid line shows the mean of the posterior fitted trend; shaded region around the line bounds the 95% Bayesian credible interval of the fitted trend. Data are shown as means (points) plus and minus the standard deviation (error bars) across all observation locations within the station. Observations were grouped by month for aggregating.

Table A-38. Estimated rates of elevation and accretion trends at Watch Hill in Fire Island National Seashore. Values in parentheses are the 95% Bayesian credible intervals. Pr(trend > 0) columns report the posterior probability that the estimated trend is greater than zero.

SET	Response	Trend estimate (mm/yr)	Pr(trend > 0)	Pr(trend > slr)	Pr(trend < slr)
WH1	Accretion	3.81 (3.24 – 4.36)	0.99	0.07	0.88
WH2	Accretion	3.56 (2.98 – 4.13)	0.99	0.04	0.93
WH3	Accretion	4.7 (4.06 – 5.27)	1.00	0.29	0.61
WH1	Elevation	3.69 (3.35 – 4.04)	0.31	0.00	1.00
WH2	Elevation	3.96 (3.61 – 4.3)	0.46	0.00	1.00
WH3	Elevation	5.33 (4.92 – 5.69)	0.99	0.01	0.99
Overall	**Accretion**	**4.02 (3.63 – 4.36)**	**1.00**	**0.05**	**0.48**
Overall	**Elevation**	**4.33 (4.1 – 4.52)**	**1.00**	**0.62**	**0.00**

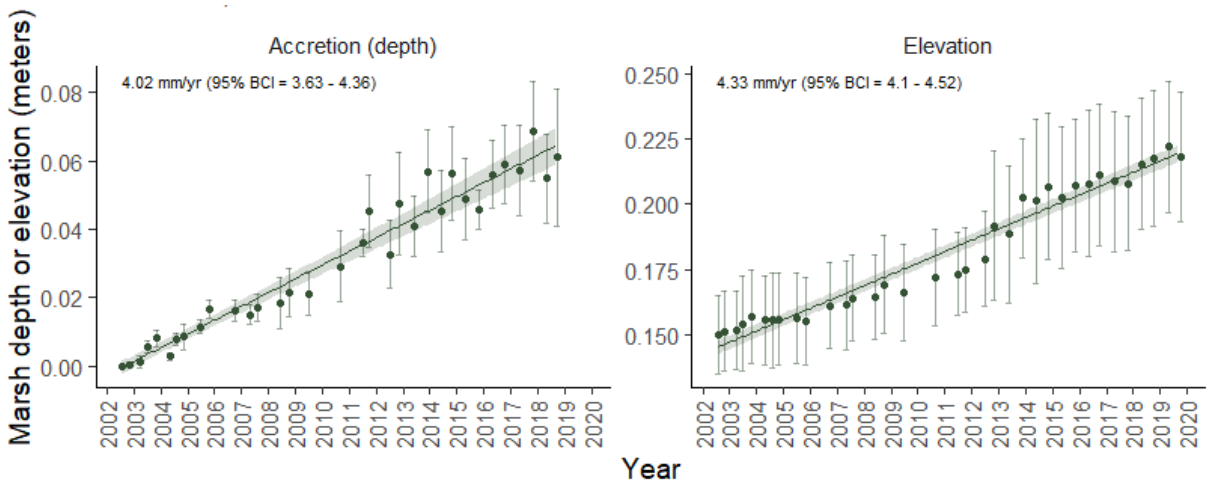


Figure A-67. Overall accretion and elevation trends for the Watch Hill site at Fire Island National Seashore. Solid line shows the mean of the posterior fitted trend; shaded region around the line bounds the 95% Bayesian credible interval of the fitted trend. These trend lines were computed using the mean of the intercept posteriors across SETs within the site and the mean of the slope posteriors across SETs within a site. Data are shown as means (points) plus and minus the standard deviation (error bars) across all observation locations within the site. Observations were grouped by month for aggregating.

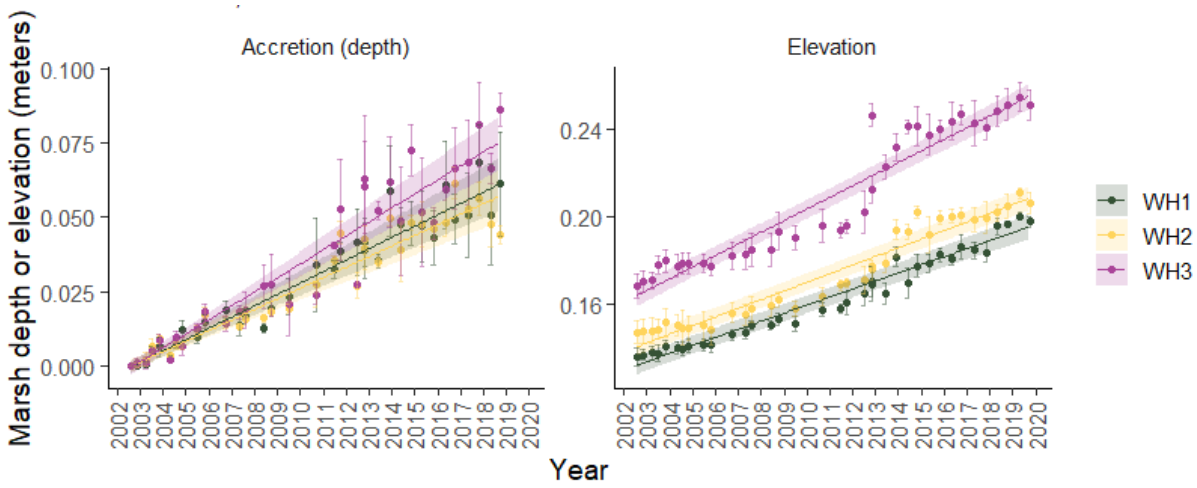


Figure A-68. Accretion and elevation trends at each station for the Watch Hill site at Fire Island National Seashore. Solid line shows the mean of the posterior fitted trend; shaded region around the line bounds the 95% Bayesian credible interval of the fitted trend. Data are shown as means (points) plus and minus the standard deviation (error bars) across all observation locations within the station. Observations were grouped by month for aggregating.

Gateway National Recreation Area

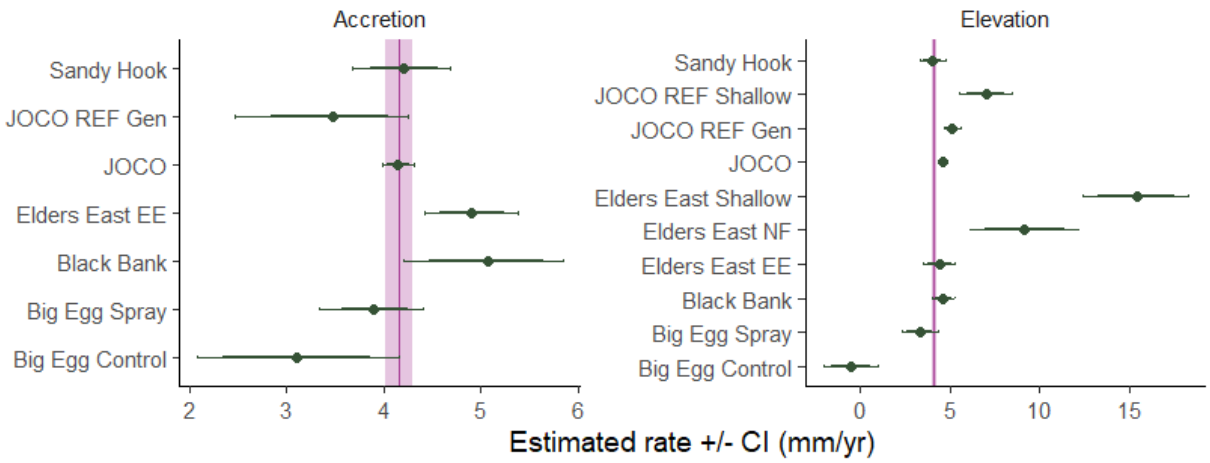


Figure A-69. Estimated accretion and elevation trends at the site level for Gateway National Recreation Area. The estimates are averages of the posteriors of the set-level trend estimates. The point shows the mean of the posterior; the thick error bars show the 85% Bayesian credible interval; the thin error bars show the 95% Bayesian credible interval. The vertical pink line shows the mean estimate of sea level rise and the pink rectangle bounds the 95% confidence interval.

Table A-39. Posterior trends (mean and 95% Bayesian credible interval) and the posterior probabilities that the trends in elevation or accretion are greater than 0 [Pr(trend > 0)], that the trend is greater than the upper bound of sea level rise [Pr(trend > slr)], and that the trend is less than the lower bound of sea level rise [Pr(trend < slr)] at each site in Gateway National Recreation Area. The final column [Pr(trend_i < trend_j)] is the probability that the trend specified in the row (either elevation or accretion) is less than the other estimated trend (either accretion or elevation) at the same site.

Site	Response	Trend estimate (mm/yr)	Pr(trend > 0)	Pr(trend > slr)	Pr(trend < slr)	Pr(trend_i < trend_j)
Big Egg Control	Accretion	3.1 (2.09 – 4.16)	1.00	0.01	0.96	0.00
Big Egg Spray	Accretion	3.9 (3.34 – 4.41)	1.00	0.05	0.72	0.15
Black Bank	Accretion	5.07 (4.2 – 5.84)	1.00	0.96	0.01	0.21
Elders East	Accretion	4.9 (4.43 – 5.37)	1.00	0.99	0.00	0.19
JOCO	Accretion	4.15 (3.98 – 4.32)	1.00	0.04	0.07	1.00
JOCO REF	Accretion	3.48 (2.47 – 4.24)	1.00	0.02	0.92	1.00
Sandy Hook	Accretion	4.21 (3.68 – 4.69)	1.00	0.37	0.21	0.37
Big Egg Control	Elevation	-0.46 (-2 – 1.07)	0.27	0.00	1.00	1.00
Big Egg Spray	Elevation	3.34 (2.36 – 4.35)	1.00	0.03	0.93	0.85
Black Bank	Elevation	4.66 (4.03 – 5.27)	1.00	0.88	0.02	0.79
Elders East	Elevation	4.46 (3.53 – 5.33)	1.00	0.66	0.17	0.81
Elders East NF	Elevation	9.15 (6.14 – 12.11)	1.00	1.00	0.00	NA
Elders East Shallow	Elevation	15.37 (12.41 – 18.23)	1.00	1.00	0.00	NA
JOCO	Elevation	4.65 (4.54 – 4.76)	1.00	1.00	0.00	0.00
JOCO REF	Elevation	5.15 (4.67 – 5.61)	1.00	1.00	0.00	0.00
JOCO REF Shallow	Elevation	7.03 (5.58 – 8.44)	1.00	1.00	0.00	NA
Sandy Hook	Elevation	4.06 (3.34 – 4.77)	1.00	0.25	0.43	0.63

Big Egg Control

Table A-40. Estimated rates of elevation and accretion trends at Big Egg Control in Gateway National Recreation Area. Values in parentheses are the 95% Bayesian credible intervals. Pr(trend > 0) columns report the posterior probability that the estimated trend is greater than zero.

SET	Response	Trend estimate (mm/yr)	Pr(trend > 0)	Pr(trend > slr)	Pr(trend < slr)
BEC1	Accretion	3.3 (2.12 – 4.52)	0.72	0.00	1.00
BEC2	Accretion	3.22 (2 – 4.56)	0.62	0.00	1.00
BEC3	Accretion	2.78 (1.33 – 4.04)	0.35	0.00	1.00
BEC1	Elevation	7.45 (4.44 – 10.1)	1.00	0.94	0.05
BEC2	Elevation	-9.02 (-11.64 – -5.93)	0.00	0.00	1.00
BEC3	Elevation	0.2 (-2.47 – 2.75)	0.57	0.03	0.96
Overall	**Accretion**	**3.1 (2.09 – 4.16)**	**1.00**	**0.01**	**0.96**
Overall	**Elevation**	**-0.46 (-2 – 1.07)**	**0.27**	**0.00**	**1.00**

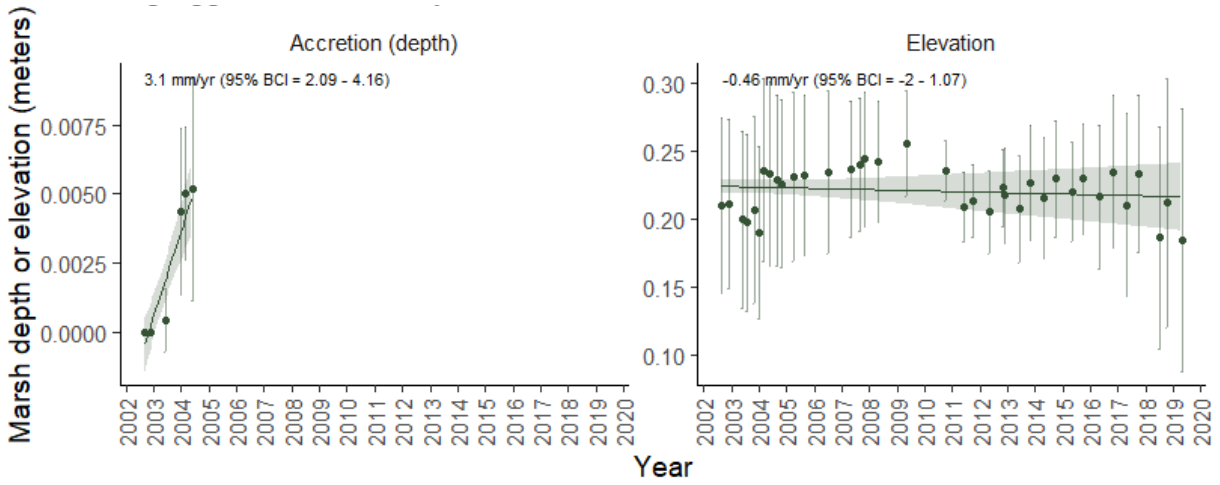


Figure A-70. Overall accretion and elevation trends for the Big Egg Control site at Gateway National Recreation Area. Solid line shows the mean of the posterior fitted trend; shaded region around the line bounds the 95% Bayesian credible interval of the fitted trend. These trend lines were computed using the mean of the intercept posteriors across SETs within the site and the mean of the slope posteriors across SETs within a site. Data are shown as means (points) plus and minus the standard deviation (error bars) across all observation locations within the site. Observations were grouped by month for aggregating.

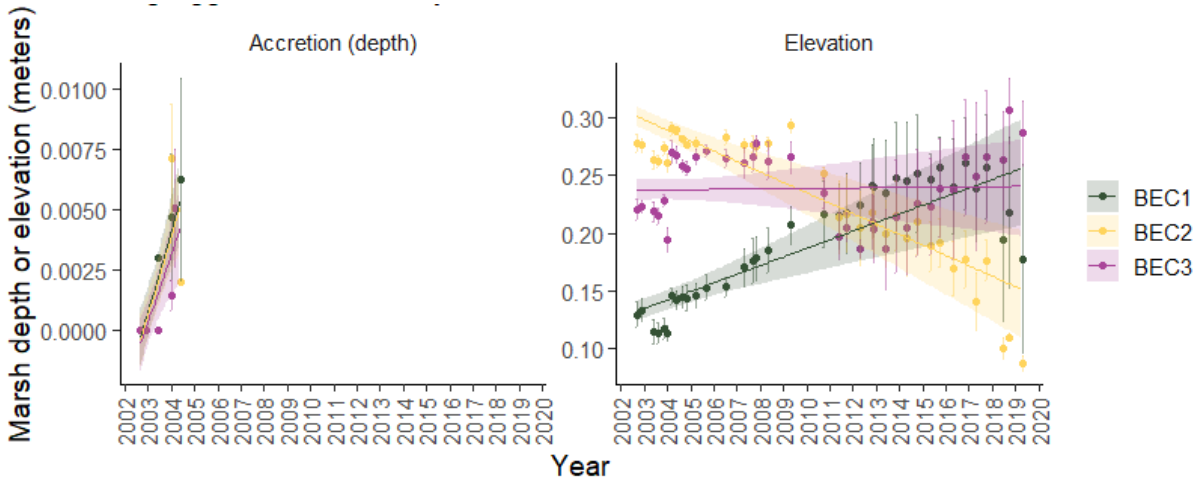


Figure A-71. Accretion and elevation trends at each station for the Big Egg Control site at Gateway National Recreation Area. Solid line shows the mean of the posterior fitted trend; shaded region around the line bounds the 95% Bayesian credible interval of the fitted trend. Data are shown as means (points) plus and minus the standard deviation (error bars) across all observation locations within the station. Observations were grouped by month for aggregating.

Big Egg Spray

Table A-41. Estimated rates of elevation and accretion trends at Big Egg Spray in Gateway National Recreation Area. Values in parentheses are the 95% Bayesian credible intervals. Pr(trend > 0) columns report the posterior probability that the estimated trend is greater than zero.

SET	Response	Trend estimate (mm/yr)	Pr(trend > 0)	Pr(trend > slr)	Pr(trend < slr)
BES1	Accretion	3.72 (2.94 – 4.54)	0.48	0.00	1.00
BES2	Accretion	3.98 (3.3 – 4.55)	0.73	0.00	1.00
BES3	Accretion	3.99 (3.22 – 4.66)	0.72	0.00	1.00
BES1	Elevation	6.5 (3.94 – 8.31)	0.99	0.60	0.35
BES2	Elevation	1.9 (0.17 – 3.58)	0.53	0.02	0.97
BES3	Elevation	1.61 (0.03 – 3.5)	0.46	0.01	0.98
Overall	**Accretion**	**3.9 (3.34 – 4.41)**	**1.00**	**0.05**	**0.72**
Overall	**Elevation**	**3.34 (2.36 – 4.35)**	**1.00**	**0.03**	**0.93**

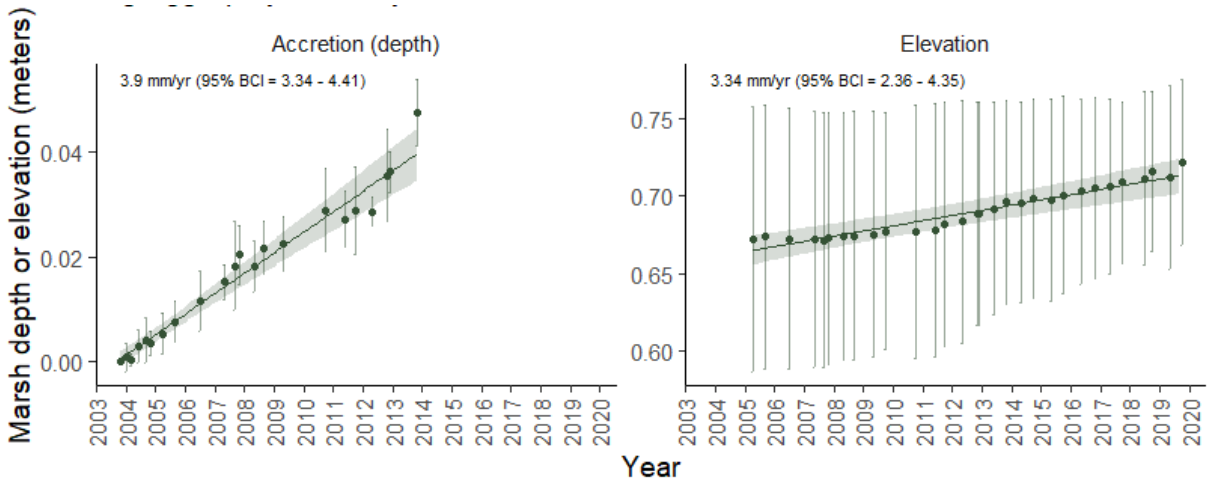


Figure A-72. Overall accretion and elevation trends for the Big Egg Spray site at Gateway National Recreation Area. Solid line shows the mean of the posterior fitted trend; shaded region around the line bounds the 95% Bayesian credible interval of the fitted trend. These trend lines were computed using the mean of the intercept posteriors across SETs within the site and the mean of the slope posteriors across SETs within a site. Data are shown as means (points) plus and minus the standard deviation (error bars) across all observation locations within the site. Observations were grouped by month for aggregating.

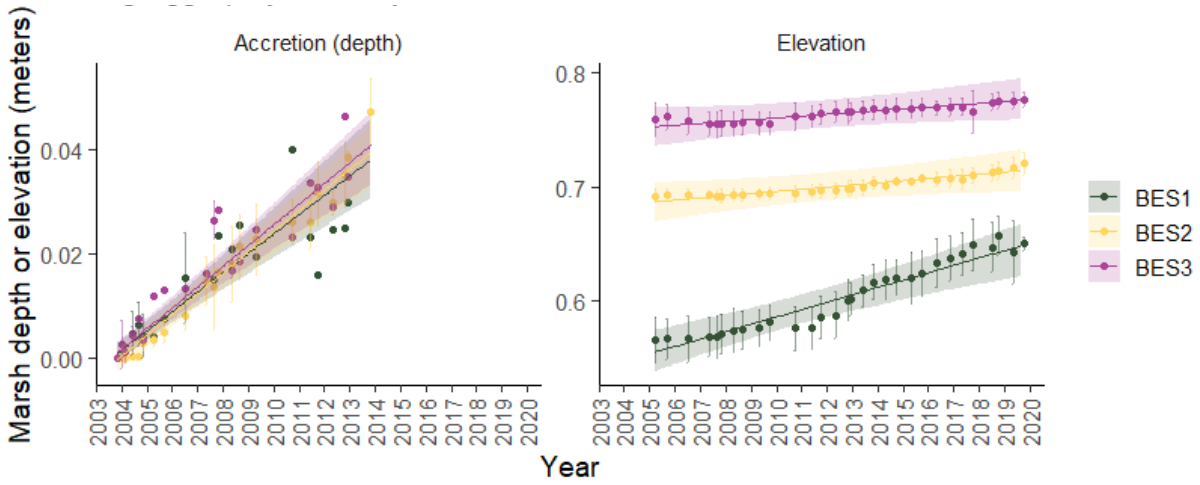


Figure A-73. Accretion and elevation trends at each station for the Big Egg Spray site at Gateway National Recreation Area. Solid line shows the mean of the posterior fitted trend; shaded region around the line bounds the 95% Bayesian credible interval of the fitted trend. Data are shown as means (points) plus and minus the standard deviation (error bars) across all observation locations within the station. Observations were grouped by month for aggregating.

Black Bank

Table A-42. Estimated rates of elevation and accretion trends at Black Bank in Gateway National Recreation Area. Values in parentheses are the 95% Bayesian credible intervals. Pr(trend > 0) columns report the posterior probability that the estimated trend is greater than zero.

SET	Response	Trend estimate (mm/yr)	Pr(trend > 0)	Pr(trend > slr)	Pr(trend < slr)
BB1	Accretion	4.8 (3.71 – 5.82)	0.78	0.06	0.91
BB2	Accretion	4.79 (3.78 – 5.76)	0.78	0.06	0.92
BB3	Accretion	5.63 (4.23 – 7.14)	0.91	0.18	0.79
BB1	Elevation	4.35 (3.39 – 5.25)	0.43	0.00	0.99
BB2	Elevation	4.48 (3.53 – 5.44)	0.51	0.01	0.99
BB3	Elevation	5.15 (4.18 – 6.13)	0.89	0.02	0.98
Overall	**Accretion**	**5.07 (4.2 – 5.84)**	**1.00**	**0.96**	**0.01**
Overall	**Elevation**	**4.66 (4.03 – 5.27)**	**1.00**	**0.88**	**0.02**

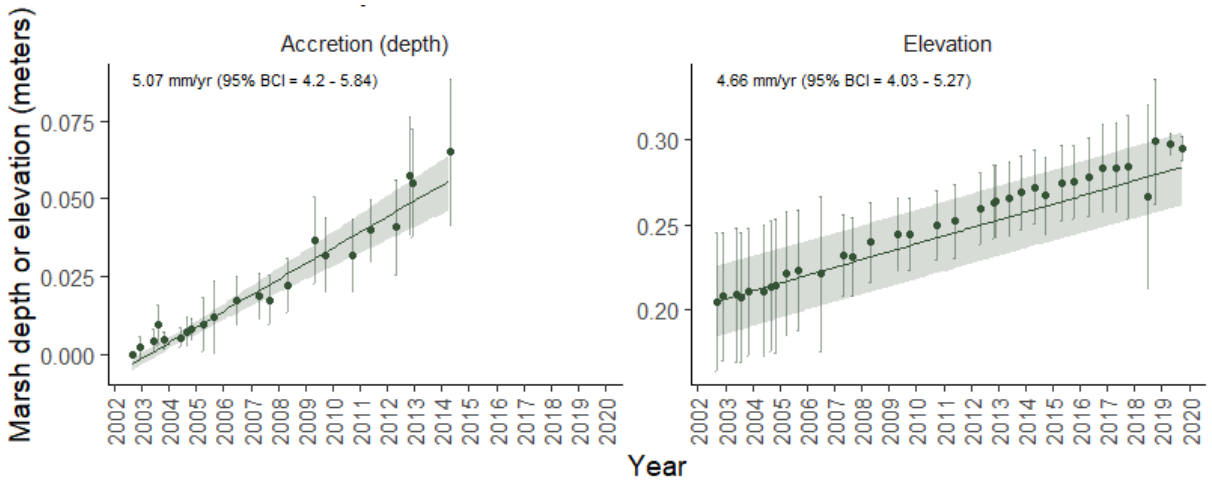


Figure A-74. Overall accretion and elevation trends for the Black Bank site at Gateway National Recreation Area. Solid line shows the mean of the posterior fitted trend; shaded region around the line bounds the 95% Bayesian credible interval of the fitted trend. These trend lines were computed using the mean of the intercept posteriors across SETs within the site and the mean of the slope posteriors across SETs within a site. Data are shown as means (points) plus and minus the standard deviation (error bars) across all observation locations within the site. Observations were grouped by month for aggregating.

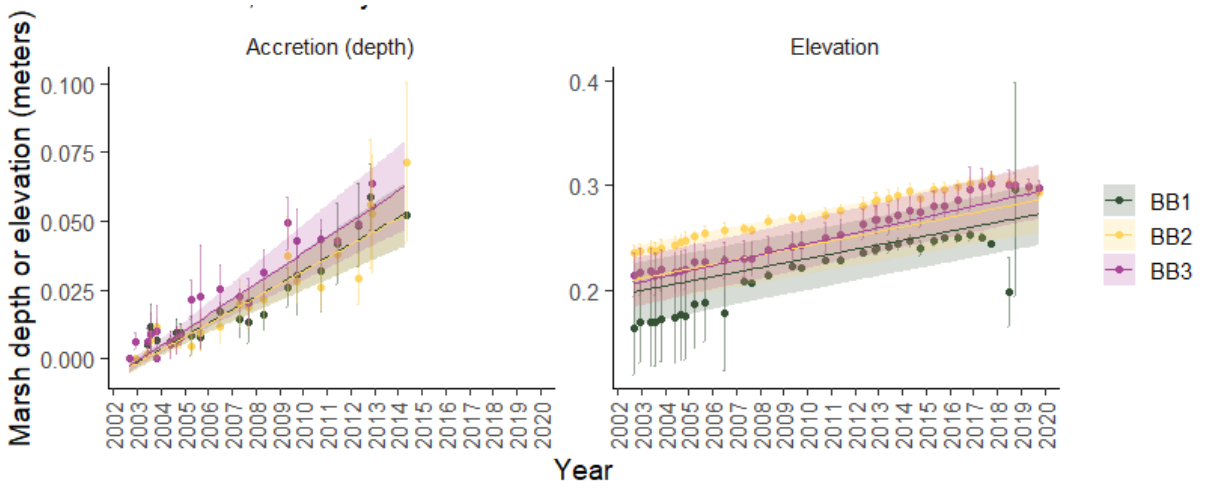


Figure A-75. Accretion and elevation trends at each station for the Black Bank site at Gateway National Recreation Area. Solid line shows the mean of the posterior fitted trend; shaded region around the line bounds the 95% Bayesian credible interval of the fitted trend. Data are shown as means (points) plus and minus the standard deviation (error bars) across all observation locations within the station. Observations were grouped by month for aggregating.

Elders East

Table A-43. Estimated rates of elevation and accretion trends at Elders East in Gateway National Recreation Area. Values in parentheses are the 95% Bayesian credible intervals. Pr(trend > 0) columns report the posterior probability that the estimated trend is greater than zero.

SET	Response	Trend estimate (mm/yr)	Pr(trend > 0)	Pr(trend > slr)	Pr(trend < slr)
EE1	Accretion	4.9 (4.2 – 5.62)	0.67	0.02	0.98
EE2	Accretion	4.82 (4.28 – 5.33)	0.61	0.01	0.98
EE3	Accretion	4.99 (4.42 – 5.58)	0.76	0.02	0.97
EE1	Elevation	4.29 (3.01 – 5.37)	0.46	0.00	1.00
EE2	Elevation	4.61 (3.49 – 5.77)	0.68	0.01	0.99
EE3	Elevation	4.5 (3.41 – 5.55)	0.62	0.00	1.00
Overall	**Accretion**	**4.9 (4.43 – 5.37)**	**1.00**	**0.99**	**0.00**
Overall	**Elevation**	**4.46 (3.53 – 5.33)**	**1.00**	**0.66**	**0.17**

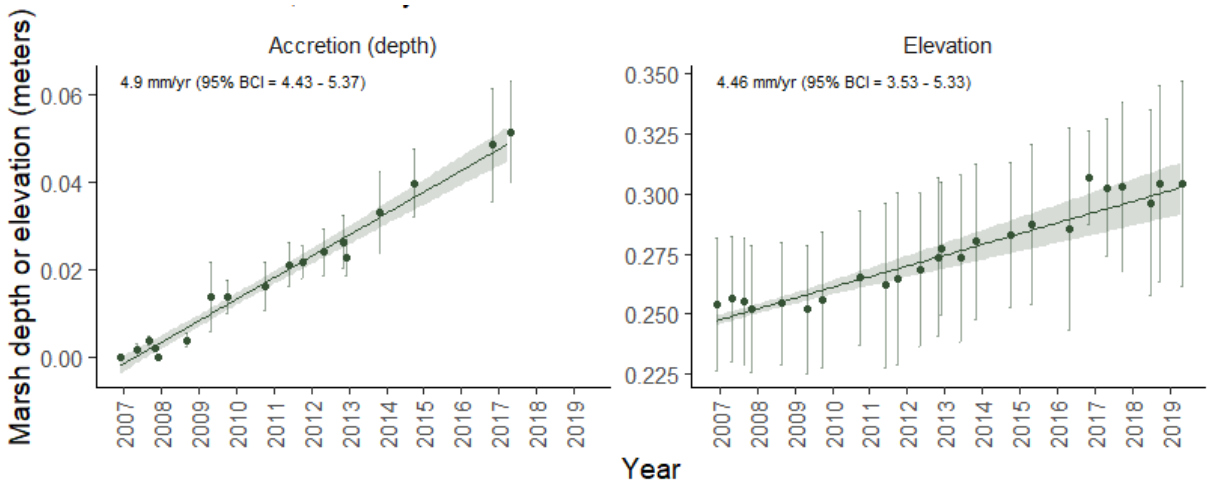


Figure A-76. Overall accretion and elevation trends for the Elders East site at Gateway National Recreation Area. Solid line shows the mean of the posterior fitted trend; shaded region around the line bounds the 95% Bayesian credible interval of the fitted trend. These trend lines were computed using the mean of the intercept posteriors across SETs within the site and the mean of the slope posteriors across SETs within a site. Data are shown as means (points) plus and minus the standard deviation (error bars) across all observation locations within the site. Observations were grouped by month for aggregating.

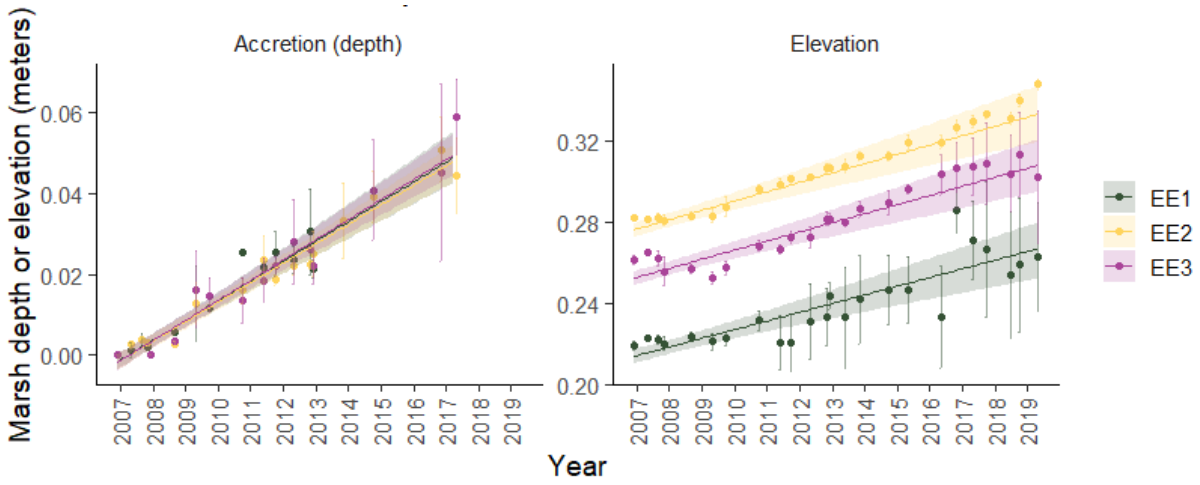


Figure A-77. Accretion and elevation trends at each station for the Elders East site at Gateway National Recreation Area. Solid line shows the mean of the posterior fitted trend; shaded region around the line bounds the 95% Bayesian credible interval of the fitted trend. Data are shown as means (points) plus and minus the standard deviation (error bars) across all observation locations within the station. Observations were grouped by month for aggregating.

Elders East NF

Table A-44. Estimated rates of elevation and accretion trends at Elders East NF in Gateway National Recreation Area. Values in parentheses are the 95% Bayesian credible intervals. Pr(trend > 0) columns report the posterior probability that the estimated trend is greater than zero.

SET	Response	Trend estimate (mm/yr)	Pr(trend > 0)	Pr(trend > slr)	Pr(trend < slr)
EE NF1	Elevation	3.35 (-0.69 – 7.87)	0.74	0.22	0.76
EE NF2	Elevation	16.62 (10.78 – 23.71)	1.00	1.00	0.00
EE NF3	Elevation	7.49 (1.15 – 12.76)	0.96	0.69	0.28
Overall	**Elevation**	**9.15 (6.14 – 12.11)**	**1.00**	**1.00**	**0.00**

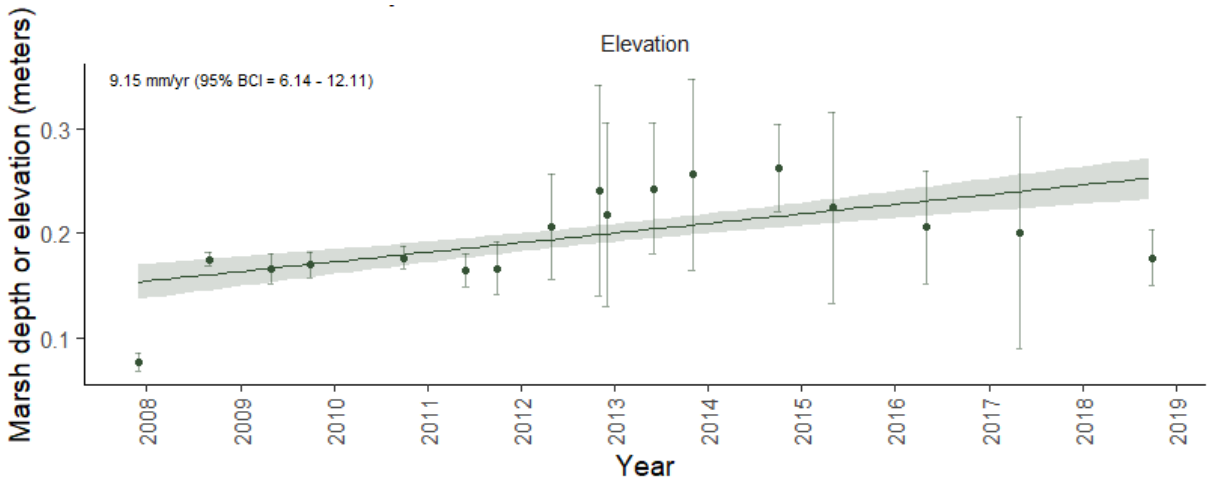


Figure A-78. Overall accretion and elevation trends for the Elders East NF site at Gateway National Recreation Area. Solid line shows the mean of the posterior fitted trend; shaded region around the line bounds the 95% Bayesian credible interval of the fitted trend. These trend lines were computed using the mean of the intercept posteriors across SETs within the site and the mean of the slope posteriors across SETs within a site. Data are shown as means (points) plus and minus the standard deviation (error bars) across all observation locations within the site. Observations were grouped by month for aggregating.

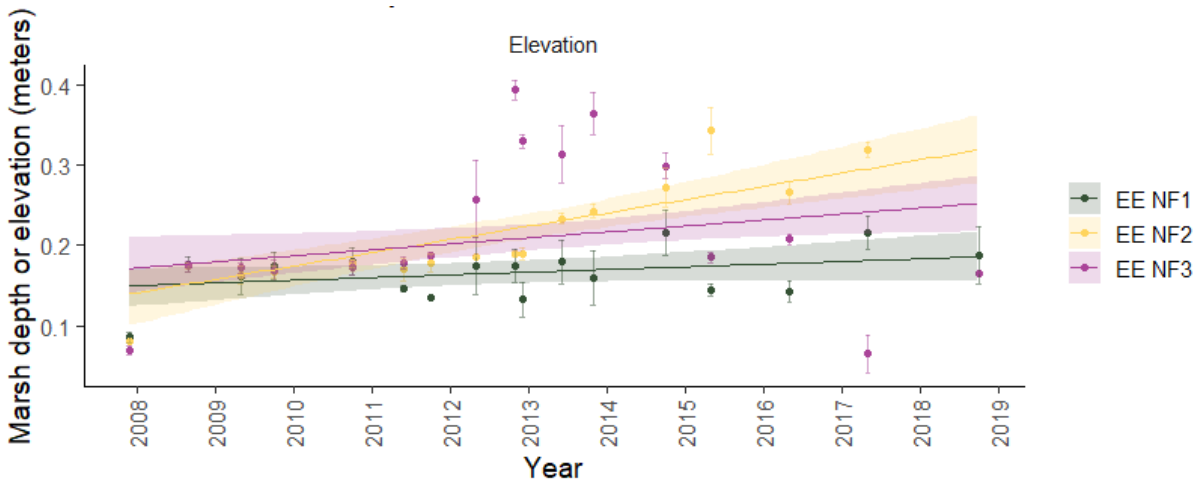


Figure A-79. Accretion and elevation trends at each station for the Elders East NF site at Gateway National Recreation Area. Solid line shows the mean of the posterior fitted trend; shaded region around the line bounds the 95% Bayesian credible interval of the fitted trend. Data are shown as means (points) plus and minus the standard deviation (error bars) across all observation locations within the station. Observations were grouped by month for aggregating.

Elders East Shallow

Table A-45. Estimated rates of elevation and accretion trends at Elders East Shallow in Gateway National Recreation Area. Values in parentheses are the 95% Bayesian credible intervals. Pr(trend > 0) columns report the posterior probability that the estimated trend is greater than zero.

SET	Response	Trend estimate (mm/yr)	Pr(trend > 0)	Pr(trend > slr)	Pr(trend < slr)
EE1 Shallow	Elevation	24.53 (17.89 – 31.12)	1	1.00	0.00
EE2 Shallow	Elevation	10.64 (6.85 – 14.27)	1	0.97	0.03
EE3 Shallow	Elevation	10.95 (7.28 – 14.66)	1	0.98	0.02
Overall	**Elevation**	**15.37 (12.41 – 18.23)**	**1**	**1.00**	**0.00**

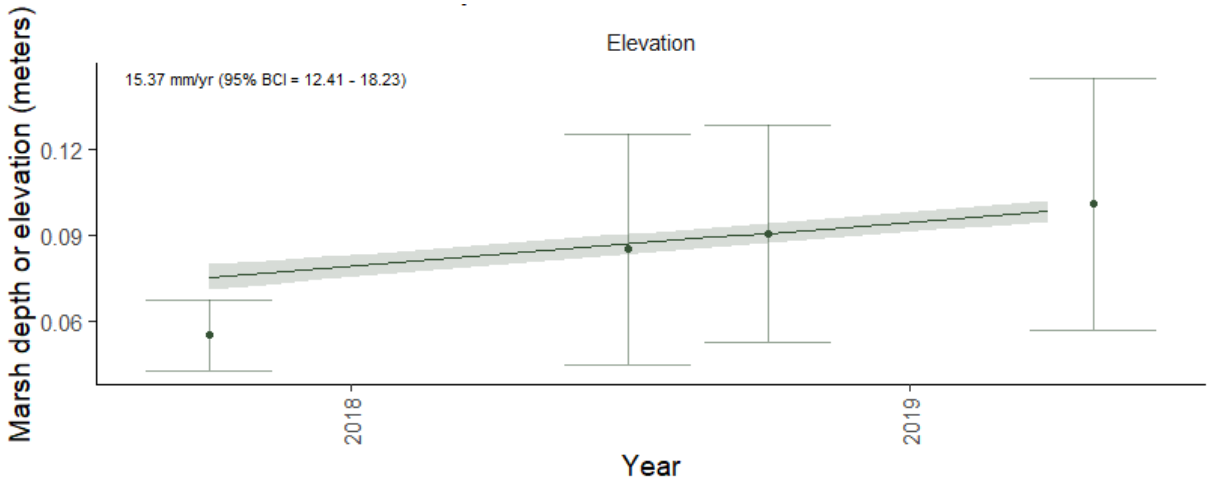


Figure A-80. Overall accretion and elevation trends for the Elders East Shallow site at Gateway National Recreation Area. Solid line shows the mean of the posterior fitted trend; shaded region around the line bounds the 95% Bayesian credible interval of the fitted trend. These trend lines were computed using the mean of the intercept posteriors across SETs within the site and the mean of the slope posteriors across SETs within a site. Data are shown as means (points) plus and minus the standard deviation (error bars) across all observation locations within the site. Observations were grouped by month for aggregating.

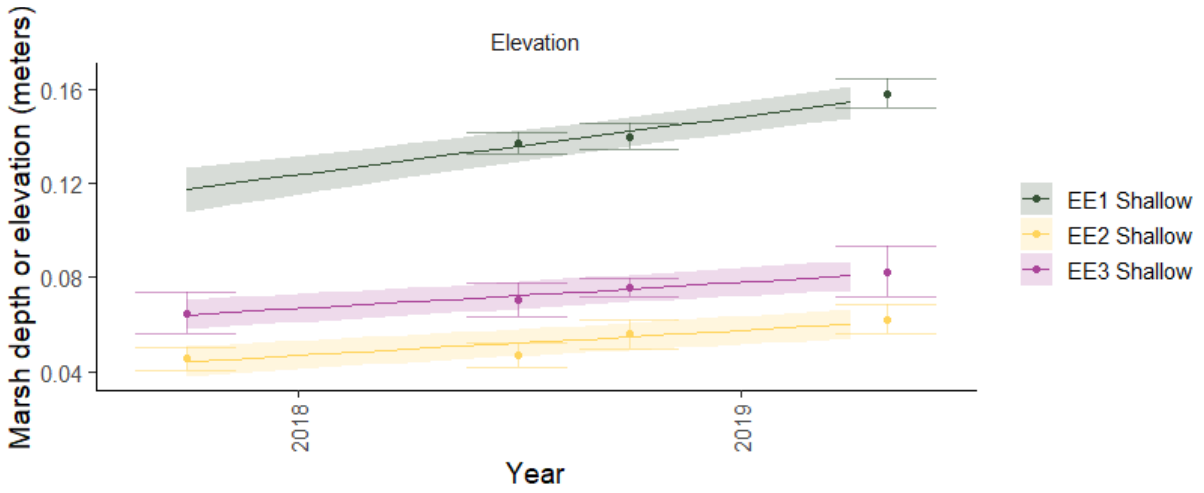


Figure A-81. Accretion and elevation trends at each station for the Elders East Shallow site at Gateway National Recreation Area. Solid line shows the mean of the posterior fitted trend; shaded region around the line bounds the 95% Bayesian credible interval of the fitted trend. Data are shown as means (points) plus and minus the standard deviation (error bars) across all observation locations within the station. Observations were grouped by month for aggregating.

JOCO

Table A-46. Estimated rates of elevation and accretion trends at JOCO in Gateway National Recreation Area. Values in parentheses are the 95% Bayesian credible intervals. Pr(trend > 0) columns report the posterior probability that the estimated trend is greater than zero.

SET	Response	Trend estimate (mm/yr)	Pr(trend > 0)	Pr(trend > slr)	Pr(trend < slr)
Joco1	Accretion	4.14 (3.89 – 4.39)	0.92	0.03	0.94
Joco2	Accretion	4 (3.74 – 4.25)	0.86	0.02	0.96
Joco3	Accretion	4.31 (4.03 – 4.59)	0.97	0.05	0.92
Joco1	Elevation	4.35 (4.17 – 4.57)	0.26	0.00	1.00
Joco2	Elevation	4.56 (4.37 – 4.75)	0.49	0.00	1.00
Joco3	Elevation	5.04 (4.81 – 5.23)	0.96	0.00	1.00
Overall	**Accretion**	**4.15 (3.98 – 4.32)**	**1.00**	**0.04**	**0.07**
Overall	**Elevation**	**4.65 (4.54 – 4.76)**	**1.00**	**1.00**	**0.00**

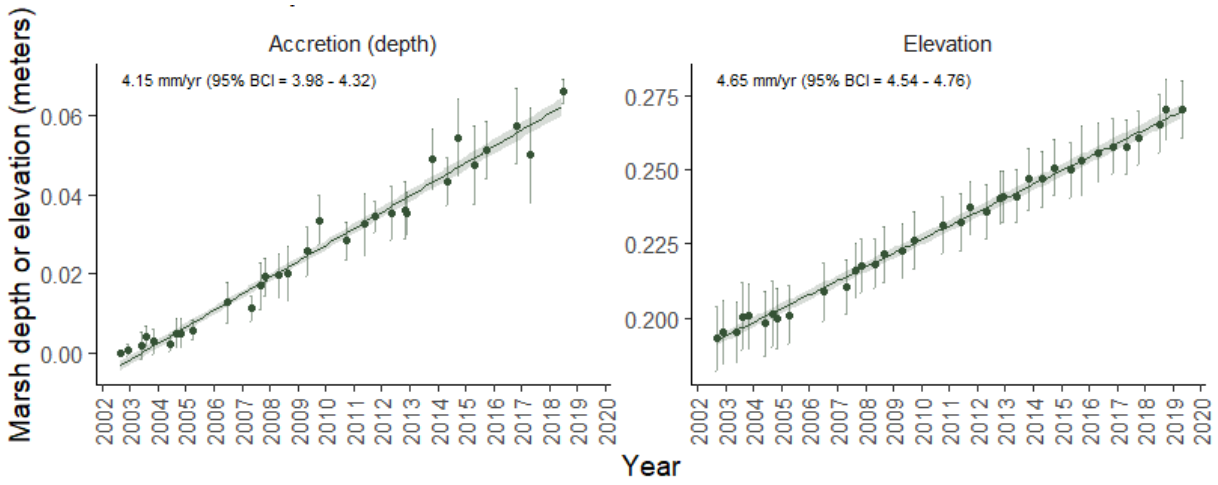


Figure A-82. Overall accretion and elevation trends for the JOCO site at Gateway National Recreation Area. Solid line shows the mean of the posterior fitted trend; shaded region around the line bounds the 95% Bayesian credible interval of the fitted trend. These trend lines were computed using the mean of the intercept posteriors across SETs within the site and the mean of the slope posteriors across SETs within a site. Data are shown as means (points) plus and minus the standard deviation (error bars) across all observation locations within the site. Observations were grouped by month for aggregating.

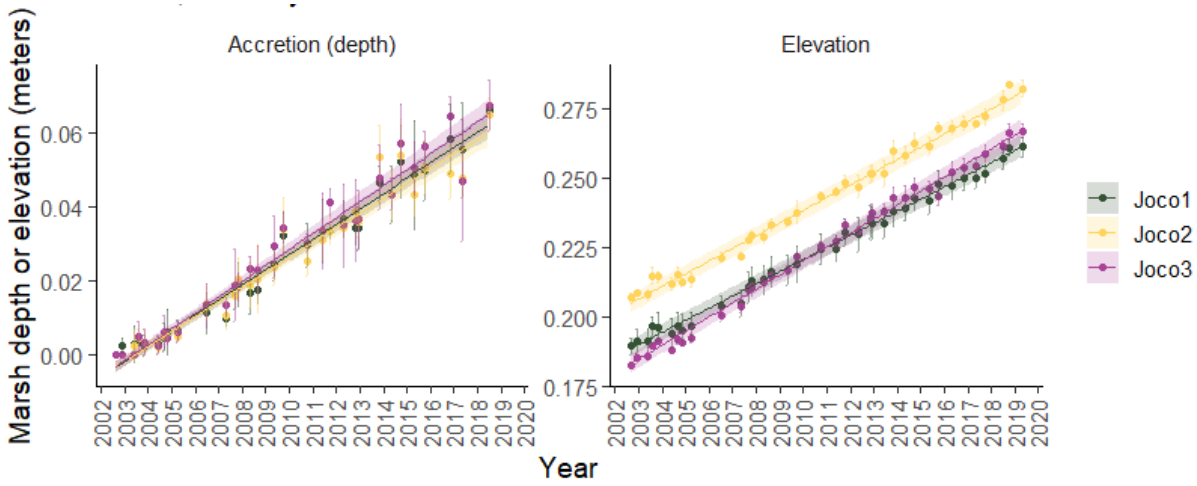


Figure A-83. Accretion and elevation trends at each station for the JOCO site at Gateway National Recreation Area. Solid line shows the mean of the posterior fitted trend; shaded region around the line bounds the 95% Bayesian credible interval of the fitted trend. Data are shown as means (points) plus and minus the standard deviation (error bars) across all observation locations within the station. Observations were grouped by month for aggregating.

JOCO REF

Table A-47. Estimated rates of elevation and accretion trends at JOCO REF in Gateway National Recreation Area. Values in parentheses are the 95% Bayesian credible intervals. Pr(trend > 0) columns report the posterior probability that the estimated trend is greater than zero.

SET	Response	Trend estimate (mm/yr)	Pr(trend > 0)	Pr(trend > slr)	Pr(trend < slr)
JocoRef1	Accretion	3.63 (2.34 – 4.83)	0.78	0.01	0.98
JocoRef2	Accretion	3.27 (1.96 – 4.28)	0.61	0.00	0.99
JocoRef3	Accretion	3.52 (2.32 – 4.56)	0.74	0.01	0.99
JocoRef1	Elevation	5.3 (4.63 – 6.02)	0.74	0.00	0.99
JocoRef2	Elevation	4.95 (4.24 – 5.54)	0.39	0.00	1.00
JocoRef3	Elevation	5.2 (4.54 – 5.89)	0.64	0.01	0.99
Overall	**Accretion**	**3.48 (2.47 – 4.24)**	**1.00**	**0.02**	**0.92**
Overall	**Elevation**	**5.15 (4.67 – 5.61)**	**1.00**	**1.00**	**0.00**

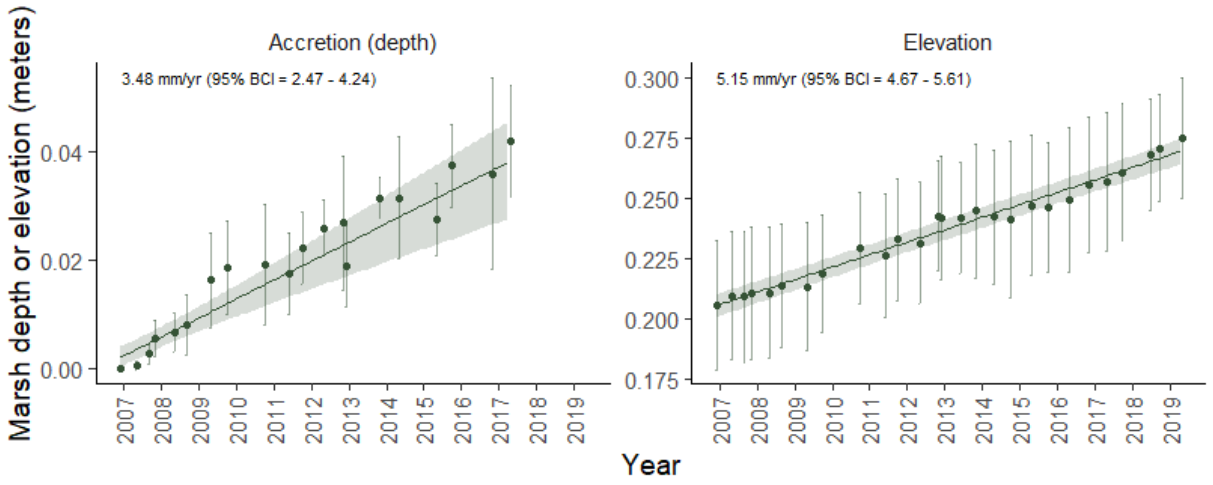


Figure A-84. Overall accretion and elevation trends for the JOCO REF site at Gateway National Recreation Area. Solid line shows the mean of the posterior fitted trend; shaded region around the line bounds the 95% Bayesian credible interval of the fitted trend. These trend lines were computed using the mean of the intercept posteriors across SETs within the site and the mean of the slope posteriors across SETs within a site. Data are shown as means (points) plus and minus the standard deviation (error bars) across all observation locations within the site. Observations were grouped by month for aggregating.

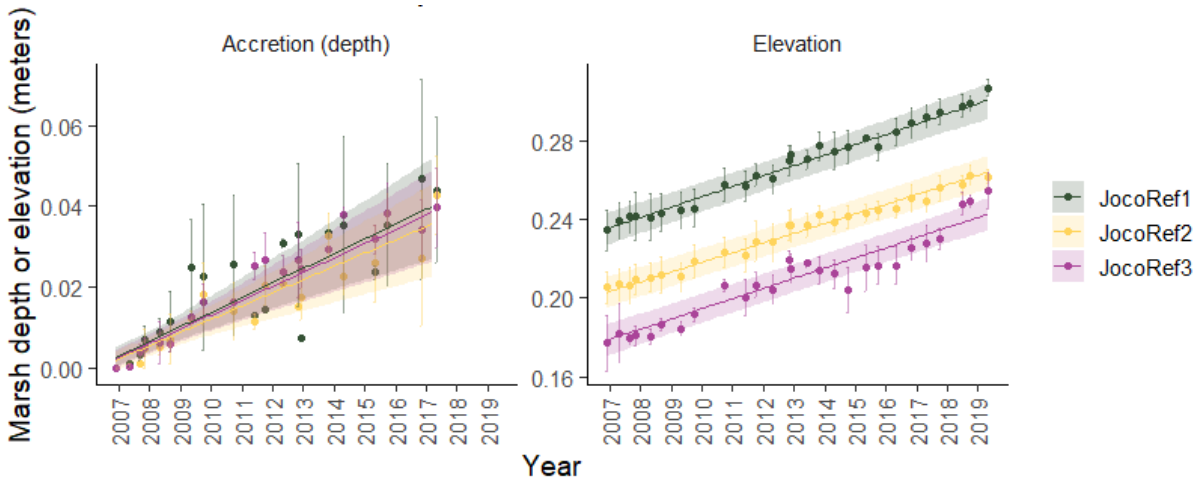


Figure A-85. Accretion and elevation trends at each station for the JOCO REF site at Gateway National Recreation Area. Solid line shows the mean of the posterior fitted trend; shaded region around the line bounds the 95% Bayesian credible interval of the fitted trend. Data are shown as means (points) plus and minus the standard deviation (error bars) across all observation locations within the station. Observations were grouped by month for aggregating.

JOCO REF Shallow

Table A-48. Estimated rates of elevation and accretion trends at JOCO REF Shallow in Gateway National Recreation Area. Values in parentheses are the 95% Bayesian credible intervals. Pr(trend > 0) columns report the posterior probability that the estimated trend is greater than zero.

SET	Response	Trend estimate (mm/yr)	Pr(trend > 0)	Pr(trend > slr)	Pr(trend < slr)
JocoRef1 Shallow	Elevation	7.69 (5.49 – 10.28)	0.85	0.24	0.75
JocoRef2 Shallow	Elevation	6.88 (4.95 – 8.87)	0.74	0.16	0.82
JocoRef3 Shallow	Elevation	6.53 (4.58 – 8.3)	0.67	0.12	0.86
Overall	**Elevation**	**7.03 (5.58 – 8.44)**	**1.00**	**1.00**	**0.00**

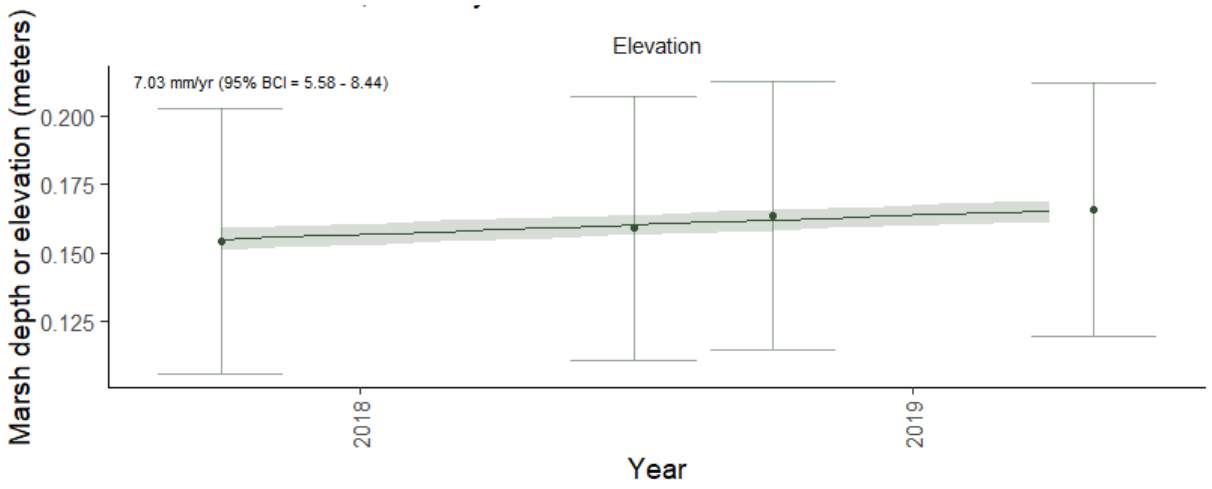


Figure A-86. Overall accretion and elevation trends for the JOCO REF Shallow site at Gateway National Recreation Area. Solid line shows the mean of the posterior fitted trend; shaded region around the line bounds the 95% Bayesian credible interval of the fitted trend. These trend lines were computed using the mean of the intercept posteriors across SETs within the site and the mean of the slope posteriors across SETs within a site. Data are shown as means (points) plus and minus the standard deviation (error bars) across all observation locations within the site. Observations were grouped by month for aggregating.

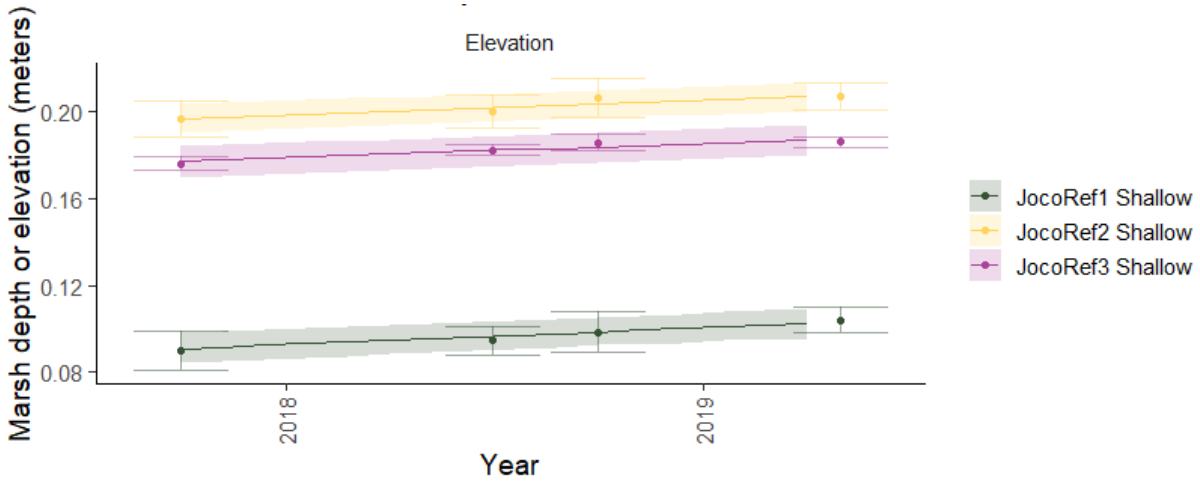


Figure A-87. Accretion and elevation trends at each station for the JOCO REF Shallow site at Gateway National Recreation Area. Solid line shows the mean of the posterior fitted trend; shaded region around the line bounds the 95% Bayesian credible interval of the fitted trend. Data are shown as means (points) plus and minus the standard deviation (error bars) across all observation locations within the station. Observations were grouped by month for aggregating.

Sandy Hook

Table A-49. Estimated rates of elevation and accretion trends at Sandy Hook in Gateway National Recreation Area. Values in parentheses are the 95% Bayesian credible intervals. Pr(Trend > 0) columns report the posterior probability that the estimated trend is greater than zero.

SET	Response	Trend estimate (mm/yr)	Pr(trend > 0)	Pr(trend > slr)	Pr(trend < slr)
SH1	Accretion	4.7 (3.86 – 5.48)	1.00	0.54	0.36
SH2	Accretion	4.5 (3.66 – 5.32)	1.00	0.45	0.43
SH3	Accretion	3.43 (2.53 – 4.25)	1.00	0.12	0.82
SH1	Elevation	4.92 (3.52 – 6.39)	0.94	0.10	0.88
SH2	Elevation	5.16 (3.93 – 6.22)	0.98	0.11	0.87
SH3	Elevation	2.11 (0.54 – 3.69)	0.23	0.00	1.00
Overall	**Accretion**	**4.21 (3.68 – 4.69)**	**1.00**	**0.37**	**0.21**
Overall	**Elevation**	**4.06 (3.34 – 4.77)**	**1.00**	**0.25**	**0.43**

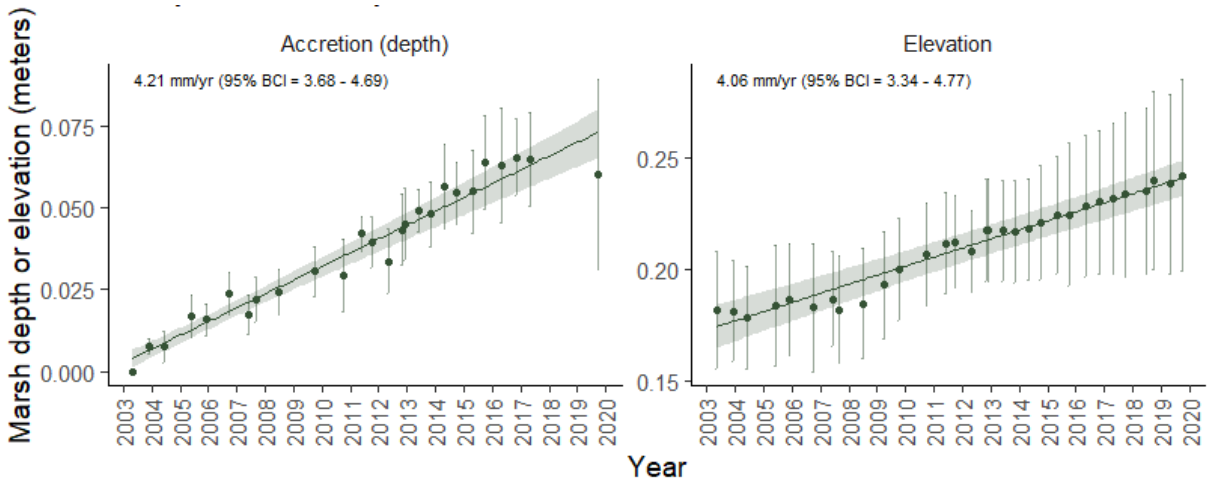


Figure A-88. Overall accretion and elevation trends for the Sandy Hook site at Gateway National Recreation Area. Solid line shows the mean of the posterior fitted trend; shaded region around the line bounds the 95% Bayesian credible interval of the fitted trend. These trend lines were computed using the mean of the intercept posteriors across SETs within the site and the mean of the slope posteriors across SETs within a site. Data are shown as means (points) plus and minus the standard deviation (error bars) across all observation locations within the site. Observations were grouped by month for aggregating.

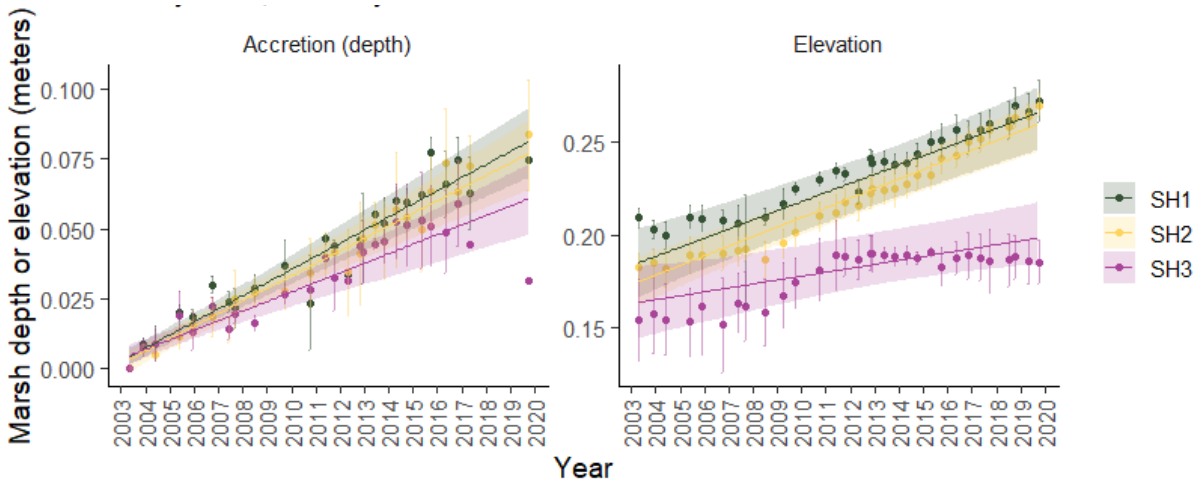


Figure A-89. Accretion and elevation trends at each station for the Sandy Hook site at Gateway National Recreation Area. Solid line shows the mean of the posterior fitted trend; shaded region around the line bounds the 95% Bayesian credible interval of the fitted trend. Data are shown as means (points) plus and minus the standard deviation (error bars) across all observation locations within the station. Observations were grouped by month for aggregating.

George Washington Memorial Parkway

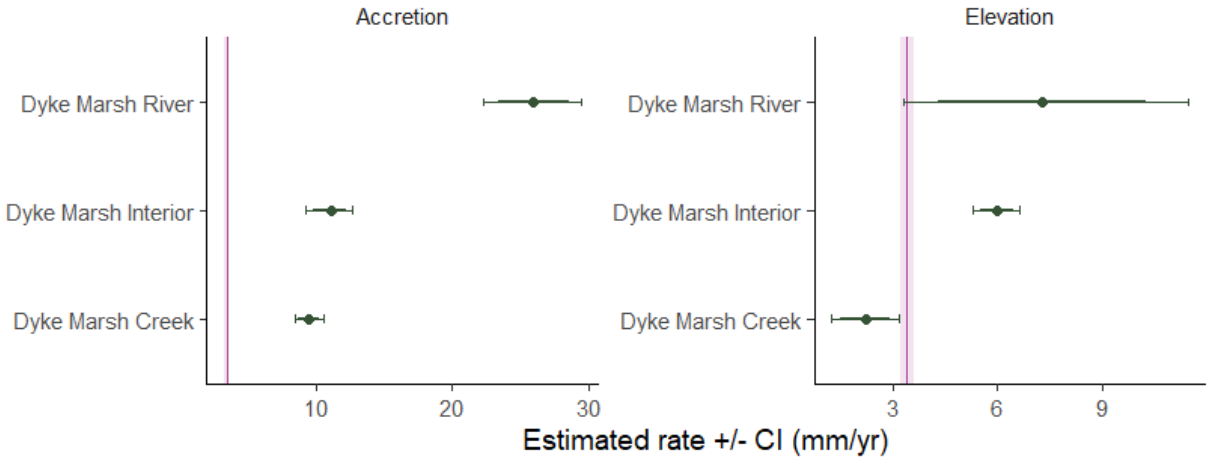


Figure A-90. Estimated accretion and elevation trends at the site level for George Washington Memorial Parkway. The estimates are averages of the posteriors of the set-level trend estimates. The point shows the mean of the posterior; the thick error bars show the 85% Bayesian credible interval; the thin error bars show the 95% Bayesian credible interval. The vertical pink line shows the mean estimate of sea level rise and the pink rectangle bounds the 95% confidence interval.

Table A-50. Posterior trends (mean and 95% Bayesian credible interval) and the posterior probabilities that the trends in elevation or accretion are greater than 0 [Pr(trend > 0)], that the trend is greater than the upper bound of sea level rise [Pr(trend > slr)], and that the trend is less than the lower bound of sea level rise [Pr(trend < slr)] at each site in George Washington Memorial Parkway. The final column [Pr(trend_i < trend_j)] is the probability that the trend specified in the row (either elevation or accretion) is less than the other estimated trend (either accretion or elevation) at the same site.

Site	Response	Trend estimate (mm/yr)	Pr(trend > 0)	Pr(trend > slr)	Pr(trend < slr)	Pr(trend_i < trend_j)
Dyke Marsh Creek	Accretion	9.48 (8.44 – 10.59)	1	1.00	0.00	0
Dyke Marsh Interior	Accretion	11.05 (9.23 – 12.67)	1	1.00	0.00	0
Dyke Marsh River	Accretion	25.99 (22.32 – 29.48)	1	1.00	0.00	0
Dyke Marsh Creek	Elevation	2.23 (1.27 – 3.21)	1	0.00	0.98	1
Dyke Marsh Interior	Elevation	5.98 (5.29 – 6.61)	1	1.00	0.00	1
Dyke Marsh River	Elevation	7.28 (3.31 – 11.45)	1	0.96	0.02	1

Dyke Marsh Creek

Table A-51. Estimated rates of elevation and accretion trends at Dyke Marsh Creek in George Washington Memorial Parkway. Values in parentheses are the 95% Bayesian credible intervals. Pr(trend > 0) columns report the posterior probability that the estimated trend is greater than zero.

SET	Response	Trend estimate (mm/yr)	Pr(trend > 0)	Pr(trend > slr)	Pr(trend < slr)
Creek Bank 1	Accretion	5.64 (4.28 – 7.08)	1.00	1.00	0.00
Creek Bank 2	Accretion	10.67 (9.08 – 12.36)	1.00	1.00	0.00
Creek Bank 3	Accretion	12.12 (10.64 – 13.6)	1.00	1.00	0.00
Creek Bank 1	Elevation	3.57 (1.89 – 5.25)	0.94	0.16	0.78
Creek Bank 2	Elevation	4.22 (2.51 – 5.83)	0.98	0.27	0.64
Creek Bank 3	Elevation	-1.11 (-2.79 – 0.82)	0.04	0.00	1.00
Overall	**Accretion**	**9.48 (8.44 – 10.59)**	**1.00**	**1.00**	**0.00**
Overall	**Elevation**	**2.23 (1.27 – 3.21)**	**1.00**	**0.00**	**0.98**

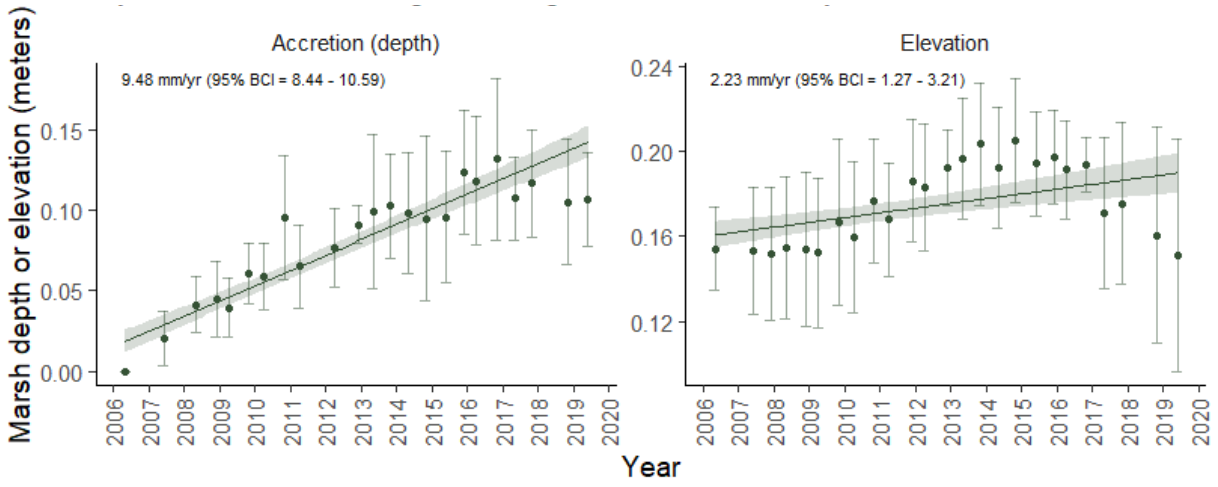


Figure A-91. Overall accretion and elevation trends for the Dyke Marsh Creek site at George Washington Memorial Parkway. Solid line shows the mean of the posterior fitted trend; shaded region around the line bounds the 95% Bayesian credible interval of the fitted trend. These trend lines were computed using the mean of the intercept posteriors across SETs within the site and the mean of the slope posteriors across SETs within a site. Data are shown as means (points) plus and minus the standard deviation (error bars) across all observation locations within the site. Observations were grouped by month for aggregating.

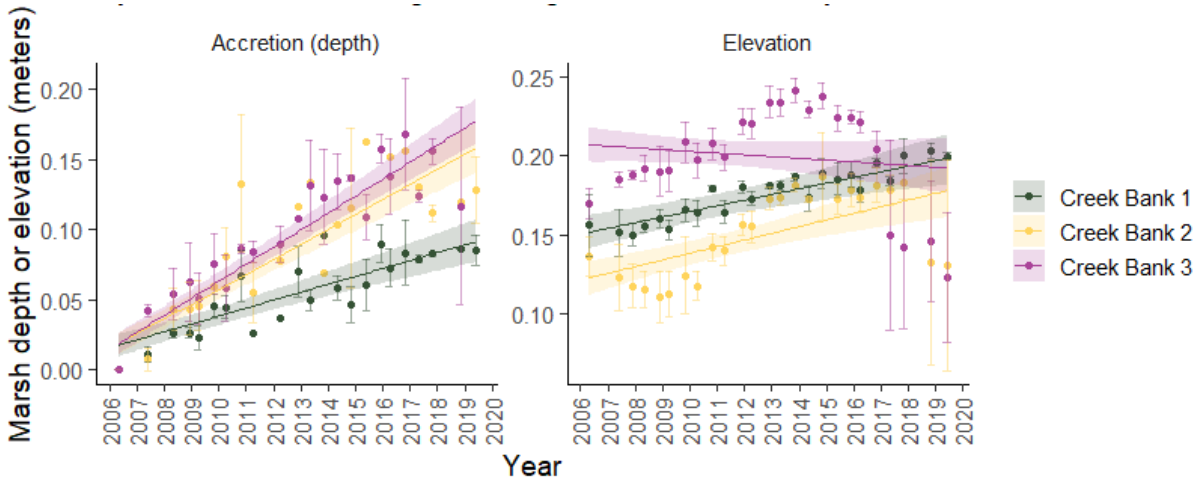


Figure A-92. Accretion and elevation trends at each station for the Dyke Marsh Creek site at George Washington Memorial Parkway. Solid line shows the mean of the posterior fitted trend; shaded region around the line bounds the 95% Bayesian credible interval of the fitted trend. Data are shown as means (points) plus and minus the standard deviation (error bars) across all observation locations within the station. Observations were grouped by month for aggregating.

Dyke Marsh Interior

Table A-52. Estimated rates of elevation and accretion trends at Dyke Marsh Interior in George Washington Memorial Parkway. Values in parentheses are the 95% Bayesian credible intervals. Pr(Trend > 0) columns report the posterior probability that the estimated trend is greater than zero.

SET	Response	Trend estimate (mm/yr)	Pr(trend > 0)	Pr(trend > slr)	Pr(trend < slr)
Interior 1	Accretion	8.17 (5.34 – 10.99)	1.00	1.00	0.00
Interior 2	Accretion	12.1 (9.09 – 14.95)	1.00	1.00	0.00
Interior 3	Accretion	12.87 (9.79 – 15.65)	1.00	1.00	0.00
Interior 1	Elevation	3.75 (2.66 – 4.89)	0.43	0.06	0.92
Interior 2	Elevation	6.78 (5.67 – 7.88)	0.99	0.35	0.59
Interior 3	Elevation	7.4 (6.25 – 8.54)	1.00	0.46	0.48
Overall	**Accretion**	**11.05 (9.23 – 12.67)**	**1.00**	**1.00**	**0.00**
Overall	**Elevation**	**5.98 (5.29 – 6.61)**	**1.00**	**1.00**	**0.00**

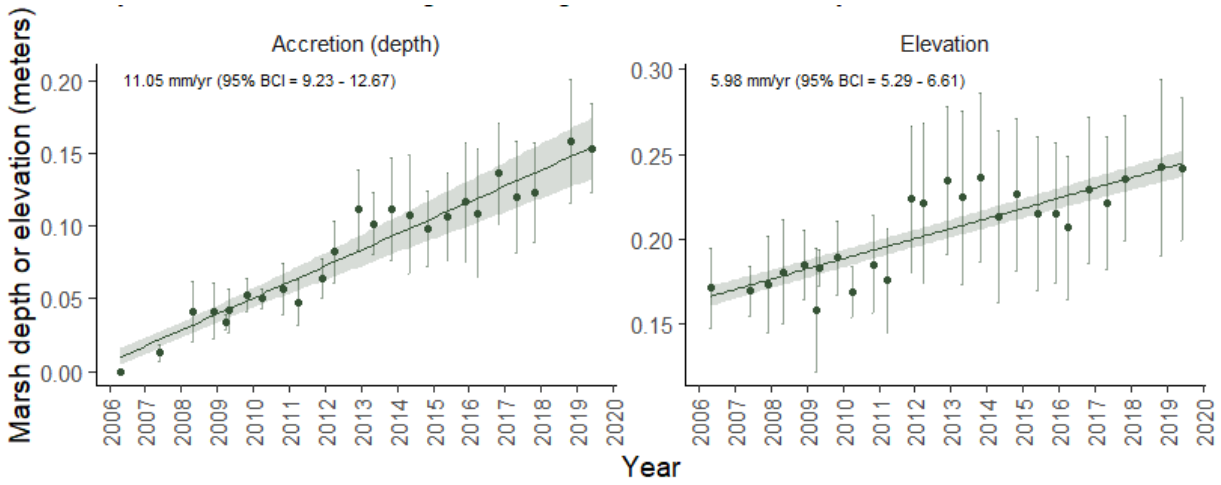


Figure A-93. Overall accretion and elevation trends for the Dyke Marsh Interior site at George Washington Memorial Parkway. Solid line shows the mean of the posterior fitted trend; shaded region around the line bounds the 95% Bayesian credible interval of the fitted trend. These trend lines were computed using the mean of the intercept posteriors across SETs within the site and the mean of the slope posteriors across SETs within a site. Data are shown as means (points) plus and minus the standard deviation (error bars) across all observation locations within the site. Observations were grouped by month for aggregating.

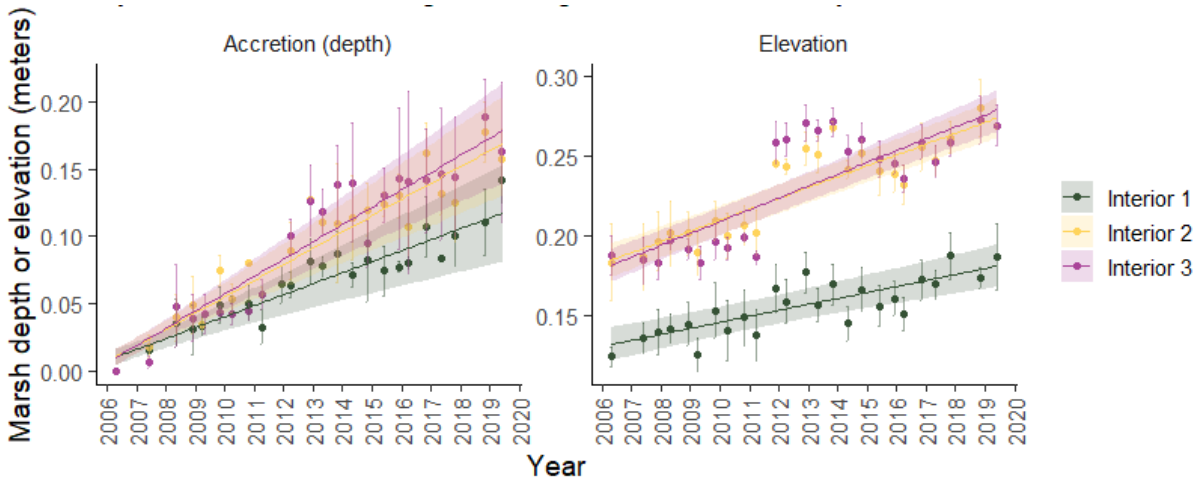


Figure A-94. Accretion and elevation trends at each station for the Dyke Marsh Interior site at George Washington Memorial Parkway. Solid line shows the mean of the posterior fitted trend; shaded region around the line bounds the 95% Bayesian credible interval of the fitted trend. Data are shown as means (points) plus and minus the standard deviation (error bars) across all observation locations within the station. Observations were grouped by month for aggregating.

Dyke Marsh River

Table A-53. Estimated rates of elevation and accretion trends at Dyke Marsh River in George Washington Memorial Parkway. Values in parentheses are the 95% Bayesian credible intervals. Pr(trend > 0) columns report the posterior probability that the estimated trend is greater than zero.

SET	Response	Trend estimate (mm/yr)	Pr(trend > 0)	Pr(trend > slr)	Pr(trend < slr)
River 1	Accretion	14.51 (6.18 – 23.06)	1.00	1.00	0.00
River 1A	Accretion	16.05 (12.83 – 19.15)	1.00	1.00	0.00
River 2	Accretion	32.63 (27.24 – 38.16)	1.00	1.00	0.00
River 3	Accretion	40.76 (37.67 – 43.85)	1.00	1.00	0.00
River 1	Elevation	-2.25 (-10.61 – 7.82)	0.24	0.08	0.91
River 1A	Elevation	1.46 (-2.54 – 5.17)	0.60	0.14	0.83
River 2	Elevation	6.81 (0.91 – 12.87)	0.96	0.75	0.22
River 3	Elevation	23.08 (19.5 – 26.54)	1.00	1.00	0.00
Overall	**Accretion**	**25.99 (22.32 – 29.48)**	**1.00**	**1.00**	**0.00**
Overall	**Elevation**	**7.28 (3.31 – 11.45)**	**1.00**	**0.96**	**0.02**

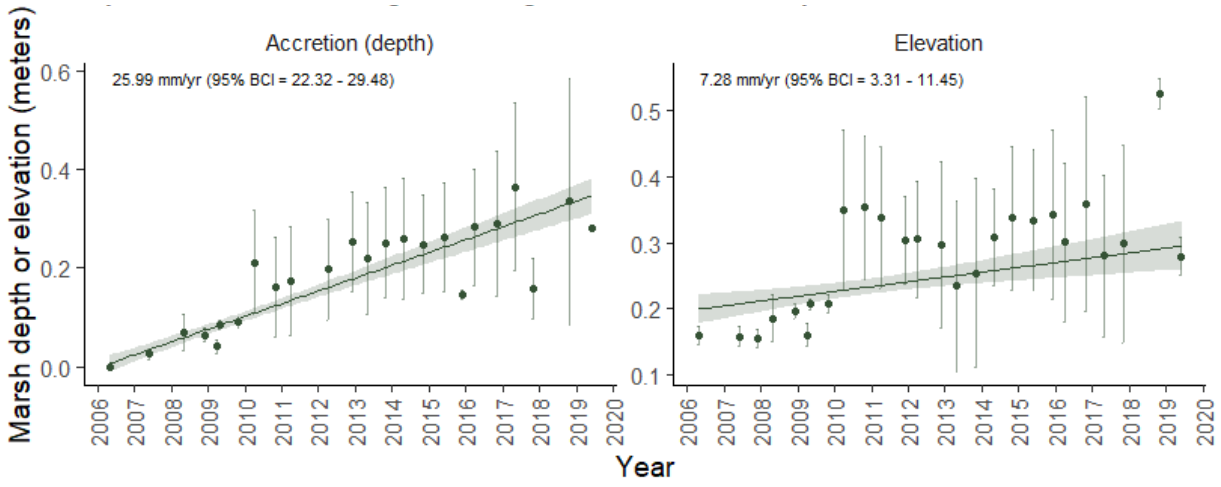


Figure A-95. Overall accretion and elevation trends for the Dyke Marsh River site at George Washington Memorial Parkway. Solid line shows the mean of the posterior fitted trend; shaded region around the line bounds the 95% Bayesian credible interval of the fitted trend. These trend lines were computed using the mean of the intercept posteriors across SETs within the site and the mean of the slope posteriors across SETs within a site. Data are shown as means (points) plus and minus the standard deviation (error bars) across all observation locations within the site. Observations were grouped by month for aggregating.

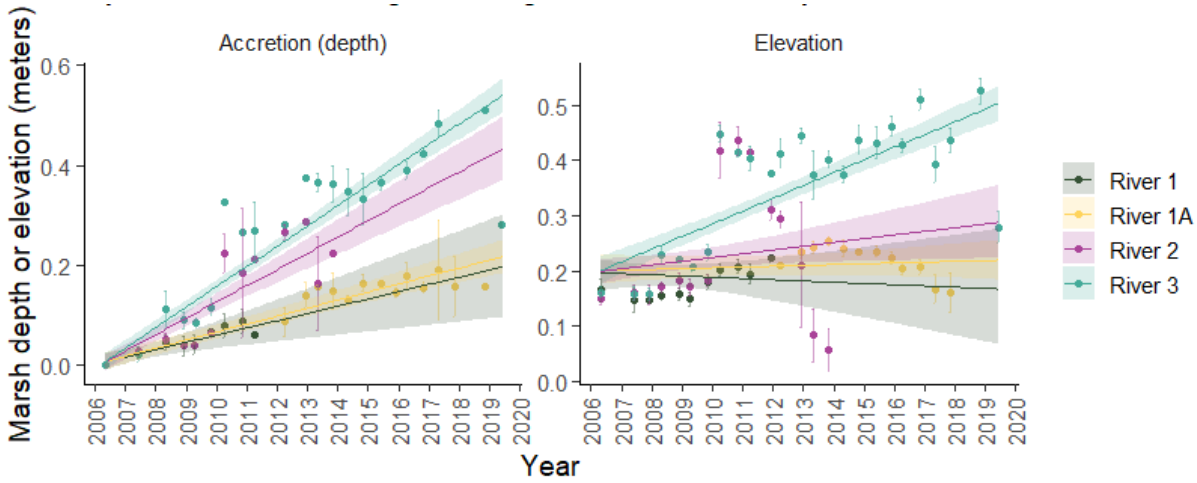


Figure A-96. Accretion and elevation trends at each station for the Dyke Marsh River site at George Washington Memorial Parkway. Solid line shows the mean of the posterior fitted trend; shaded region around the line bounds the 95% Bayesian credible interval of the fitted trend. Data are shown as means (points) plus and minus the standard deviation (error bars) across all observation locations within the station. Observations were grouped by month for aggregating.

National Capital Parks-East

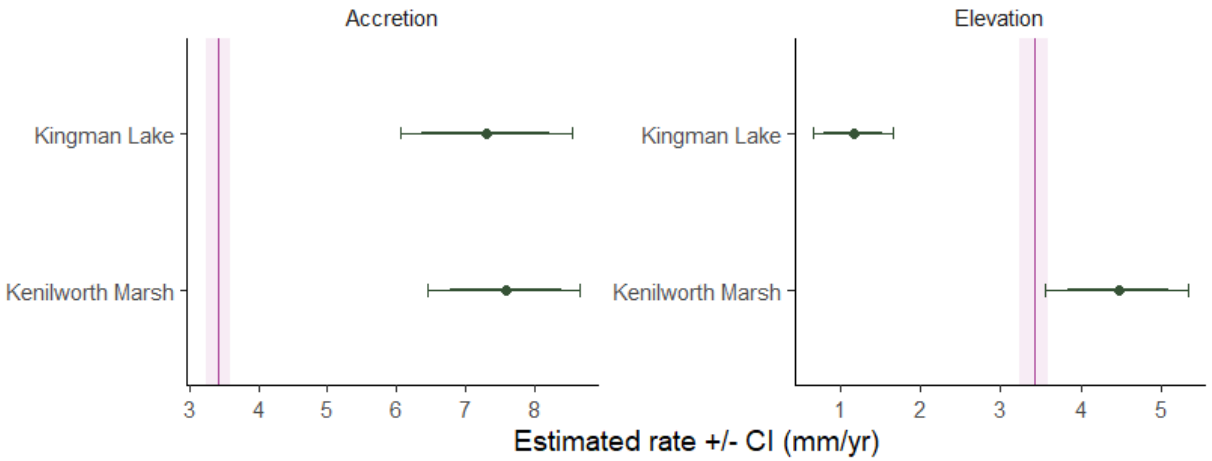


Figure A-97. Estimated accretion and elevation trends at the site level for National Capital Parks-East. The estimates are averages of the posteriors of the set-level trend estimates. The point shows the mean of the posterior; the thick error bars show the 85% Bayesian credible interval; the thin error bars show the 95% Bayesian credible interval. The vertical pink line shows the mean estimate of sea level rise and the pink rectangle bounds the 95% confidence interval.

Table A-54. Posterior trends (mean and 95% Bayesian credible interval) and the posterior probabilities that the trends in elevation or accretion are greater than 0 [Pr(trend > 0)], that the trend is greater than the upper bound of sea level rise [Pr(trend > slr)], and that the trend is less than the lower bound of sea level rise [Pr(trend < slr)] at each site in National Capital Parks-East. The final column [Pr(trend_i < trend_j)] is the probability that the trend specified in the row (either elevation or accretion) is less than the other estimated trend (either accretion or elevation) at the same site.

Site	Response	Trend estimate (mm/yr)	Pr(trend > 0)	Pr(trend > slr)	Pr(trend < slr)	Pr(trend_i < trend_j)
Kenilworth Marsh	Accretion	7.59 (6.45 – 8.67)	1	1.00	0	0
Kingman Lake	Accretion	7.3 (6.06 – 8.56)	1	1.00	0	0
Kenilworth Marsh	Elevation	4.48 (3.55 – 5.34)	1	0.97	0	1
Kingman Lake	Elevation	1.16 (0.66 – 1.66)	1	0.00	1	1

Kenilworth Marsh

Table A-55. Estimated rates of elevation and accretion trends at Kenilworth Marsh in National Capital Parks-East. Values in parentheses are the 95% Bayesian credible intervals. Pr(trend > 0) columns report the posterior probability that the estimated trend is greater than zero.

SET	Response	Trend estimate (mm/yr)	Pr(trend > 0)	Pr(trend > slr)	Pr(trend < slr)
Kenilworth 1	Accretion	7.6 (5.63 – 9.62)	0.93	0.71	0.28
Kenilworth 2	Accretion	7.33 (5.22 – 9.4)	0.94	0.69	0.29
Kenilworth 3	Accretion	8.1 (5.98 – 10.62)	0.94	0.72	0.26
Kenilworth 4	Accretion	7.43 (5.3 – 9.53)	0.93	0.70	0.29
Kenilworth 5	Accretion	7.5 (5.35 – 9.8)	0.93	0.70	0.28
Kenilworth 1	Elevation	5.39 (3.62 – 7.25)	0.95	0.23	0.70
Kenilworth 2	Elevation	1.94 (-0.47 – 4.03)	0.24	0.01	0.99
Kenilworth 3	Elevation	6.14 (4.28 – 7.92)	0.99	0.37	0.55
Kenilworth 4	Elevation	7.11 (4.92 – 9.06)	0.99	0.60	0.32
Kenilworth 5	Elevation	1.84 (-0.11 – 3.92)	0.21	0.00	1.00
Overall	**Accretion**	**7.59 (6.45 – 8.67)**	**1.00**	**1.00**	**0.00**
Overall	**Elevation**	**4.48 (3.55 – 5.34)**	**1.00**	**0.97**	**0.00**

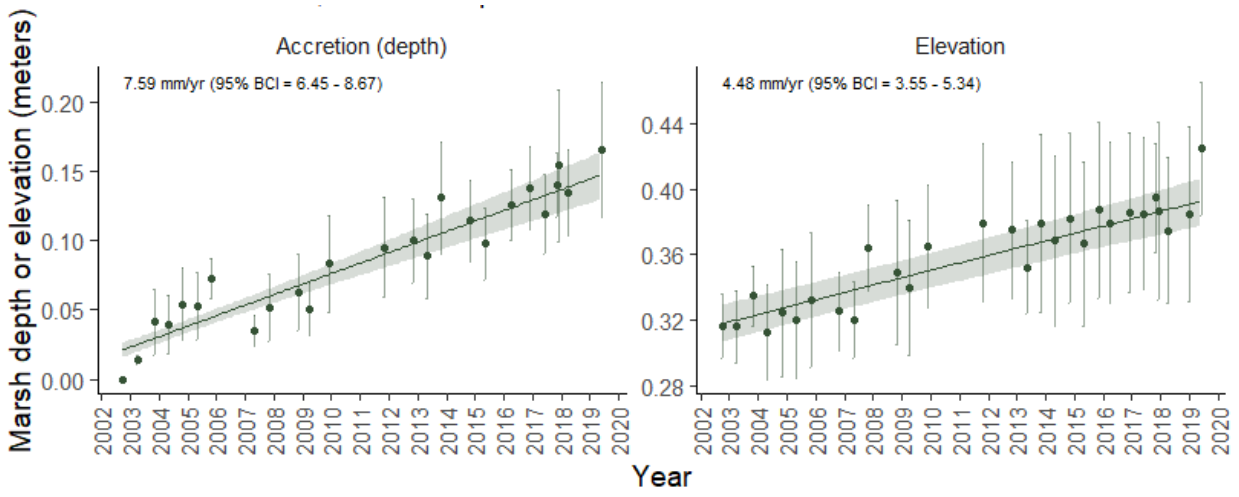


Figure A-98. Overall accretion and elevation trends for the Kenilworth Marsh site at National Capital Parks-East. Solid line shows the mean of the posterior fitted trend; shaded region around the line bounds the 95% Bayesian credible interval of the fitted trend. These trend lines were computed using the mean of the intercept posteriors across SETs within the site and the mean of the slope posteriors across SETs within a site. Data are shown as means (points) plus and minus the standard deviation (error bars) across all observation locations within the site. Observations were grouped by month for aggregating.

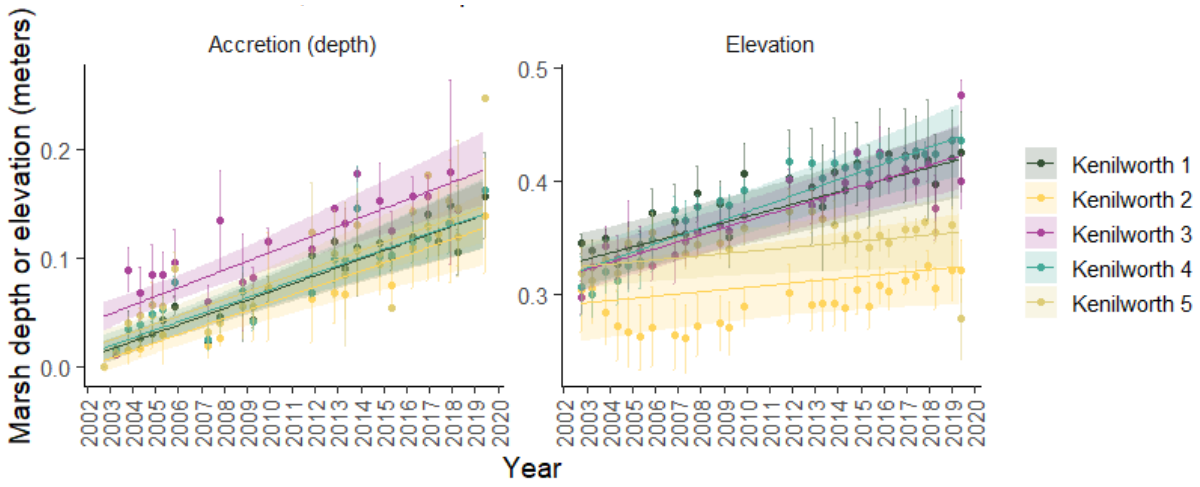


Figure A-99. Accretion and elevation trends at each station for the Kenilworth Marsh site at National Capital Parks-East. Solid line shows the mean of the posterior fitted trend; shaded region around the line bounds the 95% Bayesian credible interval of the fitted trend. Data are shown as means (points) plus and minus the standard deviation (error bars) across all observation locations within the station. Observations were grouped by month for aggregating.

Kingman Lake

Table A-56. Estimated rates of elevation and accretion trends at Kingman Lake in National Capital Parks-East. Values in parentheses are the 95% Bayesian credible intervals. Pr(trend > 0) columns report the posterior probability that the estimated trend is greater than zero.

SET	Response	Trend estimate (mm/yr)	Pr(trend > 0)	Pr(trend > slr)	Pr(trend < slr)
Kingman 1	Accretion	5.62 (1.06 – 10.41)	0.97	0.71	0.25
Kingman 2	Accretion	6.31 (3.52 – 9.03)	0.99	0.82	0.14
Kingman 3	Accretion	4.7 (2.86 – 6.62)	0.97	0.63	0.32
Kingman 4	Accretion	8.87 (7.23 – 10.67)	1.00	0.98	0.01
Kingman 5	Accretion	10.99 (9.13 – 12.91)	1.00	1.00	0.00
Kingman 1	Elevation	0.1 (-0.98 – 1.18)	0.48	0.01	0.98
Kingman 2	Elevation	-9.06 (-10.21 – -7.89)	0.00	0.00	1.00
Kingman 3	Elevation	4.81 (3.72 – 5.9)	1.00	0.73	0.19
Kingman 4	Elevation	4.67 (3.55 – 5.72)	1.00	0.72	0.21
Kingman 5	Elevation	5.3 (4.19 – 6.45)	1.00	0.84	0.12
Overall	**Accretion**	**7.3 (6.06 – 8.56)**	**1.00**	**1.00**	**0.00**
Overall	**Elevation**	**1.16 (0.66 – 1.66)**	**1.00**	**0.00**	**1.00**

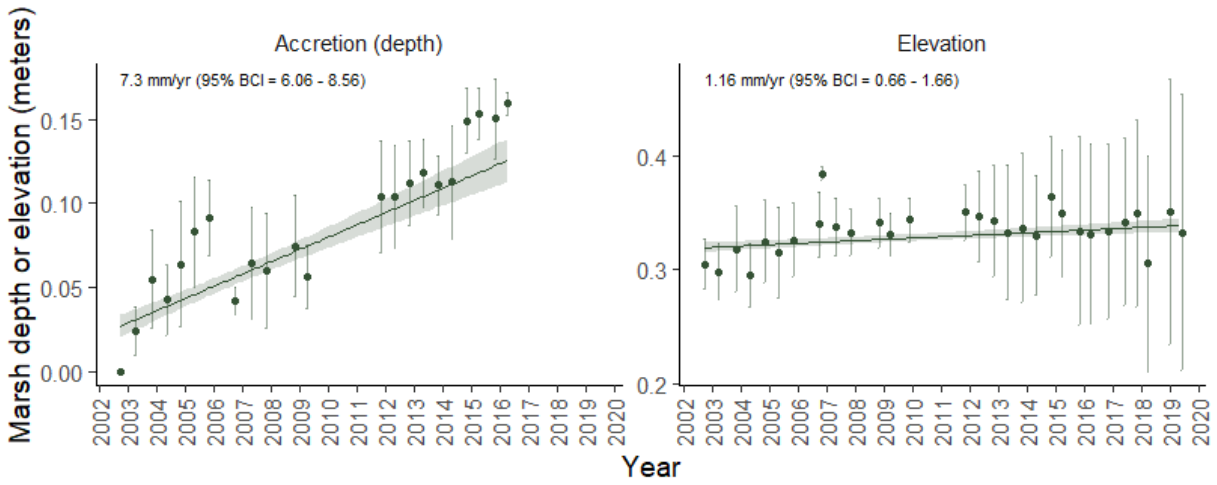


Figure A-100. Overall accretion and elevation trends for the Kingman Lake site at National Capital Parks-East. Solid line shows the mean of the posterior fitted trend; shaded region around the line bounds the 95% Bayesian credible interval of the fitted trend. These trend lines were computed using the mean of the intercept posteriors across SETs within the site and the mean of the slope posteriors across SETs within a site. Data are shown as means (points) plus and minus the standard deviation (error bars) across all observation locations within the site. Observations were grouped by month for aggregating.

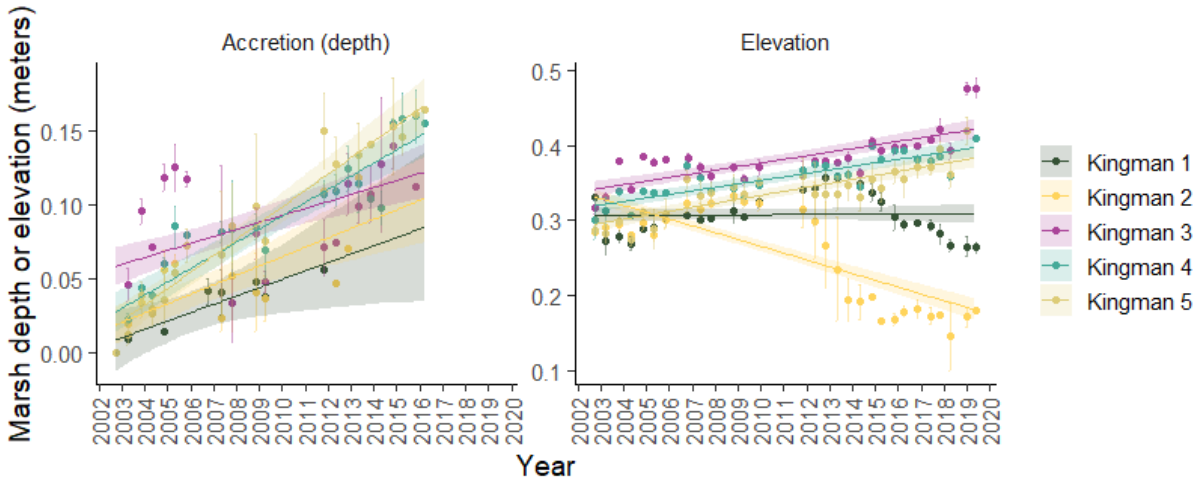


Figure A-101. Accretion and elevation trends at each station for the Kingman Lake site at National Capital Parks-East. Solid line shows the mean of the posterior fitted trend; shaded region around the line bounds the 95% Bayesian credible interval of the fitted trend. Data are shown as means (points) plus and minus the standard deviation (error bars) across all observation locations within the station. Observations were grouped by month for aggregating.

Appendix B: Details of model selection and data aggregation

Andrew T. Tredennick, Western EcoSystems Technology, Inc.
Leigh Ann Starcevich, Western EcoSystems Technology, Inc.
2021-10-29

```
# load libraries needed for analysis
library(ncbnset)  # internal package with data and helper functions
library(tidyverse)  # data wrangling
library(lubridate)  # date/time functions
library(lme4)  # mixed effects glms
```

Details on random effects structure

The nested structure of the raw data leads to a natural random effects structure of "pin-within-arm-within-set." However, this also leads to the most complicated model. To test whether complete nesting was necessary in the random effects, we conducted initial model selection tests using the **lme4** package in R. We used **lme4** (a frequentist implementation of mixed effects models) rather than the Bayesian approach because results should be similar and **lme4** is much quicker than a Bayesian algorithm.

First, we fit models with the full pin-within-arm-within-set random effects structure for each site. We counted the number of fits that were "singular." Singular fits imply that the variation among groups at some level within the random effects is essentially zero (or close enough that it cannot be easily estimated). Additionally, singular fits arise when the correlation estimate in the variance-covariance matrix is nearly 1 or -1. In these cases, it is recommended to drop the level of random effects causing the singular fit due to low among group variation. We show an example workflow for diagnosing singularity below, using the Bass Harbor site data from Acadia National Park.

```
# load data using the ncbnset package
dat <- allSETDat  # this is an internal data object of ncbnset

# format the data
fullData <- dat %>%
  # drop NA records
  filter(!is.na(PinHeight_m)) %>%
  # extract year from the measurement date
  mutate(calyear = year(Event_Date)) %>%
  # convert to mm
  mutate(elev = PinHeight_m*1000) %>%
  # rename several variables to make a tidy data frame for modeling
  rename("park" = Park_Code,
         "site" = Site_Name,
         "set" = Station_Name,
         "arm" = Pipe_Direction,
```

```
         "pin" = Pin_Position) %>%
  # update year column to account for actual days since first observation
  group_by(park, site, set, arm, pin) %>%
  mutate(year = as.numeric(Event_Date - min(Event_Date))/365.25) %>%
  ungroup() %>%
  dplyr::select(park, site, year, set, arm, pin, elev)

head(fullData)
```

```
## # A tibble: 6 x 7
##   park  site         year set           arm     pin  elev
##   <chr> <chr>       <dbl> <chr>         <chr> <dbl> <dbl>
## 1 ACAD  Bass Harbor     0 Bass Harbor 3 A         1   133
## 2 ACAD  Bass Harbor     0 Bass Harbor 3 A         2   129
## 3 ACAD  Bass Harbor     0 Bass Harbor 3 A         3   133
## 4 ACAD  Bass Harbor     0 Bass Harbor 3 A         4   132
## 5 ACAD  Bass Harbor     0 Bass Harbor 3 A         5   133
## 6 ACAD  Bass Harbor     0 Bass Harbor 3 A         6   134
```

```
# subset data to site of interest
modData <- fullData %>%
  filter(park == "ACAD", site == "Bass Harbor")

# fit the full random effects model
fullModel <- lmer(elev ~ 1 + year + (1 + year | set) +
                    (1 + year | set:arm) +
                    (1 + year | set:arm:pin),
                  data = modData)
isSingular(fullModel)
```

```
## [1] TRUE
```

The `isSingular` function returns the evaluation of `TRUE`. We can probe the model results to figure out why the model is singular.

```
## Linear mixed model fit by REML ['lmerMod']
## Formula: elev ~ 1 + year + (1 + year | set) + (1 + year | set:arm) + (1 +
##     year | set:arm:pin)
##    Data: modData
##
## REML criterion at convergence: 12440.5
##
## Scaled residuals:
##     Min      1Q  Median      3Q     Max
## -3.4202 -0.6342  0.0115  0.6609  3.5641
```

```
##
## Random effects:
##  Groups      Name        Variance  Std.Dev. Corr
##  set:arm:pin (Intercept) 1.529e+01  3.9107
##              year        9.002e-02  0.3000  -1.00
##  set:arm     (Intercept) 1.165e+02 10.7923
##              year        2.084e-01  0.4565  -0.82
##  set         (Intercept) 1.143e+03 33.8019
##              year        1.008e+01  3.1744  -0.86
##  Residual                4.538e+01  6.7367
## Number of obs: 1836, groups:  set:arm:pin, 108; set:arm, 12; set, 3
##
## Fixed effects:
##             Estimate Std. Error t value
## (Intercept)  168.127     19.769   8.505
## year           2.581      1.839   1.403
##
## Correlation of Fixed Effects:
##      (Intr)
## year -0.851
## convergence code: 0
## boundary (singular) fit: see ?isSingular
```

Here we see that the correlation between the intercept and the slope at the pin level is estimated as -1, resulting in a singular fit. We also see that the variance within that level for the slope (`year`) is relatively small (an order of magnitude smaller than variation at the other levels). These two lines of evidence suggest that the "pins" level does not need to be included in the random effects structure. For more information on singular fits, see the R help page by entering `?isSingular` in an R console.

We repeated the analysis above for all sites and found that 50% of the models resulted in singular fits. Therefore, we chose to use a "arm-within-set" random effects structure for the intercept and slope (year effect) so that all sites would be fitted with the same model. Below we show the reduced model for the same data.

```
reducedModel <- lmer(elev ~ 1 + year + (1 + year | set) +
                       (1 + year | set:arm),
                     data = modData)
isSingular(reducedModel)
```

```
## [1] FALSE
```

Details on data aggregation

Once we decided on the random effects structure, we fit preliminary models using the **brms** package for Bayesian inference. Preliminary models were fit using the raw data: one observation per pin-within-arm-within-set at each observation time (`Event_Date`). The preliminary models took a very

long time to fit (one site took over three days) and the Hamiltonian Monte Carlo (HMC) algorithm in Stan (which **brms** uses) issued warnings about divergent transitions (https://mc-stan.org/misc/warnings.html#divergent-transitions-after-warmup). We also found that fitting the model with **lme4**::`lmer()` resulted in convergence warnings (see final line of model summary):

```
## Linear mixed model fit by REML ['lmerMod']
## Formula: elev ~ 1 + year + (1 + year | set) + (1 + year | set:arm)
##    Data: modData
##
## REML criterion at convergence: 12569.5
##
## Scaled residuals:
##     Min      1Q  Median      3Q     Max
## -3.9596 -0.6502  0.0158  0.6651  3.0560
##
## Random effects:
##  Groups   Name        Variance  Std.Dev. Corr
##  set:arm  (Intercept)  118.0504 10.8651
##           year           0.2108  0.4591  -0.83
##  set      (Intercept) 1137.0873 33.7207
##           year          10.0347  3.1678  -0.85
##  Residual               52.3840  7.2377
## Number of obs: 1836, groups:  set:arm, 12; set, 3
##
## Fixed effects:
##             Estimate Std. Error t value
## (Intercept)  168.127     19.722   8.525
## year           2.581      1.835   1.406
##
## Correlation of Fixed Effects:
##      (Intr)
## year -0.851
## convergence code: 0
## Model failed to converge with max|grad| = 0.00445525 (tol = 0.002,
component 1)
```

We found that aggregating the data over pins (average of pins for each arm-within-set observation) and using informative priors (see main report) allowed us to avoid the algorithm warnings. We can also see that using the aggregated data with `lmer` results in successful convergence of the model fit.

```
aggData <- modData %>%
  group_by(park, site, year, set, arm) %>%
  summarise(elev = mean(elev),
            .groups = "drop")
```

```
reducedModel <- lmer(elev ~ 1 + year + (1 + year | set) +
                       (1 + year | set:arm),
                     data = aggData)
summary(reducedModel)
```

```
## Linear mixed model fit by REML ['lmerMod']
## Formula: elev ~ 1 + year + (1 + year | set) + (1 + year | set:arm)
##    Data: aggData
##
## REML criterion at convergence: 1371.9
##
## Scaled residuals:
##      Min       1Q   Median       3Q      Max
## -2.61700 -0.59202 -0.01786  0.66864  2.62994
##
## Random effects:
##  Groups   Name        Variance Std.Dev. Corr
##  set:arm  (Intercept)  114.318 10.6920
##           year           0.122  0.3493  -1.00
##  set      (Intercept) 1143.053 33.8091
##           year          10.024  3.1661  -0.86
##  Residual               37.237  6.1022
## Number of obs: 204, groups:  set:arm, 12; set, 3
##
## Fixed effects:
##             Estimate Std. Error t value
## (Intercept)  168.127     19.780   8.500
## year           2.581      1.839   1.403
##
## Correlation of Fixed Effects:
##      (Intr)
## year -0.852
## convergence code: 0
## boundary (singular) fit: see ?isSingular
```

Note that the "isSingular" warning is issued again. However, we were able to overcome this warning by fitting the model using a fully Bayesian method. To quote the R help, one suggestion is to "use a fully Bayesian method that both regularizes the model via informative priors and gives estimates and credible intervals for all parameters that average over the uncertainty in the random effects parameters (Gelman and Hill 2006, McElreath 2015; MCMCglmm, rstanarm and brms packages)." Thus, between aggregating data and using the fully Bayesian approach, we were able to design a workflow that is computationally efficient, passes model convergence diagnostics, and allows us to still explicitly model *most* of the nested structure of the data.

We used the same random effects structure and data aggregation scheme for the accretion data so that the models will be directly comparable. Note that the accretion data were averaged over replicate observations rather than pins, matching the data structure. Example accretion data are shown below.

```
## # A tibble: 6 x 7
##   park  site        set           horizon date        year  accr
##   <chr> <chr>       <chr>         <chr>   <date>     <dbl> <dbl>
## 1 ACAD  Bass Harbor Bass Harbor 1 A       2011-09-20 0      0
## 2 ACAD  Bass Harbor Bass Harbor 1 A       2012-05-23 0.674  2.67
## 3 ACAD  Bass Harbor Bass Harbor 1 A       2012-09-10 0.975  2.75
## 4 ACAD  Bass Harbor Bass Harbor 1 A       2013-05-21 1.67   5
## 5 ACAD  Bass Harbor Bass Harbor 1 A       2013-09-17 1.99   6.75
## 6 ACAD  Bass Harbor Bass Harbor 1 A       2014-05-13 2.64  11.3
```

Appendix C: Example of fitting hierarchical Bayesian generalized additive model for trend estimates

Andrew T. Tredennick, Western EcoSystems Technology, Inc.
Leigh Ann Starcevich, Western EcoSystems Technology, Inc.
2021-10-29

GAMM vs. GLMM

We used generalized linear mixed effects models (GLMMs) in the main report because a majority of the trends were in fact linear over time. Likewise, the use of GLMMs allows for direct comparison with previous trend estimates produced by the NPS team. However, GLMMs are not appropriate in all cases, specifically when the trend is not linear but rather fluctuates over time. We produced a suite of visual model checks (Tredennick et al. 2021) that provide evidence of when a GLMM might not be appropriate. Our recommendation is to simply view the raw data and decide whether a "wiggly" generalized additive mixed-effects model (GAMM) makes more sense. Also, with the method we demonstrate below, the hierarchical Bayesian GAMM should converge on the GLMM trend estimate if no "wiggliness" is required.

An important caveat is that hierarchical Bayesian GAMMs, especially with nested random effects, are relatively new and difficult to code appropriately without writing custom model code. The example we provide is accurate to the best of our knowledge, but the documentation and examples for hierarchical Bayesian GAMMs are few. This is part of the reason why we opted for GLMMs in the main report. With those caveats in mind, the hierarchical Bayesian GAMM could be a one-size-fits-all model for truly linear trends, non-linear trends that fluctuate, and trends that have a breakpoint between two distinct linear trends.

Hierarchical Bayesian GAMM: An exemplar

Here we demonstrate how to fit a hierarchical Bayesian GAMM (HB-GAMM) using a prototypical site from the dataset where the trend fluctuates over time (FIIS Watch Hill site). We use the **brms** package as in the main report. We also demonstrate how to estimate the posterior distribution of the trend over time.

```
# load all the packages we will need
library(ncbnset)  # internal package with data and helper functions
library(tidyverse)  # data wrangling
library(lubridate)  # date/time functions
library(brms)  # bayesian modeling functions
```

We will use the Watch Hill site from Fire Island National Seashore because it shows a distinct non-linear trend over time.

```
# load data
dat <- allSETDat  # internal data from the ncbcnset package
```

```
# format data for analysis
dat <- FormatData(df = allSETDat, type = "elev")

# subset to site of interest
dat <- dat %>%
  filter(park == "FIIS", site == "Watch Hill")
head(dat)
```

```
## # A tibble: 6 x 7
##   park  site       set   arm   date        year  elev
##   <chr> <chr>      <chr> <chr> <date>     <dbl> <dbl>
## 1 FIIS  Watch Hill WH1   A     2002-08-15 0      132.
## 2 FIIS  Watch Hill WH1   A     2002-11-14 0.249  135.
## 3 FIIS  Watch Hill WH1   A     2003-04-03 0.632  135.
## 4 FIIS  Watch Hill WH1   A     2003-07-15 0.914  136.
## 5 FIIS  Watch Hill WH1   A     2003-10-24 1.19   138.
## 6 FIIS  Watch Hill WH1   A     2004-04-30 1.71   140
```

```
ggplot(dat, aes(x = date, y = elev, color = arm)) +
  geom_point() +
  facet_wrap(~set)
```

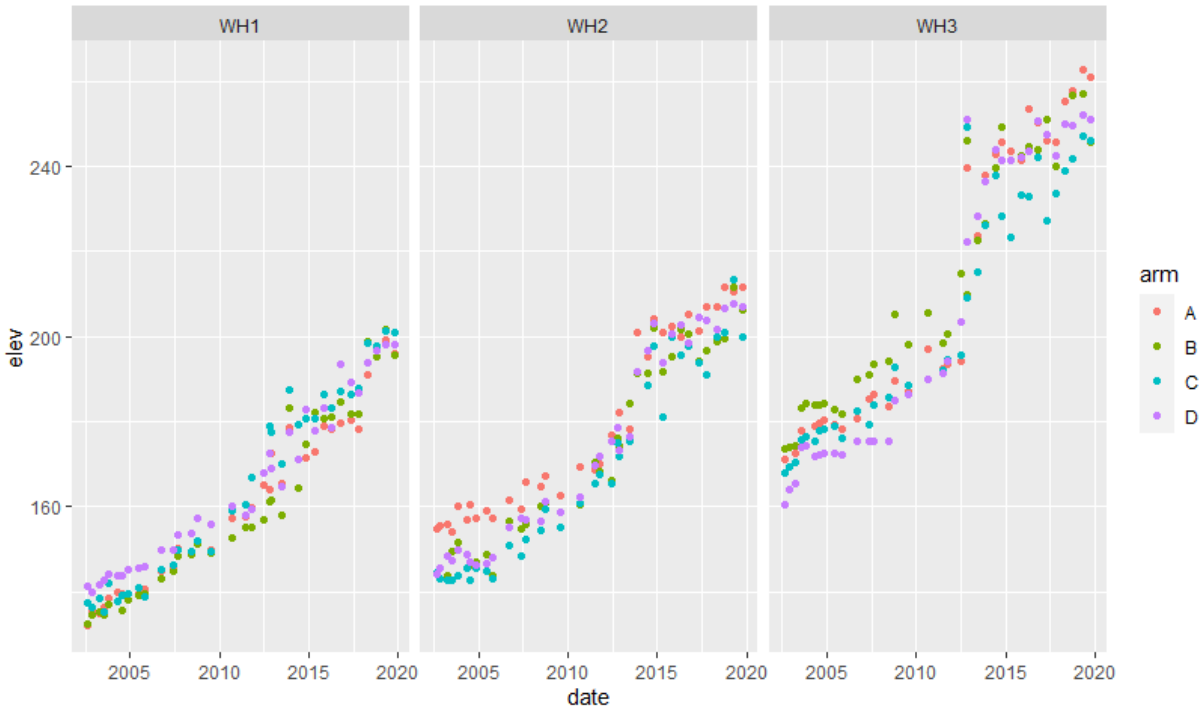


Figure C-1. Elevation data over time at the three Watch Hill SETs, Fire Island National Seashore

For the GAMM, we need to explicitly set `arm` and `set` as factors in the data frame. We also add a `dummy` column that is all 1s so we can "turn off" the arm random effect for making predictions. This will become clearer later in the code.

```
dat <- dat %>%
  mutate(set = as.factor(set),
         arm = as.factor(arm)) %>%
  mutate(dummy = 1)  # this is so we can turn off the arm effect
```

Now we can fit the HB-GAMM using **brms**.

```
mod <- brm(elev ~ s(year, bs = "cr") +  # population (global) level
             # random intercept for set
             s(set, bs = "re") +
             # random intercept for set-within-arm
             s(set, arm, bs = "re", by = dummy)  +
             # random slope for set
             s(set, year, bs = "re") +
             # random slope for set-within-arm
             s(set, arm, year, bs = "re", by = dummy),
           data = dat,
           chains = 1,
           iter = 2000,
           warmup = 1000)

print(mod)
```

```
##  Family: gaussian
##   Links: mu = identity; sigma = identity
## Formula: elev ~ s(year, bs = "cr") + s(set, year, bs = "re") + s(set, arm,
year, bs = "re", by = dummy) + s(set, bs = "re") + s(set, arm, bs = "re", by
= dummy)
##    Data: df (Number of observations: 432)
## Samples: 1 chains, each with iter = 2000; warmup = 1000; thin = 1;
##          total post-warmup samples = 1000
##
## Smooth Terms:
##                           Estimate Est.Error l-95% CI u-95% CI Rhat Bulk_ESS
## sds(syear_1)                  2.87      1.05     1.44     5.40 1.00      270
## sds(ssetyear_1)              22.50     13.41     7.42    59.51 1.00      464
## sds(ssetarmyeardummy_1)       5.91      2.00     2.87    10.84 1.00      366
## sds(sset_1)                  24.22     13.42     8.88    58.02 1.00      431
## sds(ssetarmdummy_1)           4.94      1.57     2.75     8.73 1.01      419
##                           Tail_ESS
## sds(syear_1)                   309
```

```
## sds(ssetyear_1)                721
## sds(ssetarmyeardummy_1)        532
## sds(sset_1)                    571
## sds(ssetarmdummy_1)            592
##
## Population-Level Effects:
##           Estimate Est.Error l-95% CI u-95% CI Rhat Bulk_ESS Tail_ESS
## Intercept   181.50     14.26   153.54   211.86 1.00      622      518
## syear_1      10.95      1.93     7.17    15.05 1.00      460      375
##
## Family Specific Parameters:
##       Estimate Est.Error l-95% CI u-95% CI Rhat Bulk_ESS Tail_ESS
## sigma     5.65      0.21     5.23     6.07 1.00     1064      718
##
## Samples were drawn using sampling(NUTS). For each parameter, Bulk_ESS
## and Tail_ESS are effective sample size measures, and Rhat is the potential
## scale reduction factor on split chains (at convergence, Rhat = 1).
```

The model summary is not super intuitive. It is easier to understand the model fits and the overall trend estimates. First, to get a sense of what the model is producing, we can plot the fitted trend over time.

```
# set up a new data frame for evaluating fit
years <- unique(sort(dat$year))
sets <- unique(sort(dat$set))
newdata <- tibble(
  year = rep(years, times = length(sets)),
  set = rep(sets, each = length(years))
) %>%
  mutate(arm = "A") %>%  # set arm to arbitrary value found in the data
  mutate(dummy = 0)  # zero out the arm-within-set effect

# get fit summaries at different quantiles of the posterior distribution
quants <- c(0.025, 0.075, 0.16, 0.5, 0.84, 0.925, 0.975)
fits <- fitted(mod, newdata, probs = quants)

# create dataframe with calendar date associated with each year
datJoin <- dat %>%
  filter(arm == "A") %>%
  dplyr::select(set, date, year)

# format as tibble/dataframe and merge in the year and set values
fits <- as_tibble(fits) %>%
  bind_cols(newdata) %>%  # year and set values
```

```
  left_join(datJoin, by = c("set", "year"))

# summarise the data for plotting
sumdf <- dat %>%
  group_by(set, date) %>%
  summarise(meanelev = mean(elev),
            sdev = sd(elev))

ggplot(data = sumdf, aes(x = date)) +
  geom_point(aes(y = meanelev)) +
  geom_errorbar(aes(ymin = meanelev-sdev, ymax= meanelev+sdev), width = 0.1)
+
  geom_line(data = fits, aes(y = Estimate), color = "salmon", size = 1) +
  geom_ribbon(data = fits, aes(ymin = `Q2.5`, ymax = `Q97.5`),
              alpha = 0.2,
              fill = "salmon") +
  facet_wrap(~set) +
  labs(x = "Date", y = "Elevation (millimeters)")
```

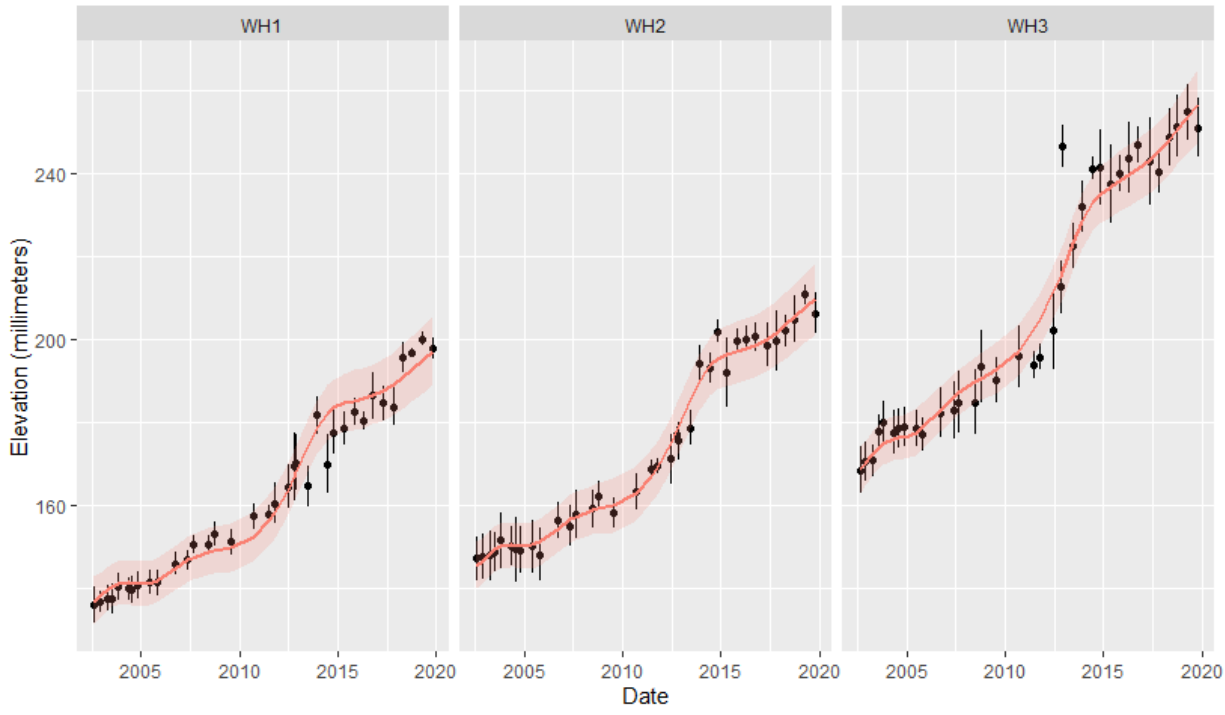


Figure C-2. Fitted elevation trends from the hierarchical Bayesian generalized linear mixed effects model. Line shows the mean of the posterior predictive distribution and shaded regions delimits the 95% Bayesian credible interval.

Because the trend is allowed to fluctuate over time, the model summary does not report single trend estimates. However, trend estimates can be calculated by summarizing the first derivatives of the fitted curves shown above. In brief, we make predictions at the new data points (years) and then make predictions at those some years adjust by a small factor. We then calculate the difference in the two predictions divided by the small factor, which yields the first derivative of the curve at that point. We can then take the average of the first derivatives to approximate the posterior distribution of the overall trend estimate. This is demonstrated below (it is easier done than said). Note that this approach is adapted from the tutorial provided here: https://dilshersinghdhillon.netlify.app/post/estimating-smooth-trends-and-identifying-periods-of-change-using-bayesian-inference/.

```
# first derivatives
epsilon <- 1e-6  # small factor
first <- newdata  # use same data frame as above for predictions
second <- newdata %>%
  mutate(year = year + epsilon)  # adjust the year by small factor

# get predictions
first_preds <- posterior_linpred(
   mod,
   newdata = first,
   summary = FALSE  # summary is FALSE because we want entire distribution
)

second_preds <- posterior_linpred(
   mod,
   newdata = second,
   summary = FALSE  # summary is FALSE because we want entire distribution
)


# calculate the differennce and divide by epsilon, which is analgous to dx/dt
diff <- (second_preds - first_preds) / epsilon

# using the posterior samples, calculate the mean and lower and upper
quantiles
meanDiff  <- apply(diff, MARGIN = 2, FUN = mean)
lowerDiff <- apply(diff, MARGIN = 2, FUN = quantile, prob = 0.025)
upperDiff <- apply(diff, MARGIN = 2, FUN = quantile, prob = 0.975)

# make a data frame of results
res <- data.frame(meanDiff) %>%
  cbind(lowerDiff) %>%
```

```
  cbind(upperDiff) %>%
  cbind(first) %>%
  left_join(datJoin)

# plot the first derivatives over time
ggplot(res, aes(x = date, y = meanDiff, group = set)) +
  geom_line(color = "salmon", size = 1)  +
  geom_ribbon(aes(ymin = lowerDiff, ymax = upperDiff),
              alpha = 0.2, fill = "salmon") +
  labs(y = "First derivative (trend, mm/yr)", x = "Date") +
  facet_wrap(~set)
```

Figure C-3 shows the estimated trend (first derivative of the GAMM or spline) at modeled time points. The figure allows one to see not only the general trend over time, but also times at which elevation is changing the most. For example, the trend is highest around 2012, when hurricane Sandy came through.

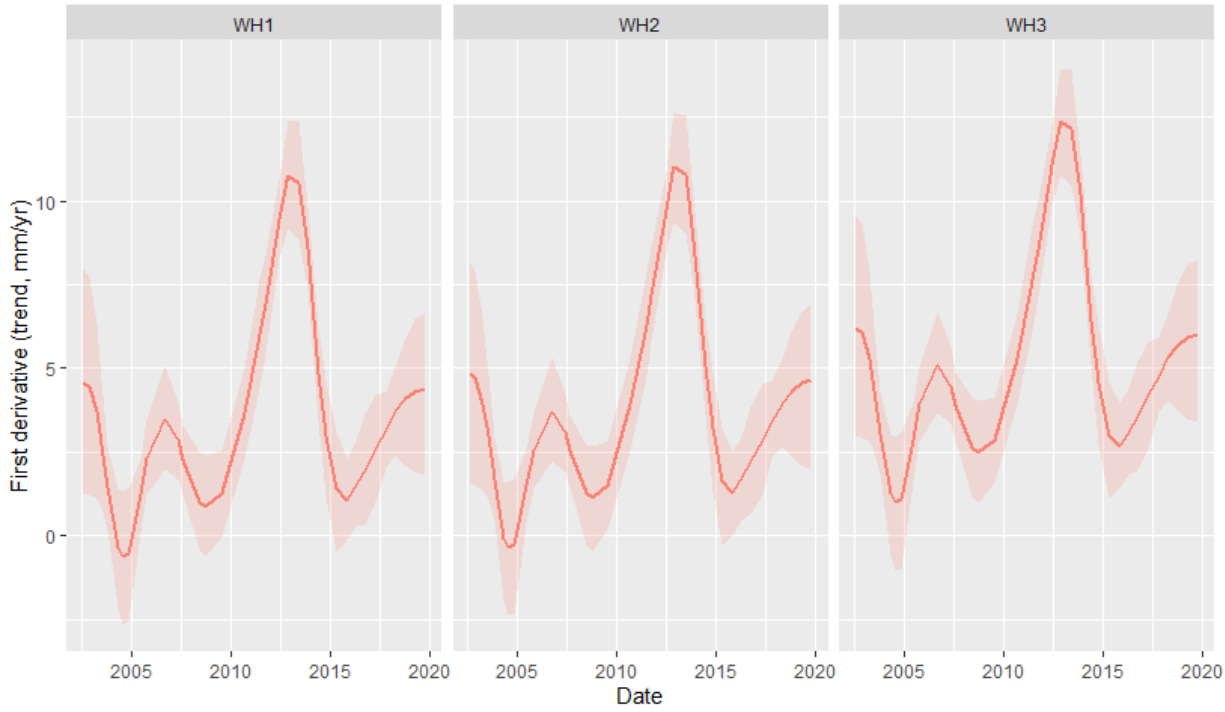


Figure C-3. Posterior distribution of first derivatives of the fitted trends over time.

```
# summarise the diffs distributions
diffDf <- as.data.frame(t(diff)) %>%
  bind_cols(first) %>%
  pivot_longer(cols = starts_with("V"),
               names_to = "rep",
               values_to = "diff") %>%
```

```
  group_by(set, rep) %>%
  summarise(OverallDiff = mean(diff),
            .groups = "drop") %>%
  group_by(set) %>%
  summarise(`Estimated Trend (mm/yr)` = mean(OverallDiff),
            Lower95 = round(quantile(OverallDiff, 0.025), 2),
            Upper95 = round(quantile(OverallDiff, 0.975), 2),
            .groups = "drop") %>%
  mutate(`95% BCI` = paste(Lower95, " - ", Upper95)) %>%
  dplyr::select(-Lower95, -Upper95) %>%
  rename("SET" = set)

knitr::kable(diffDf, digits = 2, caption = "Elevation trend estimates from
the hierarchical Bayesian generalized additive model, computed from estimates
of the first derivatives.")
```

Table C-1. Elevation trend estimates from the hierarchical Bayesian generalized additive model, computed from estimates of the first derivatives.

SET	Elevation trend (mm/yr)	95% BCI
WH1	3.70	3.18 – 4.2
WH2	3.95	3.44 – 4.43
WH3	5.31	4.83 – 5.8

Table C-2. Elevation trend estimates from the hierarchical Bayesian generalized linear mixed-effects model from the main report.

SET	Elevation trend (mm/yr)	95% BCI
WH1	3.70	3.34 – 4.05
WH2	3.96	3.62 – 4.29
WH3	5.34	4.94 – 5.7

Additional resources

The paper by Pedersen et al. (2019) covers several examples of hierarchical generalized additive models in ecology. However, it does not show implementation in **brms** or how to handle nested random effects. It is still an exceedingly useful resource, though.

References

Pedersen, E. J., D. L. Miller, G. L. Simpson, and N. Ross. 2019. Hierarchical generalized additive models in ecology: An introduction with mgcv. PeerJ 7:e6876.

Appendix D: Example of fitting a Bayesian piece-wise linear regression to detect changepoints in trends over time

Mikey Tabak, Western EcoSystems Technology, Inc.
Andrew T. Tredennick, Western EcoSystems Technology, Inc.
Leigh Ann Starcevich, Western EcoSystems Technology, Inc.
2021-11-05

Changepoint analysis for a SET within a site

Here we provide an example of a changepoint analysis for one SET station within a site (Fire Island National Seashore Watch Hill SET 3). There are three main components. First we fit a mixed effects model with a changepoint effect and one without a changepoint effect and determine which is more appropriate using Leave One Out cross-validation following Vehtari et al. 2017. Then, if the best model includes a changepoint effect, we find the posterior distribution of the changepoint. Finally, we find the slope of the line before and after the changepoint.

Note that we use a simpler random effects structure for this example. We fit a model with an arm random effect on the intercept, and the model is fit at the SET level rather than the site level. We used a simpler random effects structure to make the example tractable and computationally feasible. Moreover, specifying the correct random effects structure for the changepoint model is difficult using the **brms** model specification. We recommend coding the model "by hand" in the Stan language if a more complex random effects structure is desired. For sake of consistency, we avoid manually coding a Stan mode here, and instead use a simpler random effects structure in **brms**.

Data

We will use the WH3 SET station at the Watch Hill site from Fire Island National Seashore because it shows a distinct changepoint.

```
# load the data
dat <- FormatData(allSETDat, type = 'elev')

# site with piecewise effect
subDat <- dat %>%
  filter(park == "FIIS") %>%
  filter(site == "Watch Hill") %>%
  filter(set == 'WH3')

ggplot(subDat, aes(x = date, y = elev, color = arm)) +
  geom_point()
```

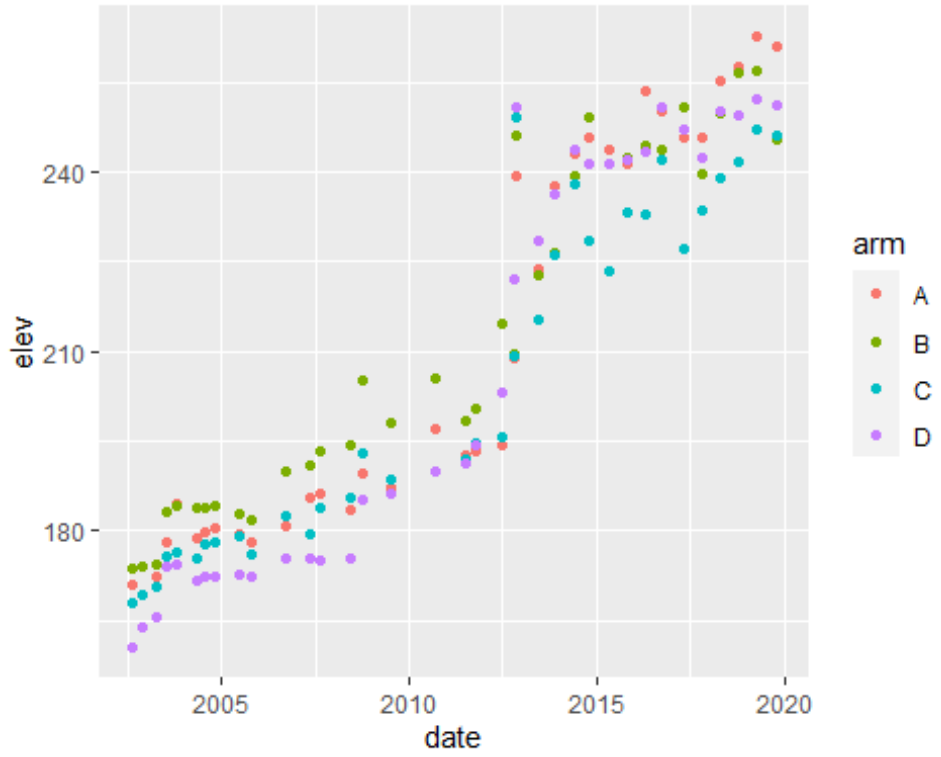


Figure D-1. Elevation data over time at Watch Hill, Fire Island National Seashore.

To help the MCMC algorithm along, we extract some information from the dataset that will be used as informative prior information. Specifically, we will find the initial elevation and its standard deviation across SET stations and use that distribution as a prior for the intercept when we fit the model.

```
# extract intercept information
startElev <- subDat %>%
  filter(year == min(year)) %>%
  pull(elev) %>%
  mean()
s1 <- sd(subDat$elev)
intp <- startElev

# set prior parameters to be passed to Stan via brms
stanvars <- stanvar(intp, name='intp') + stanvar(s1, name='s1')
```

Changepoint model

Set up a changepoint model. Note that we use the **brms**::`bf()` function to specify the model rather than **brms**::`brm`, which we used in the main analysis. The `bf` function allows for more complicated model structures.

```
# specify model structure
bform <- bf(
  elev ~ b0 + b1*(year-omega) * step(omega-year) +
    b2 * (year - omega) * step(year-omega),
    b0 + b1 + b2 + alpha ~ (1|arm),
  nlf(omega ~ inv_logit(alpha) * 20),
  nl = TRUE
)

# specify priors
priorsGLMM <- prior(normal(intp, s1), nlpar = "b0") +
  prior(normal(0, 3), nlpar = "b1") +
  prior(normal(0, 3), nlpar = "b2") +
  prior(normal(0, 20), nlpar = "alpha")
```

A couple notes on the model above. `b0` is the overall intercept. `alpha` is the inverse logit transformed changepoint (`omega` is the change point on the estimation scale). Using the inverse logit transform makes estimation easier because `alpha` can then range from -Inf to Inf. `alpha` is then transformed to `omega` by first constraining to 0-1 range and then multiplying by 20, which is just beyond the maximum possible changepoint year for this site. The `step()` function returns a 0 if the result is negative and returns a 1 if the result is positive. So, if the change point is year 4.09 (`omega = 4.09`), then `step(omega - year)` is equal to 1 when the year is less than 4.09, which "activates" the `b1` slope.

Specify some of the model conditions. You will likely need more iterations. In Stan, the bulk of the work is done in `warmup`. We find that once this stage is complete, only an additional 1000 iterations are needed. Therefore, if the model does not converge (as described below), try increasing `warmup`.

```
# These conditions are for illustration.
# You will probably want to increase warmup in practice.
warmup = 3000
iter = warmup + 1000
chains = 3
cores = 3
thin = 1
```

Fit the changepoint model

```
fit_cp <- brm(
  data = subDat,
  family = gaussian,
  formula = bform,
  warmup = warmup,
  iter = iter,
```

```
  chains = chains,
  cores = cores,
  thin = thin,
  prior = priorsGLMM,
  stanvars = stanvars,
  control = list(adapt_delta = 0.99, max_treedepth = 15)
)
```

Calculate Leave One Out Crossvalidation metrics (see Vehtari et al. 2017 for details)

```
fit_cp <- add_criterion(fit, 'loo')
```

Look at the model summary and check for convergence (Rhat < 1.05).

```
summary(fit_cp)
```

```
##  Family: gaussian
##   Links: mu = identity; sigma = identity
## Formula: elev ~ b0 + b1 * (year - omega) * step(omega - year) + b2 * (year
- omega) * step(year - omega)
##          b0 ~ (1 | arm)
##          b1 ~ (1 | arm)
##          b2 ~ (1 | arm)
##          alpha ~ (1 | arm)
##          omega ~ inv_logit(alpha) * 20
##    Data: subDat (Number of observations: 144)
## Samples: 3 chains, each with iter = 4000; warmup = 3000; thin = 1;
##          total post-warmup samples = 3000
##
## Group-Level Effects:
## ~arm (Number of levels: 4)
##                     Estimate Est.Error l-95% CI u-95% CI Rhat Bulk_ESS
Tail_ESS
## sd(b0_Intercept)        7.06      6.71     0.41    26.17 1.00     1087
1399
## sd(b1_Intercept)        7.26     19.48     0.04    63.17 1.04       74
93
## sd(b2_Intercept)        2.03      2.78     0.20     8.89 1.00      334
746
## sd(alpha_Intercept)     4.59     14.59     0.02    40.11 1.03       85
160
##
## Population-Level Effects:
##                 Estimate Est.Error l-95% CI u-95% CI Rhat Bulk_ESS
Tail_ESS
```

```
## b0_Intercept      178.87      9.08   160.69   194.16 1.04       79
163
## b1_Intercept        1.48      1.92    -3.64     4.26 1.02      606
253
## b2_Intercept        5.48      1.46     1.16     7.31 1.01      432
928
## alpha_Intercept    -4.43      9.23   -35.41    -0.08 1.04      101
110
##
## Family Specific Parameters:
##       Estimate Est.Error l-95% CI u-95% CI Rhat Bulk_ESS Tail_ESS
## sigma     9.39      0.69     8.20    10.90 1.02      111      198
##
## Samples were drawn using sampling(NUTS). For each parameter, Bulk_ESS
## and Tail_ESS are effective sample size measures, and Rhat is the potential
## scale reduction factor on split chains (at convergence, Rhat = 1).
```

Look at traceplots and check for convergence

```
plot(fit_cp, '^b_')
```

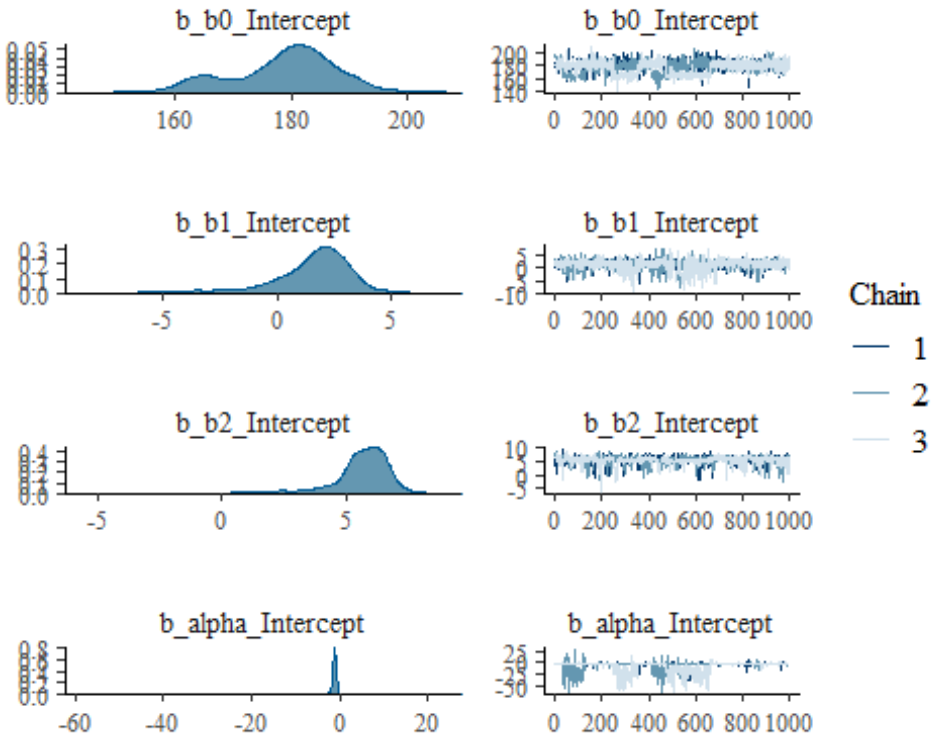


Figure D-2. Density (right column) and trace (left column) plots for model fit_cp.The lower row shows an example of a coefficient with moderately poor convergence

If the model has not converged, it may be necessary to add iterations and warmup.

Model without a changepoint effect

Set up model and priors.

```
# specify model structure
bform <- bf(
  elev ~ b0 + b1*year,
  b0 + b1  ~  (1|arm),
  nl = TRUE
)
# specify priors
priorsGLMM <- prior(normal(intp, s1), nlpar = "b0") +
  prior(normal(0, 3), nlpar = "b1")
```

Fit the non-changepoint model.

```
# fit model
fit_ncp <- brm(
  data = subDat,
  family = gaussian,
  formula = bform,
  warmup = warmup,
  iter = iter,
  chains = chains,
  cores = cores,
  thin = thin,
  prior = priorsGLMM,
  stanvars = stanvars,
  control = list(adapt_delta = 0.99, max_treedepth = 15)
)

# calculate loo
fit_ncp <- add_criterion(fit_ncp, 'loo')
```

Look at the model summary and check for convergence

```
summary(fit_ncp)
```

```
##  Family: gaussian
##   Links: mu = identity; sigma = identity
## Formula: elev ~ b0 + b1 * year
##          b0 ~ (1 | arm)
##          b1 ~ (1 | arm)
##    Data: subDat (Number of observations: 144)
## Samples: 3 chains, each with iter = 4000; warmup = 3000; thin = 1;
```

```
##          total post-warmup samples = 3000
##
## Group-Level Effects:
## ~arm (Number of levels: 4)
##                   Estimate Est.Error l-95% CI u-95% CI Rhat Bulk_ESS
Tail_ESS
## sd(b0_Intercept)     7.35      6.13     0.95    24.69 1.01      527
1051
## sd(b1_Intercept)     0.80      0.92     0.06     3.10 1.00      509
686
##
## Population-Level Effects:
##              Estimate Est.Error l-95% CI u-95% CI Rhat Bulk_ESS Tail_ESS
## b0_Intercept   164.28      4.66   154.18   173.50 1.00     1104      990
## b1_Intercept     5.18      0.62     3.50     5.99 1.01      743      524
##
## Family Specific Parameters:
##       Estimate Est.Error l-95% CI u-95% CI Rhat Bulk_ESS Tail_ESS
## sigma    10.18      0.61     9.05    11.46 1.00     2124     1752
##
## Samples were drawn using sampling(NUTS). For each parameter, Bulk_ESS
## and Tail_ESS are effective sample size measures, and Rhat is the potential
## scale reduction factor on split chains (at convergence, Rhat = 1).
```

Look at traceplots and check for convergence

```
plot(fit_ncp, '^b_')
```

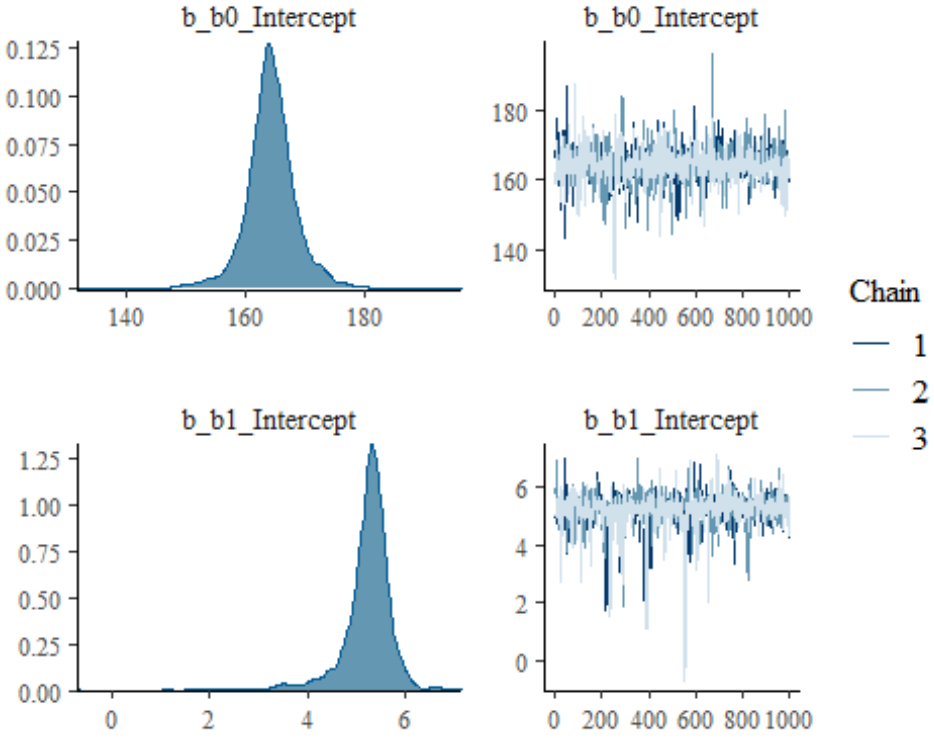


Figure D-3. Density (right column) and trace (left column) plots for model fit_ncp. Both coefficients show convergence.

Compare LOO; the model with the lowest score is best

```
print(loo_compare(fit_cp, fit_ncp), simplify=FALSE)
```

```
##         elpd_diff se_diff elpd_loo se_elpd_loo p_loo  se_p_loo looic
se_looic
## fit_cp     0.0       0.0  -532.8     13.4        12.9    2.8   1065.6
26.8
## fit_ncp   -8.7       4.5  -541.5     10.4         6.7    1.1   1082.9
20.9
```

In our example the changepoint model is best because it has the lowest LOO score. This function automatically puts the best model on top. If you find that the changepoint model is best, the next step is to find the changepoint. Otherwise, you can conclude that this dataset does not include a changepoint; there is a consistent change in elevation over time.

Find the value of the changepoint

First define an inverse logit function, which we'll use to reconstruct `omega`.

```
inv_logit <- function(x){
  exp(x)/(exp(x) + 1)
}
```

Calculate the site/set-level date for changepoint (irrespective of arms).

```
alpha <- posterior_samples(fit_cp, pars="alpha")$b_alpha_Intercept
omega <- inv_logit(alpha)*20
med_omega <- median(omega)
omega_index <- which.min(abs(subDat$year - med_omega))
omega_day0 <- subDat[omega_index, ]$date
omega_day <- as.Date(omega_day0, origin = "1970-01-01")
```

The model estimates that the median posterior changepoint date is 2006-09-18. Interestingly, this date is *not* the date we would have expected based on knowledge of the site. Based on our knowledge, we would have expected that changepoint to have occurred in 2012/13 after Hurricane Sandy. This is an important reminder that the best statistical model might not always agree with the underlying process we expect.

We can also look at the posterior distribution for slope before and after changepoint.

```
# before
b1 <- posterior_samples(fit_cp, pars='b1')$b_b1_Intercept
# after
b2 <- posterior_samples(fit_cp, pars='b2')$b_b2_Intercept
```

The median slope before the changepoint is 1.86 mm/year. After the changepoint, the median slope is 5.77 mm/year. And we can plot the fitted model to examine the model fit (subjectively).

```
# set up a new data frame for evaluating fit
years <- unique(sort(subDat$year))

newdata <- tibble(
  year = years
) %>%
  mutate(arm = "A")  # set arm to arbitrary value found in the data

# get fit summaries at different quantiles of the posterior distribution
quants <- c(0.025, 0.075, 0.16, 0.5, 0.84, 0.925, 0.975)
fits <- fitted(fit_cp, newdata, probs = quants)

# create dataframe with calendar date associated with each year
datJoin <- subDat %>%
  filter(set == "WH3") %>%
  filter(arm == "A") %>%
  dplyr::select(date, year)

# format as tibble/dataframe and merge in the year and set values
fits <- as_tibble(fits) %>%
```

```
  bind_cols(newdata) %>%  # year
  left_join(datJoin, by = c("year"))

# summarise the data for plotting
sumdf <- subDat %>%
  filter(set == "WH3") %>%
  filter(arm == "A") %>%
  group_by(date) %>%
  summarise(meanelev = mean(elev),
            sdev = sd(elev))

outlist <- list(fits = fits,
                data = sumdf,
                omegaday = omega_day)
saveRDS(outlist, "ChangePointResults.RDS")

ggplot(data = sumdf, aes(x = date)) +
  geom_point(aes(y = meanelev)) +
  geom_errorbar(aes(ymin = meanelev-sdev, ymax= meanelev+sdev), width = 0.1)
+
  geom_line(data = fits, aes(y = Estimate), color = "salmon", size = 1) +
  geom_ribbon(data = fits, aes(ymin = `Q2.5`, ymax = `Q97.5`),
              alpha = 0.2,
              fill = "salmon") +
  geom_vline(aes(xintercept = omega_day), linetype = 2) +
  labs(x = "Date", y = "Elevation (millimeters)")
```

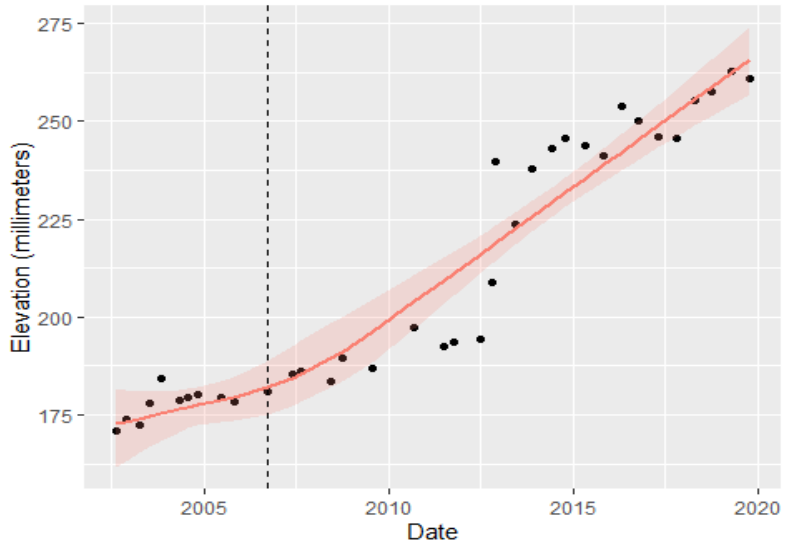


Figure D-4. Fitted changepoint model for Watch Hill WH3 SET station, arm 'A.' The horizontal line shows the estimated changepoint data from the model.

Another approach using segmented

Using **brms** is time consuming because of the HMC algorithm. This means that testing multiple models (e.g., models with different numbers of change-points) is very time consuming. One possibility is to conduct model selection using the **segmented** package to identify how many breakpoints might be supported by the data and then fitting a **brms** model with the identified structure. Here we show a brief example.

```
library(segmented)  # load the segmented package

# fit a simple linear model with no random effects
linearmod <- lm(elev ~ year, data = subDat)

# update the model fit with 1 breakpoint (psi), and give an initial
# guess of year 10 (about 2012)
segmod1 <- segmented(linearmod,
                     seg.Z = ~ year,
                     psi = c(10))
segmod1$psi  # estimate is year 5.53 for the breakpoint, similar to the BRMS
model

##           Initial     Est.    St.Err
## psi1.year      10 5.530807 0.9744456

# update the model to have 2 breakpoints (psi)
segmod2 <- segmented(linearmod,
                     seg.Z = ~ year,
                     psi = c(5.53, 10))
segmod2$psi  # years 9.12 and 10.93

##           Initial      Est.    St.Err
## psi1.year    5.53  9.126737 0.2261852
## psi2.year   10.00 10.936580 0.2264506

# compare models with AIC
AIC(segmod1, segmod2, linearmod)  # 2 breakpoint model has lowest AIC

##           df      AIC
## segmod1    5 1074.721
## segmod2    7 1018.092
## linearmod  3 1095.048

# plot the results
# get the fitted data
fits <- fitted(segmod2)
final <- data.frame(year = subDat$year, elev = fits)
```

```
final <- final %>%
  left_join(subDat %>% dplyr::select(-elev))

# extract breakpoint dates
bp1id <- which.min(abs(subDat$year - segmod2$psi[1,2]))
bpd1 <- subDat[bp1id, ]$date
bpd1 <- as.Date(bpd1, origin = "1970-01-01")
bp2id <- which.min(abs(subDat$year - segmod2$psi[2,2]))
bpd2 <- subDat[bp2id, ]$date
bpd2 <- as.Date(bpd2, origin = "1970-01-01")
bps <- c(bpd1, bpd2)

# plot the fitted model
ggplot(final, aes(x = date, y = elev)) +
  geom_line() +
  geom_point(data = subDat, aes(color = arm)) +
  labs(x = "Date", y = "Elevation (millimeters)") +
  theme(axis.text.x = element_text(angle = 45, vjust = 1, hjust=1)) +
  scale_x_date(date_breaks = "1 years", date_labels = "%Y")
```

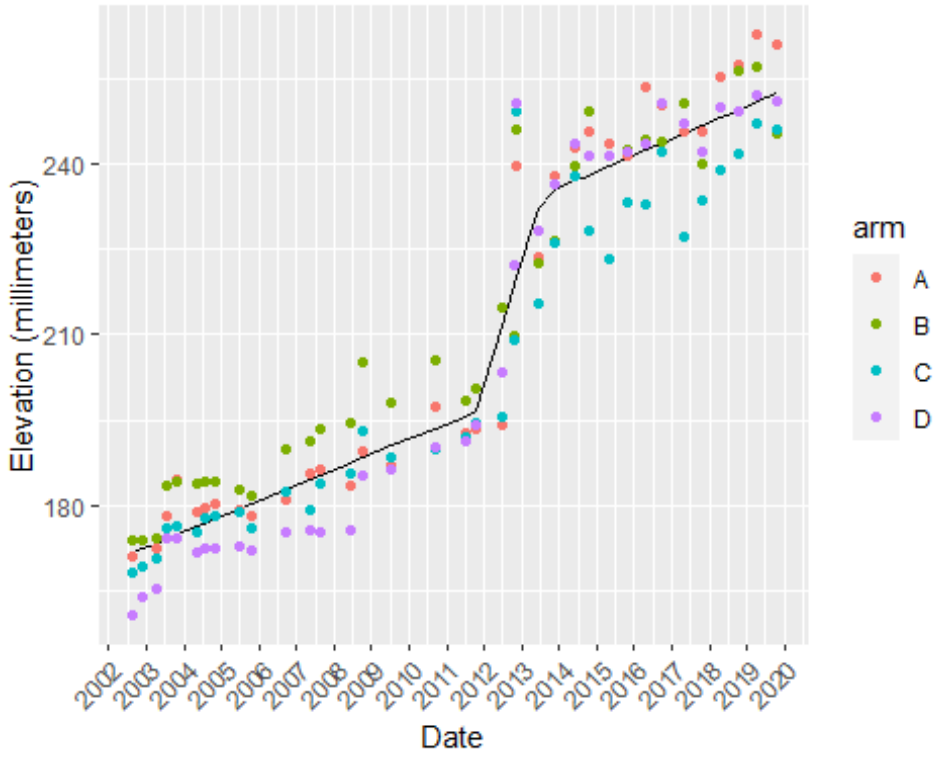


Figure D-5. Model with two breakpoints showing a better representation of the data. The changepoint dates are 2011-10-06 and 2013-06-12.

Here we see that the model with two breakpoints is a better representation of the data. The changepoint dates are 2011-10-06 and 2013-06-12. This kind of model (more than one break point) is difficult to implement in **brms** because it requires constraining the order of break points (each break point year needs to be greater than the last one). Thus, a Bayesian analysis would require Stan and **rstan** along with custom code.

Conclusions

The piece-wise linear model is able to detect change-points in the linear trend, but these change points might not occur at the time we expect a priori. In this case, the estimate of a single change-point date was associated with high uncertainty (95% BCI = 2002-08-15, 2012-06-20). More precise estimates could be achieved with a more complex model that is fitted at the site level using the same random effects structure as presented for the main analyses. As mentioned above, that more complex model is easier to design in Stan itself rather than the **brms** syntax, which we focused on here. Another approach would be to fit set level models and then average the posterior distributions of `omega` over the sets to arrive at an approximate posterior distribution for the site-level change-point date. Note that averaging posteriors decreases the variance of the averaged posterior relative to the posterior distribution from a fully random effects model.

We also found that the single break-point model produced non-intuitive results. The **segmented** package provides an easy interface to fit break-point models with more than one break-point, and those models provided a better fit. However, it is not straightforward to fit a random effects model with breakpoints using **segmented**.

These conclusions lead us to the following recommendations:

1. If the goal is to best portray the trend over time when the trend is potentially nonlinear, we suggest using Generalized Additive Models (Appendix C).

2. If the goal is to identify changepoints to model shorter time periods, we suggest using the **segmented** package (or another appropriate R package) to fit several models with different numbers of change-points and then fitting the segmented data separately using the general **brms** methods provided.

3. If the goal is to best portray the trend over time *and* identify changepoints in a Bayesian random effects framework, we suggest working with a qualified statistician (either at NPS or elsewhere) to design the statistical model and implement in an appropriate Bayesian modeling computer language (or a custom MCMC algorithm).

Appendix E: Seasonal analysis of elevation and accretion

John Lombardi, Western EcoSystems Technology, Inc.
Andrew T. Tredennick, Western EcoSystems Technology, Inc.
Mikey Tabak, Western EcoSystems Technology, Inc.
Leigh Ann Starcevich, Western EcoSystems Technology, Inc.
2021-10-29

Introduction

The seasonal analysis below was conducted to determine if there is a necessity in sampling in both spring and fall. Currently, samples are collected in both the spring and fall within a given year. The primary comparison that was done was to fit a model to the data subset to the fall, fit a model to the data subset to the spring, then assess if the credible intervals no longer overlap with the overall trend which was fit using all the data. If the credible intervals do not overlap with the model that utilizes all the data, then the trend estimate has changed when using a subset of the data. This would suggest that a yearly trend cannot be estimated well by one season of data in a year alone. Below, a summary of the groups that did have seasonal trends that varied from their overall trend are shown. Additionally, credible interval plots for every single park, site, and set are shown for the accretion and elevation metric.

General Summary

The primary conclusion of this analysis was that fitting a model to a spring only data set or a fall only data set does not typically result in a change in the overall trend estimate. The vast majority of parks, sites, and sets had credible intervals that overlapped with the model that was fit to their respective entire data set. The instances for which there was a spring or fall estimate that did not overlap with the overall are shown below.

Summary of credible interval overlaps for elevation

To test whether the seasonal estimates are different from one another, we evaluated whether the 95% confidence intervals for Spring and Fall overlap and whether the median of either season estimate falls within the 95% confidence interval of the other season. If the 95% confidence intervals do not overlap, this strongly suggests that sampling in just one season will bias the trend estimate. If the median of one season does not fall within the 95% CI of the other, this suggests there may be some bias in the trend estimate if just one season is sampled. Most confidence intervals overlapped, with only 8 out of 155 SET stations having confidence intervals for seasonal estimates that did not overlap. However, 46 out of 155 SET stations had median estimates in one season that did not fall within the 95% CI of the other season. These results are presented in the table below and figures for all estimates follow this overview section.

Table E-1. SET stations for which the median elevation trend estimate of one season did not fall within the 95% CI of the estimate for the other season.

Park*	Site	SET	CI overlap?	Median within CI?
ACAD	Bass Harbor	Bass Harbor 1	Yes	No
ACAD	Bass Harbor	Bass Harbor 3	Yes	No
ACAD	Maine Coast Heritage	MCHT 2	Yes	No
ACAD	Maine Coast Heritage	MCHT 3	Yes	No
ACAD	Schoodic	Schoodic 1	Yes	No
ACAD	Schoodic	Schoodic 2	Yes	No
ACAD	Schoodic	Schoodic 3	Yes	No
ACAD	Thompson Island	Thompson 1	Yes	No
ACAD	Thompson Island	Thompson 2	Yes	No
ASIS	Marsh 11	M11-1	Yes	No
ASIS	Marsh 11	M11-4	No	No
ASIS	Marsh 6	M6-3	Yes	No
ASIS	Marsh 8	M8-1	Yes	No
ASIS	Marsh 8	M8-2	No	No
ASIS	Marsh 8	M8-3	Yes	No
ASIS	Marsh 8	M8-4	No	No
ASIS	Marsh Exclosure	M8-4	Yes	No
ASIS	Marsh non-Exclosure	M11-1	Yes	No
ASIS	Marsh non-Exclosure	M11-4	No	No
ASIS	Marsh non-Exclosure	M6-1	Yes	No
ASIS	Marsh non-Exclosure	M6-3	Yes	No
ASIS	Marsh non-Exclosure	M8-1	Yes	No
ASIS	Marsh non-Exclosure	M8-2	No	No
ASIS	Marsh non-Exclosure	M8-3	Yes	No
BOHA	Calf Island	Calf 1	Yes	No
CACO	Blackfish Creek	BF1	Yes	No
CACO	Blackfish Creek	BF2	Yes	No
CACO	Blackfish Creek	BF4	Yes	No
CACO	Blackfish Creek	BF6	Yes	No
CACO	Hatches Harbor HH1	HH3	Yes	No
CACO	Hatches Harbor H1	H3	Yes	No
CACO	Hatches Harbor H2	H4	Yes	No
CACO	Hatches Harbor H2	H6	Yes	No
CACO	Herring River G	G1	Yes	No
CACO	Herring River G	G3	Yes	No
CACO	Herring River Phrag	Phrag1	Yes	No
CACO	Herring River Phrag	Phrag2	Yes	No
COLO	Marsh 30	M30 Pipe 1	Yes	No
COLO	Marsh 30	M30 Pipe 2	Yes	No
COLO	Marsh 30	M30 Pipe 3	No	No
GATE	Big Egg Control	BEC3	Yes	No
GATE	Black Bank	BB1	Yes	No
GATE	Elders East NF	EE NF1	Yes	No

Park*	Site	SET	CI overlap?	Median within CI?
GATE	Elders East NF	EE NF3	No	No
GATE	Elders East Shallow	EE2 Shallow	Yes	No
GATE	JOCO REF Shallow	JocoRef3 Shallow	Yes	No
GWMP	Dyke Marsh River	River 3	No	No

*Park abbreviations: ASIS - Assateague Island National Seashore, BOHA - Boston Harbor Islands National Recreation Area, CACO - Cape Cod National Seashore, COLO - Colonial National Historical Park, FIIS - Fire Island National Seashore, GATE - Gateway National Recreation Area, GWMP - George Washington Memorial Parkway, NACE - National Capital Parks-East.

At the site level, 16 out of 44 sites had median estimates for one season that did not fall within the 95% CI of the other season estimate. Of these, only 2 sites had 95% CIs that did not overlap (see Table D-2.).

Table D-2. Sites for which the median elevation trend estimate of one season did not fall within the 95% CI of the estimate for the other season. Site-level trend estimates are the average of the SET-level estimates within each site and season.

Park*	Site	SET	CI overlap?	Median within CI?
ACAD	Bass Harbor	Seasonal Average	Yes	No
ACAD	Maine Coast Heritage	Seasonal Average	Yes	No
ACAD	Schoodic	Seasonal Average	Yes	No
ACAD	Thompson Island	Seasonal Average	Yes	No
ASIS	Marsh 6	Seasonal Average	Yes	No
ASIS	Marsh 8	Seasonal Average	No	No
ASIS	Marsh 11	Seasonal Average	Yes	No
ASIS	Marsh Exclosure	Seasonal Average	Yes	No
ASIS	Marsh non-Exclosure	Seasonal Average	Yes	No
CACO	Blackfish Creek	Seasonal Average	Yes	No
CACO	Hatches Harbor HH1	Seasonal Average	Yes	No
CACO	Hatches Harbor H2	Seasonal Average	Yes	No
CACO	Herring River G	Seasonal Average	Yes	No
COLO	Marsh 30	Seasonal Average	No	No
GATE	Big Egg Control	Seasonal Average	Yes	No
GATE	Elders East NF	Seasonal Average	Yes	No
GATE	Elders East Shallow	Seasonal Average	Yes	No

*Park abbreviations: ASIS - Assateague Island National Seashore, BOHA - Boston Harbor Islands National Recreation Area, CACO - Cape Cod National Seashore, COLO - Colonial National Historical Park, FIIS - Fire Island National Seashore, GATE - Gateway National Recreation Area, GWMP - George Washington Memorial Parkway, NACE - National Capital Parks-East.

Summary of credible interval overlaps for accretion

To test whether the seasonal estimates are different from one another, we evaluated whether the 95% confidence intervals for Spring and Fall overlap and whether the median of either season estimate falls within the 95% confidence interval of the other season. If the 95% confidence intervals do not overlap, this strongly suggests that sampling in just one season will bias the trend estimate. If the

median of one season does not fall within the 95% CI of the other, this suggests there may be some bias in the trend estimate if just one season is sampled.

Most confidence intervals overlapped, with only 4 out of 153 SET stations having confidence intervals for seasonal estimates that did not overlap. However, 31 out of 153 SET stations had median estimates in one season that did not fall within the 95% CI of the other season. These results are presented in the table below and figures for all estimates follow this overview section.

Table D-3. SET stations for which the median accretion trend estimate of one season did not fall within the 95% CI of the estimate for the other season.

Park*	Site	SET	CI overlap?	Median within CI?
ASIS	Marsh 6	M6-1	Yes	No
ASIS	Marsh 6	M6-2	Yes	No
ASIS	Marsh 8	M8-1	No	No
ASIS	Marsh 8	M8-2	Yes	No
ASIS	Marsh 8	M8-3	Yes	No
ASIS	Marsh 8	M8-4	Yes	No
ASIS	Marsh Exclosure	M8-4	Yes	No
ASIS	Marsh non-Exclosure	M5-1	Yes	No
ASIS	Marsh non-Exclosure	M6-2	Yes	No
ASIS	Marsh non-Exclosure	M8-1	No	No
ASIS	Marsh non-Exclosure	M8-2	Yes	No
BOHA	Thompson Island	Thompson 4	Yes	No
CACO	Blackfish Creek	BF4	Yes	No
CACO	Blackfish Creek	BF6	No	No
CACO	Hatches Harbor HH1	HH3	Yes	No
CACO	Herring River High Toss	HighToss3	Yes	No
CACO	Nauset Marsh N	N1	Yes	No
COLO	Marsh 5	M5 Pipe 1	Yes	No
COLO	Marsh 13	M13 Pipe 1	Yes	No
COLO	Marsh 13	M13 Pipe 2	Yes	No
COLO	Marsh 30	M30 Pipe 1	Yes	No
FIIS	Watch Hill	WH3	Yes	No
GATE	Big Egg Control	BEC2	Yes	No
GATE	Elders East	EE2	Yes	No
GATE	JOCO	Joco2	Yes	No
GATE	JOCO	Joco3	Yes	No
GATE	Sandy Hook	SH3	Yes	No
GWMP	Dyke Marsh Creek	Creek Bank 2	Yes	No
GWMP	Dyke Marsh Creek	Creek Bank 3	Yes	No
GWMP	Dyke Marsh River	River 1A	Yes	No
GWMP	Dyke Marsh River	River 2	Yes	No

*Park abbreviations: ASIS - Assateague Island National Seashore, BOHA - Boston Harbor Islands National Recreation Area, CACO - Cape Cod National Seashore, COLO - Colonial National Historical Park, FIIS - Fire Island National Seashore, GATE - Gateway National Recreation Area, GWMP - George Washington Memorial Parkway, NACE - National Capital Parks-East.

At the site level, 8 out of 40 sites had median estimates for one season that did not fall within the 95% CI of the other season estimate. Of these, only 2 sites had 95% CIs that did not overlap (see Table D-4).

Table D-4. Sites for which the median accretion trend estimate of one season did not fall within the 95% CI of the estimate for the other season. Site-level trend estimates are the average of the SET-level estimates within each site and season.

Park*	Site	SET	CI overlap?	Median within CI?
ACAD	Thompson Island	Seasonal Average	Yes	No
ASIS	Marsh 6	Seasonal Average	Yes	No
ASIS	Marsh 8	Seasonal Average	No	No
ASIS	Marsh non-Exclosure	Seasonal Average	Yes	No
CACO	Blackfish Creek	Seasonal Average	Yes	No
CACO	Hatches Harbor HH1	Seasonal Average	Yes	No
CACO	Herring River High Toss	Seasonal Average	Yes	No
COLO	Marsh 13	Seasonal Average	Yes	No
COLO	Marsh 30	Seasonal Average	Yes	No
FIIS	Watch Hill	Seasonal Average	Yes	No
GATE	Big Egg Control	Seasonal Average	Yes	No
GATE	JOCO	Seasonal Average	Yes	No
GATE	Sandy Hook	Seasonal Average	Yes	No
GWMP	Dyke Marsh Creek	Seasonal Average	Yes	No
GWMP	Dyke Marsh River	Seasonal Average	Yes	No

*Park abbreviations: ASIS - Assateague Island National Seashore, BOHA - Boston Harbor Islands National Recreation Area, CACO - Cape Cod National Seashore, COLO - Colonial National Historical Park, FIIS - Fire Island National Seashore, GATE - Gateway National Recreation Area, GWMP - George Washington Memorial Parkway, NACE - National Capital Parks-East.

Elevation Seasonal Analysis plots

The plots following are all visualizations of the credible intervals for a park, site, and set (or overall) trend for elevation. If the 3 credible intervals all overlap in a figure, then the overall trend is very similar between the fall only, spring only, and overall models that were fit. However, if the seasonal trends are very different (see tables above), then estimating the trend from just one season might bias the trend estimate.

The x-axis displays the estimated trend value, where the left endpoint is the lower limit to the 95% credible interval, the right end point is the upper limit to the 95% credible interval, and the middle point is the median value. The y-axis splits the data temporally for the spring, fall, and overall values.

Elevation Seasonal by SET plots

The plots below contain the elevation trend estimates by season for each park, site, and SET.

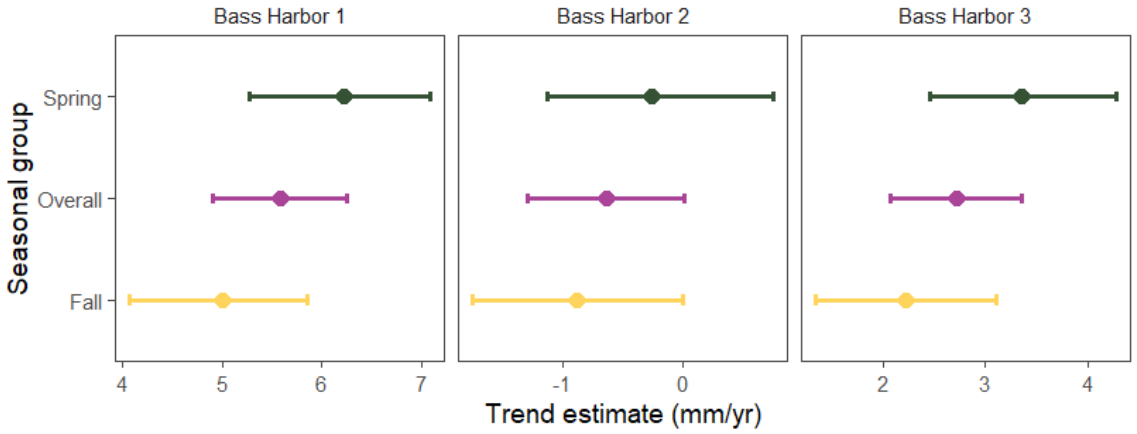


Figure E-1. Elevation trend estimates by season for each station at the Bass Harbor site, Acadia National Park.

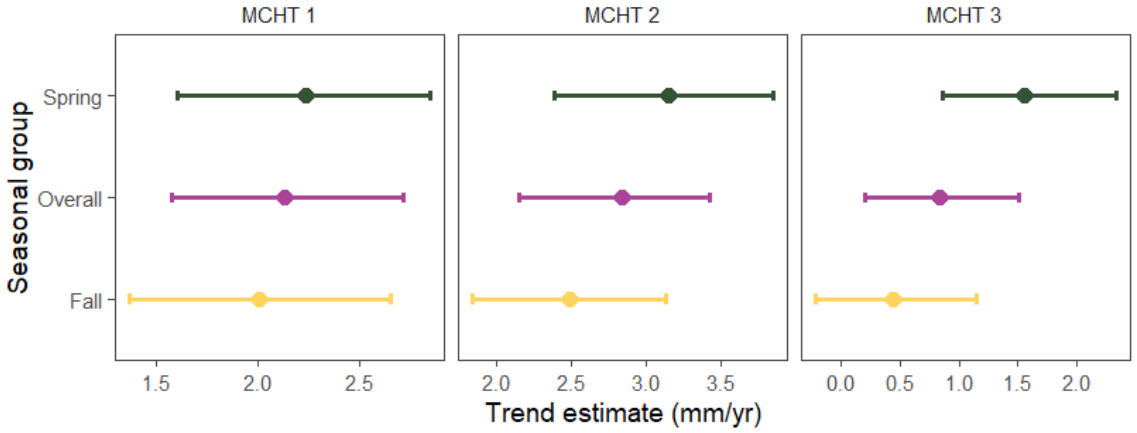


Figure E-2. Elevation trend estimates by season for each station at the Maine Coast Heritage site, Acadia National Park.

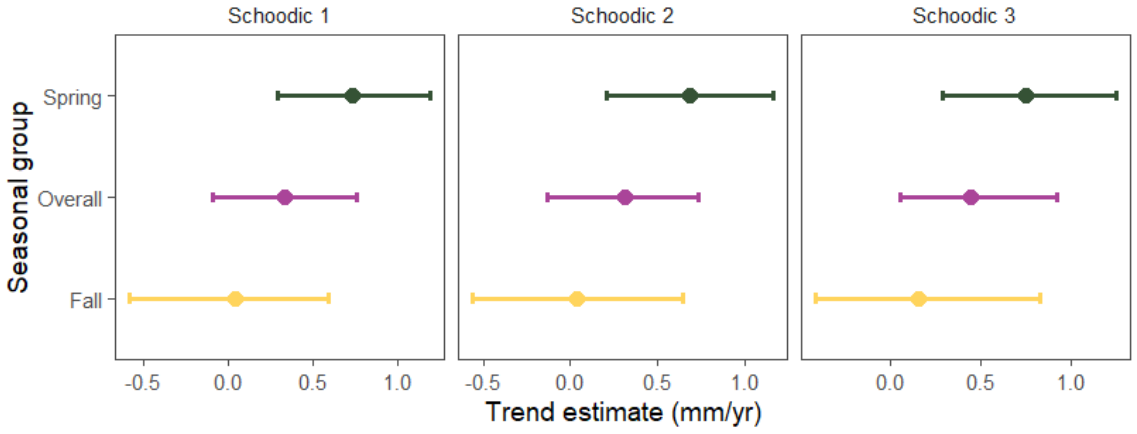


Figure E-3. Elevation trend estimates by season for each station at the Schoodic site, Acadia National Park.

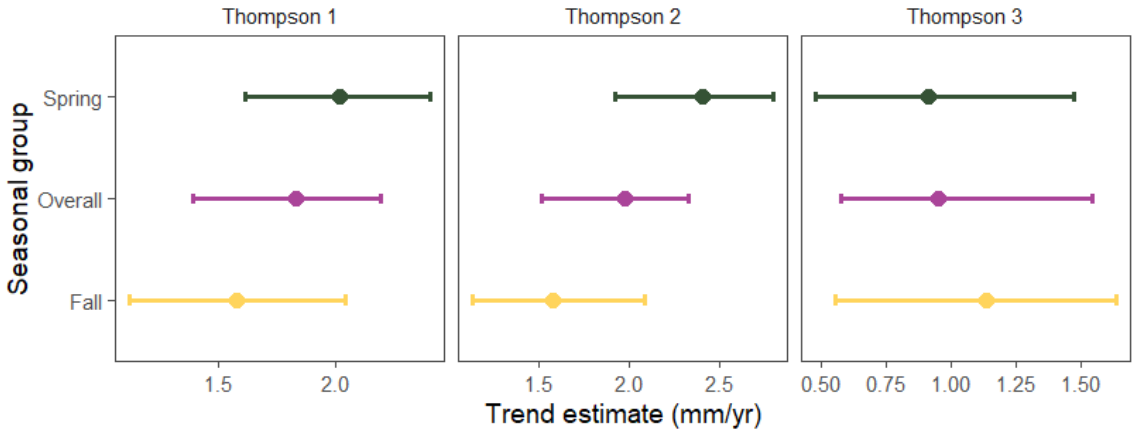


Figure E-4. Elevation trend estimates by season for each station at the Thompson Island site, Acadia National Park.

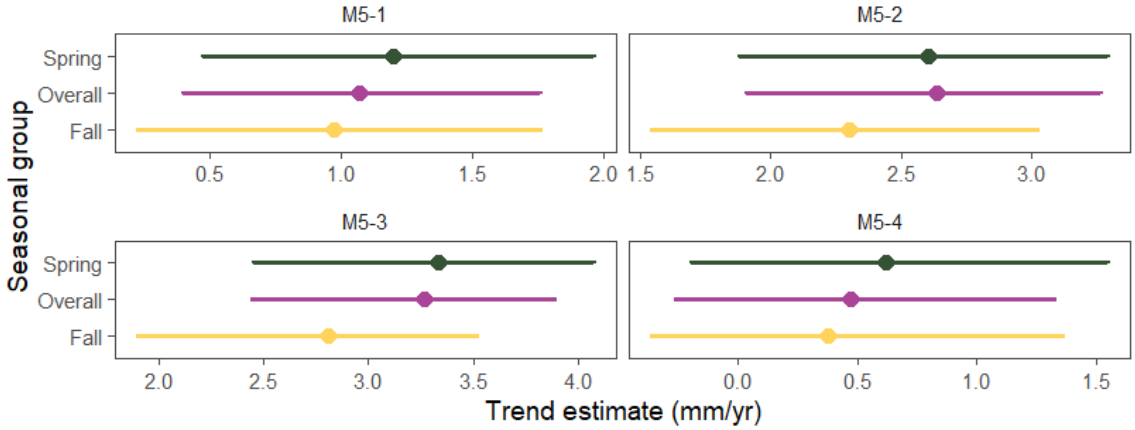


Figure E-5. Elevation trend estimates by season for each station at the Marsh 5 site, Assateague Island National Seashore.

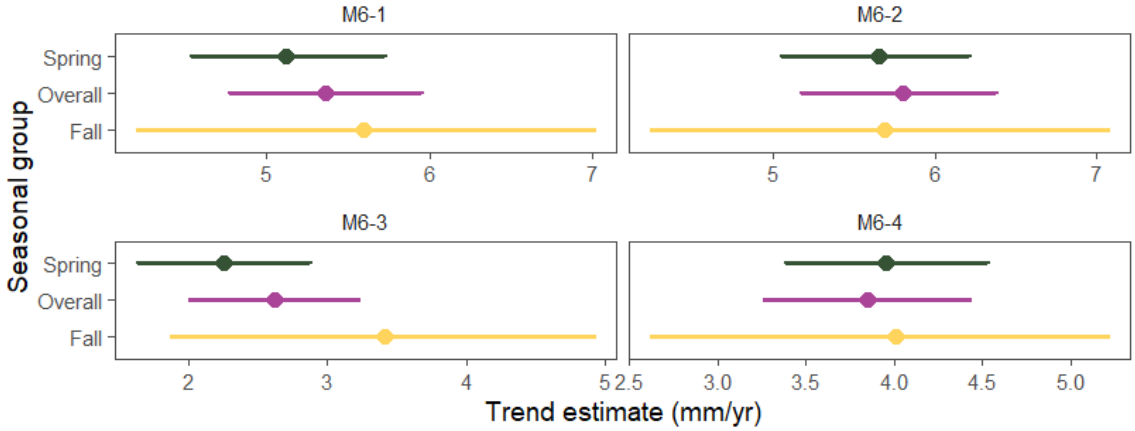


Figure E-6. Elevation trend estimates by season for each station at the Marsh 6 site, Assateague Island National Seashore.

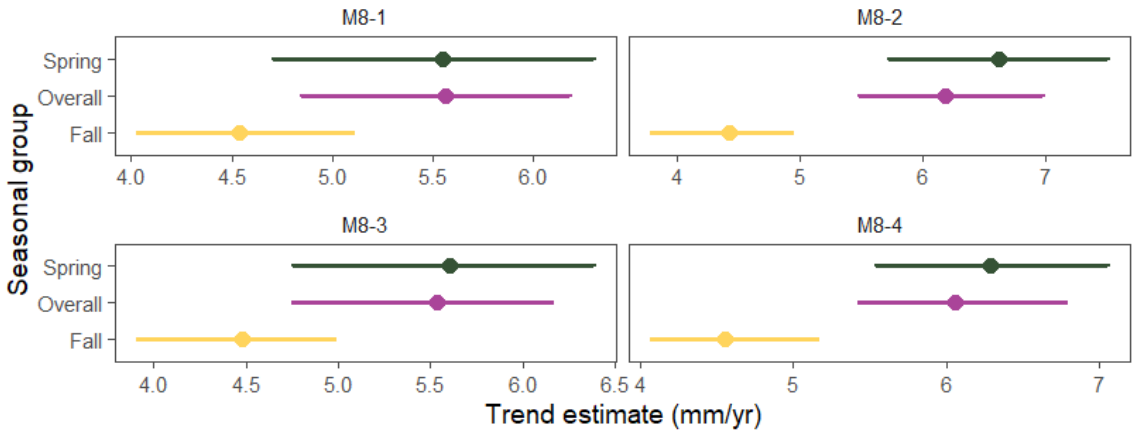


Figure E-7. Elevation trend estimates by season for each station at the Marsh 8 site, Assateague Island National Seashore.

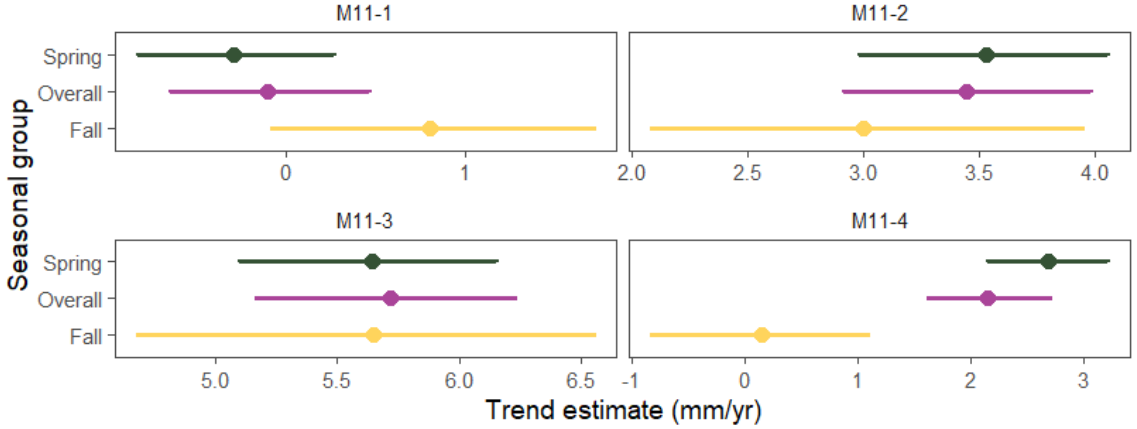


Figure E-8. Elevation trend estimates by season for each station at the Marsh 11 site, Assateague Island National Seashore.

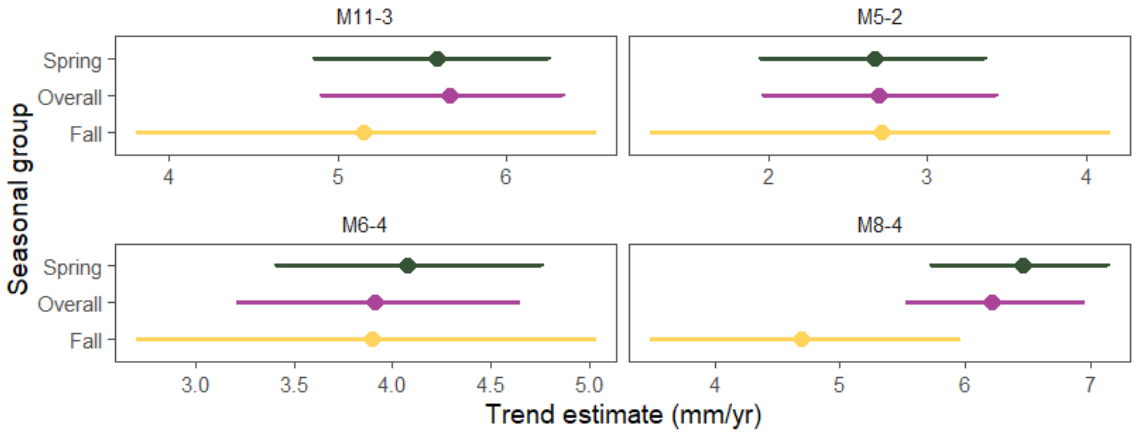


Figure E-9. Elevation trend estimates by season for each station at the Marsh Exclosure site, Assateague Island National Seashore.

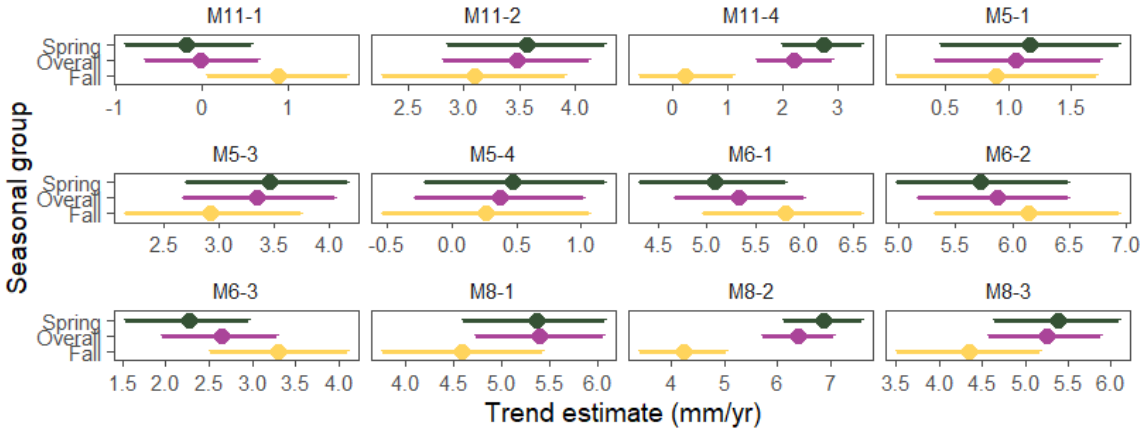


Figure E-10. Elevation trend estimates by season for each station at the Marsh non-Exclosure (Marsh 5 and 6) sites, Assateague Island National Seashore.

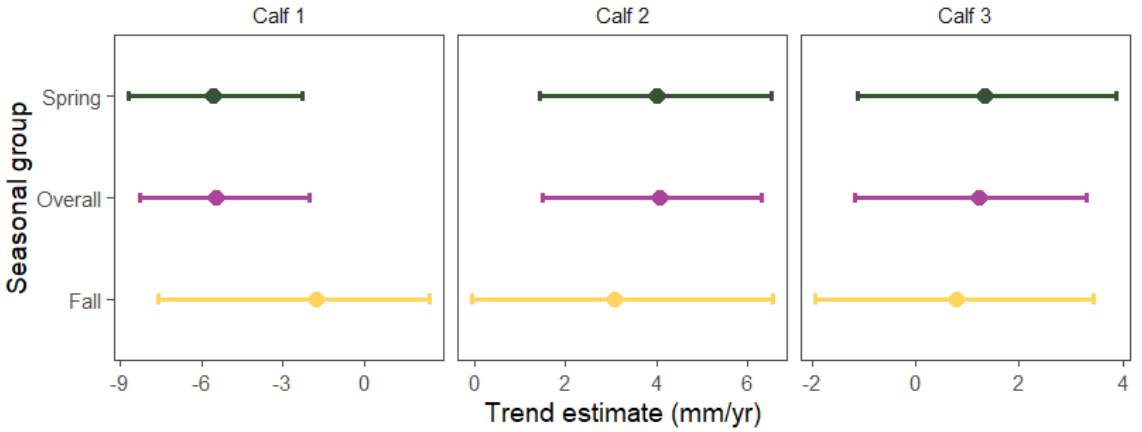


Figure E-11. Elevation trend estimates by season for each station at the Calf Island site, Boston Harbor Islands Recreation Area.

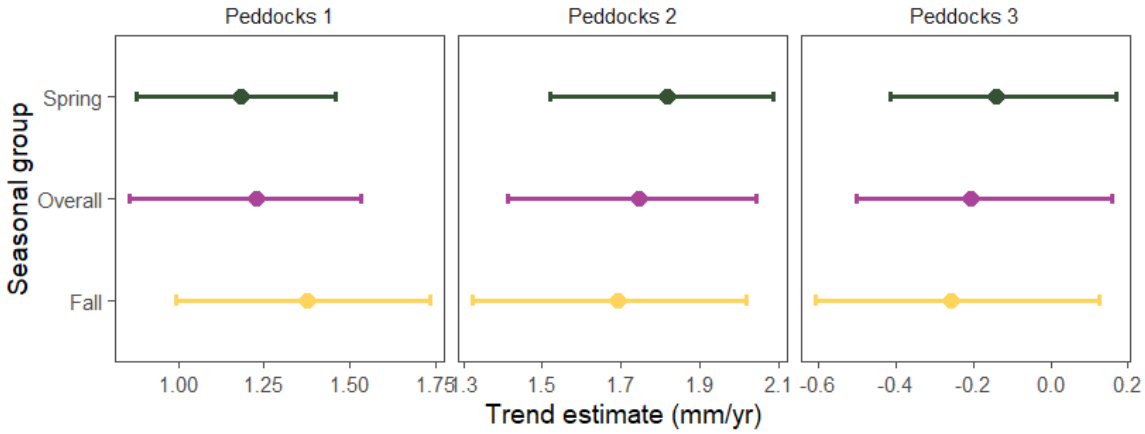


Figure E-12. Elevation trend estimates by season for each station at the Peddocks Island site, Boston Harbor Islands Recreation Area.

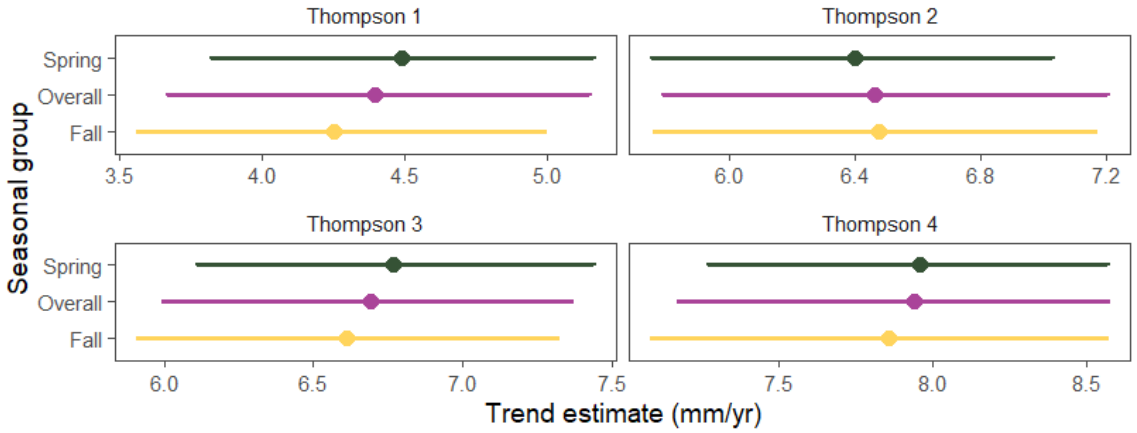


Figure E-13. Elevation trend estimates by season for each station at the Thompson Island site, Boston Harbor Islands Recreation Area.

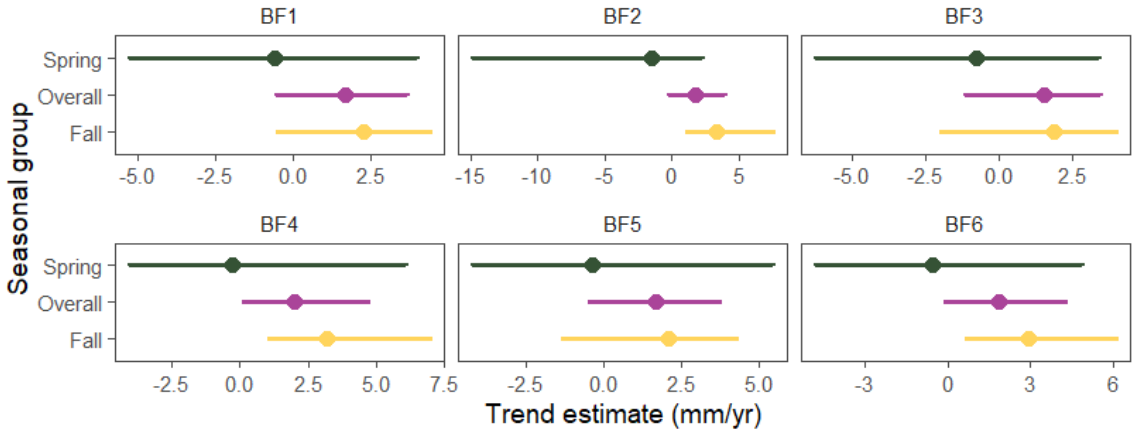


Figure E-14. Elevation trend estimates by season for each station at the Blackfish Creek site, Cape Cod National Seashore.

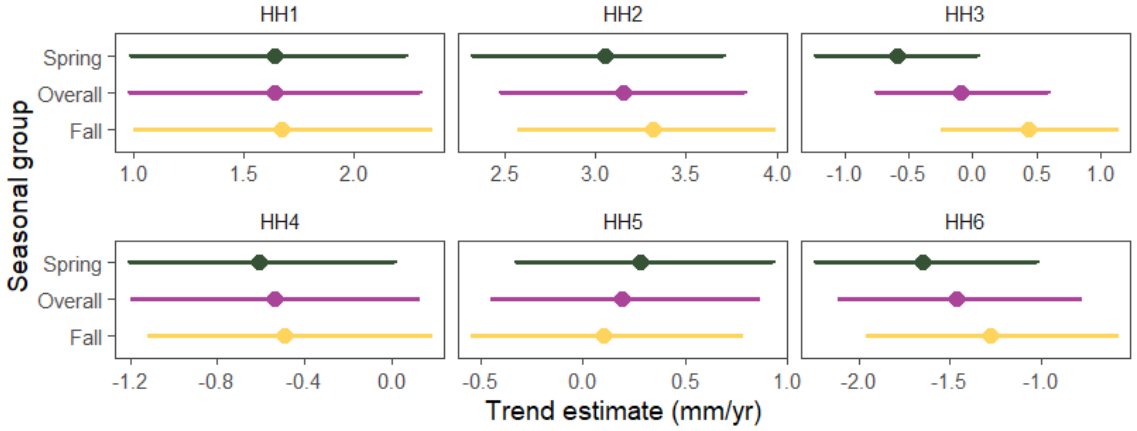


Figure E-15. Elevation trend estimates by season for each station at the Hatches Harbor HH1 site, Cape Cod National Seashore.

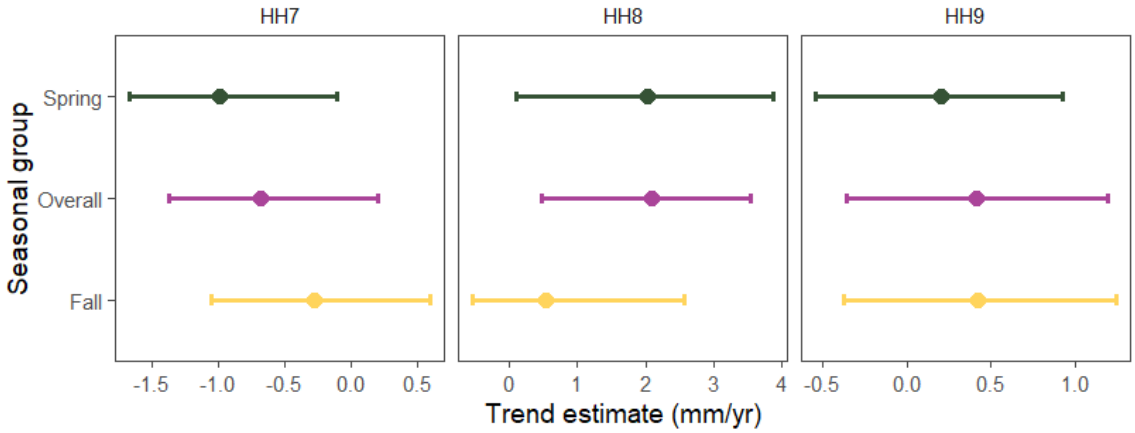


Figure E-16. Elevation trend estimates by season for each station at the Hatches Harbor HH2 site, Cape Cod National Seashore.

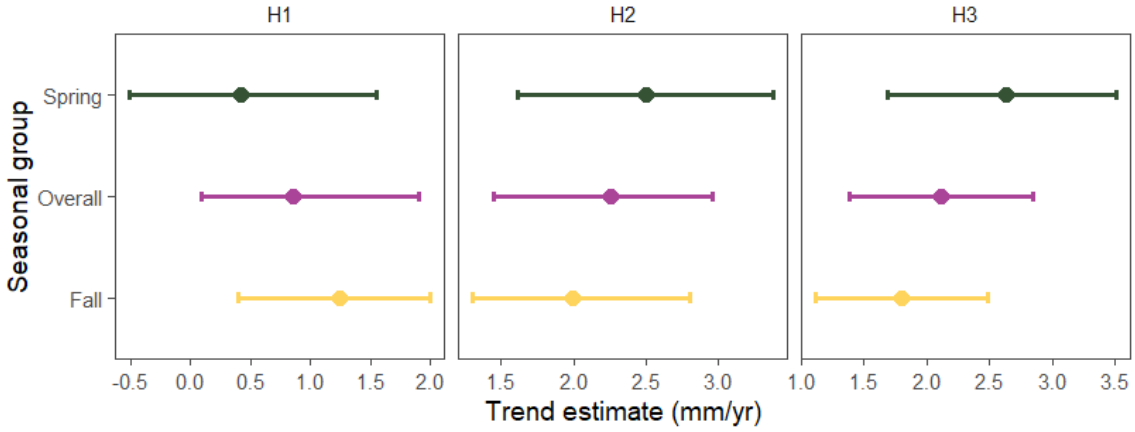


Figure E-17. Elevation trend estimates by season for each station at the Hatches Harbor H1 site, Cape Cod National Seashore.

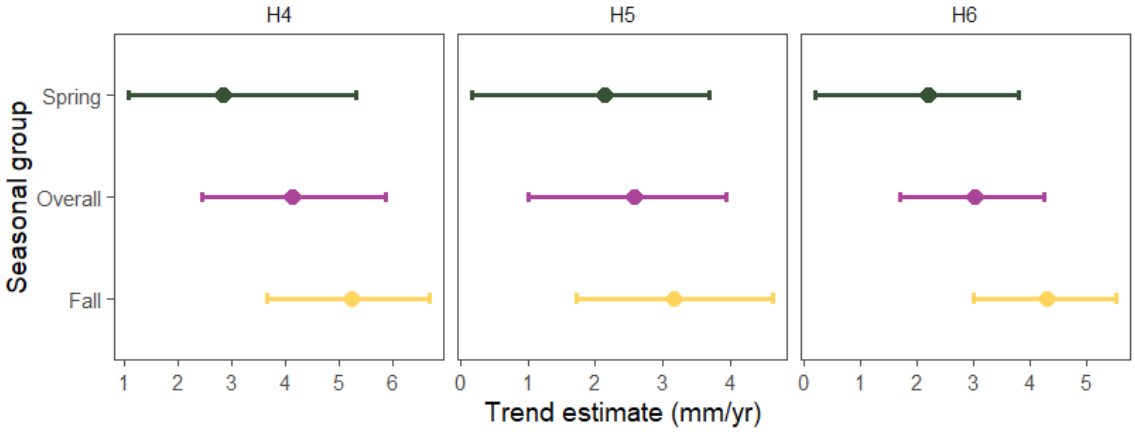


Figure E-18. Elevation trend estimates by season for each station at the Hatches Harbor H2 site, Cape Cod National Seashore.

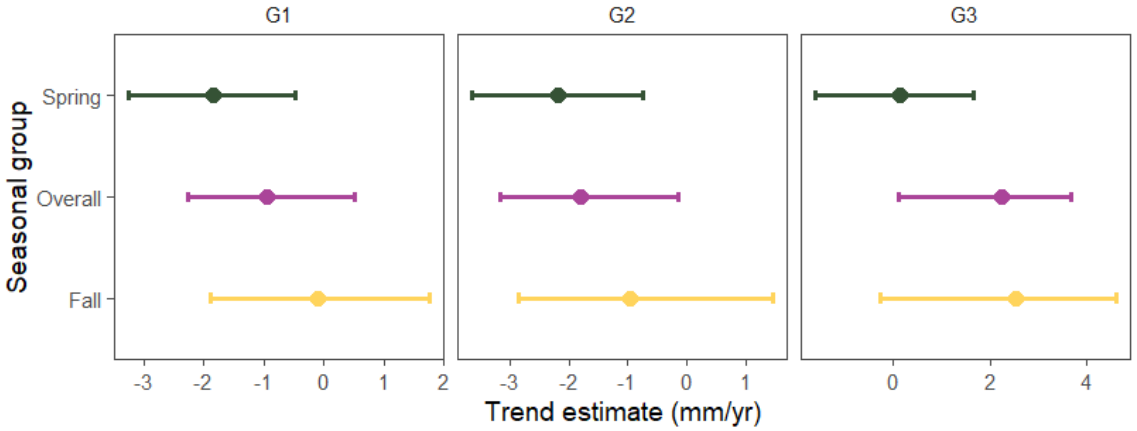


Figure E-19. Elevation trend estimates by season for each station at the Herring River G site, Cape Cod National Seashore.

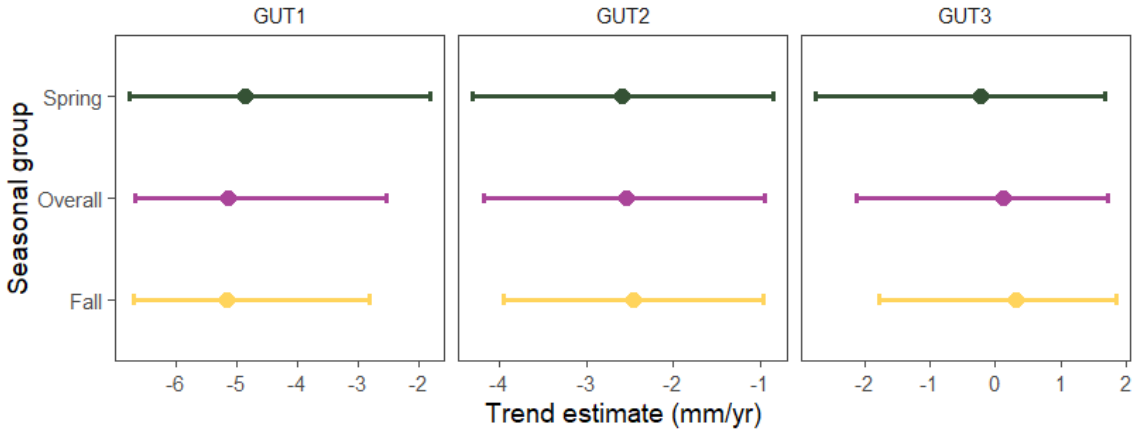


Figure E-20. Elevation trend estimates by season for each station at the Herring River GUT site, Cape Cod National Seashore.

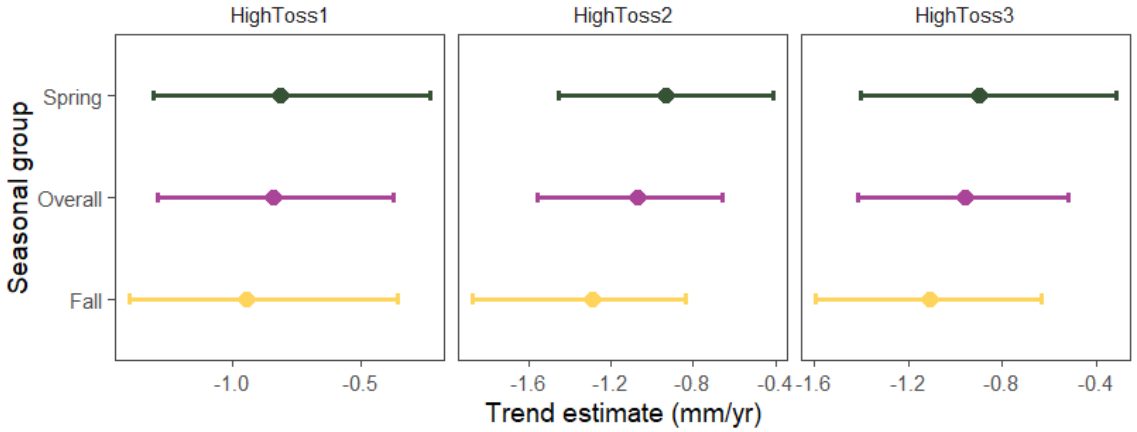


Figure E-21. Elevation trend estimates by season for each station at the Herring River High Toss site, Cape Cod National Seashore.

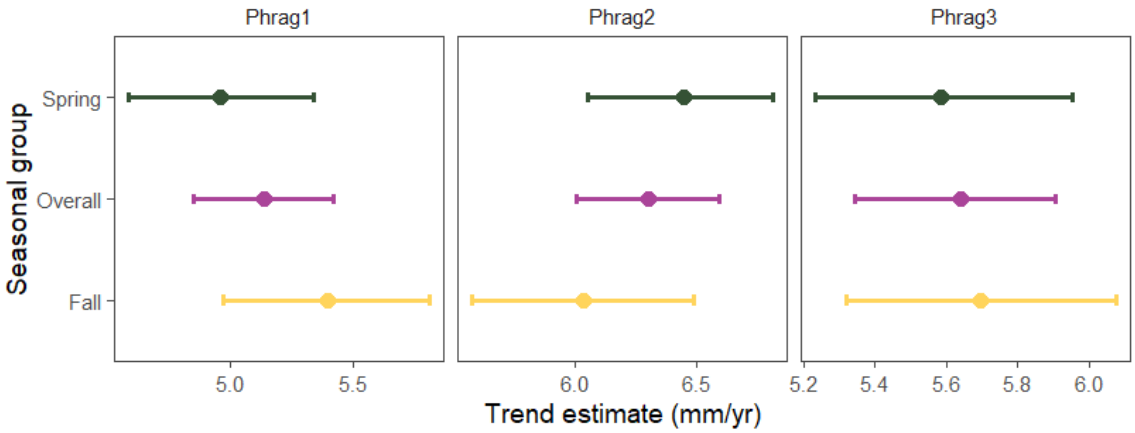


Figure E-22. Elevation trend estimates by season for each station at the Herring River Phrag site, Cape Cod National Seashore.

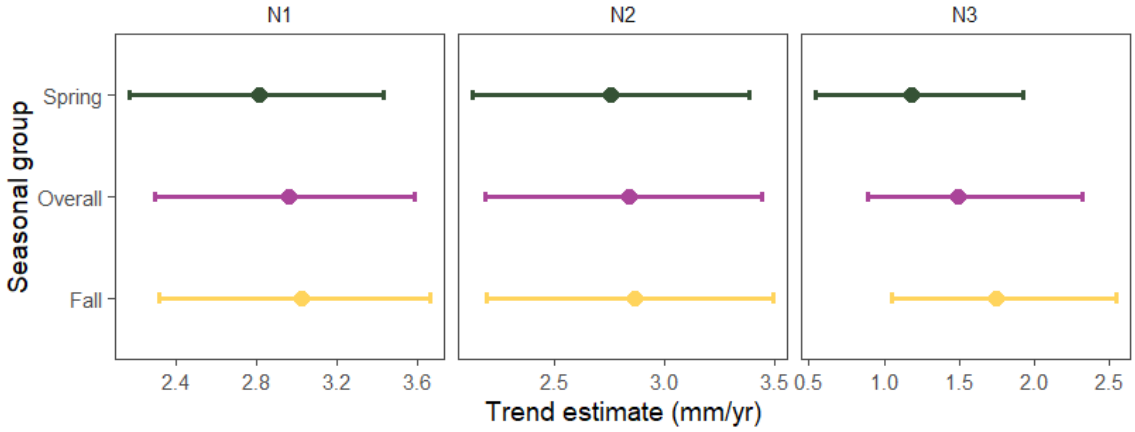


Figure E-23. Elevation trend estimates by season for each station at the Nauset Marsh N site, Cape Cod National Seashore.

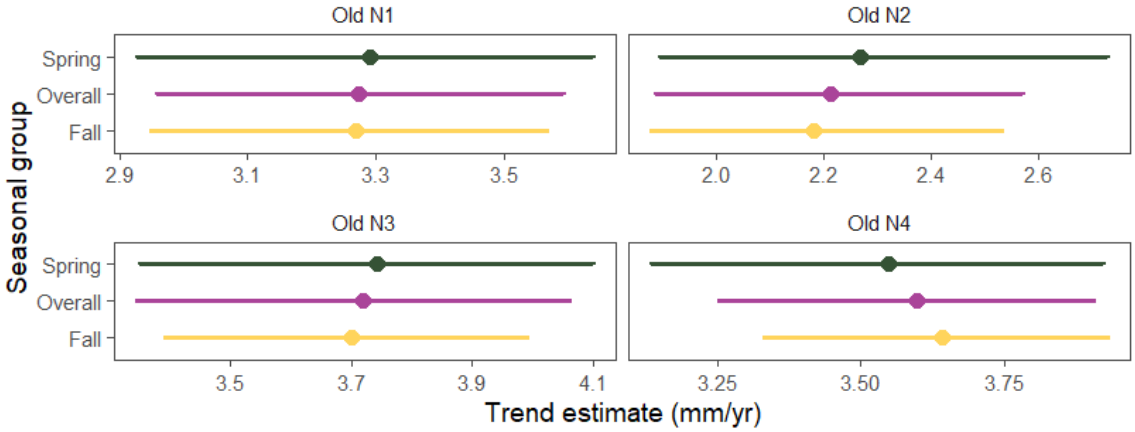


Figure E-24. Elevation trend estimates by season for each station at the Nauset Marsh Old N site, Cape Cod National Seashore.

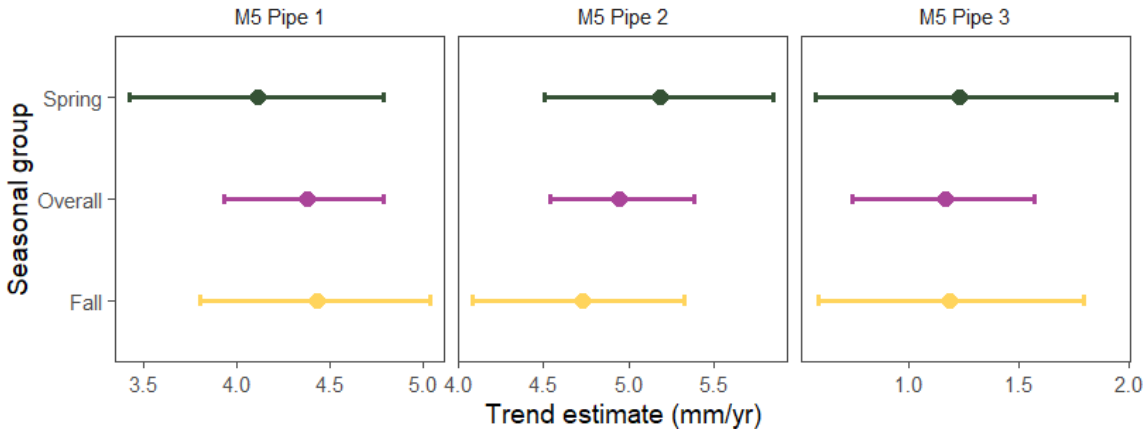


Figure E-25. Elevation trend estimates by season for each station at the Marsh 5 site, Colonial National Historical Park.

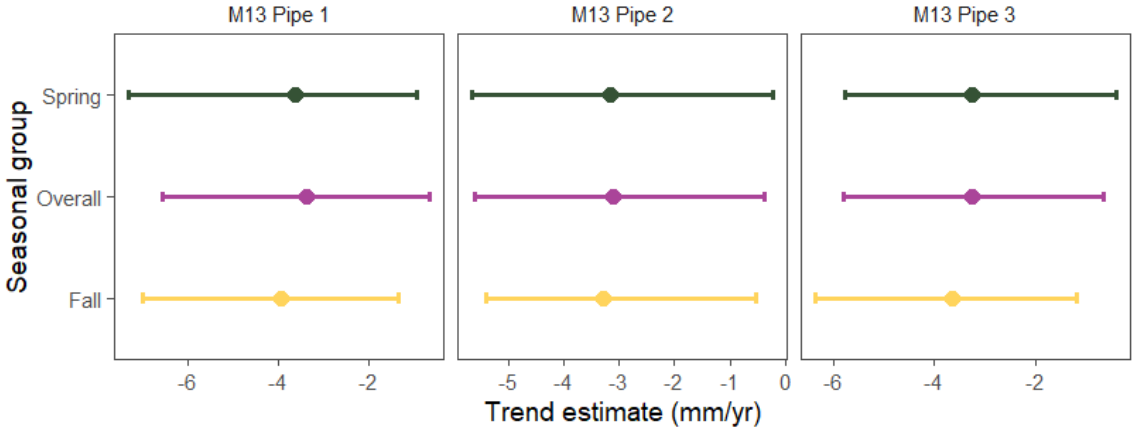


Figure E-26. Elevation trend estimates by season for each station at the Marsh 13 site, Colonial National Historical Park.

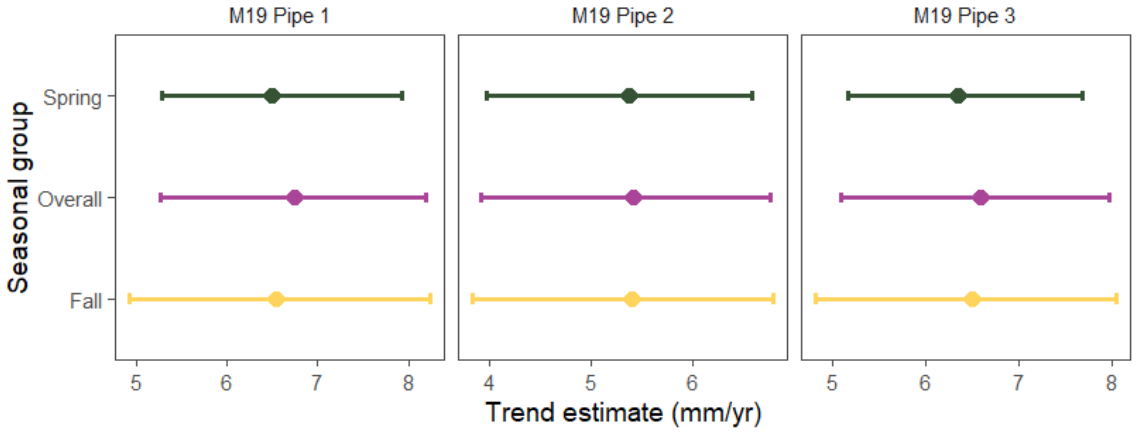


Figure E-27. Elevation trend estimates by season for each station at the Marsh 19 site, Colonial National Historical Park.

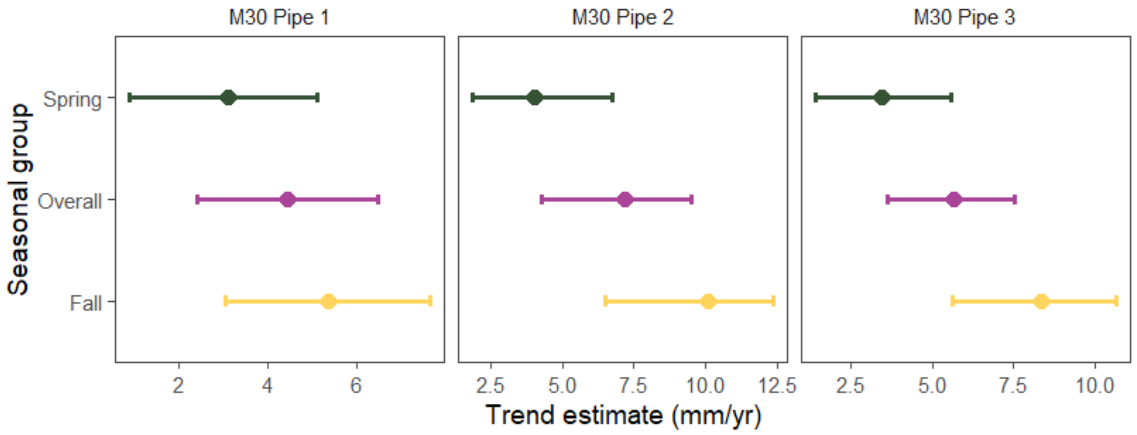


Figure E-28. Elevation trend estimates by season for each station at the Marsh 30 site, Colonial National Historical Park.

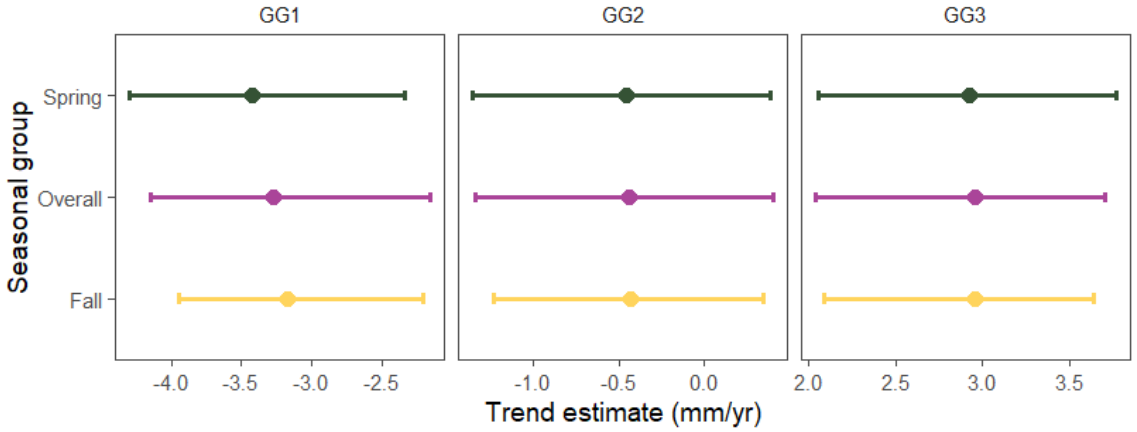


Figure E-29. Elevation trend estimates by season for each station at the Great Gun site, Fire Island National Seashore.

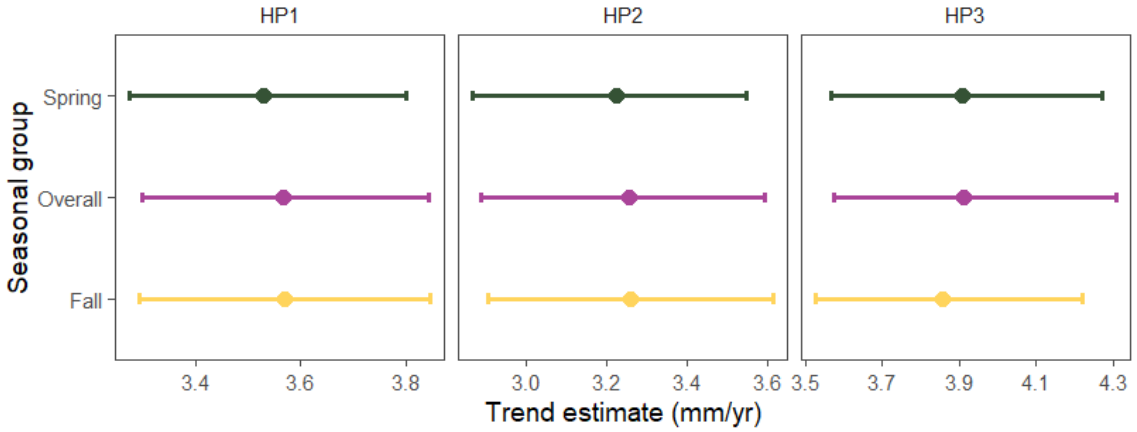


Figure E-30. Elevation trend estimates by season for each station at the Hospital Point site, Fire Island National Seashore.

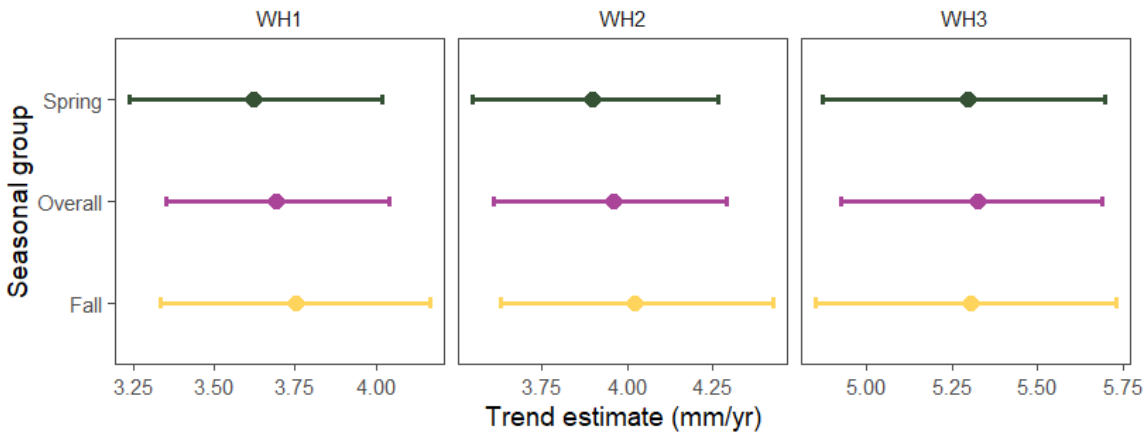


Figure E-31. Elevation trend estimates by season for each station at the Watch Hill site, Fire Island National Seashore.

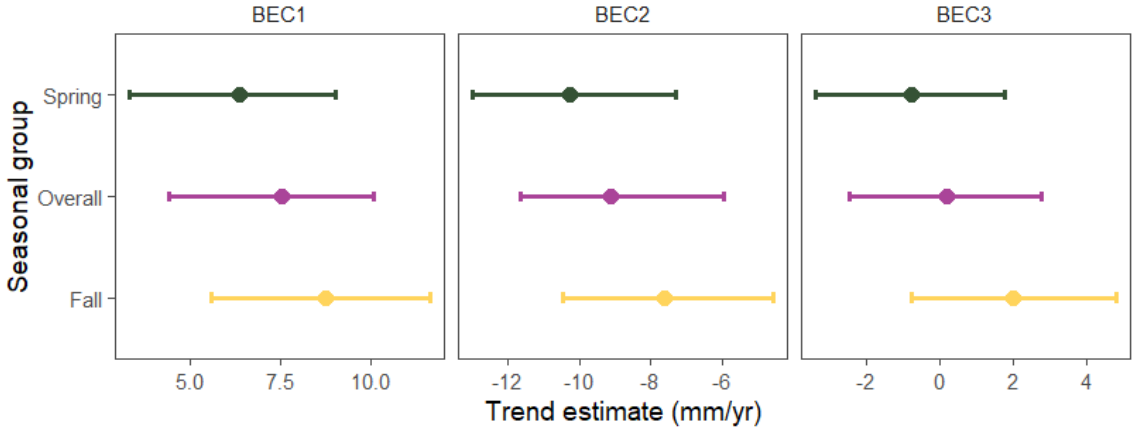


Figure E-32. Elevation trend estimates by season for each station at the Big Egg Control site, Gateway National Recreation Area.

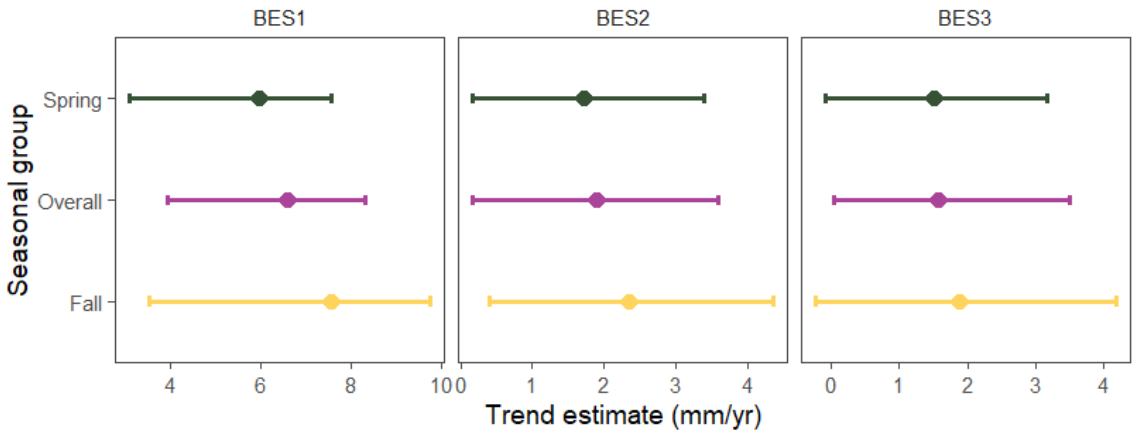


Figure E-33. Elevation trend estimates by season for each station at the Big Egg Spray site, Gateway National Recreation Area.

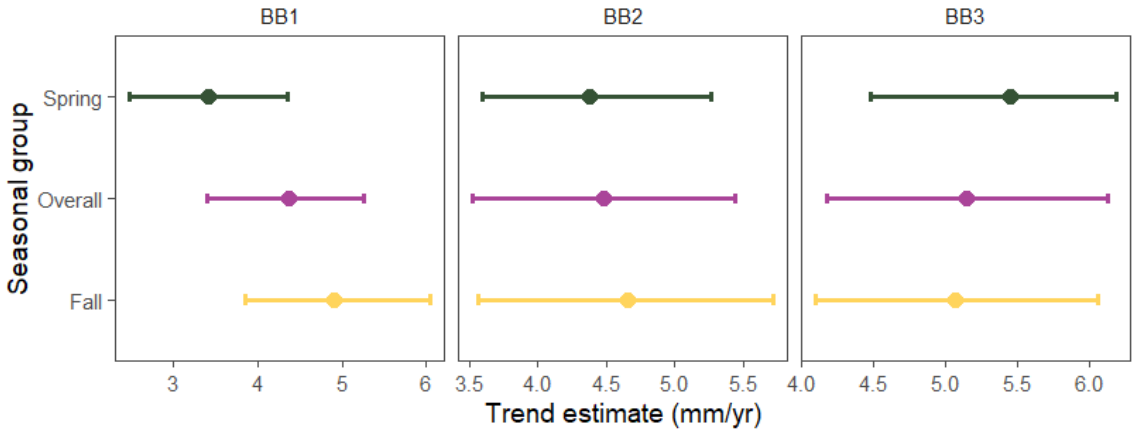


Figure E-34. Elevation trend estimates by season for each station at the Black Bank site, Gateway National Recreation Area.

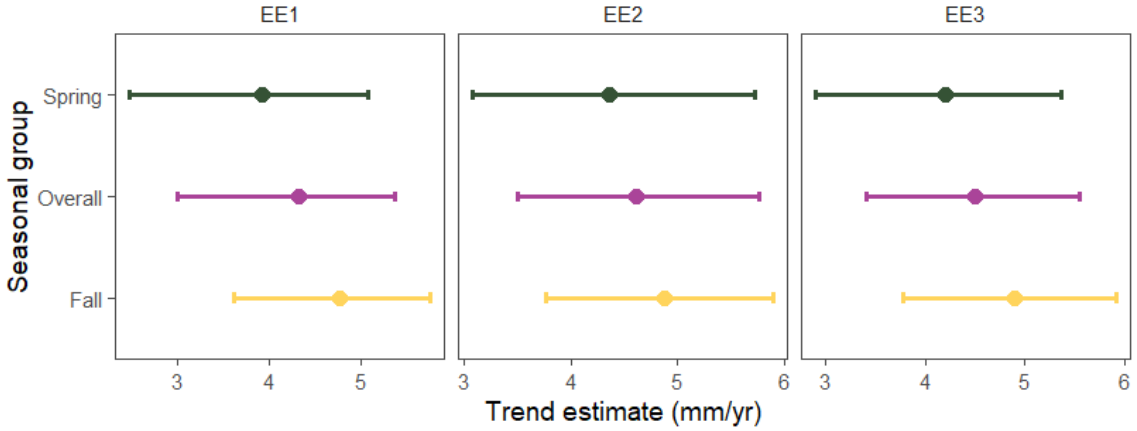


Figure E-35. Elevation trend estimates by season for each station at the Elders East site, Gateway National Recreation Area.

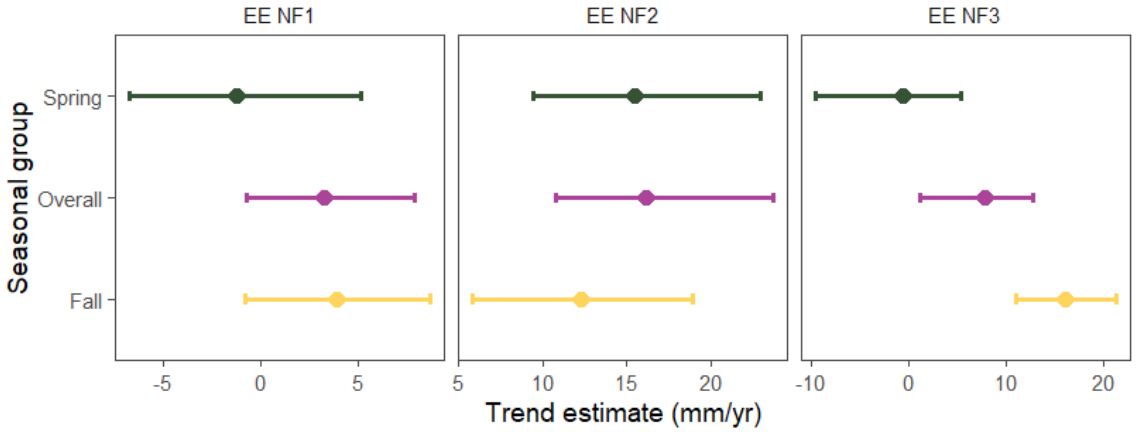


Figure E-36. Elevation trend estimates by season for each station at the Elders East NF site, Gateway National Recreation Area.

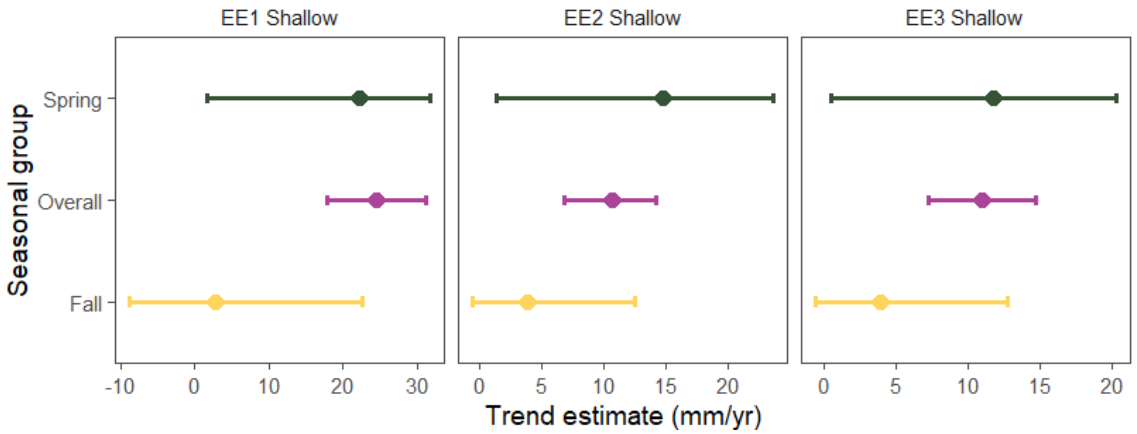


Figure E-37. Elevation trend estimates by season for each station at the Elders East Shallow site, Gateway National Recreation Area.

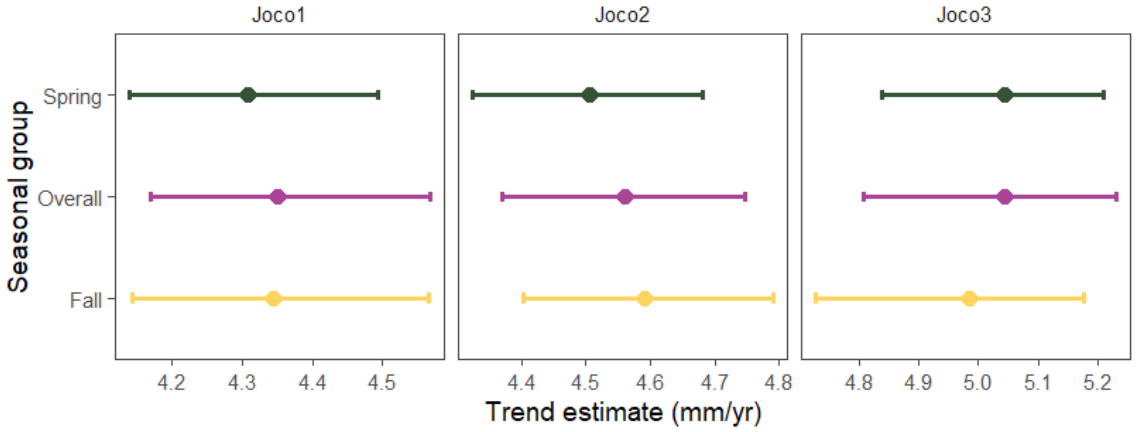


Figure E-38. Elevation trend estimates by season for each station at the JOCO site, Gateway National Recreation Area.

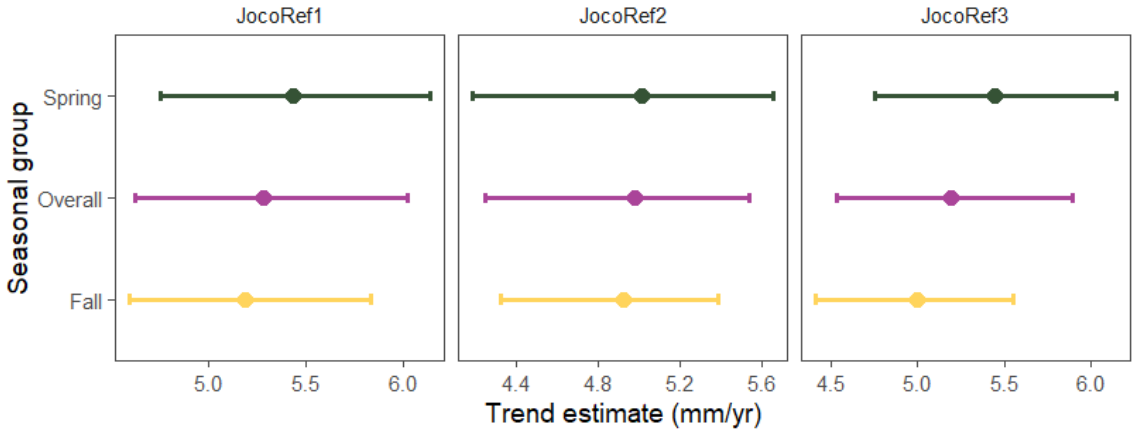


Figure E-39. Elevation trend estimates by season for each station at the JOCO REF site, Gateway National Recreation Area.

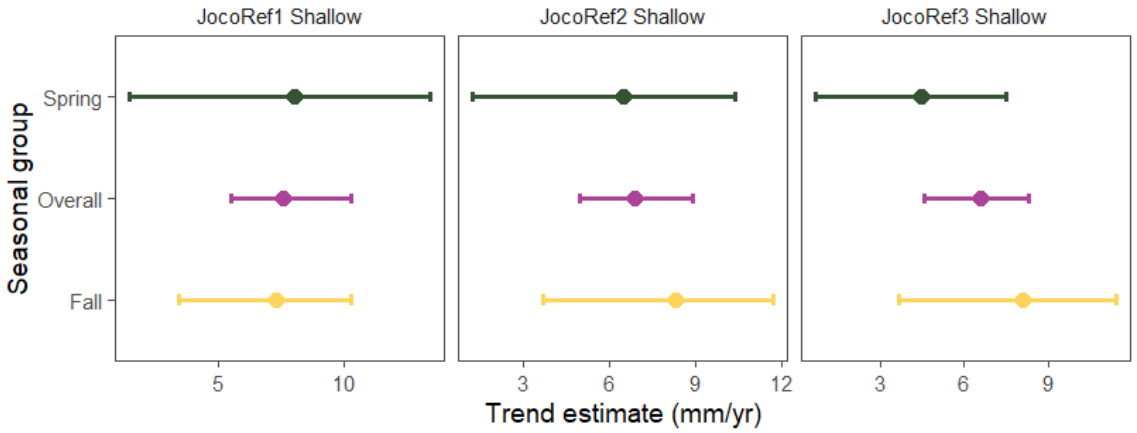


Figure E-40. Elevation trend estimates by season for each station at the JOCO REF Shallow site, Gateway National Recreation Area.

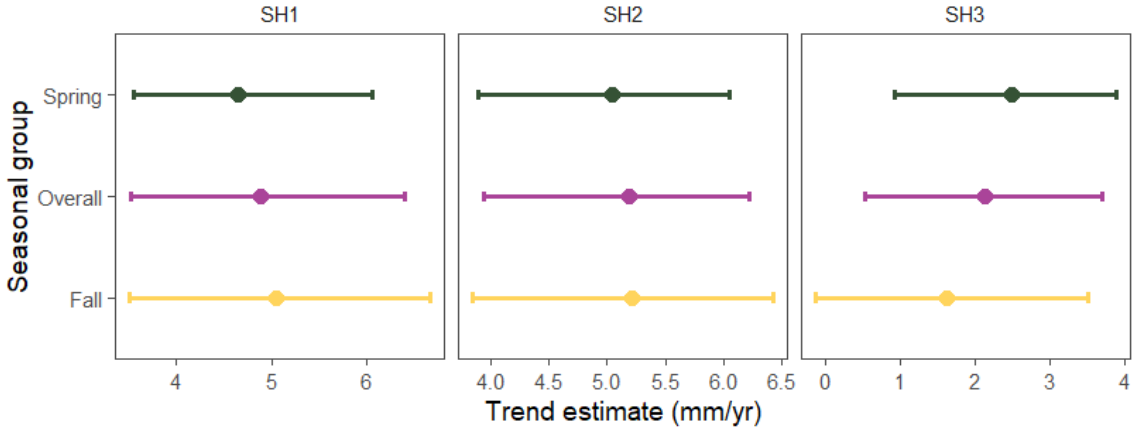


Figure E-41. Elevation trend estimates by season for each station at the Sandy Hook site, Gateway National Recreation Area.

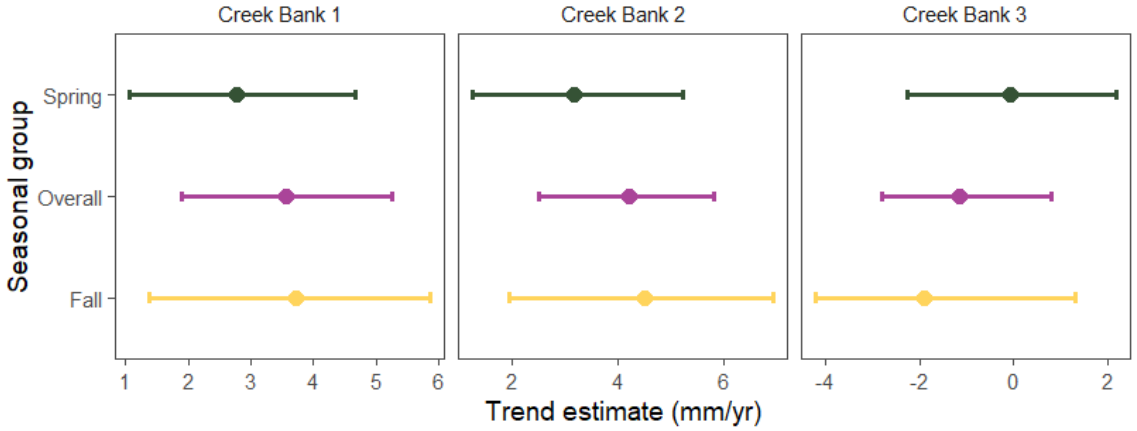


Figure E-42. Elevation trend estimates by season for each station at the Dyke Marsh Creek site, George Washington Memorial Parkway.

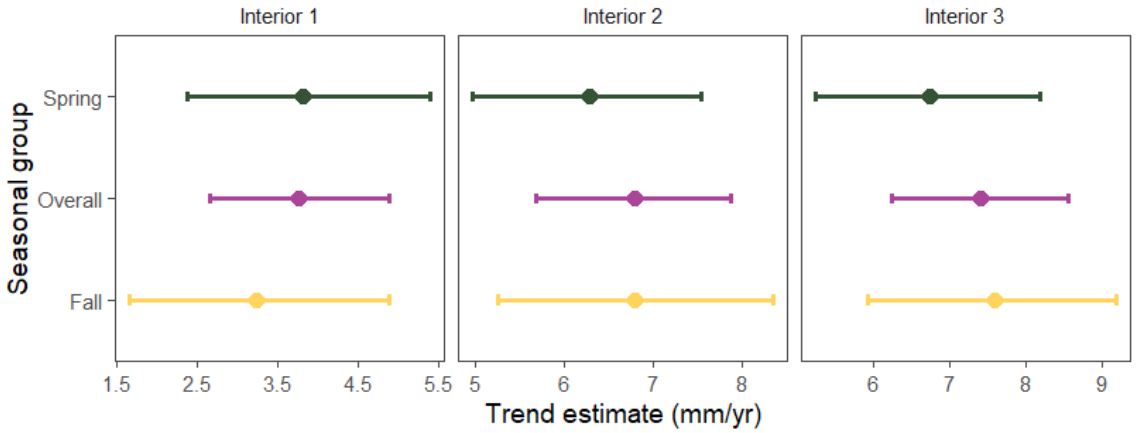


Figure E-43. Elevation trend estimates by season for each station at the Dyke Marsh Interior site, George Washington Memorial Parkway.

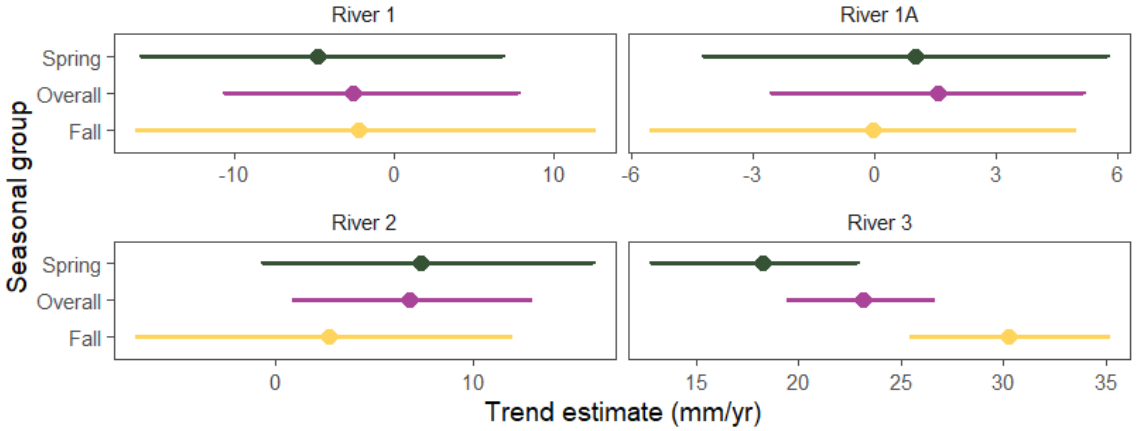


Figure E-44. Elevation trend estimates by season for each station at the Dyke Marsh River site, George Washington Memorial Parkway.

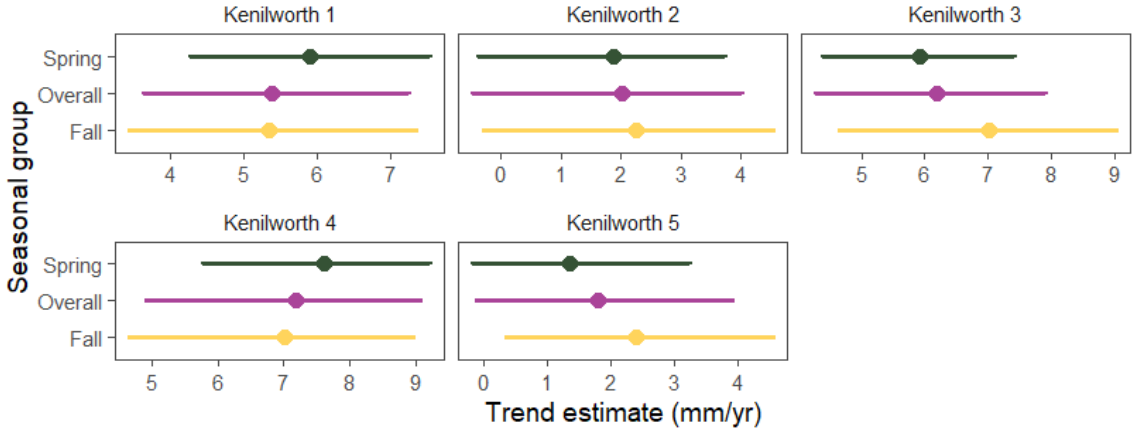


Figure E.45. Elevation trend estimates by season for each station at the Kenilworth Marsh River site, National Capital Parks-East.

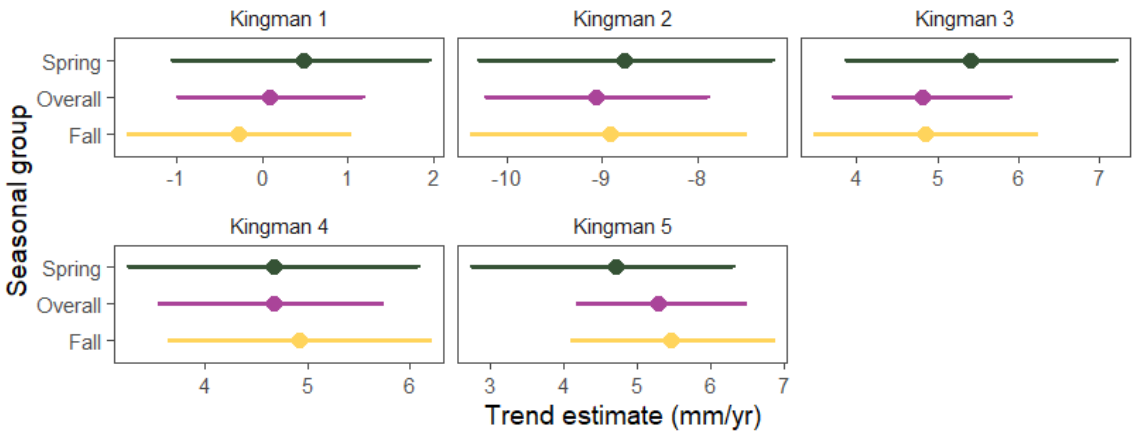


Figure E.46. Elevation trend estimates by season for each station at the Kingman Lake site, National Capital Parks-East.

Elevation Overall Plots

The plots below contain the elevation trend estimates by season for each park and site. The trend was averaged over the stations to get an 'overall elevation' trend.

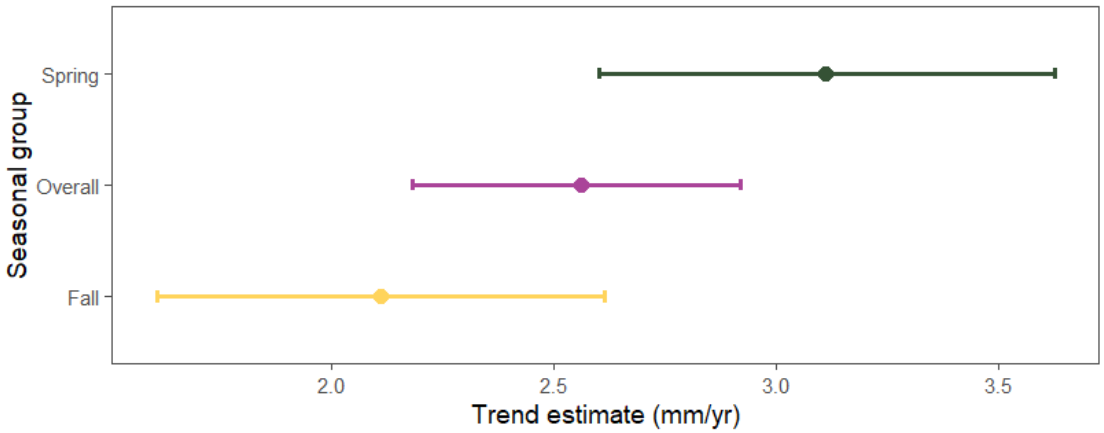


Figure E-47. Overall elevation trend estimates by season for the Bass Harbor site, Acadia National Park. The trend was averaged over the stations to get an 'overall elevation' trend.

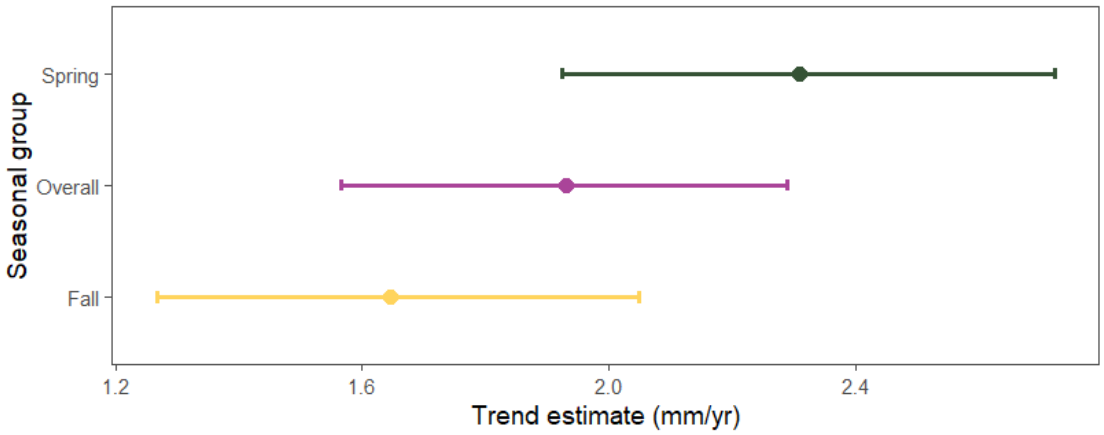


Figure E-48. Overall elevation trend estimates by season for the Maine Coast Heritage site, Acadia National Park. The trend was averaged over the stations to get an 'overall elevation' trend.

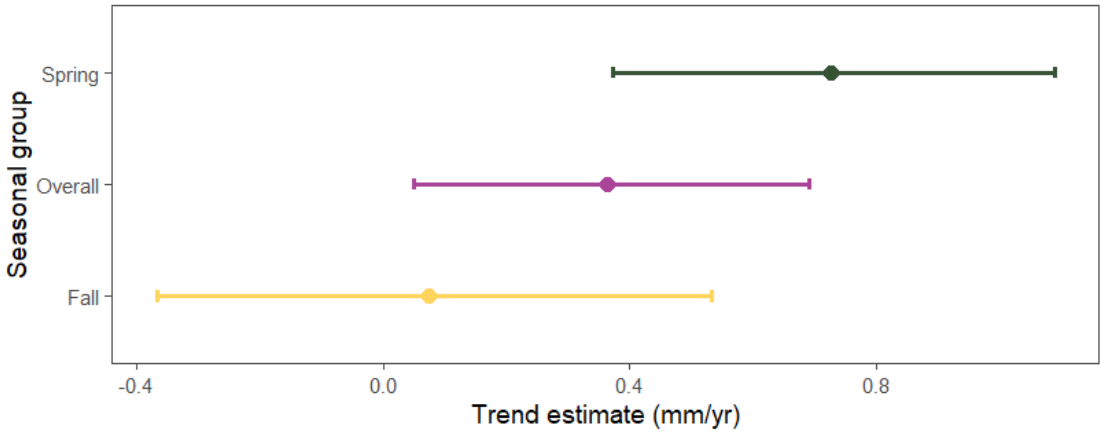


Figure E-49. Overall elevation trend estimates by season for the Schoodic site, Acadia National Park. The trend was averaged over the stations to get an 'overall elevation' trend.

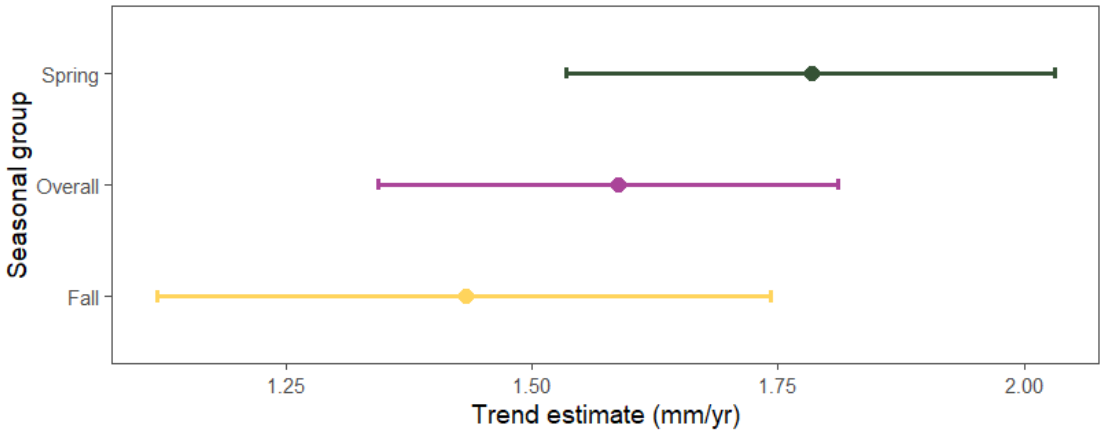


Figure E-50. Overall elevation trend estimates by season for the Thompson Island site, Acadia National Park. The trend was averaged over the stations to get an 'overall elevation' trend.

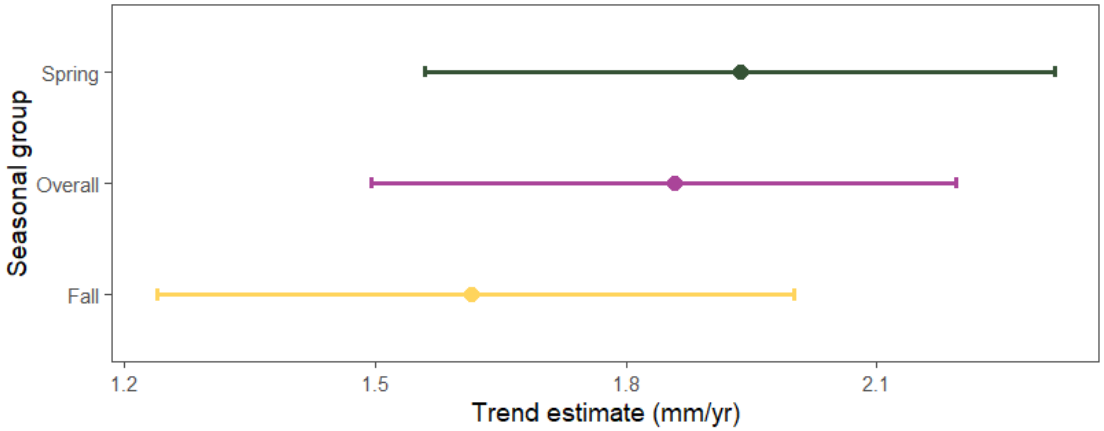


Figure E-51. Overall elevation trend estimates by season for the Marsh 5 site, Assateague Island National Seashore. The trend was averaged over the stations to get an 'overall elevation' trend.

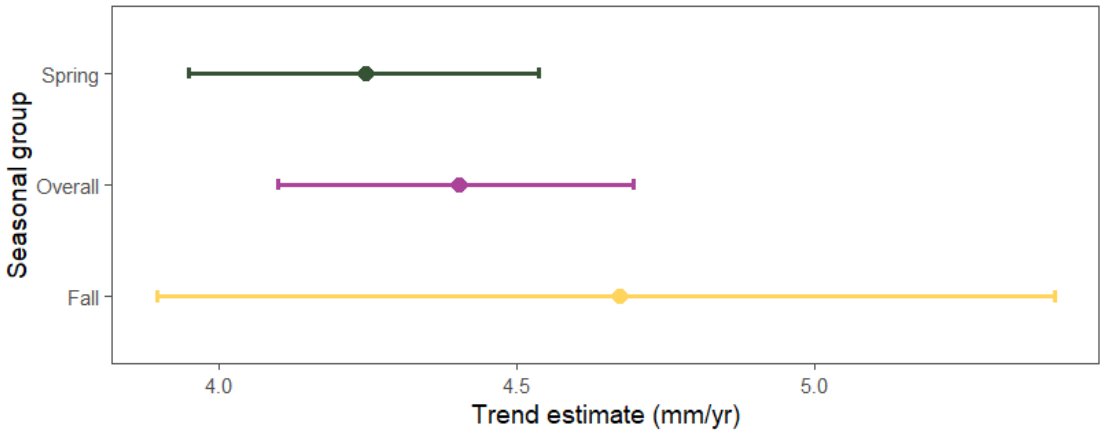


Figure E-52. Overall elevation trend estimates by season for the Marsh 6 site, Assateague Island National Seashore. The trend was averaged over the stations to get an 'overall elevation' trend.

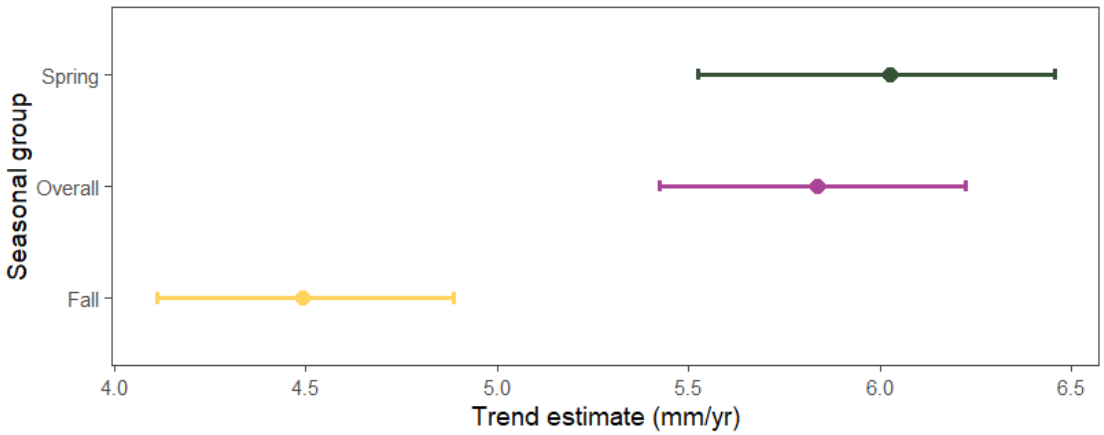


Figure E-53. Overall elevation trend estimates by season for the Marsh 8 site, Assateague Island National Seashore. The trend was averaged over the stations to get an 'overall elevation' trend.

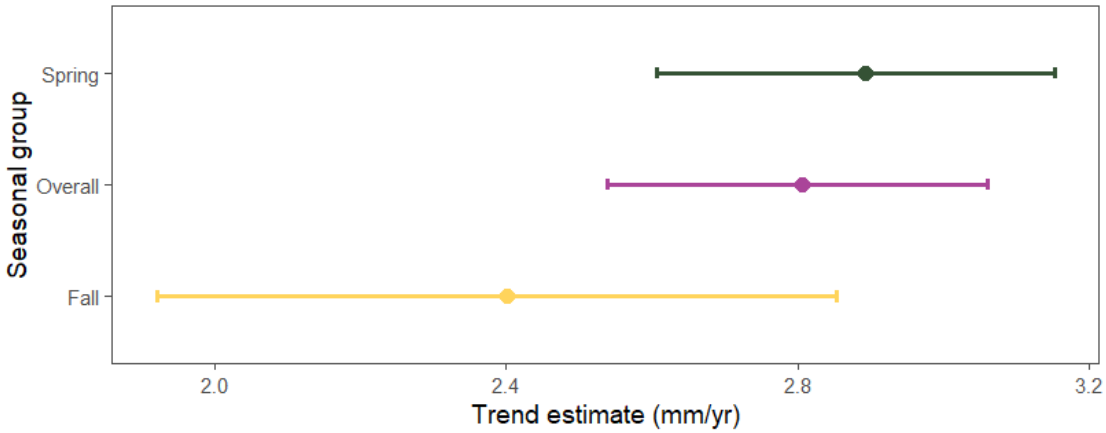


Figure E-54. Overall elevation trend estimates by season for the Marsh 11 site, Assateague Island National Seashore. The trend was averaged over the stations to get an 'overall elevation' trend.

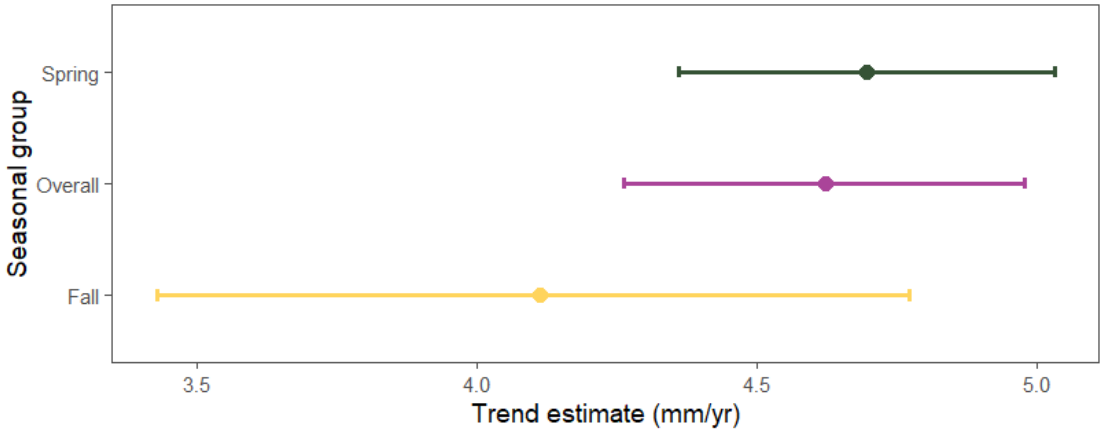


Figure E-55. Overall elevation trend estimates by season for the Marsh Exclosure site, Assateague Island National Seashore. The trend was averaged over the stations to get an 'overall elevation' trend.

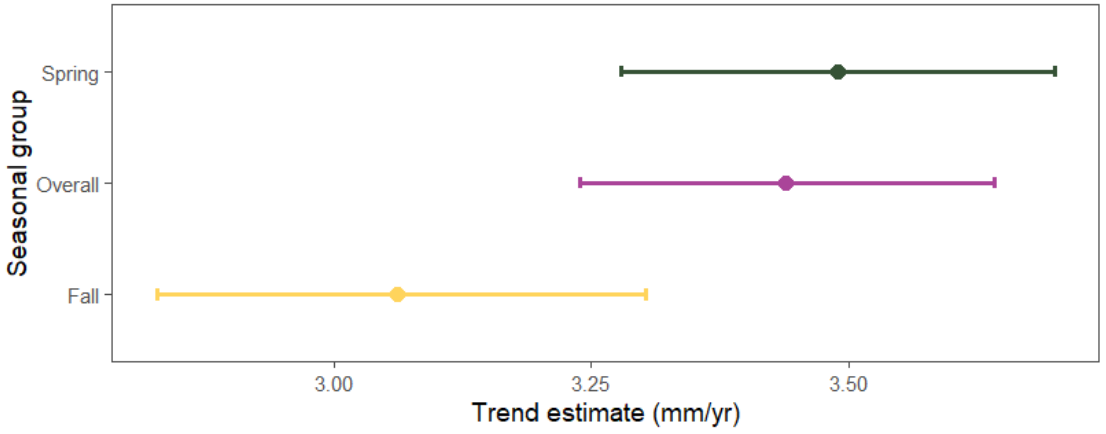


Figure E-56. Overall elevation trend estimates by season for the Marsh non-Exclosure site, Assateague Island National Seashore. The trend was averaged over the stations to get an 'overall elevation' trend.

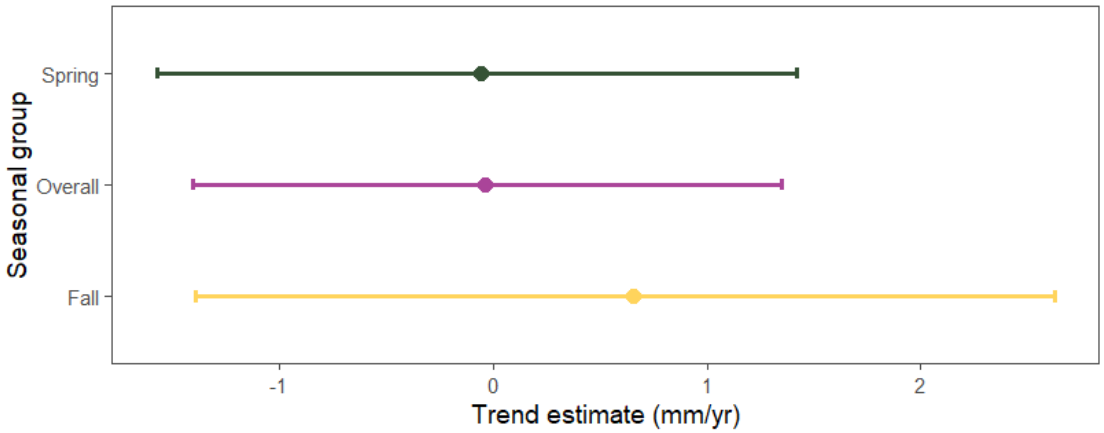


Figure E-57. Overall elevation trend estimates by season for the Calf Island site, Boston Harbor Islands Recreation Area. The trend was averaged over the stations to get an 'overall elevation' trend.

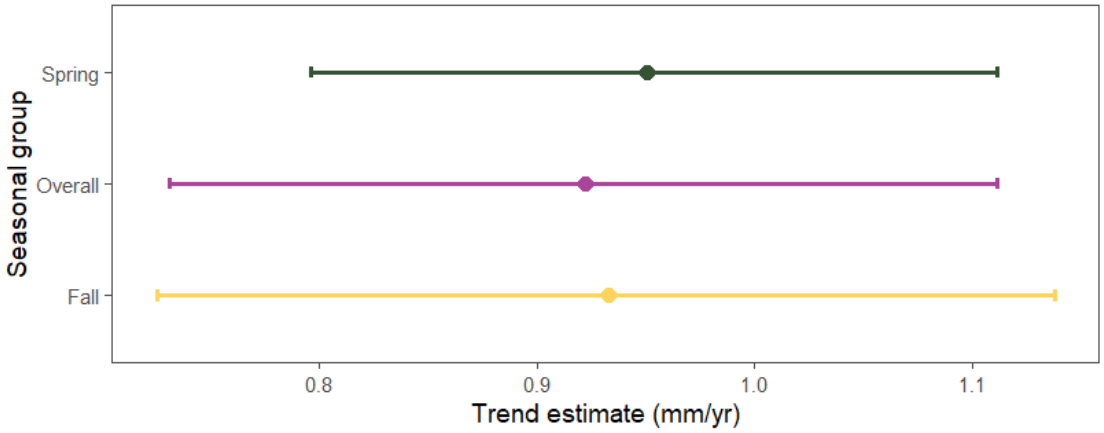


Figure E-58. Overall elevation trend estimates by season for the Peddocks Island site, Boston Harbor Islands Recreation Area. The trend was averaged over the stations to get an 'overall elevation' trend.

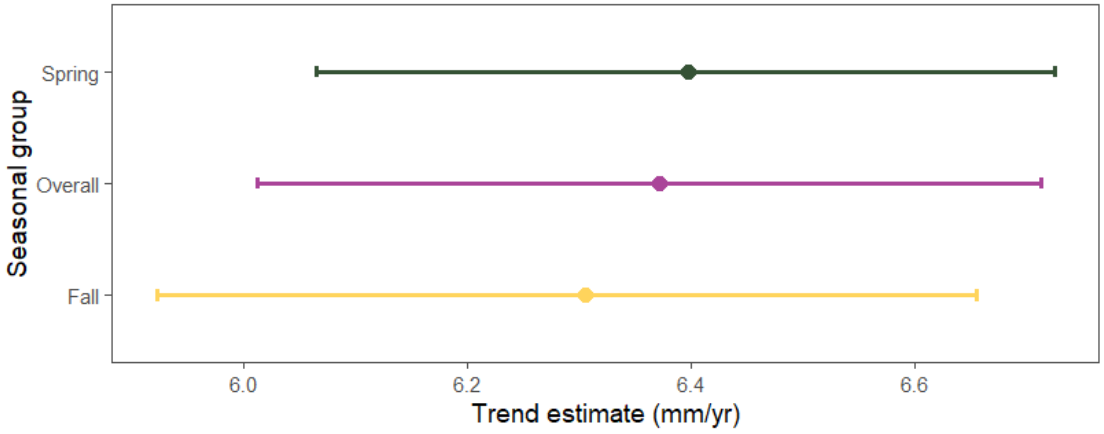


Figure E-59. Overall elevation trend estimates by season for the Thompson Island site, Boston Harbor Islands Recreation Area. The trend was averaged over the stations to get an 'overall elevation' trend.

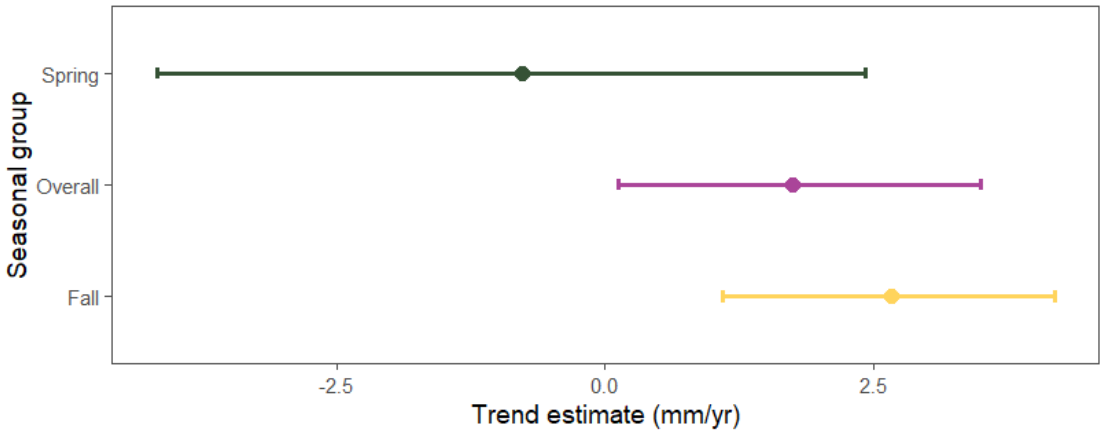


Figure E-60. Overall elevation trend estimates by season for the Blackfish Creek site, Cape Cod National Seashore. The trend was averaged over the stations to get an 'overall elevation' trend.

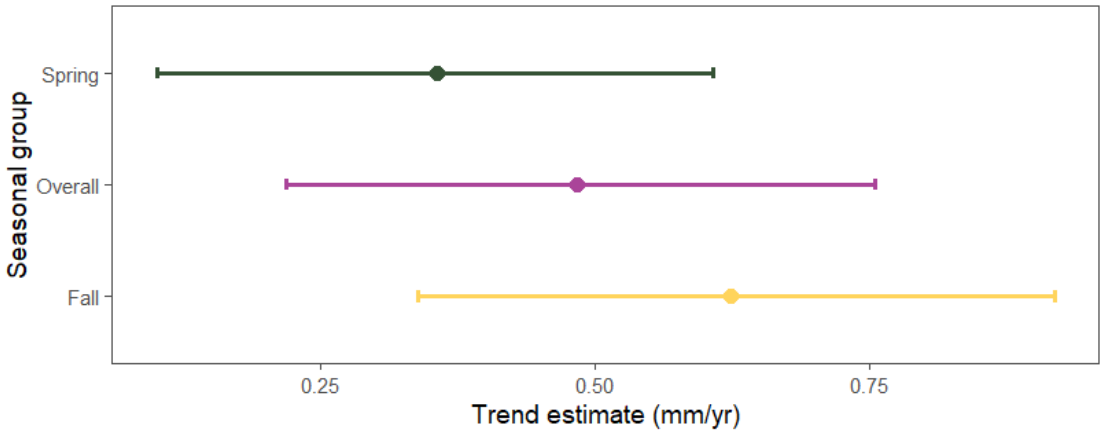


Figure E-61. Overall elevation trend estimates by season for the Hatches Harbor HH1 site, Cape Cod National Seashore. The trend was averaged over the stations to get an 'overall elevation' trend.

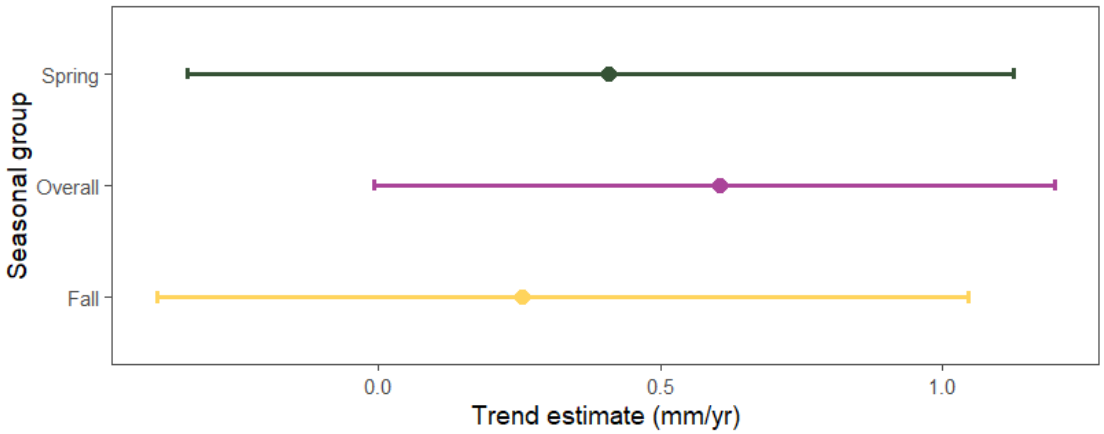


Figure E-62. Overall elevation trend estimates by season for the Hatches Harbor HH2 site, Cape Cod National Seashore. The trend was averaged over the stations to get an 'overall elevation' trend.

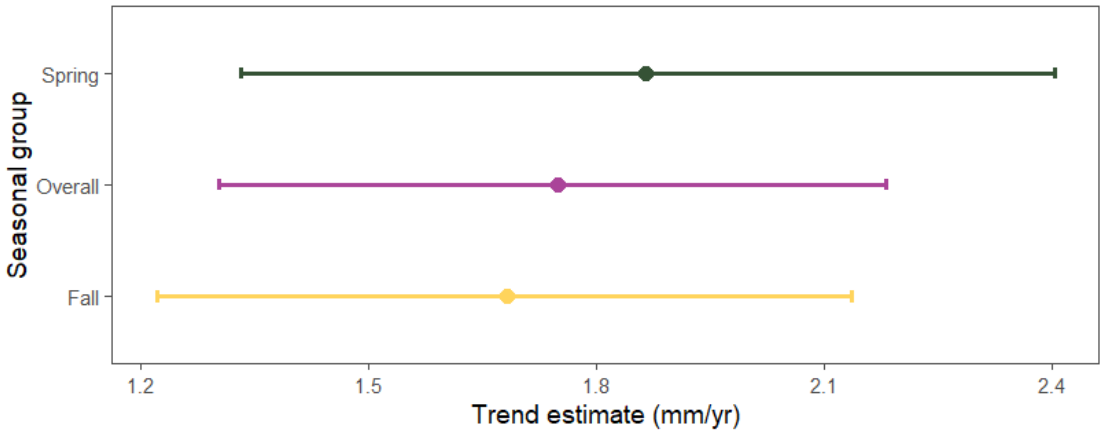


Figure E-63. Overall elevation trend estimates by season for the Hatches Harbor H1 site, Cape Cod National Seashore. The trend was averaged over the stations to get an 'overall elevation' trend.

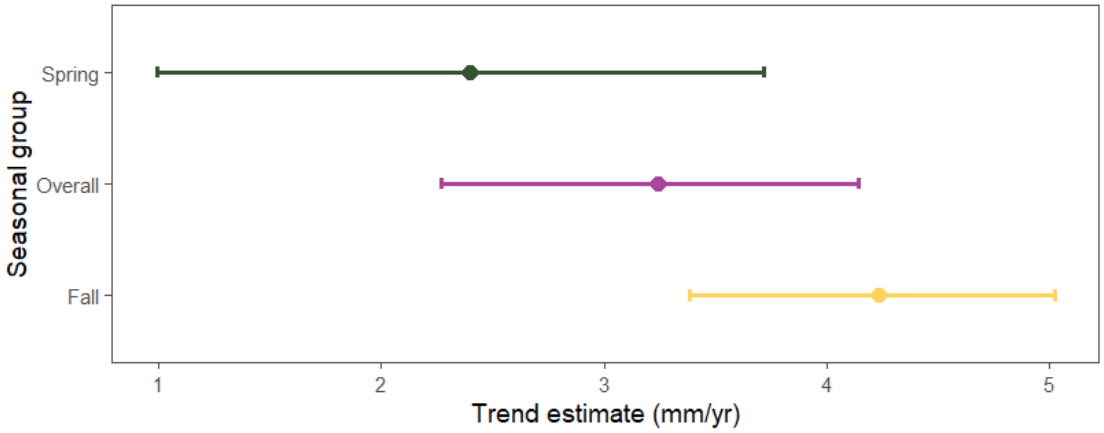


Figure E-64. Overall elevation trend estimates by season for the Hatches Harbor H2 site, Cape Cod National Seashore. The trend was averaged over the stations to get an 'overall elevation' trend.

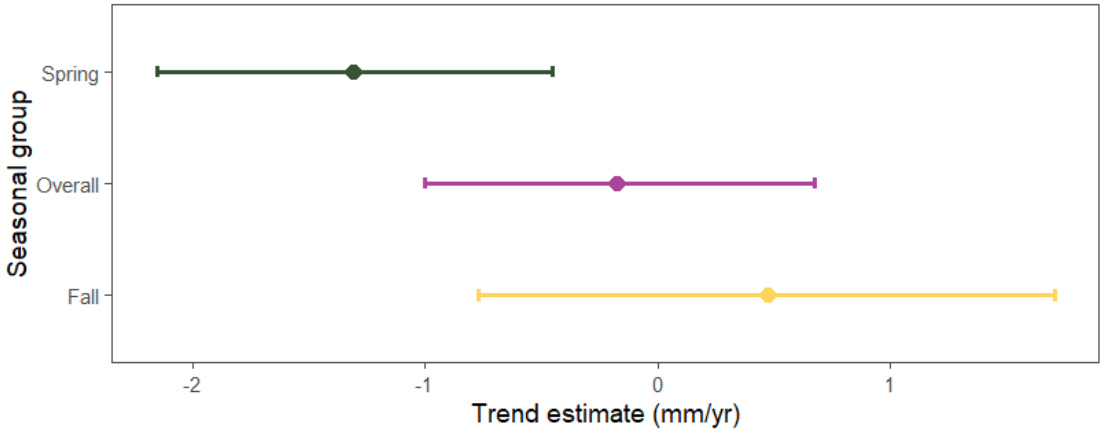


Figure E-65. Overall elevation trend estimates by season for the Herring River G site, Cape Cod National Seashore. The trend was averaged over the stations to get an 'overall elevation' trend.

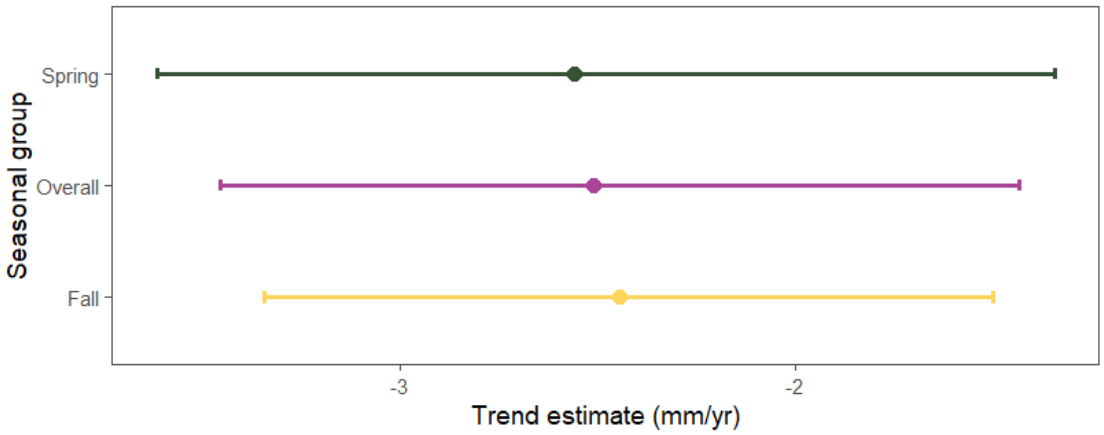


Figure E-66. Overall elevation trend estimates by season for the Herring River GUT site, Cape Cod National Seashore. The trend was averaged over the stations to get an 'overall elevation' trend.

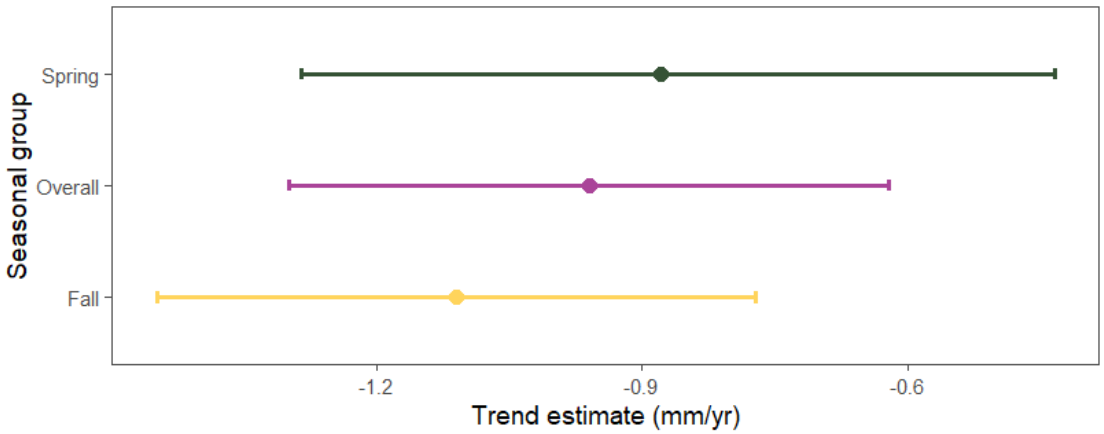


Figure E-67. Overall elevation trend estimates by season for the Herring River High Toss site, Cape Cod National Seashore. The trend was averaged over the stations to get an 'overall elevation' trend.

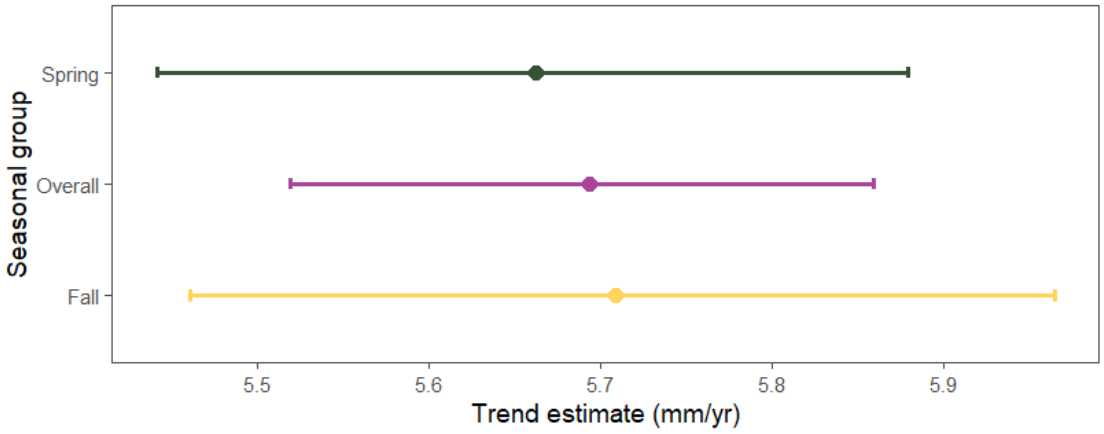


Figure E-68. Overall elevation trend estimates by season for the Herring River Phrag site, Cape Cod National Seashore. The trend was averaged over the stations to get an 'overall elevation' trend.

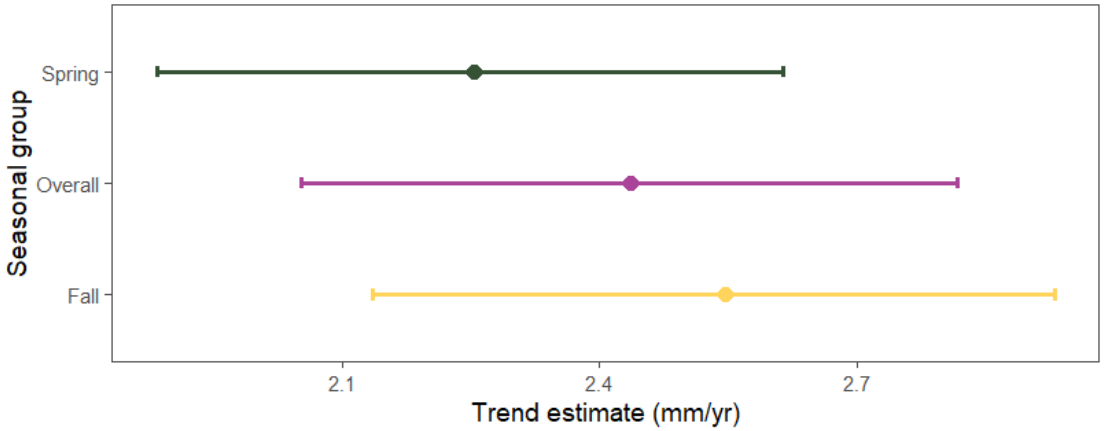


Figure E-69. Overall elevation trend estimates by season for the Nauset Marsh N site, Cape Cod National Seashore. The trend was averaged over the stations to get an 'overall elevation' trend.

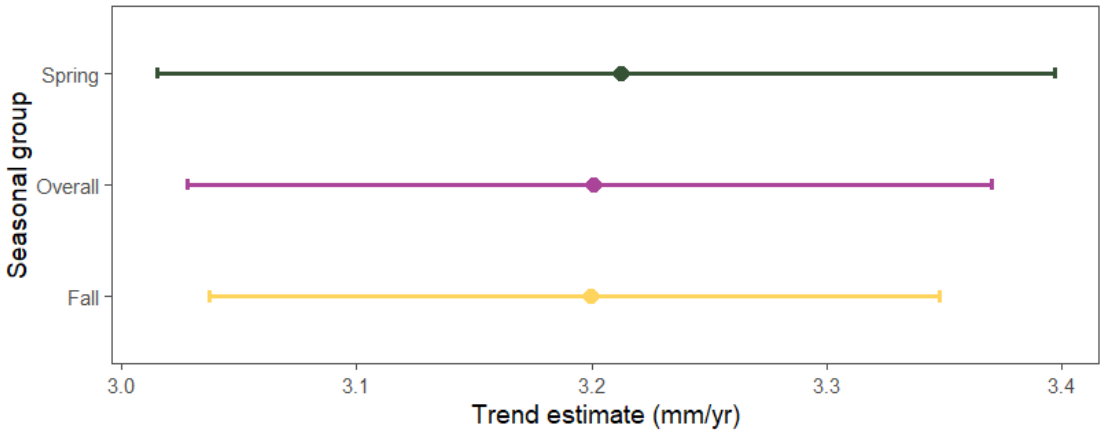


Figure E-70. Overall elevation trend estimates by season for the Nauset Marsh OldN site, Cape Cod National Seashore. The trend was averaged over the stations to get an 'overall elevation' trend.

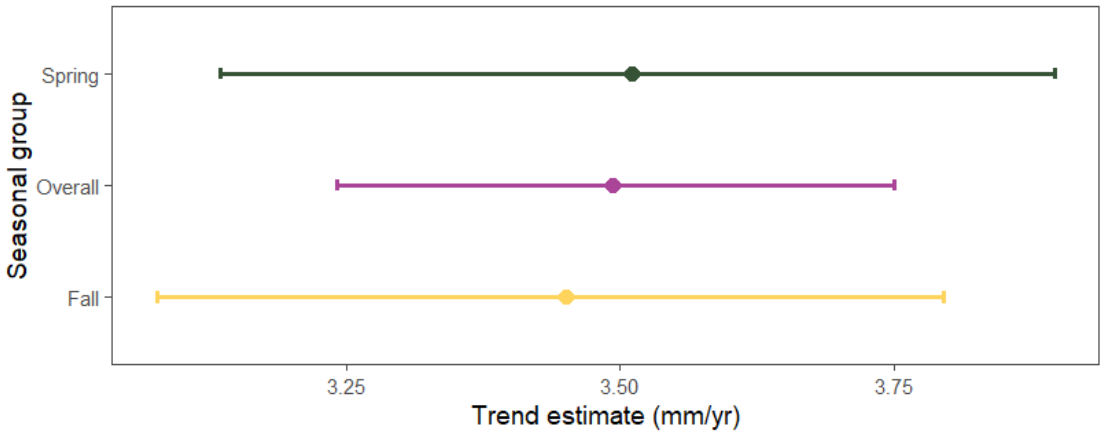


Figure E-71. Overall elevation trend estimates by season for the Marsh 5 site, Colonial National Historical Park. The trend was averaged over the stations to get an 'overall elevation' trend.

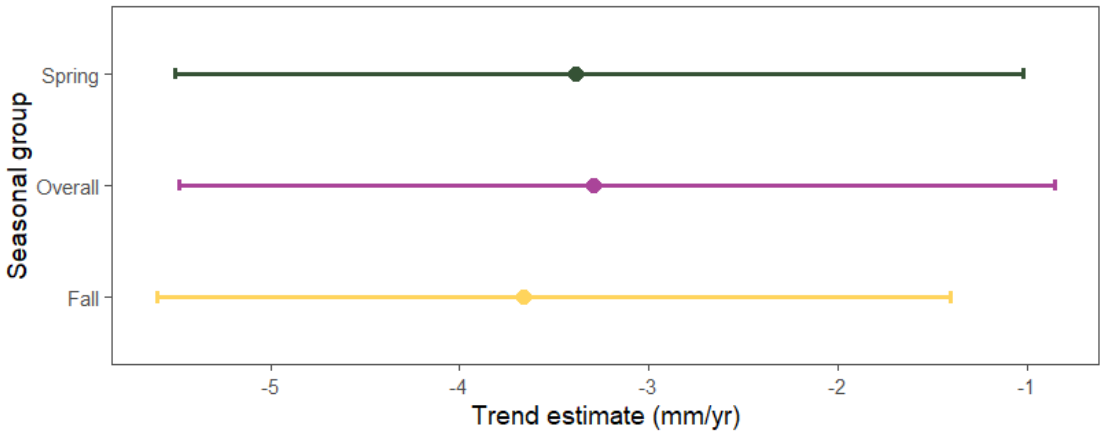


Figure E-72. Overall elevation trend estimates by season for the Marsh 13 site, Colonial National Historical Park. The trend was averaged over the stations to get an 'overall elevation' trend.

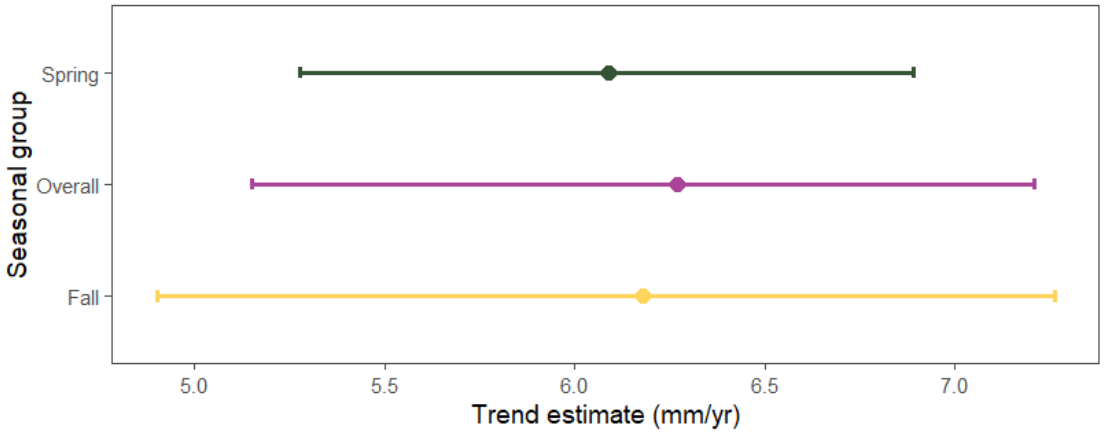


Figure E-73. Overall elevation trend estimates by season for the Marsh 19 site, Colonial National Historical Park. The trend was averaged over the stations to get an 'overall elevation' trend.

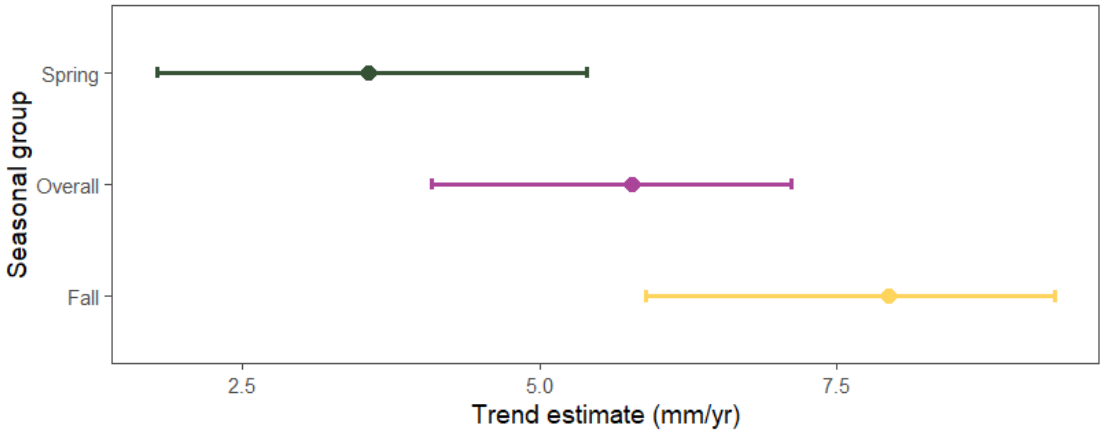


Figure E-74. Overall elevation trend estimates by season for the Marsh 30 site, Colonial National Historical Park. The trend was averaged over the stations to get an 'overall elevation' trend.

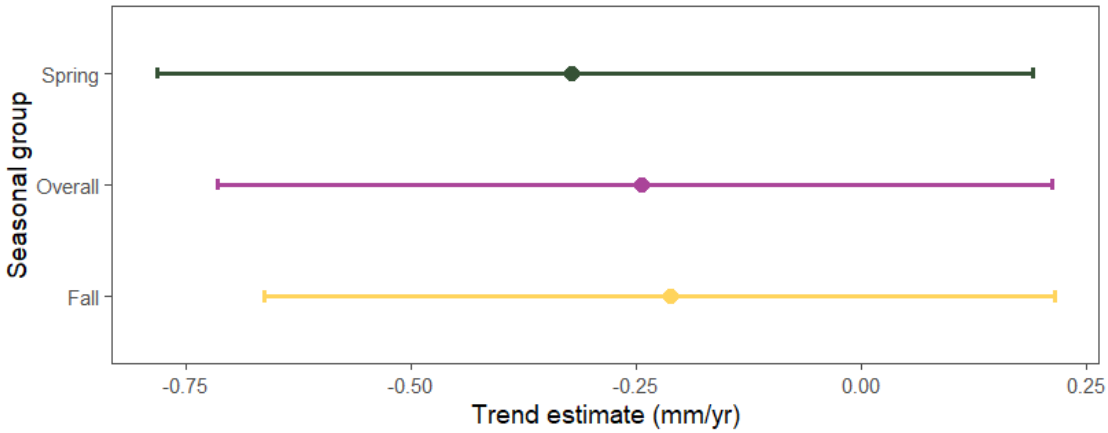


Figure E-75. Overall elevation trend estimates by season for the Great Gun site, Fire Island National Seashore. The trend was averaged over the stations to get an 'overall elevation' trend.

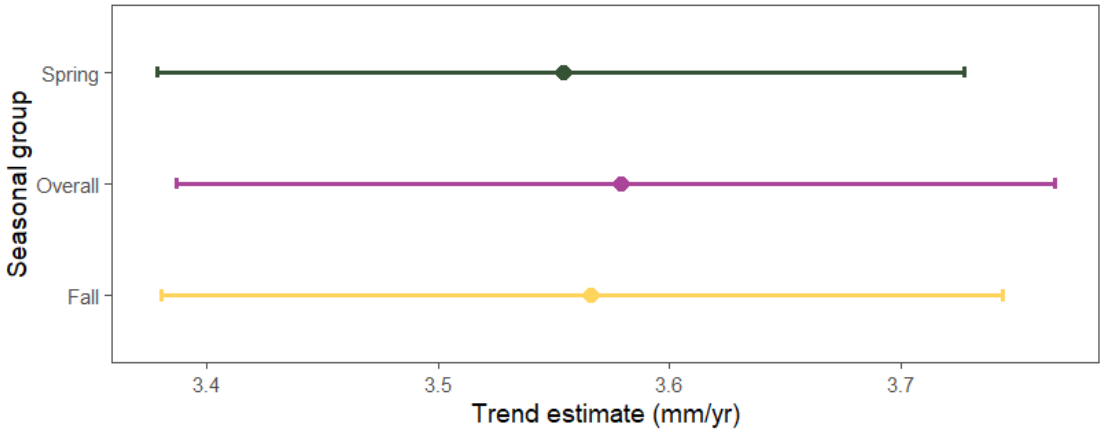


Figure E-76. Overall elevation trend estimates by season for the Hospital Point site, Fire Island National Seashore. The trend was averaged over the stations to get an 'overall elevation' trend.

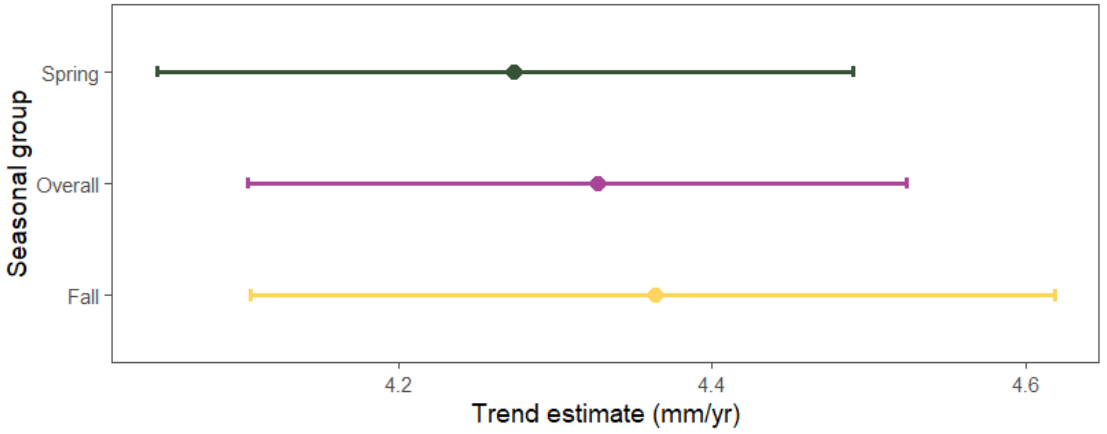


Figure E-77. Overall elevation trend estimates by season for the Watch Hill site, Fire Island National Seashore. The trend was averaged over the stations to get an 'overall elevation' trend.

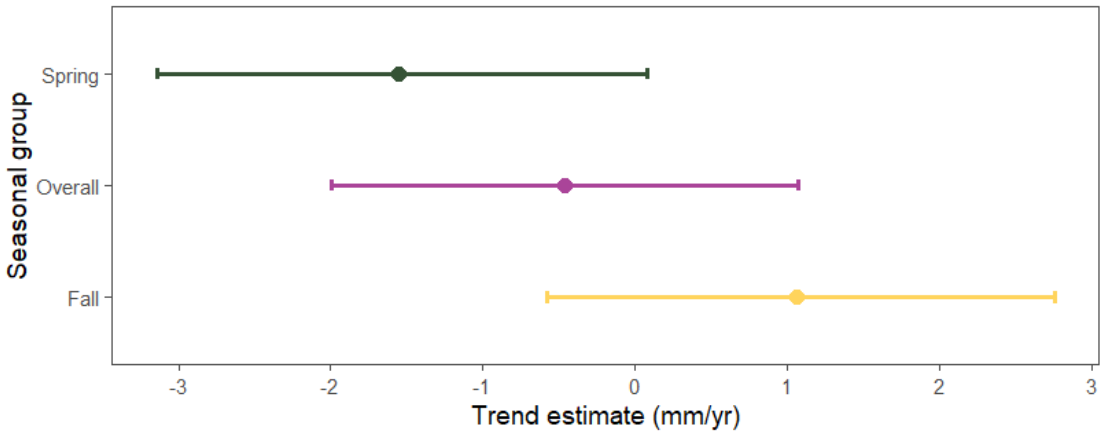


Figure E-78. Overall elevation trend estimates by season for the Big Egg Control site, Gateway National Recreation Area. The trend was averaged over the stations to get an 'overall elevation' trend.

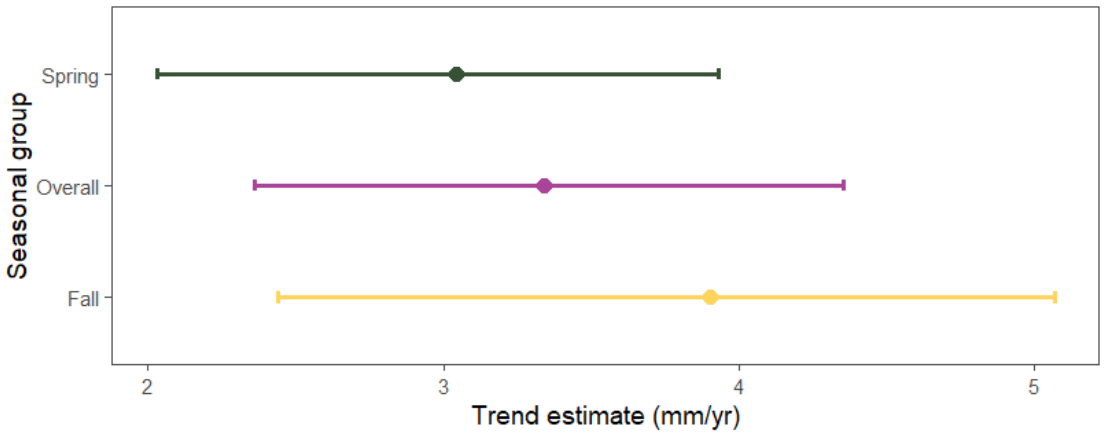


Figure E-79. Overall elevation trend estimates by season for the Big Egg Spray site, Gateway National Recreation Area. The trend was averaged over the stations to get an 'overall elevation' trend.

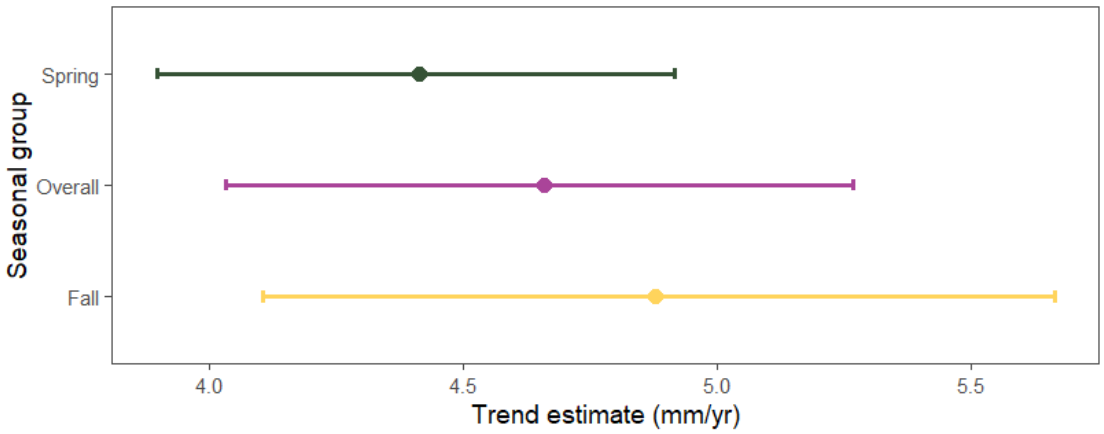


Figure E-80. Overall elevation trend estimates by season for the Black Bank site, Gateway National Recreation Area. The trend was averaged over the stations to get an 'overall elevation' trend.

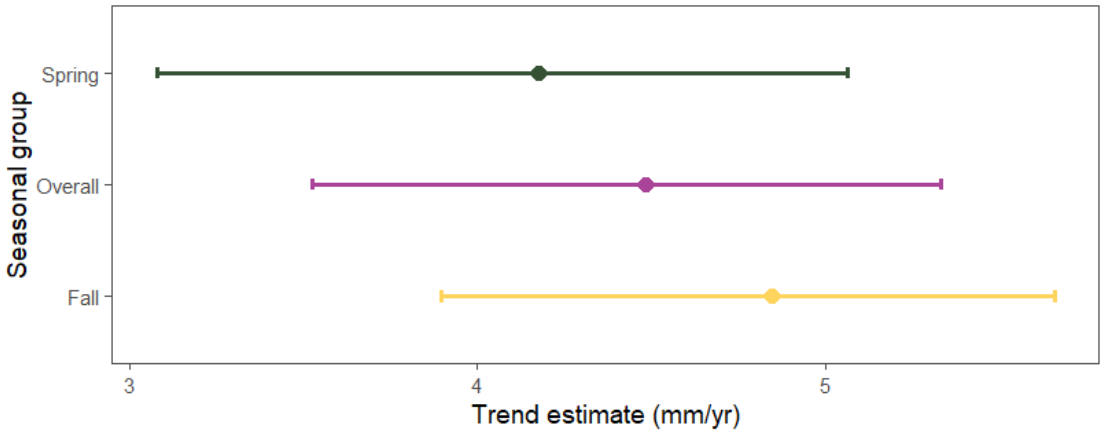


Figure E-81. Overall elevation trend estimates by season for the Elders East site, Gateway National Recreation Area. The trend was averaged over the stations to get an 'overall elevation' trend.

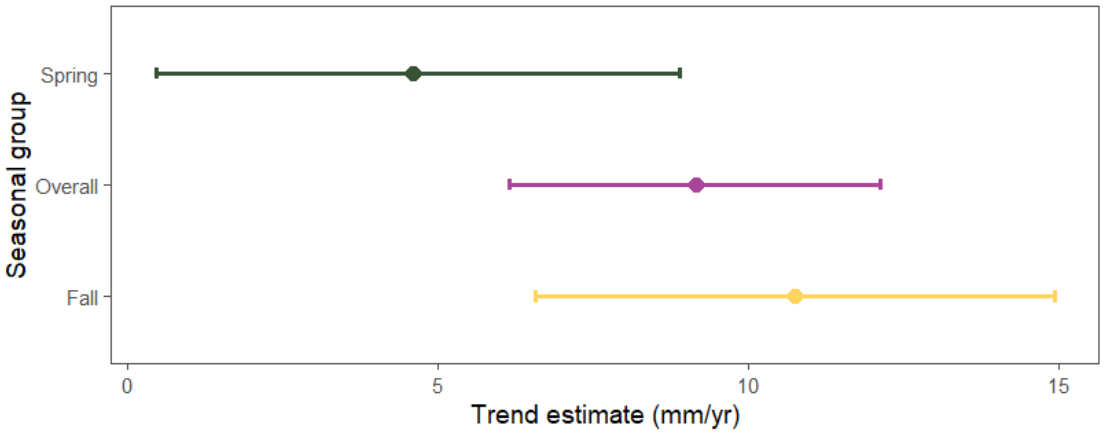


Figure E-82. Overall elevation trend estimates by season for the Elders East NF site, Gateway National Recreation Area. The trend was averaged over the stations to get an 'overall elevation' trend.

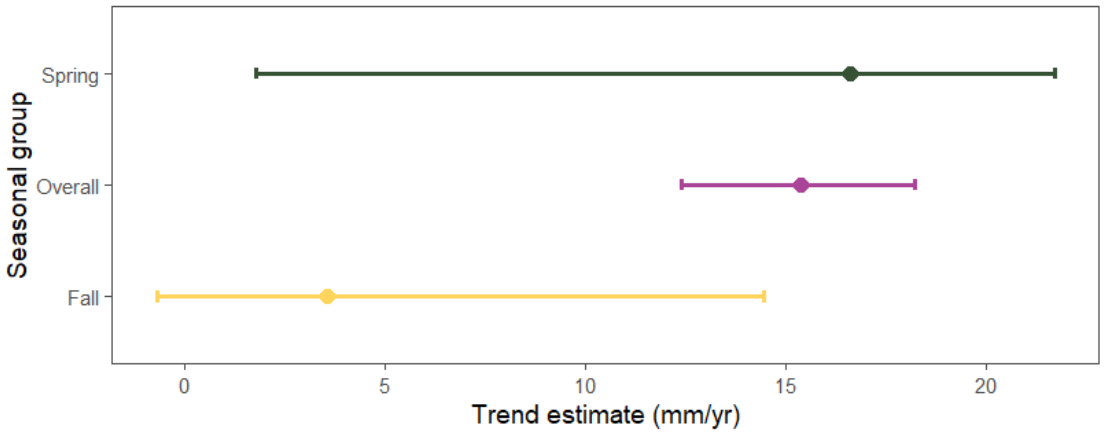


Figure E-83. Overall elevation trend estimates by season for the Elders East Shallow site, Gateway National Recreation Area. The trend was averaged over the stations to get an 'overall elevation' trend.

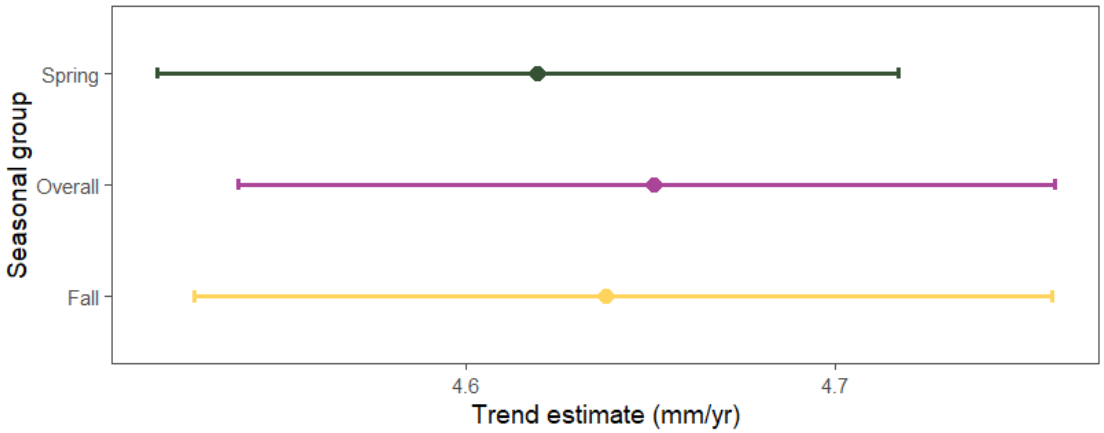


Figure E-84. Overall elevation trend estimates by season for the JOCO site, Gateway National Recreation Area. The trend was averaged over the stations to get an 'overall elevation' trend.

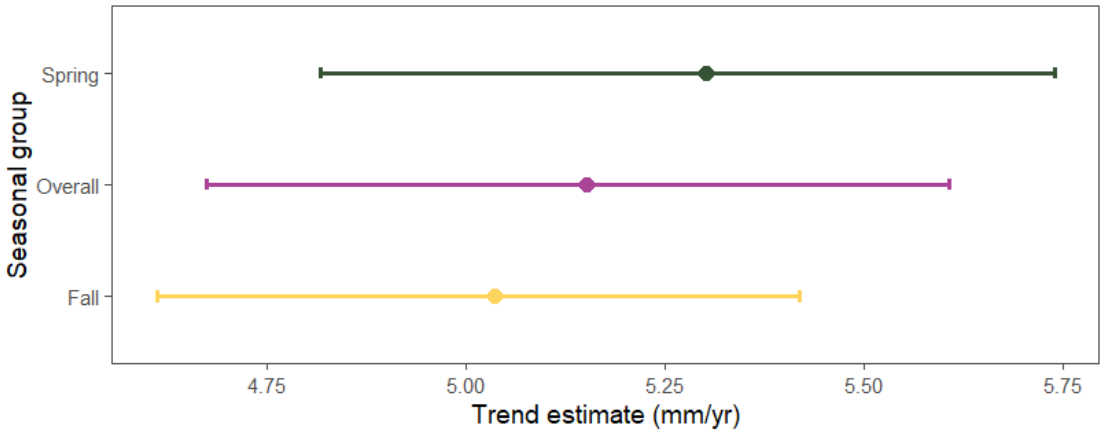


Figure E-85. Overall elevation trend estimates by season for the JOCO REF site, Gateway National Recreation Area. The trend was averaged over the stations to get an 'overall elevation' trend.

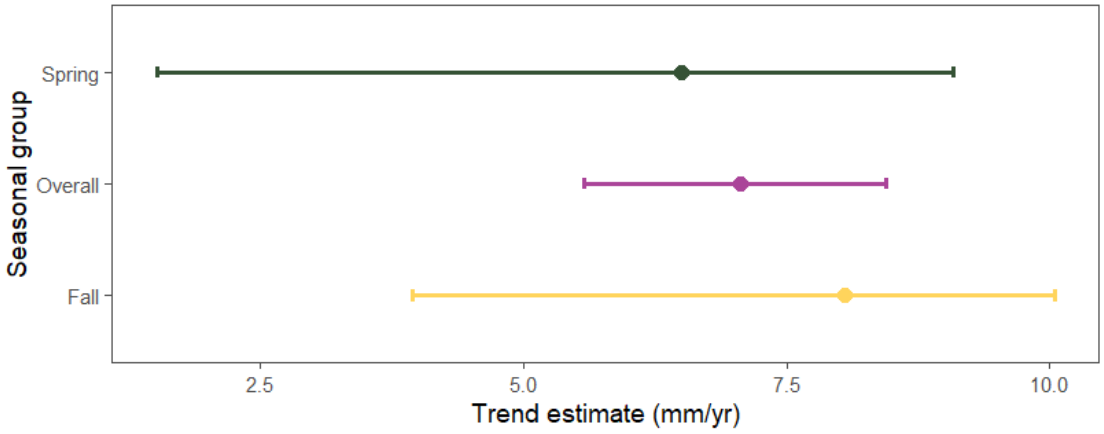


Figure E-86. Overall elevation trend estimates by season for the JOCO REF Shallow site, Gateway National Recreation Area. The trend was averaged over the stations to get an 'overall elevation' trend.

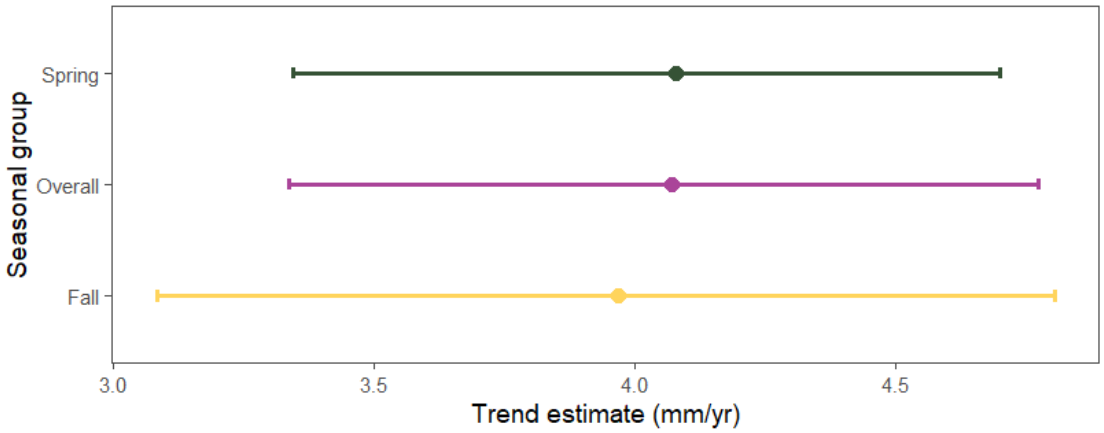


Figure E-87. Overall elevation trend estimates by season for the Sandy Hook site, Gateway National Recreation Area. The trend was averaged over the stations to get an 'overall elevation' trend.

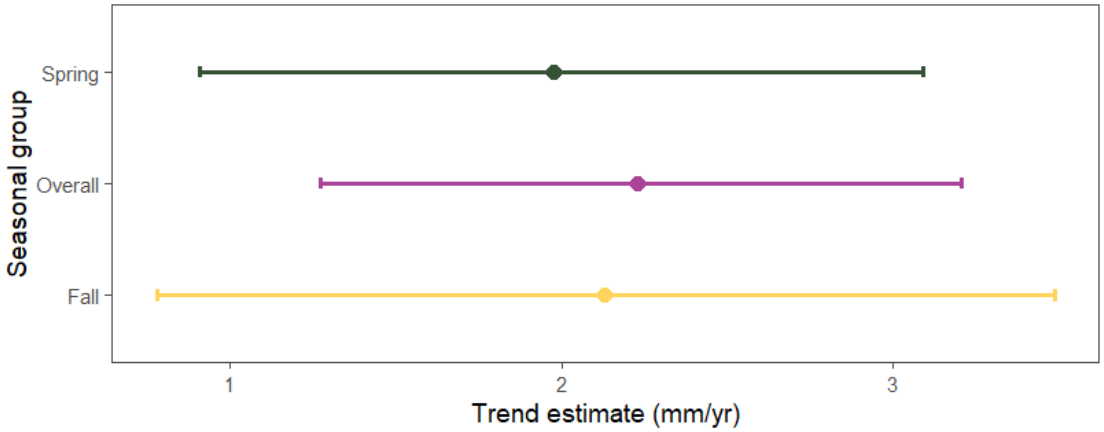


Figure E-88. Overall elevation trend estimates by season for the Dyke Marsh Creek site, George Washington Memorial Parkway. The trend was averaged over the stations to get an 'overall elevation' trend.

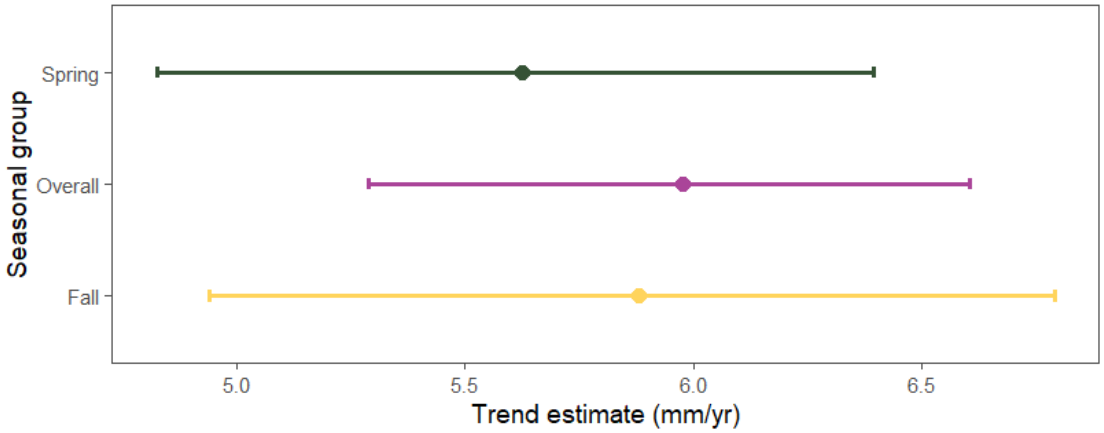


Figure E-89. Overall elevation trend estimates by season for the Dyke Marsh Interior site, George Washington Memorial Parkway. The trend was averaged over the stations to get an 'overall elevation' trend.

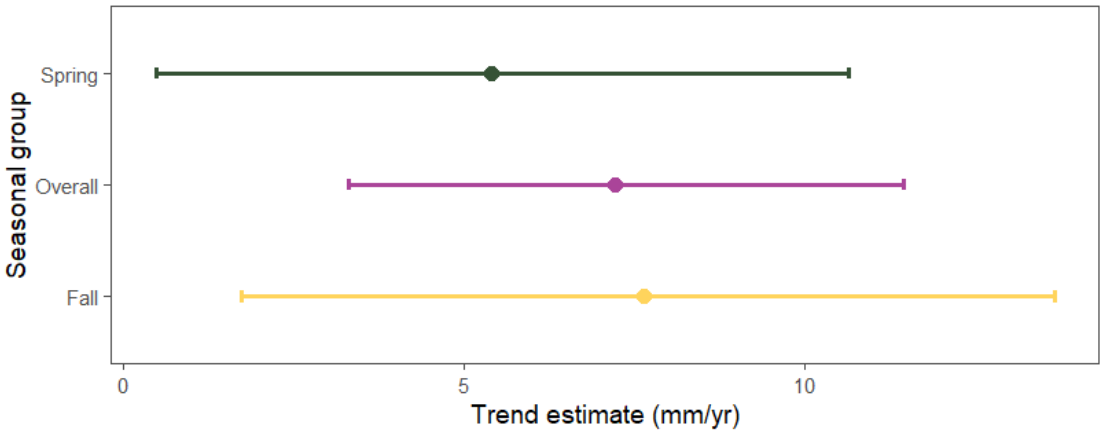


Figure E-90. Overall elevation trend estimates by season for the Dyke Marsh River site, George Washington Memorial Parkway. The trend was averaged over the stations to get an 'overall elevation' trend.

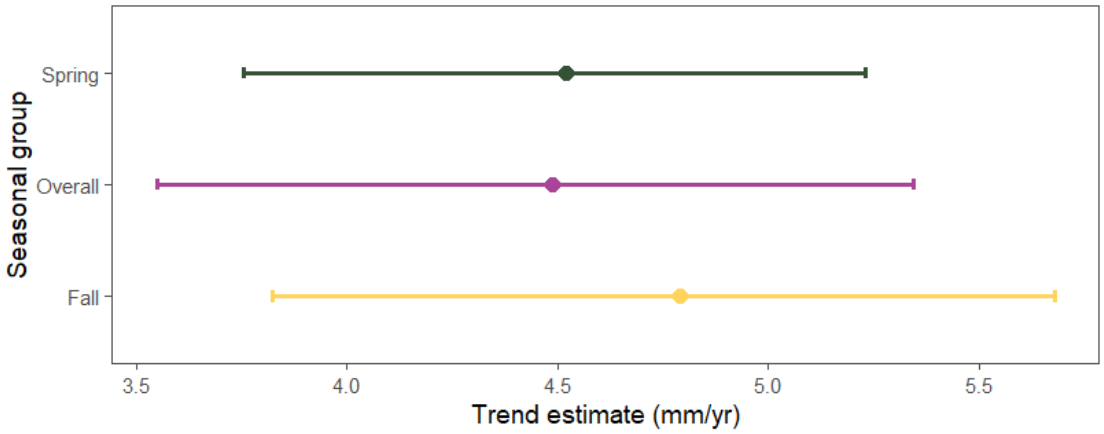


Figure E-91. Overall elevation trend estimates by season for the Kenilworth Marsh River site, National Capital Parks-East. The trend was averaged over the stations to get an 'overall elevation' trend.

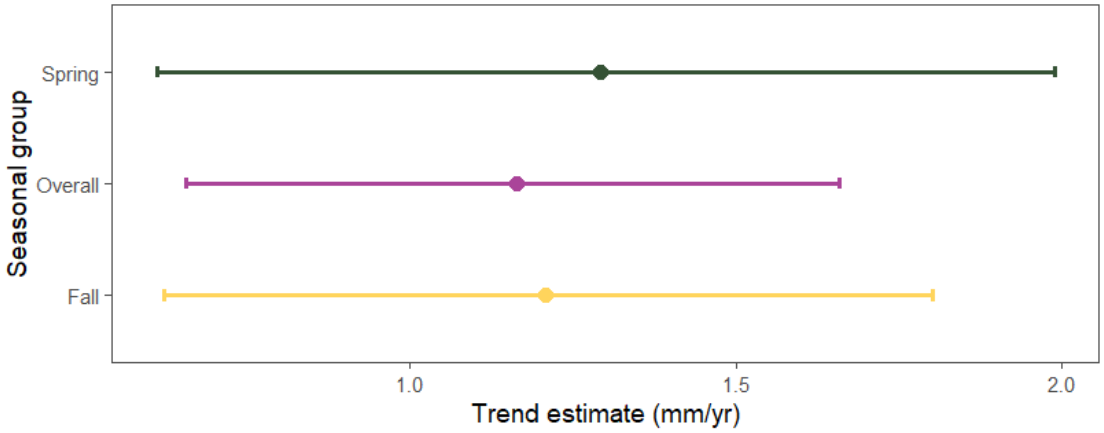


Figure E-92. Overall elevation trend estimates by season for the Kingman Lake site, National Capital Parks-East. The trend was averaged over the stations to get an 'overall elevation' trend.

Accretion Seasonal Analysis plots

The following plots are for the accretion metric. The graphs are set up identical to the elevation plots.

Accretion Seasonal Analysis by Set plots

The plots below contain the trend estimates by season for each park, site, and set.

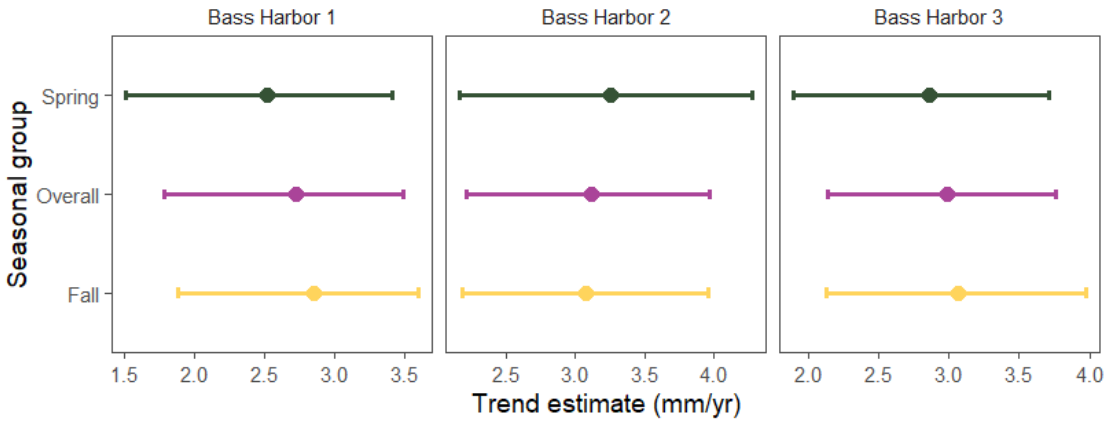


Figure E-93. Accretion trend estimates by season for each station at the Bass Harbor site, Acadia National Park.

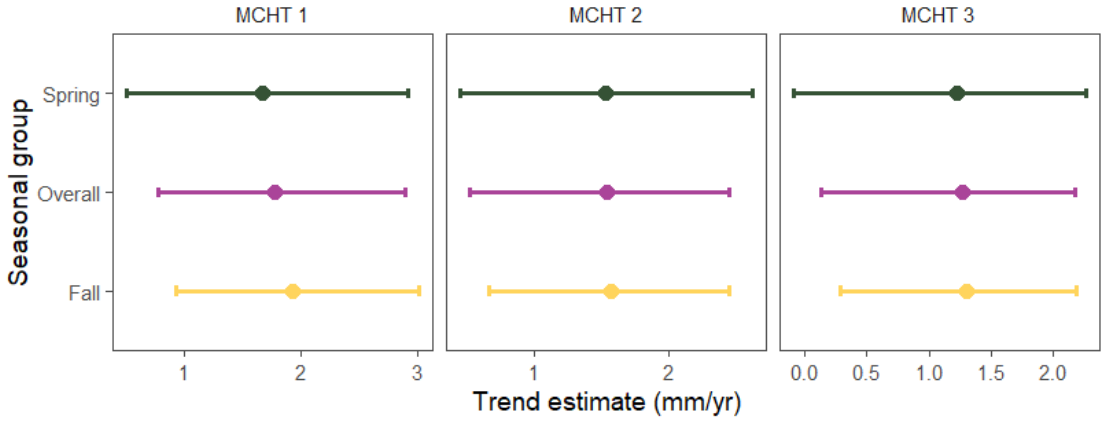


Figure E-94. Accretion trend estimates by season for each station at the Maine Coast Heritage site, Acadia National Park.

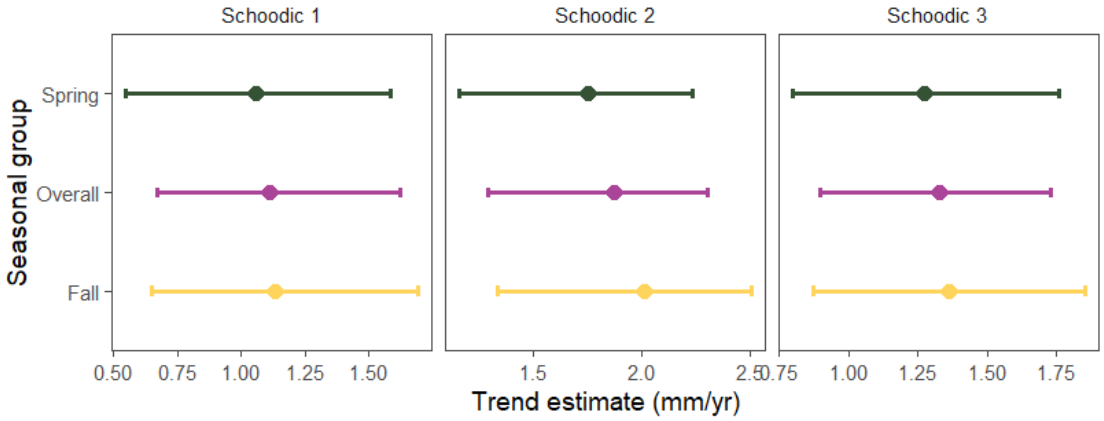


Figure E-95. Accretion trend estimates by season for each station at the Schoodic site, Acadia National Park.

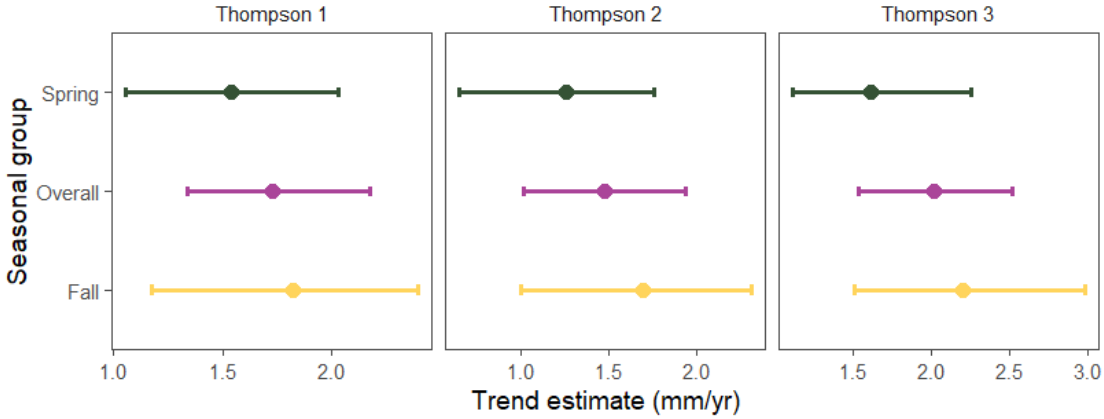


Figure E-96. Accretion trend estimates by season for each station at the Thompson Island site, Acadia National Park.

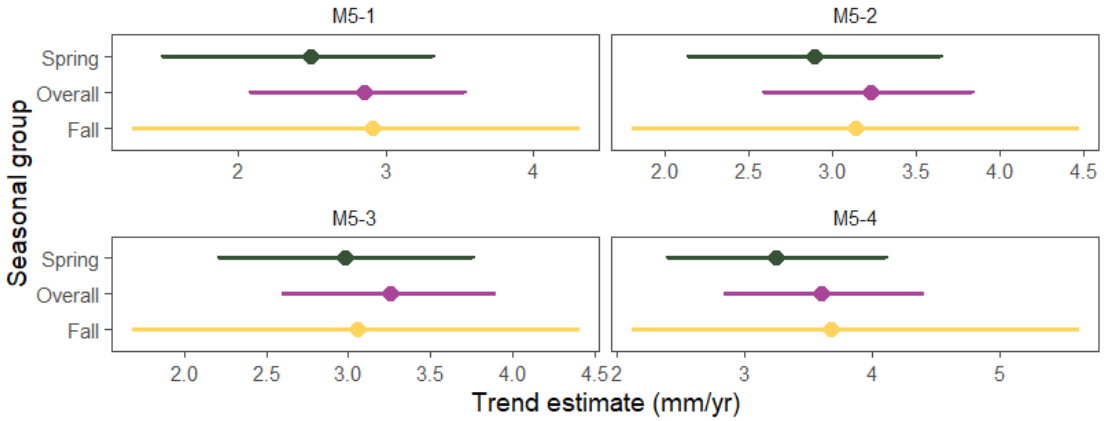


Figure E-97. Accretion trend estimates by season for each station at the Marsh 5 site, Assateague Island National Seashore.

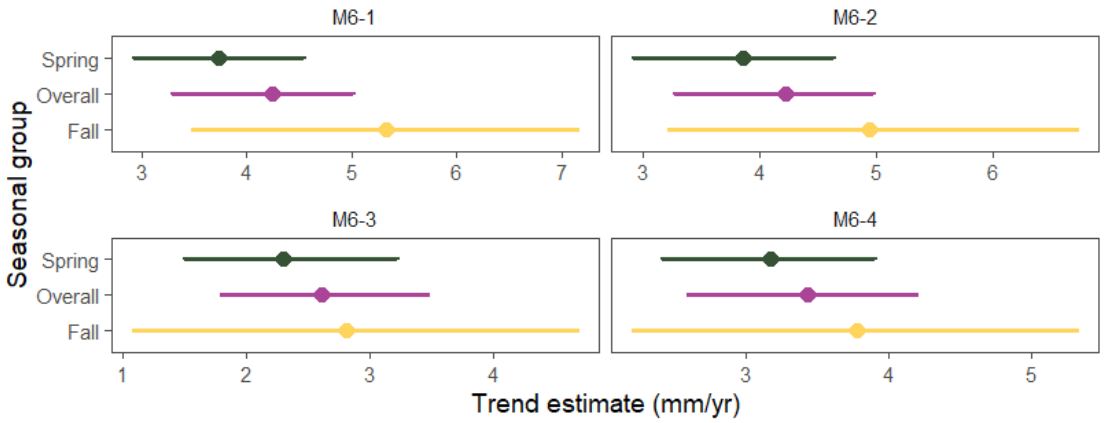


Figure E-98. Accretion trend estimates by season for each station at the Marsh 6 site, Assateague Island National Seashore.

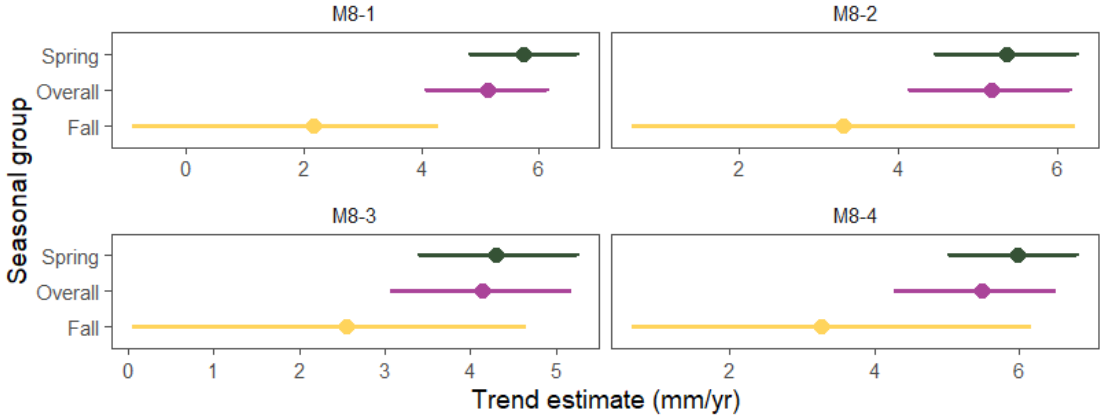


Figure E-99. Accretion trend estimates by season for each station at the Marsh 8 site, Assateague Island National Seashore.

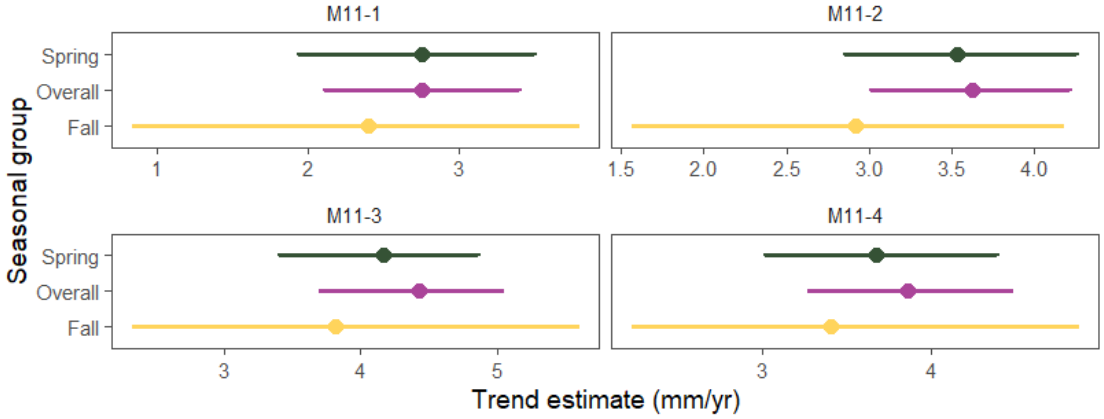


Figure E-100. Accretion trend estimates by season for each station at the Marsh 11 site, Assateague Island National Seashore.

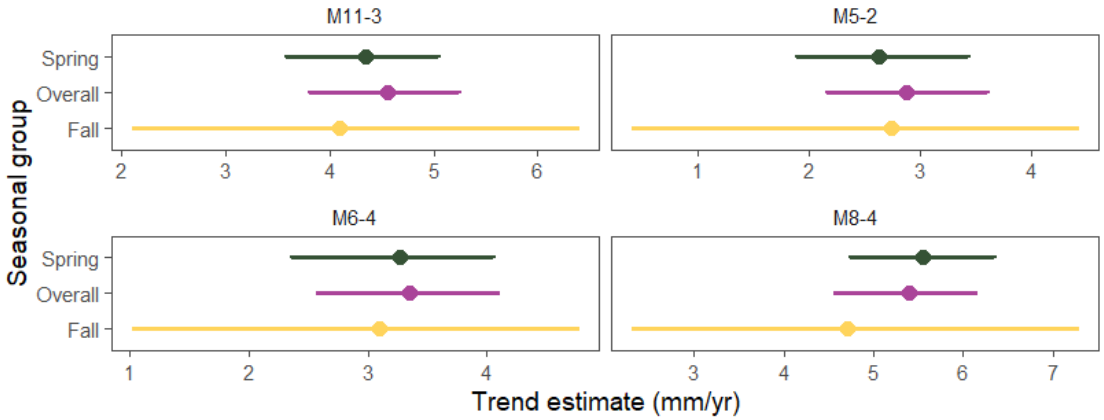


Figure E-101. Accretion trend estimates by season for each station at the Marsh Exclosure site, Assateague Island National Seashore.

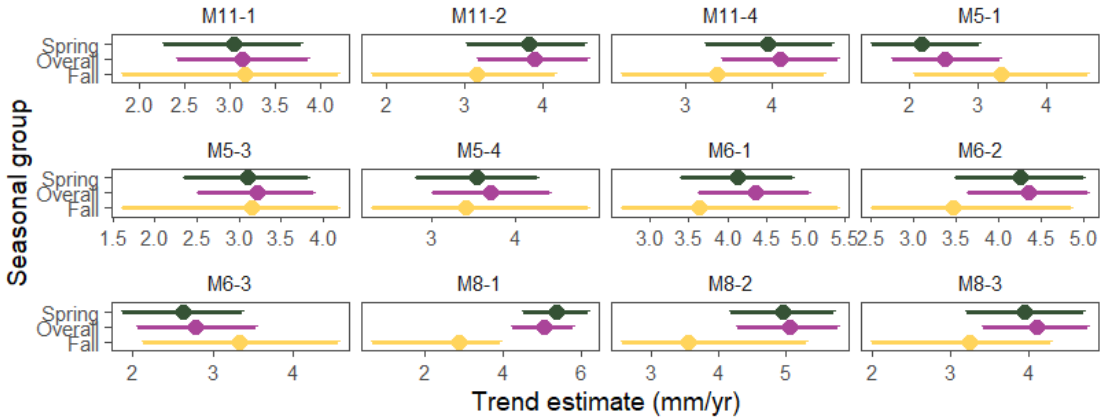


Figure E-102. Accretion trend estimates by season for each station at the Marsh non-Exclosure sites, Assateague Island National Seashore.

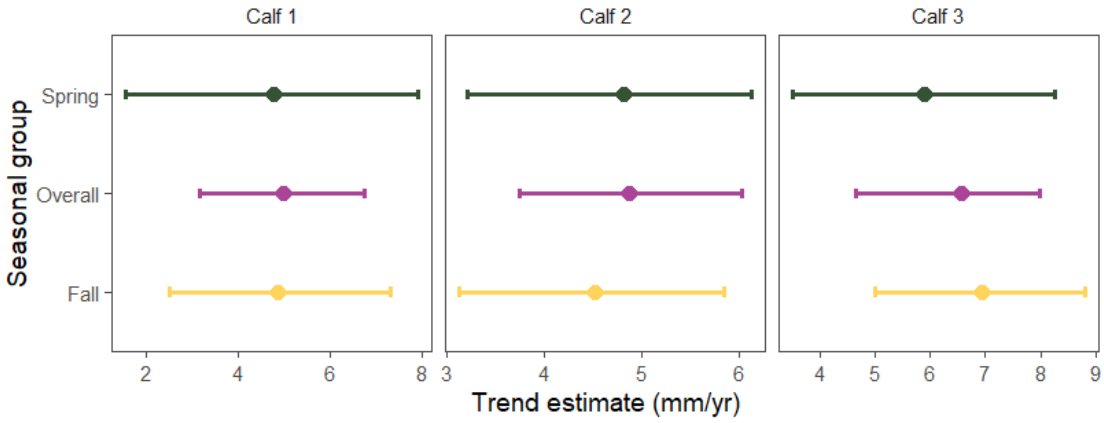


Figure E-103. Accretion trend estimates by season for each station at the Calf Island site, Boston Harbor Islands Recreation Area.

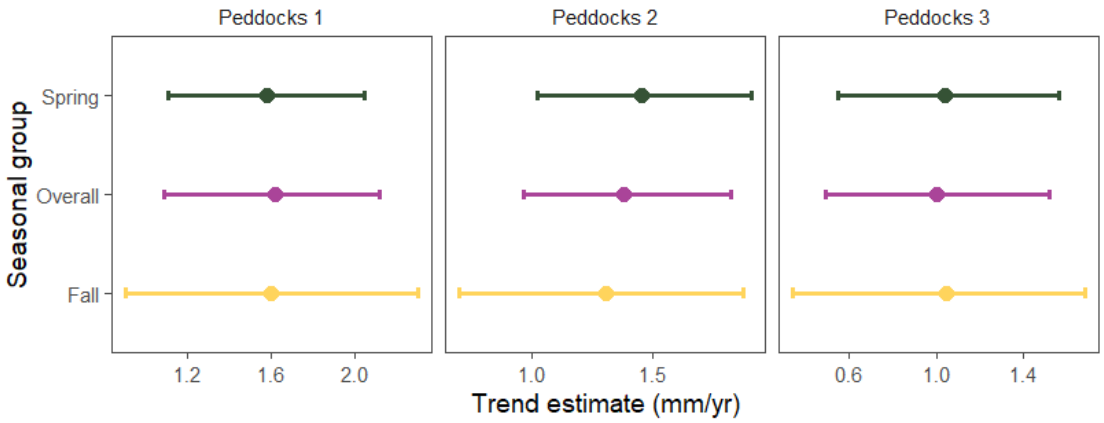


Figure E-104. Accretion trend estimates by season for each station at the Peddocks Island site, Boston Harbor Islands Recreation Area.

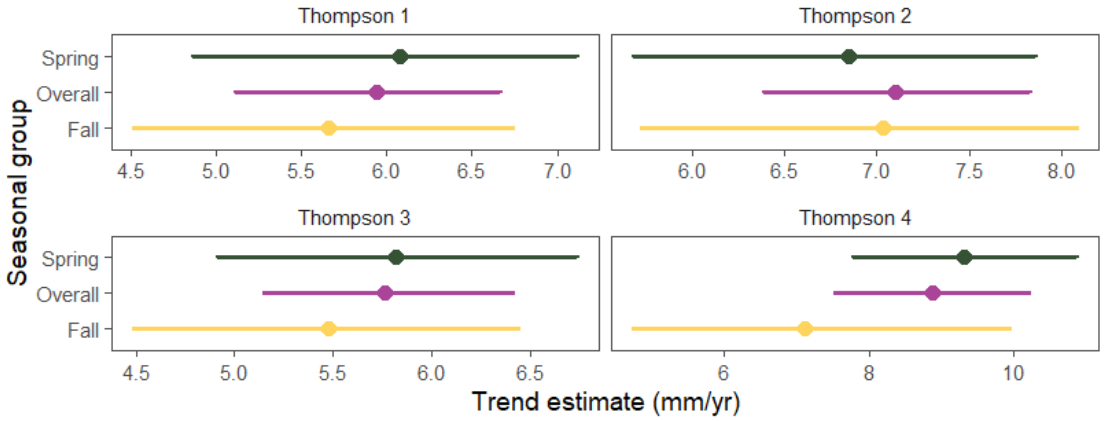


Figure E-105. Accretion trend estimates by season for each station at the Thompson Island site, Boston Harbor Islands Recreation Area.

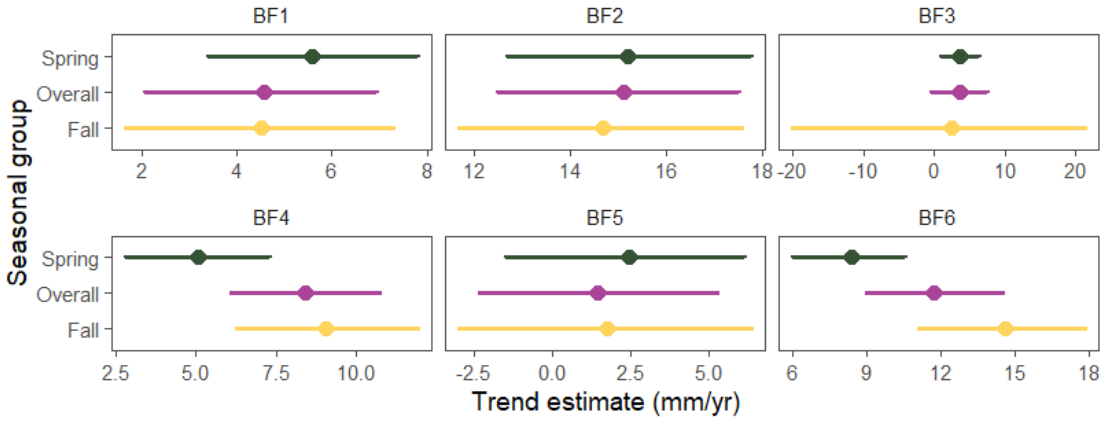


Figure E-106. Accretion trend estimates by season for each station at the Blackfish Creek site, Cape Cod National Seashore.

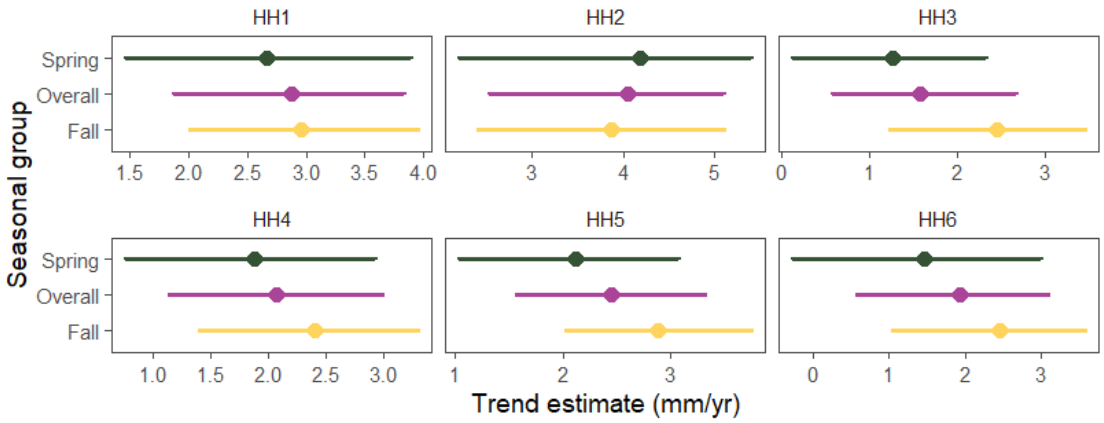


Figure E-107. Accretion trend estimates by season for each station at the Hatches Harbor HH1 site, Cape Cod National Seashore.

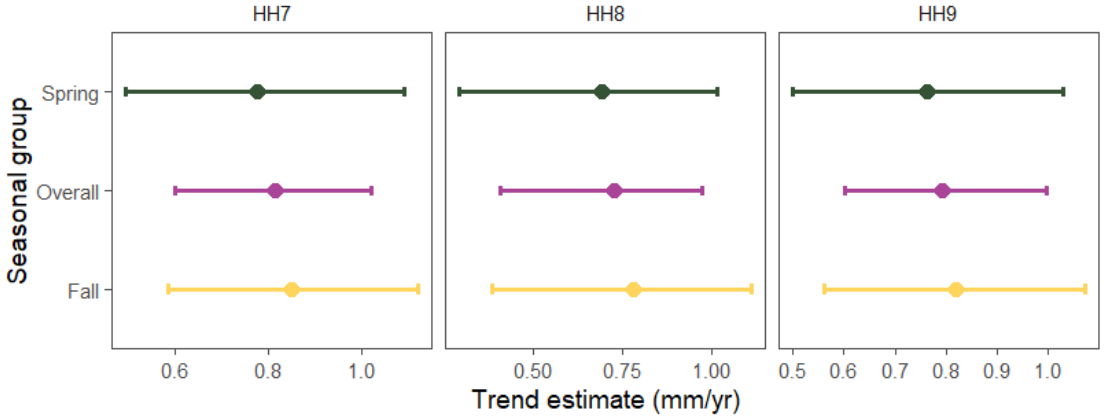


Figure E-108. Accretion trend estimates by season for each station at the Hatches Harbor HH2 site, Cape Cod National Seashore.

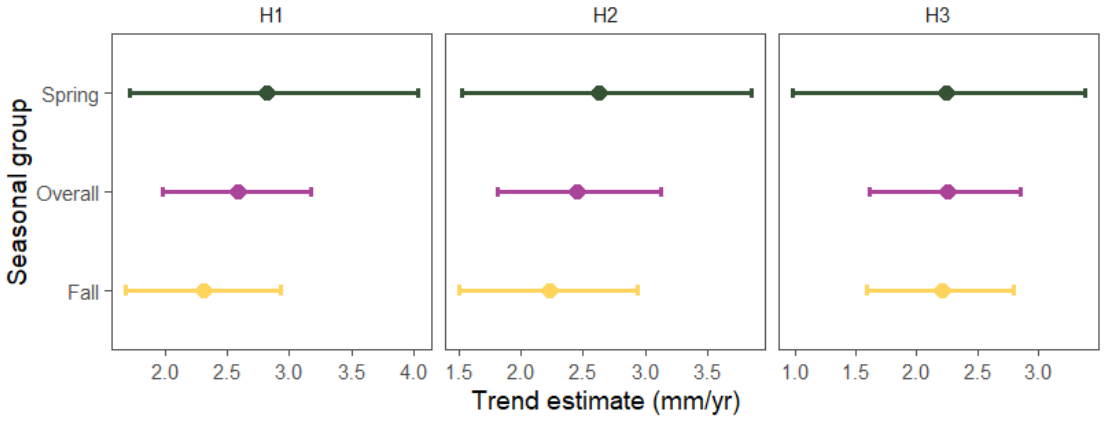


Figure E-109. Accretion trend estimates by season for each station at the Hatches Harbor H1 site, Cape Cod National Seashore.

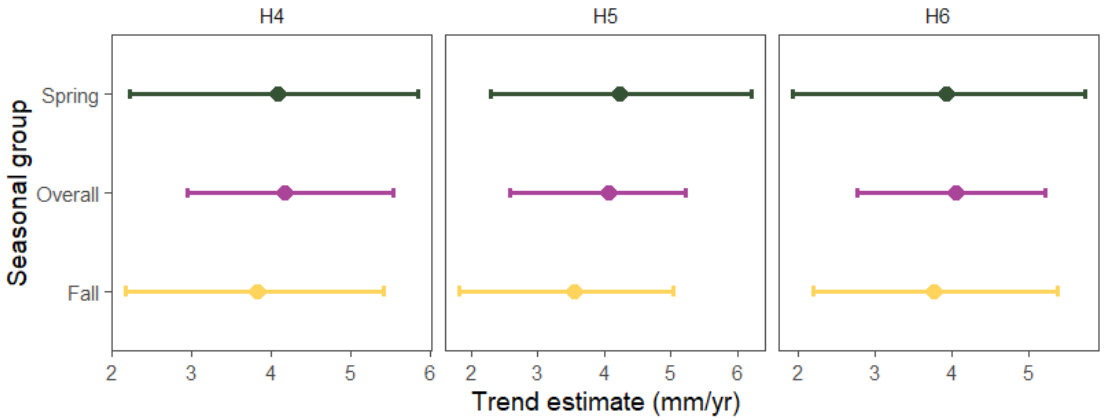


Figure E-110. Accretion trend estimates by season for each station at the Hatches Harbor H2 site, Cape Cod National Seashore.

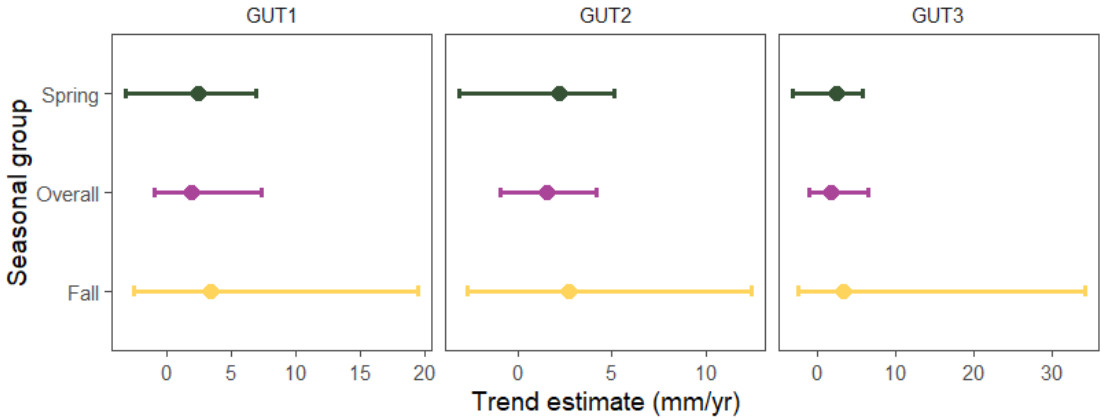


Figure E-111. Accretion trend estimates by season for each station at the Herring River GUT site, Cape Cod National Seashore.

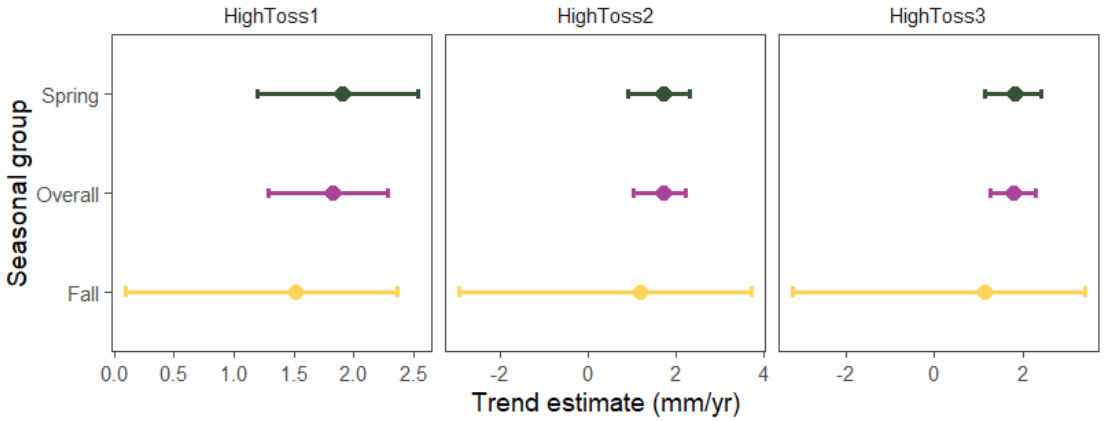


Figure E-112. Accretion trend estimates by season for each station at the Herring River High Toss site, Cape Cod National Seashore.

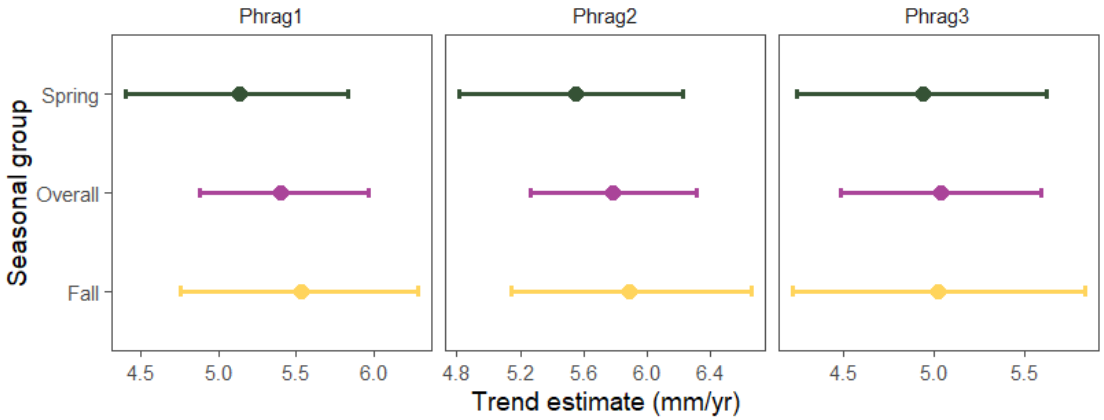


Figure E-113. Accretion trend estimates by season for each station at the Herring River Phrag site, Cape Cod National Seashore.

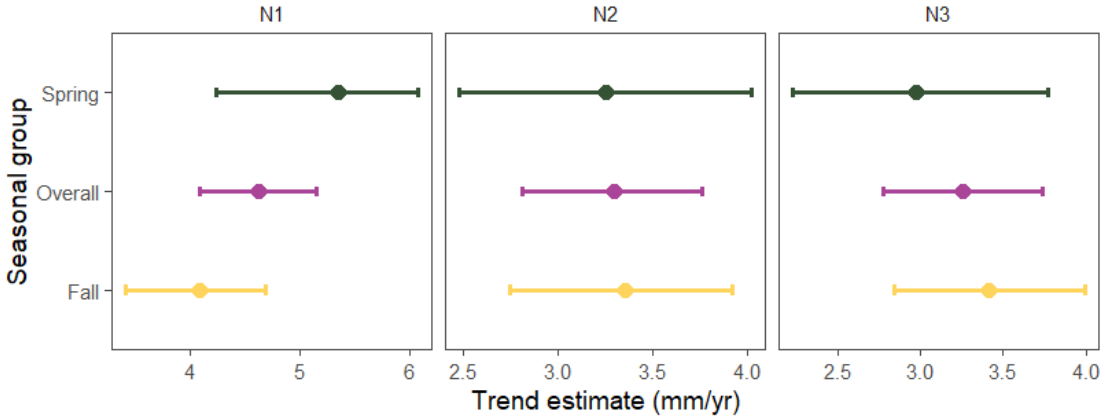


Figure E-114. Accretion trend estimates by season for each station at the Nauset Marsh N site, Cape Cod National Seashore.

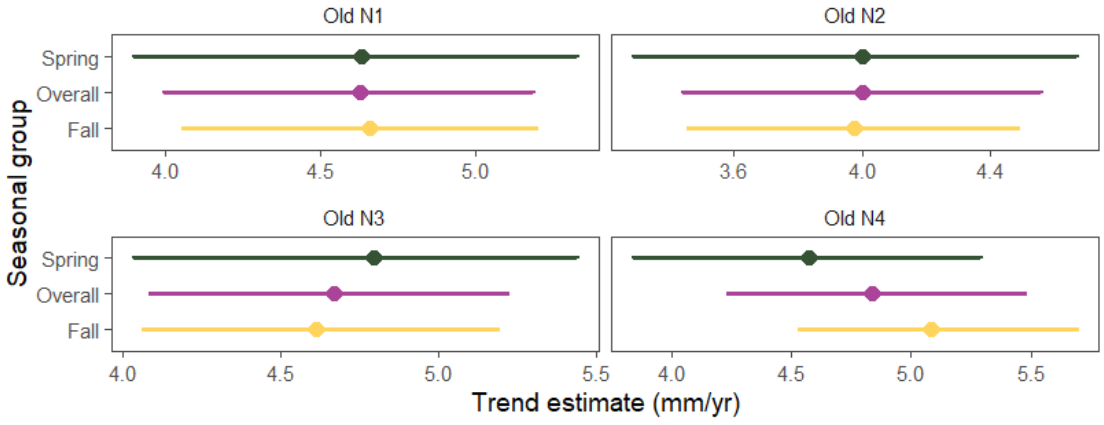


Figure E-115. Accretion trend estimates by season for each station at the Nauset Marsh OldN site, Cape Cod National Seashore.

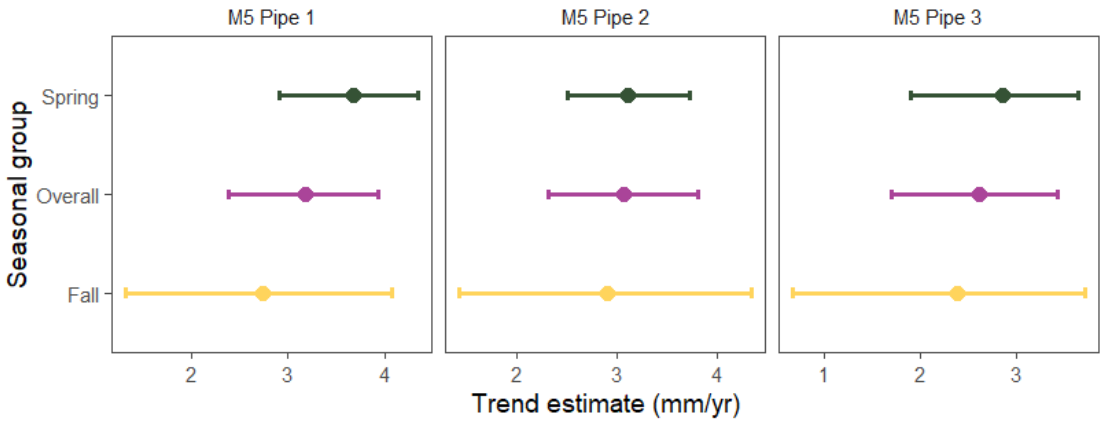


Figure E-116. Accretion trend estimates by season for each station at the Marsh 5 site, Colonial National Historical Park.

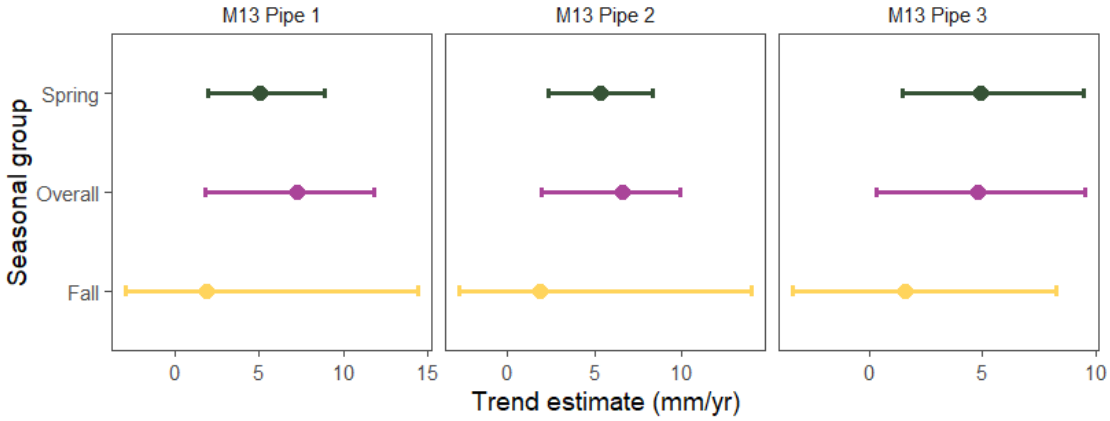


Figure E-117. Accretion trend estimates by season for each station at the Marsh 13 site, Colonial National Historical Park.

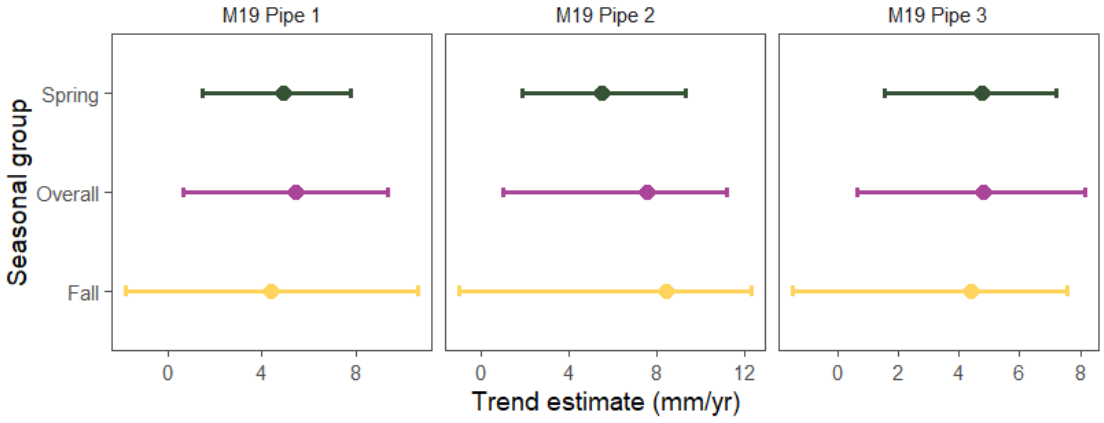


Figure E-118. Accretion trend estimates by season for each station at the Marsh 19 site, Colonial National Historical Park.

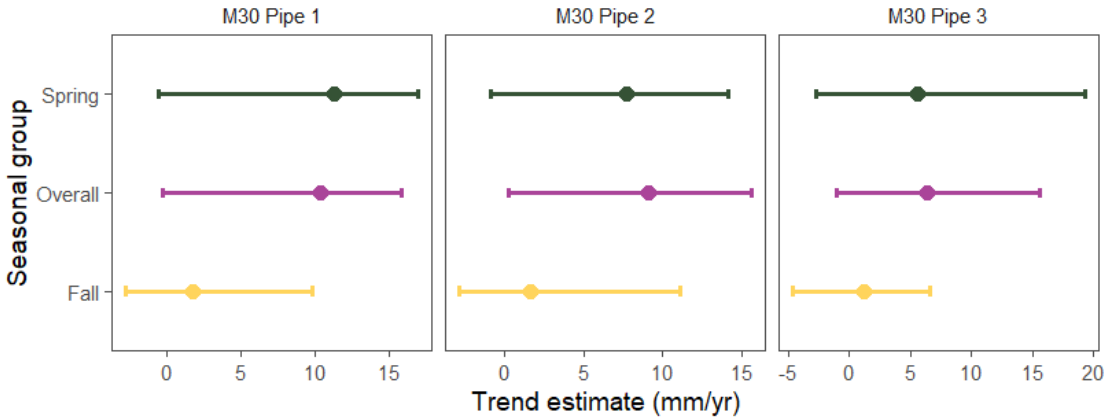


Figure E-119. Accretion trend estimates by season for each station at the Marsh 30 site, Colonial National Historical Park.

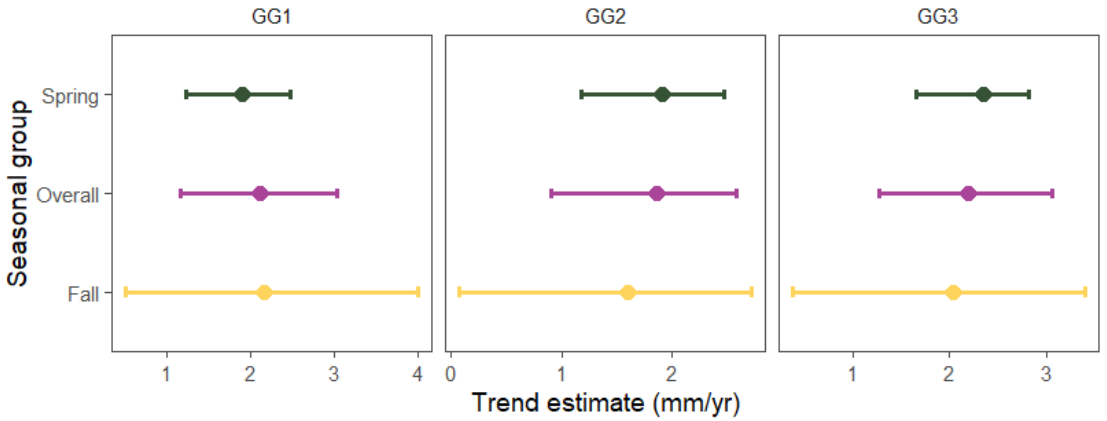


Figure E-120. Accretion trend estimates by season for each station at the Great Gun site, Fire Island National Seashore.

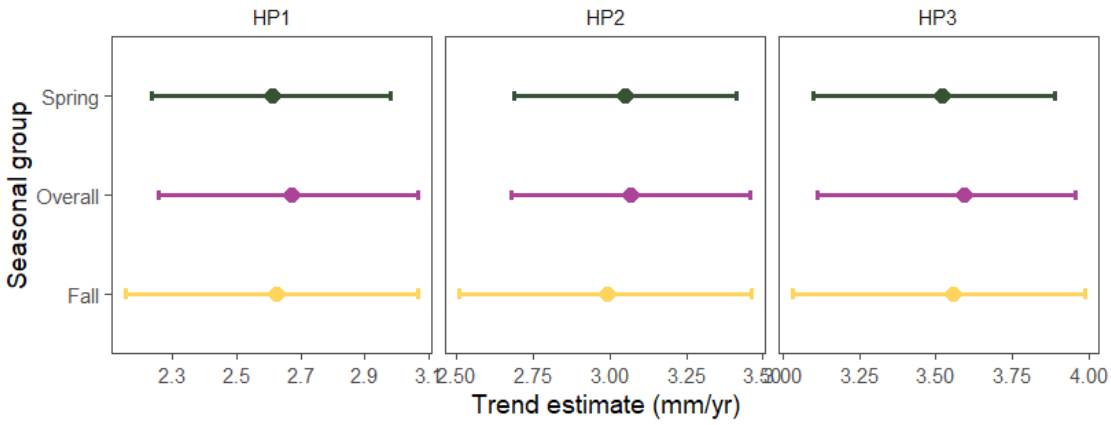


Figure E-121. Accretion trend estimates by season for each station at the Hospital Point site, Fire Island National Seashore.

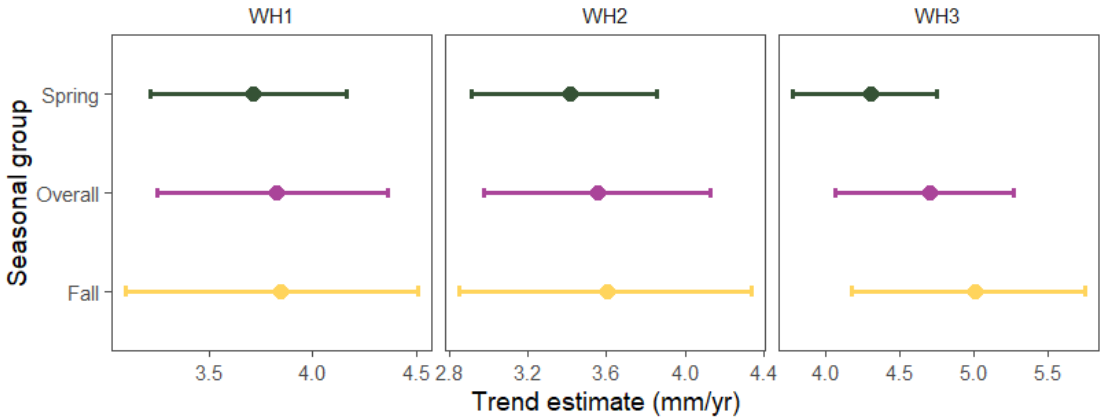


Figure E-122. Accretion trend estimates by season for each station at the Watch Hill site, Fire Island National Seashore.

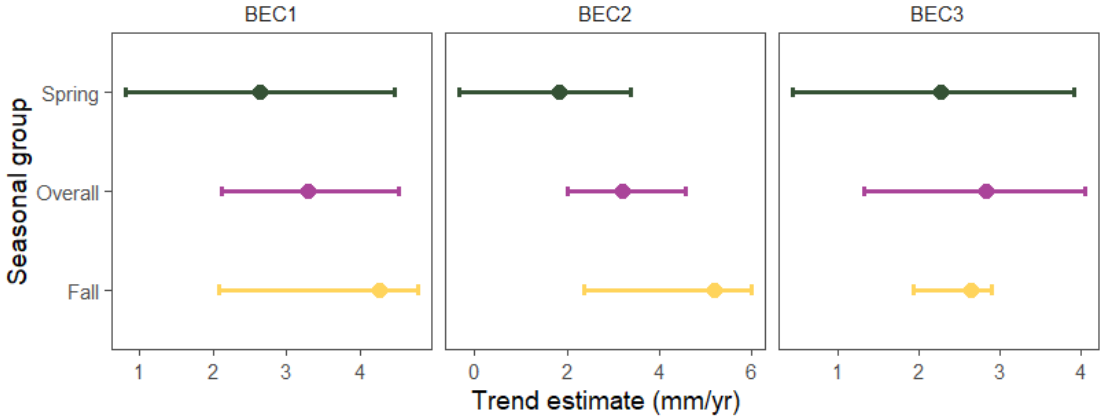


Figure E-123. Accretion trend estimates by season for each station at the Big Egg Control site, Gateway National Recreation Area.

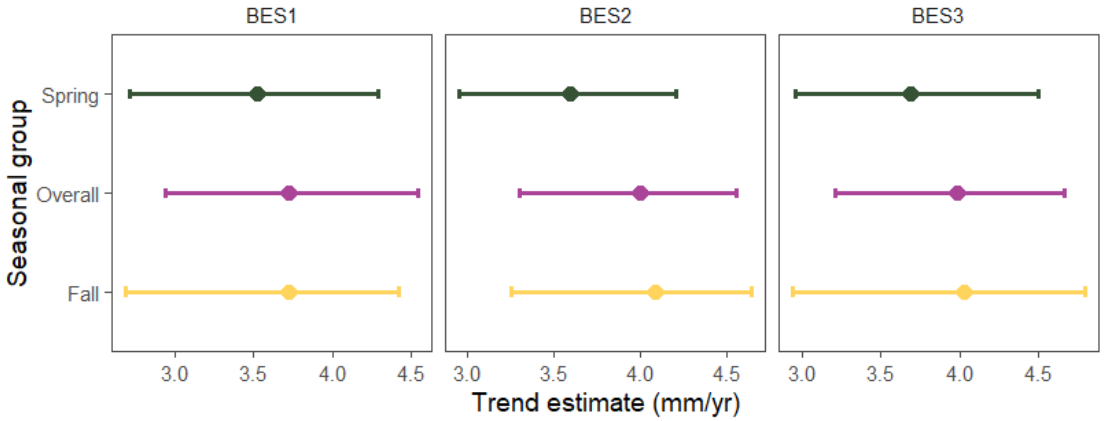


Figure E-124. Accretion trend estimates by season for each station at the Big Egg Spray site, Gateway National Recreation Area.

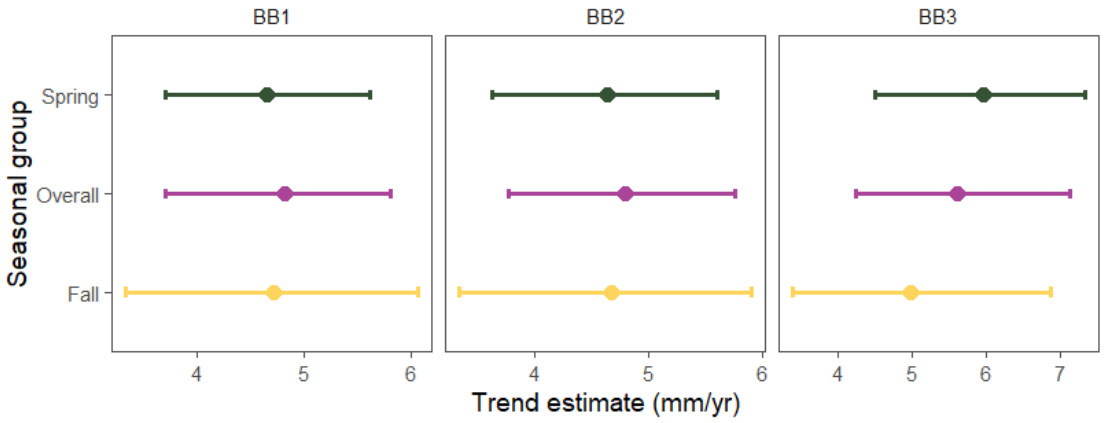


Figure E-125. Accretion trend estimates by season for each station at the Black Bank site, Gateway National Recreation Area.

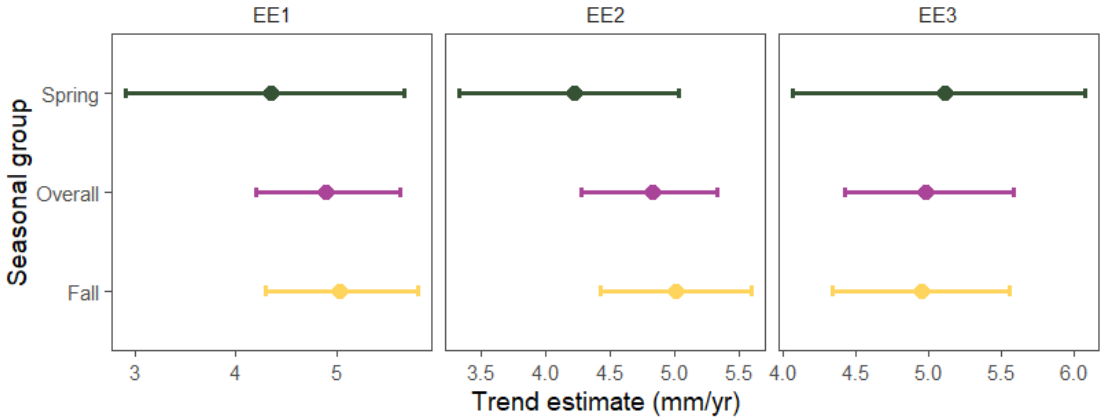


Figure E-126. Accretion trend estimates by season for each station at the Elders East site, Gateway National Recreation Area.

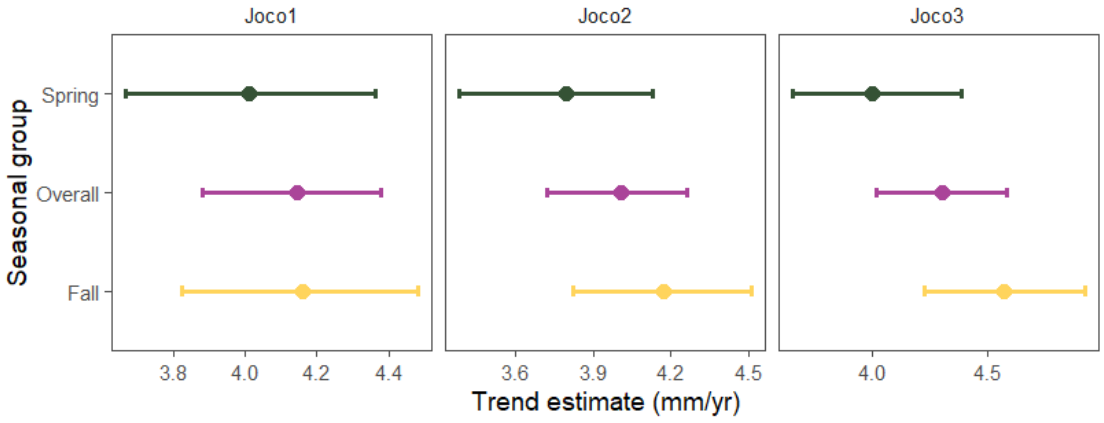


Figure E-127. Accretion trend estimates by season for each station at the JOCO site, Gateway National Recreation Area.

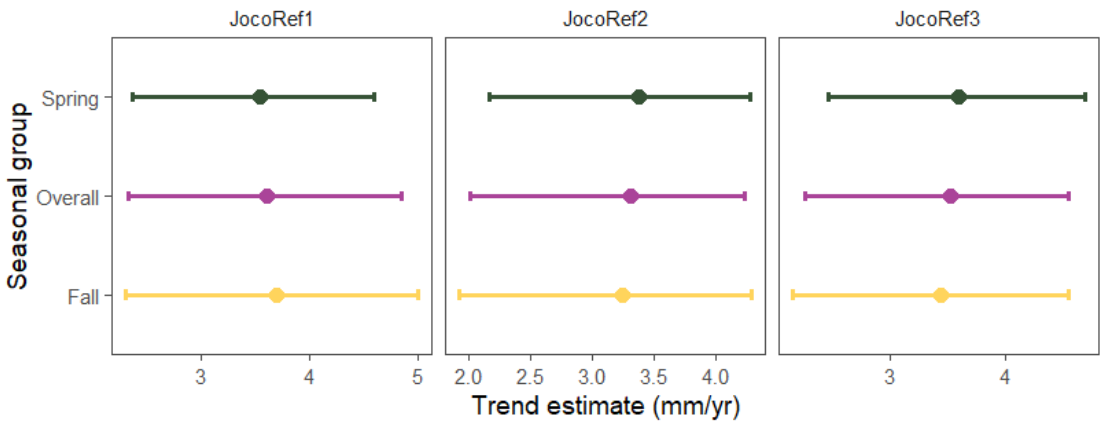


Figure E-128. Accretion trend estimates by season for each station at the JOCO REF site, Gateway National Recreation Area.

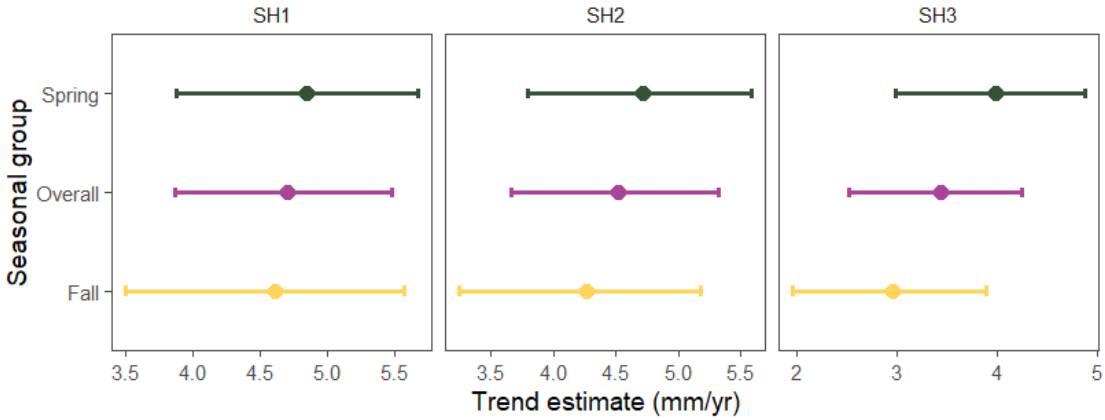


Figure E-129. Accretion trend estimates by season for each station at the JOCO REF Shallow site, Gateway National Recreation Area.

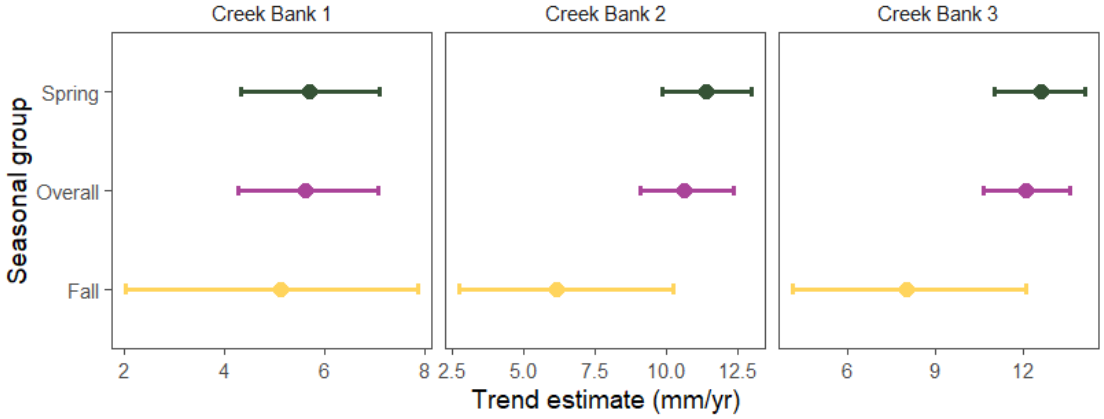


Figure E-130. Accretion trend estimates by season for each station at the Dyke Marsh Creek site, George Washington Memorial Parkway.

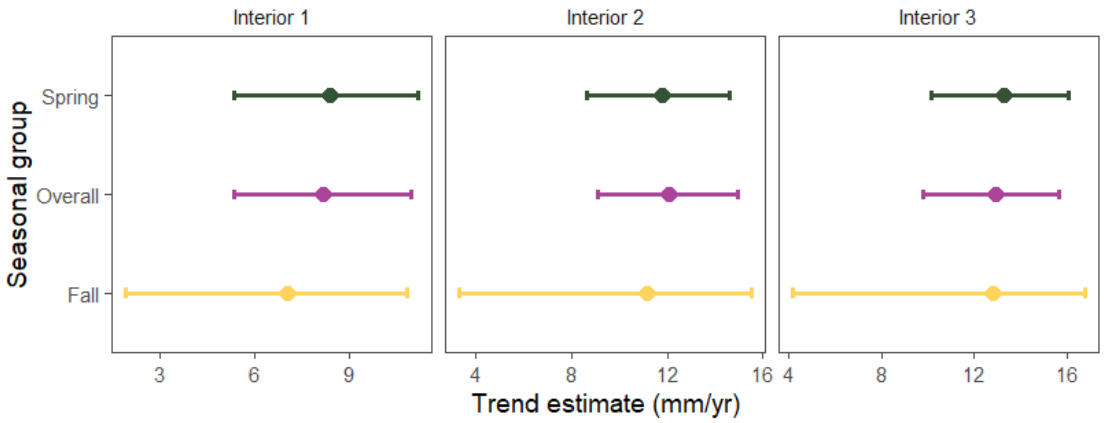


Figure E-131. Accretion trend estimates by season for each station at the Dyke Marsh Interior site, George Washington Memorial Parkway.

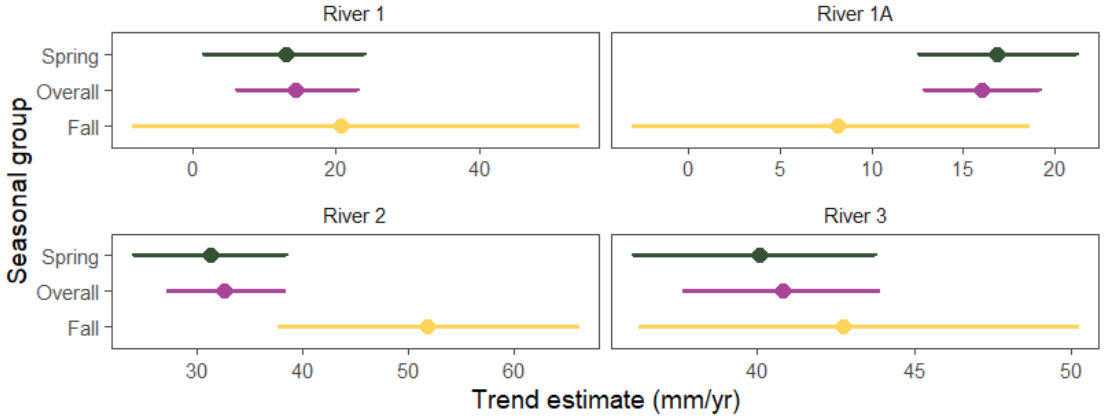


Figure E-132. Accretion trend estimates by season for each station at the Dyke Marsh River site, George Washington Memorial Parkway.

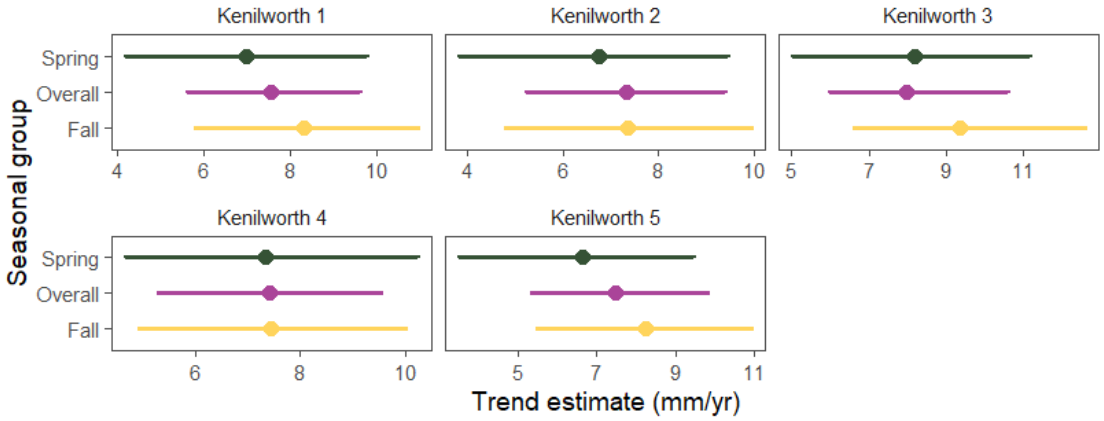


Figure E.133. Accretion trend estimates by season for each station at the Kenilworth Marsh River site, National Capital Parks-East.

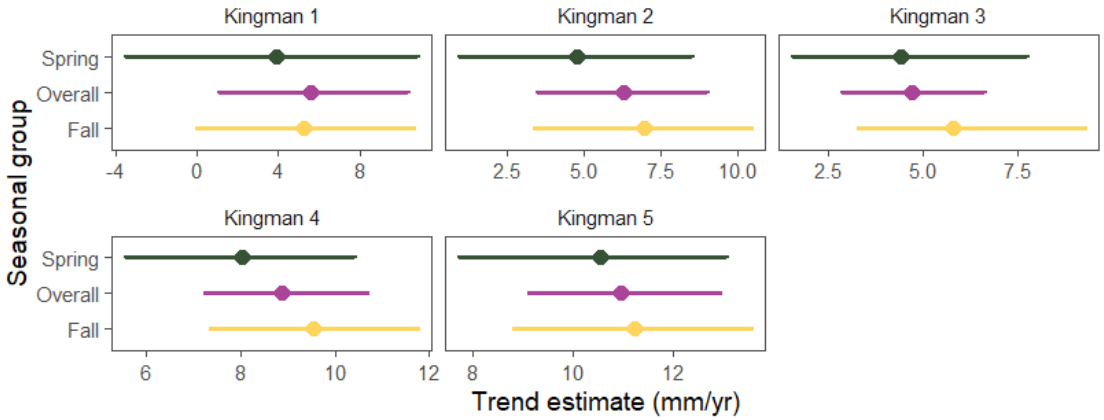


Figure E.134. Accretion trend estimates by season for each station at the Kingman Lake site, National Capital Parks-East.

Accretion Seasonal Analysis, overall plots

The plots below contain the accretion trend estimates by season for each park and site. The trend was averaged over the stations to get a 'overall accretion' trend.

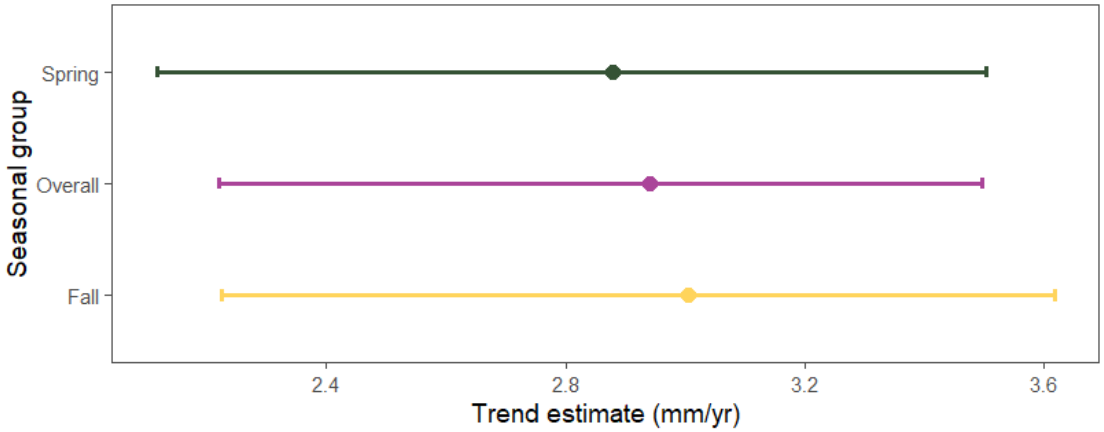


Figure E-135. Overall accretion trend estimates by season for the Bass Harbor site, Acadia National Park. The trend was averaged over the stations to get an 'overall accretion' trend.

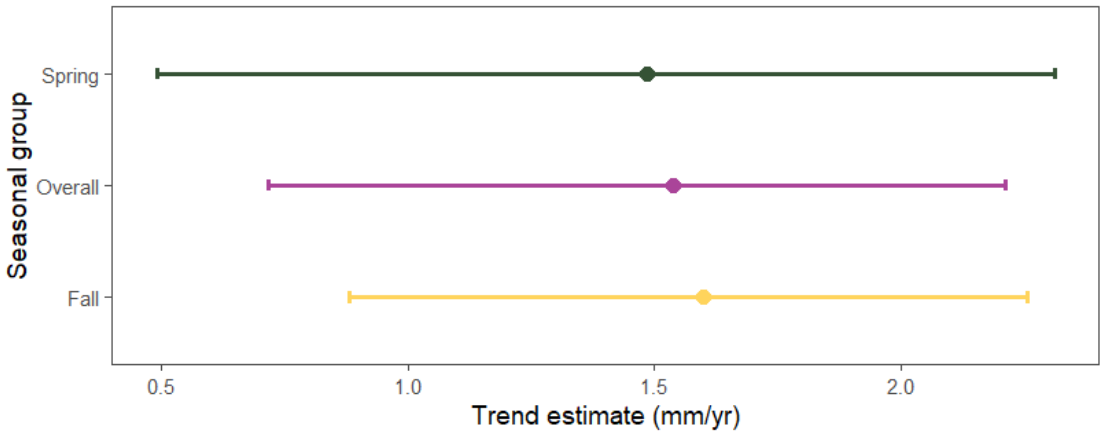


Figure E-136. Overall accretion trend estimates by season for the Maine Coast Heritage site, Acadia National Park. The trend was averaged over the stations to get an 'overall accretion' trend.

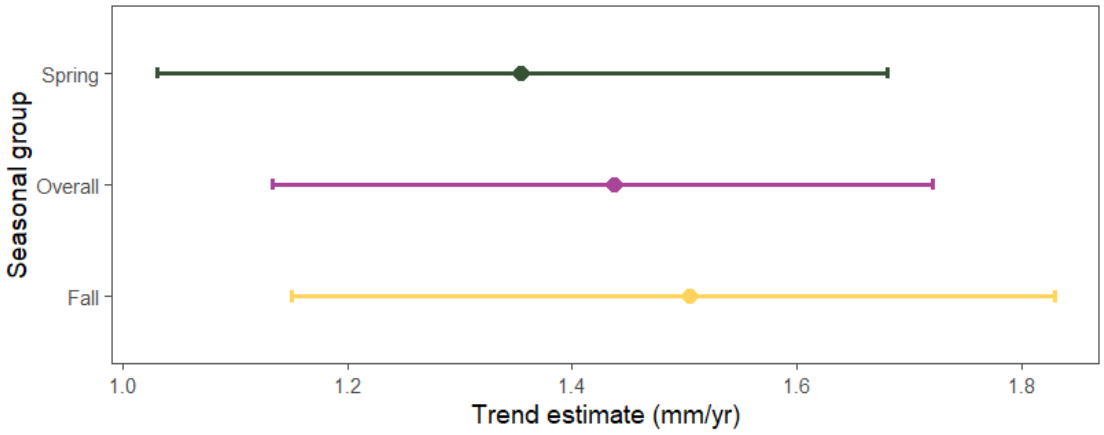


Figure E-137. Overall accretion trend estimates by season for the Schoodic site, Acadia National Park. The trend was averaged over the stations to get an 'overall accretion' trend.

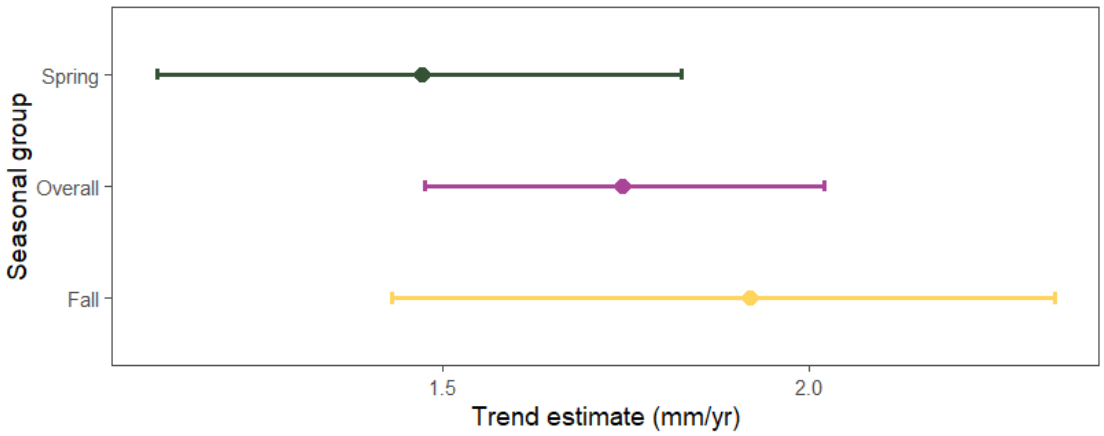


Figure E-138. Overall accretion trend estimates by season for the Thompson Island site, Acadia National Park. The trend was averaged over the stations to get an 'overall accretion' trend.

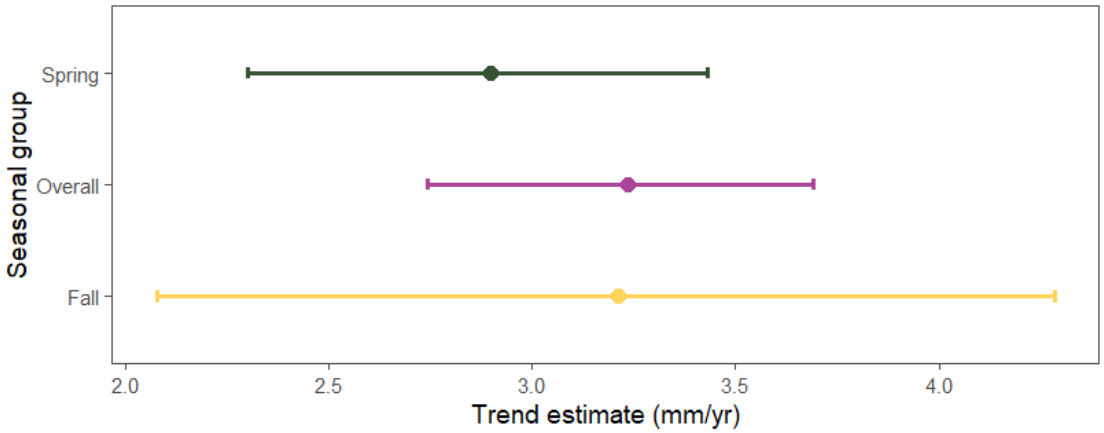


Figure E-139. Overall accretion trend estimates by season for the Marsh 5 site, Assateague Island National Seashore. The trend was averaged over the stations to get an 'overall accretion' trend.

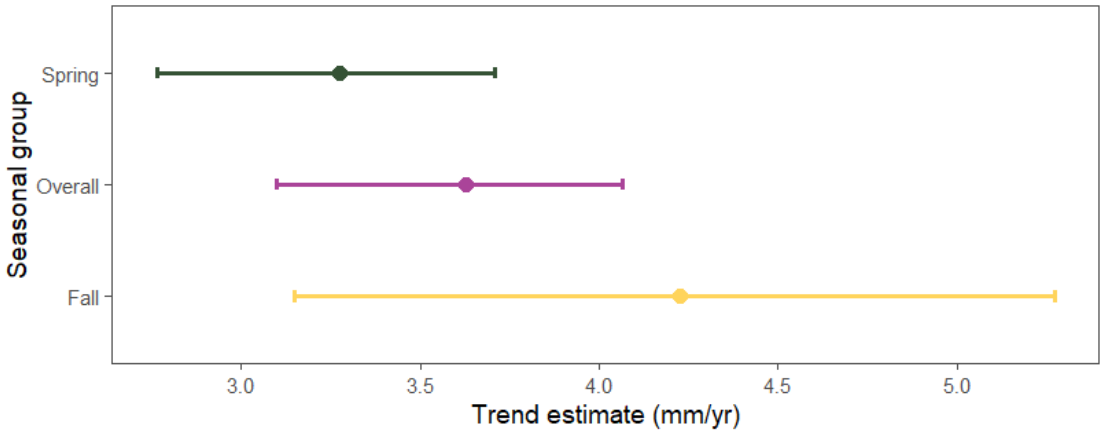


Figure E-140. Overall accretion trend estimates by season for the Marsh 6 site, Assateague Island National Seashore. The trend was averaged over the stations to get an 'overall accretion' trend.

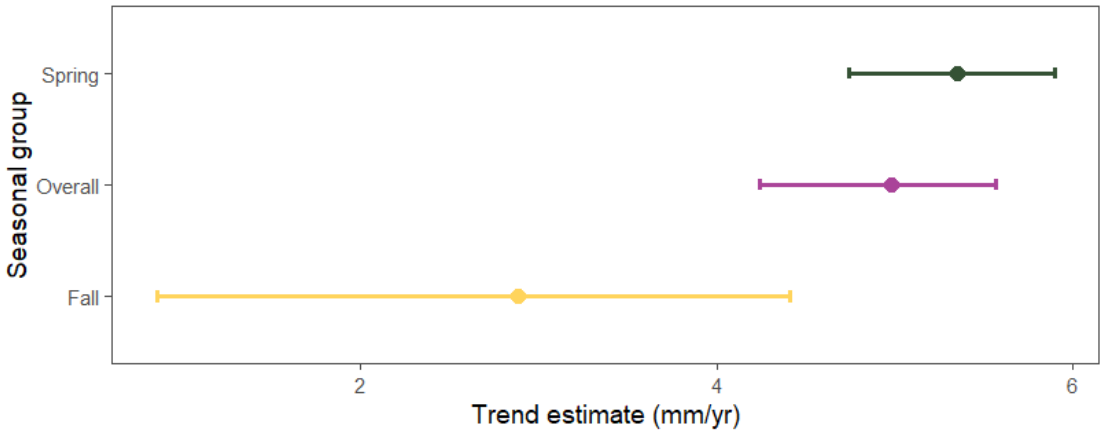


Figure E-141. Overall accretion trend estimates by season for the Marsh 8 site, Assateague Island National Seashore. The trend was averaged over the stations to get an 'overall accretion' trend.

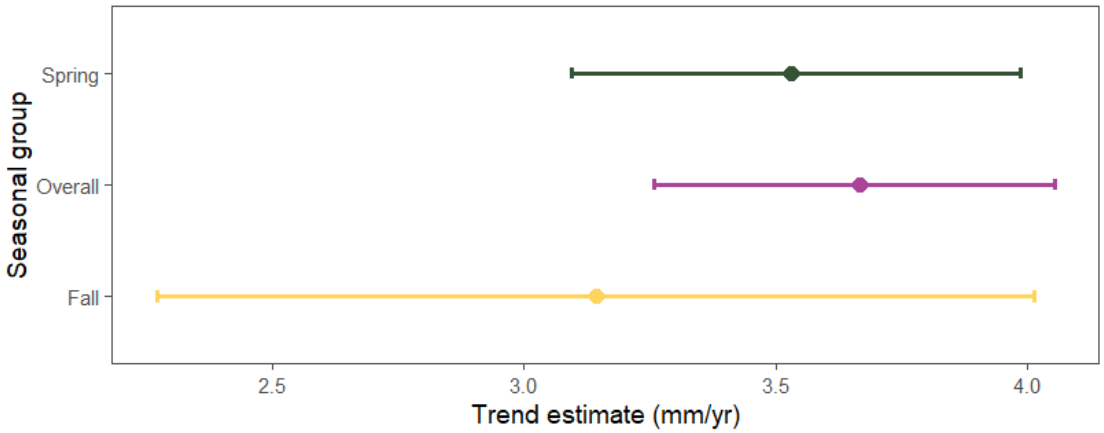


Figure E-142. Overall accretion trend estimates by season for the Marsh 11 site, Assateague Island National Seashore. The trend was averaged over the stations to get an 'overall accretion' trend.

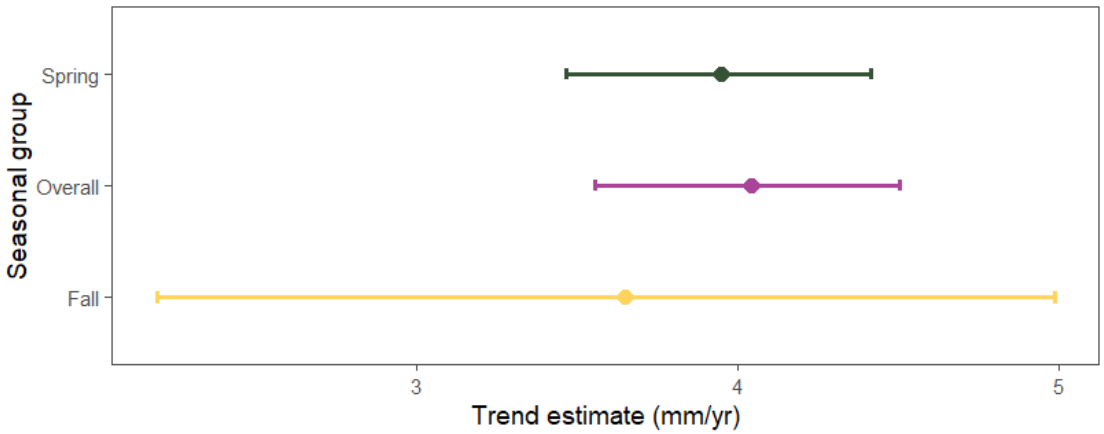


Figure E-143. Overall accretion trend estimates by season for the Marsh Exclosure site, Assateague Island National Seashore. The trend was averaged over the stations to get an 'overall accretion' trend.

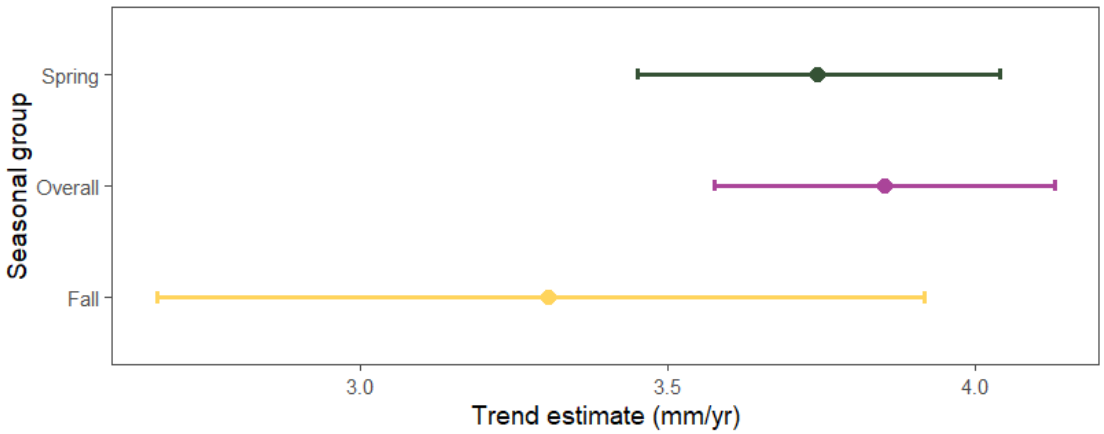


Figure E-144. Overall accretion trend estimates by season for the Marsh non-Exclosure site, Assateague Island National Seashore. The trend was averaged over the stations to get an 'overall accretion' trend.

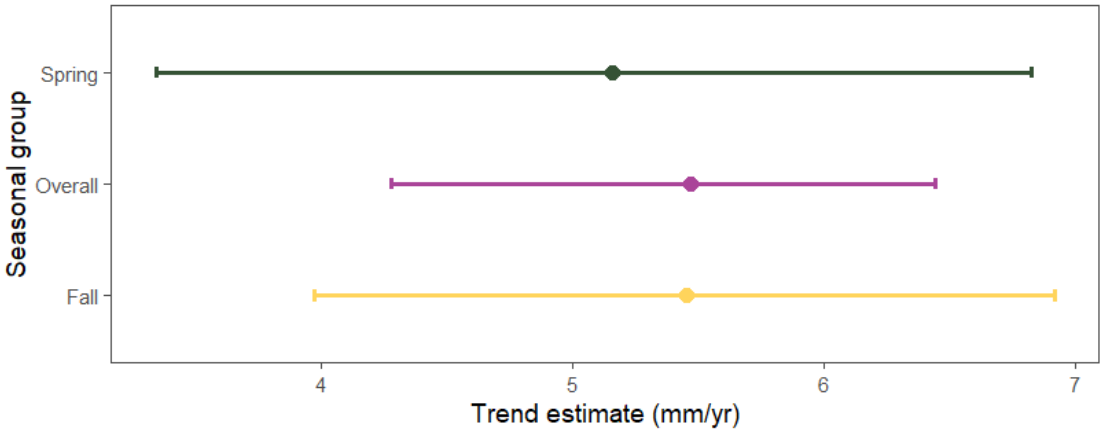


Figure E-145. Overall accretion trend estimates by season for the Calf Island site, Boston Harbor Islands Recreation Area. The trend was averaged over the stations to get an 'overall accretion' trend.

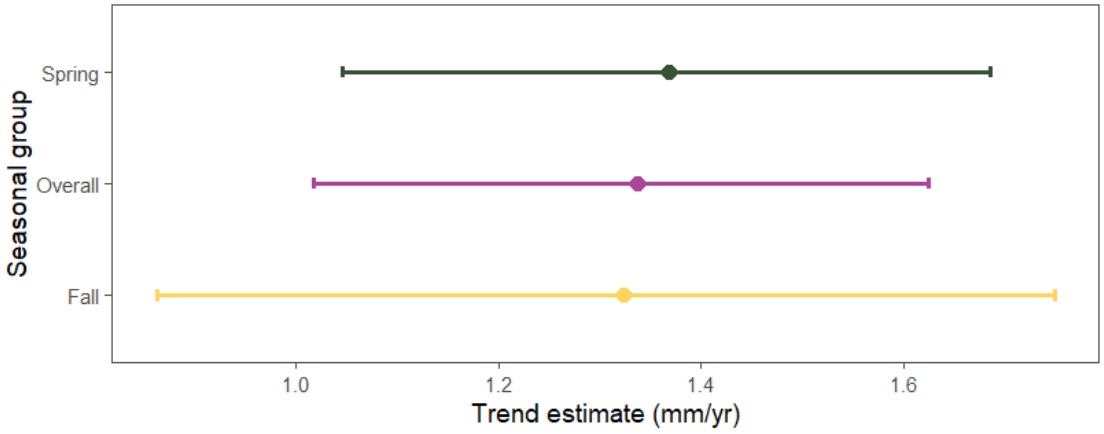


Figure E-146. Overall accretion trend estimates by season for the Peddocks Island site, Boston Harbor Islands Recreation Area. The trend was averaged over the stations to get an 'overall accretion' trend.

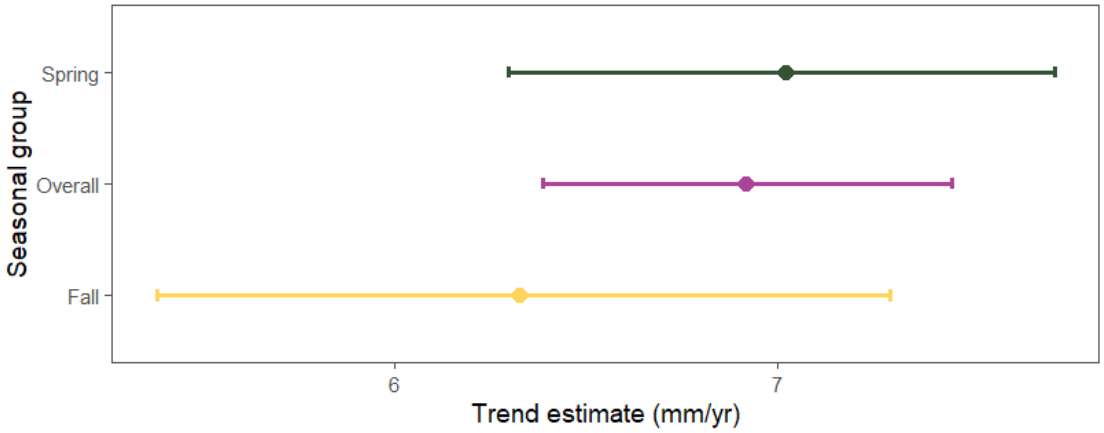


Figure E-147. Overall accretion trend estimates by season for the Thompson Island site, Boston Harbor Islands Recreation Area. The trend was averaged over the stations to get an 'overall accretion' trend.

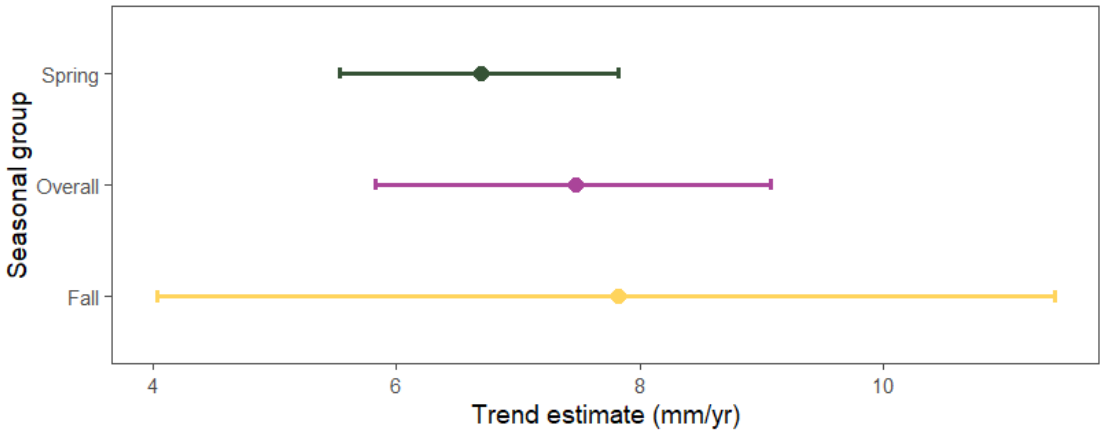


Figure E-148. Overall accretion trend estimates by season for the Blackfish Creek site, Cape Cod National Seashore. The trend was averaged over the stations to get an 'overall accretion' trend.

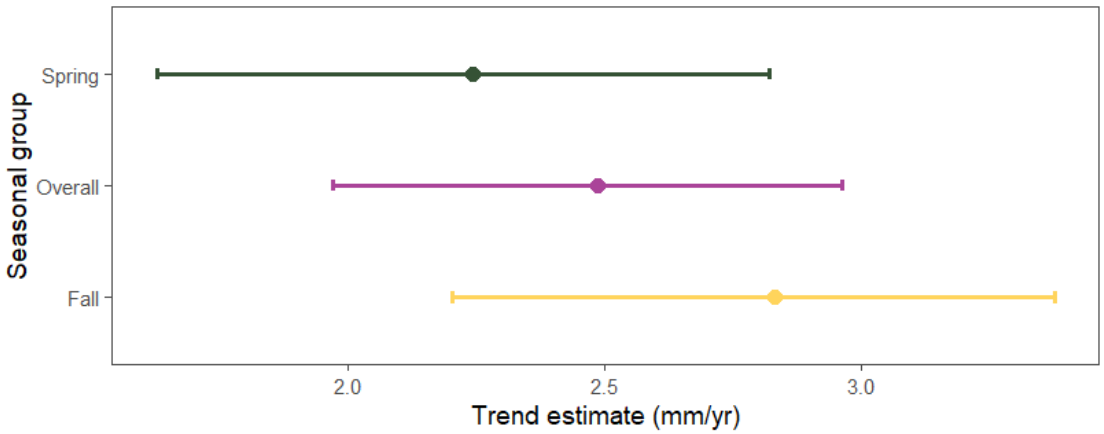


Figure E-149. Overall accretion trend estimates by season for the Hatches Harbor HH1 site, Cape Cod National Seashore. The trend was averaged over the stations to get an 'overall accretion' trend.

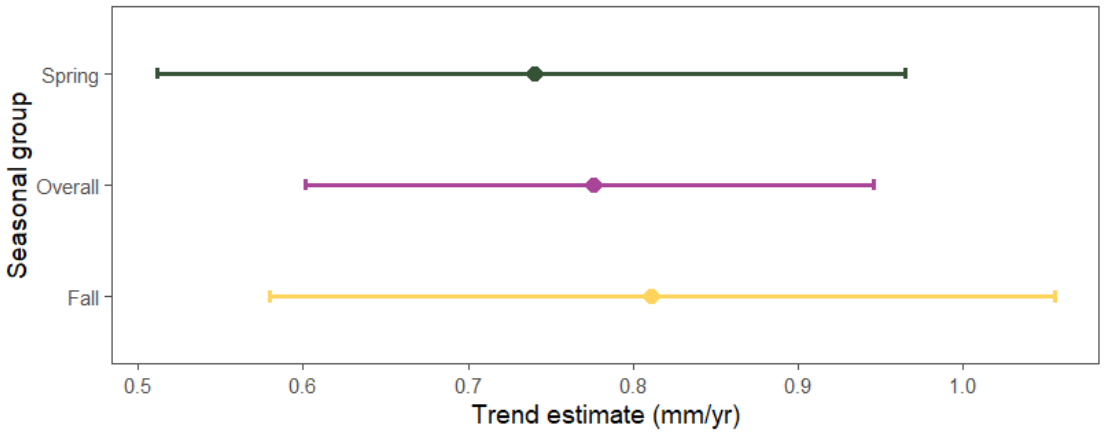


Figure E-150. Overall accretion trend estimates by season for the Hatches Harbor HH2 site, Cape Cod National Seashore. The trend was averaged over the stations to get an 'overall accretion' trend.

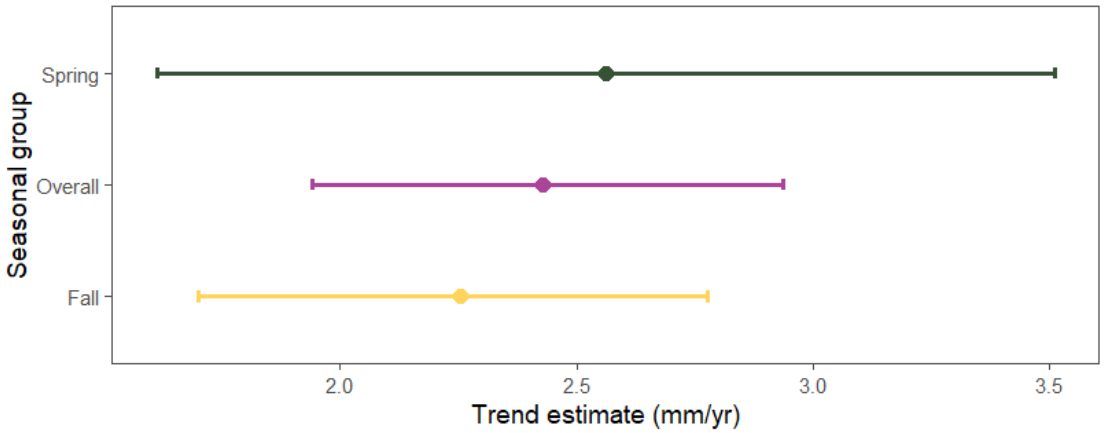


Figure E-151. Overall accretion trend estimates by season for the Hatches Harbor H1 site, Cape Cod National Seashore. The trend was averaged over the stations to get an 'overall accretion' trend.

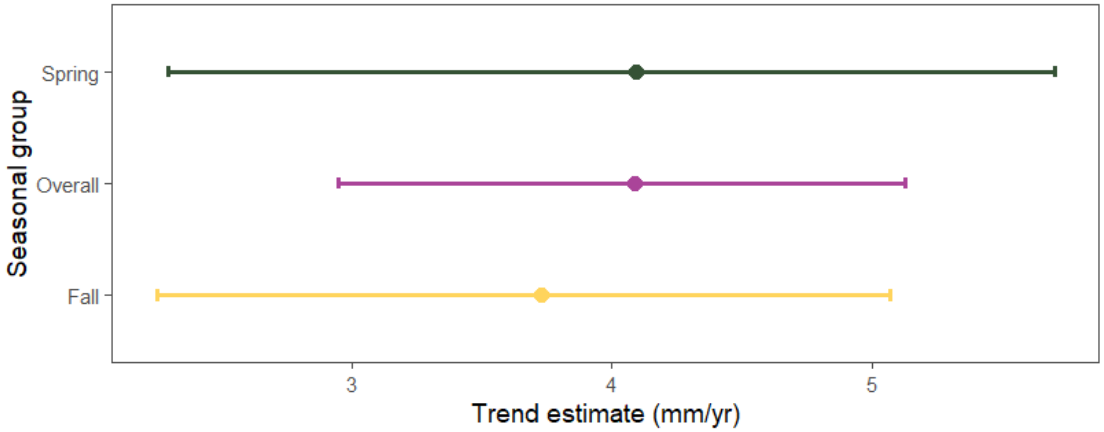


Figure E-152. Overall accretion trend estimates by season for the Hatches Harbor H2 site, Cape Cod National Seashore. The trend was averaged over the stations to get an 'overall accretion' trend.

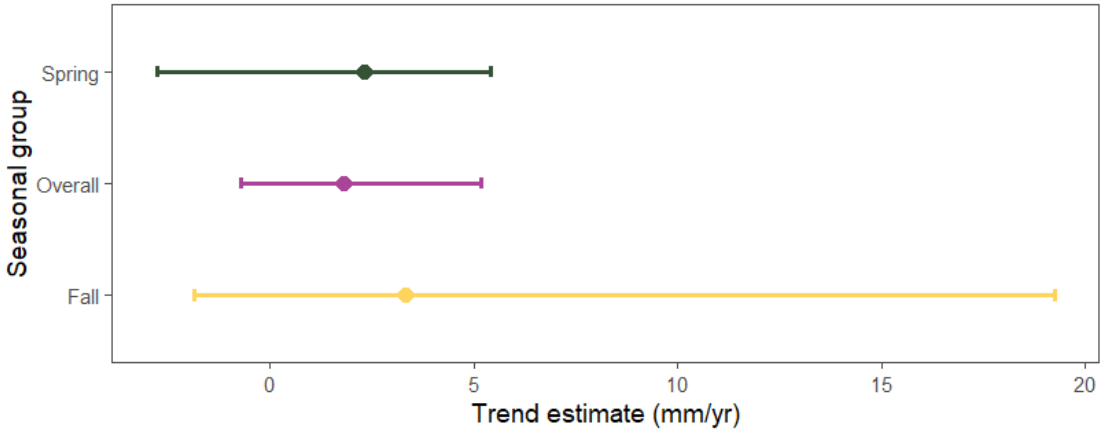


Figure E-153. Overall accretion trend estimates by season for the Herring River GUT site, Cape Cod National Seashore. The trend was averaged over the stations to get an 'overall accretion' trend.

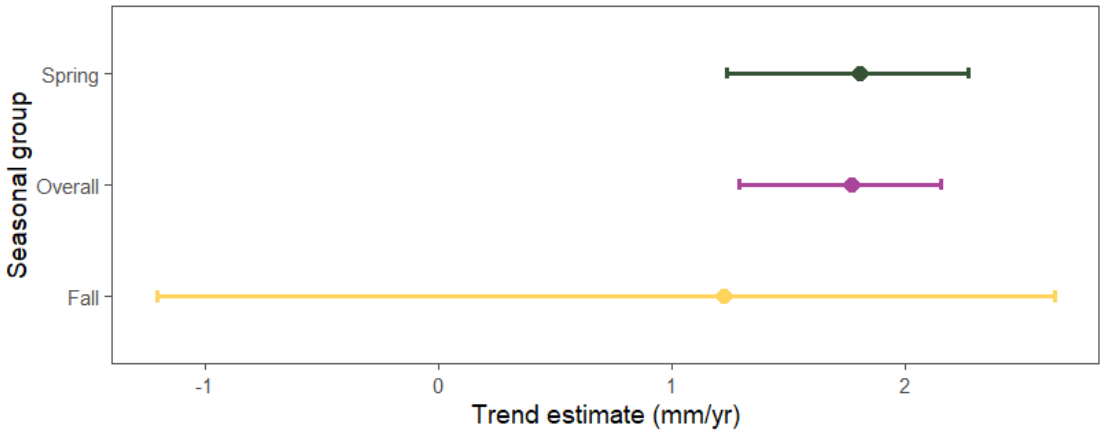


Figure E-154. Overall accretion trend estimates by season for the Herring River High Toss site, Cape Cod National Seashore. The trend was averaged over the stations to get an 'overall accretion' trend.

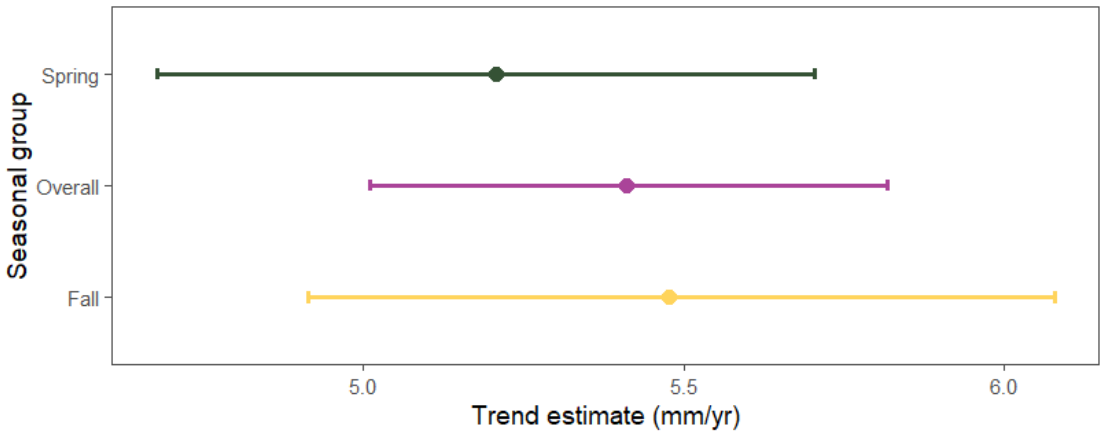


Figure E-155. Overall accretion trend estimates by season for the Herring River Phrag site, Cape Cod National Seashore. The trend was averaged over the stations to get an 'overall accretion' trend.

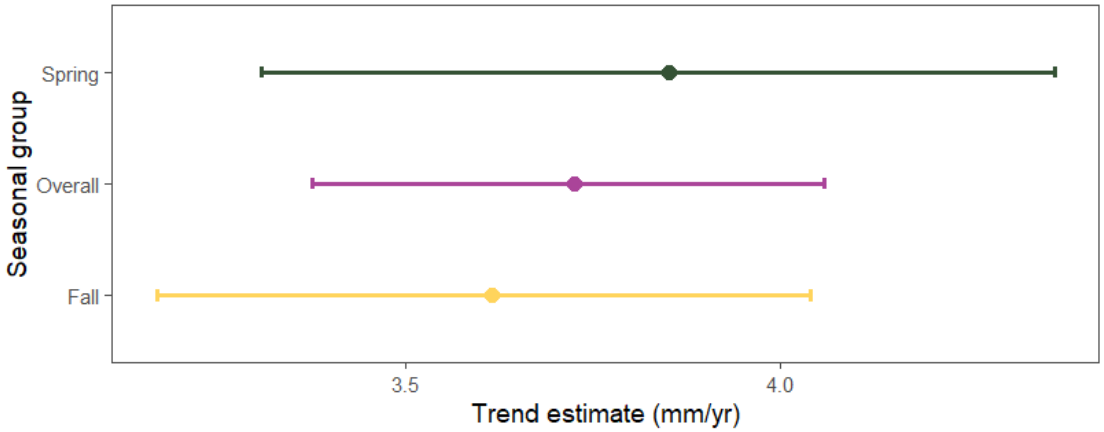


Figure E-156. Overall accretion trend estimates by season for the Nauset Marsh N site, Cape Cod National Seashore. The trend was averaged over the stations to get an 'overall accretion' trend.

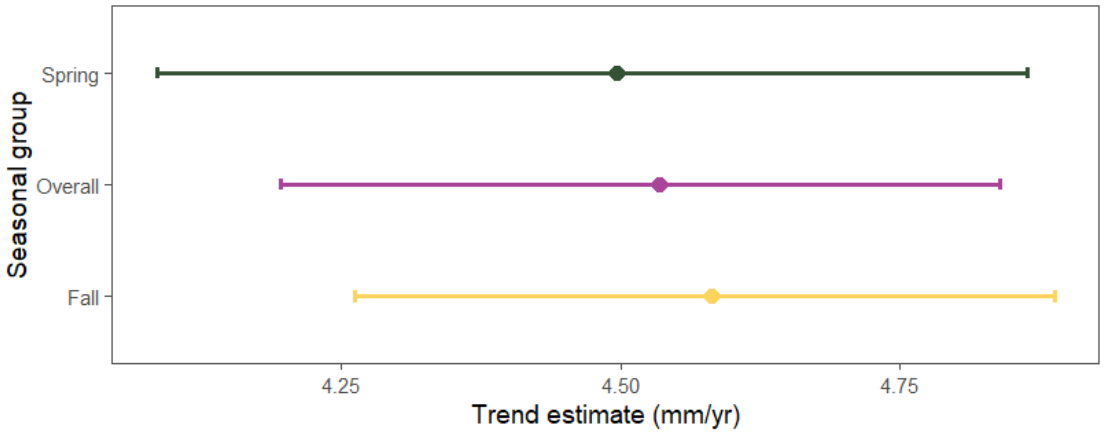


Figure E-157. Overall accretion trend estimates by season for the Nauset Marsh OldN site, Cape Cod National Seashore. The trend was averaged over the stations to get an 'overall accretion' trend.

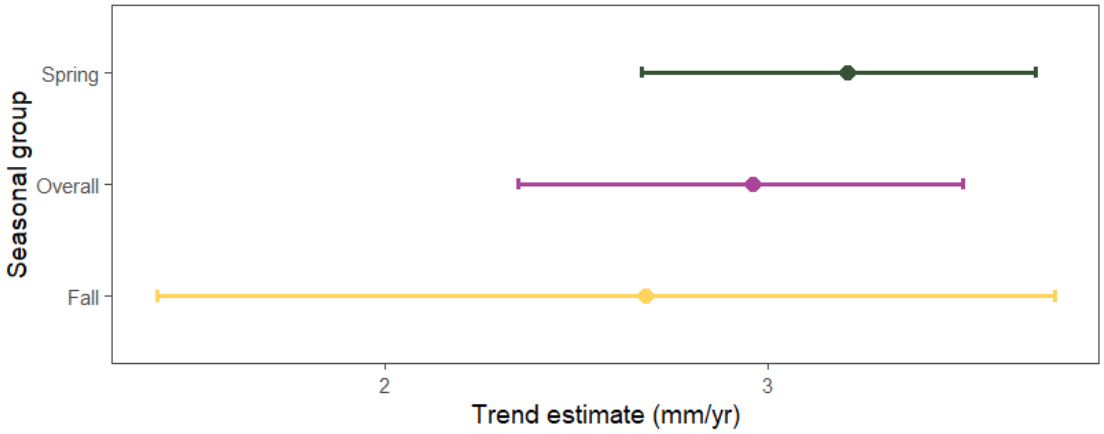


Figure E-158. Overall accretion trend estimates by season for the Marsh 5 site, Colonial National Historical Park. The trend was averaged over the stations to get an 'overall accretion' trend.

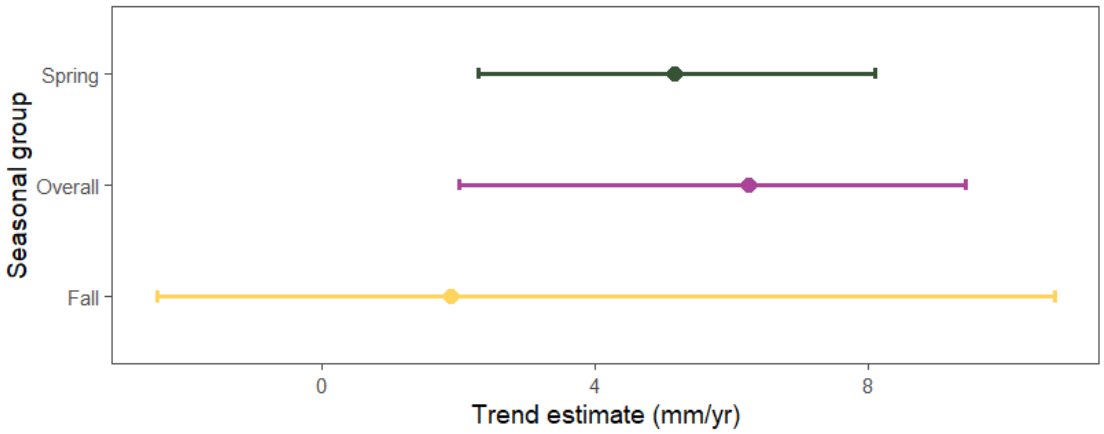


Figure E-159. Overall accretion trend estimates by season for the Marsh 13 site, Colonial National Historical Park. The trend was averaged over the stations to get an 'overall accretion' trend.

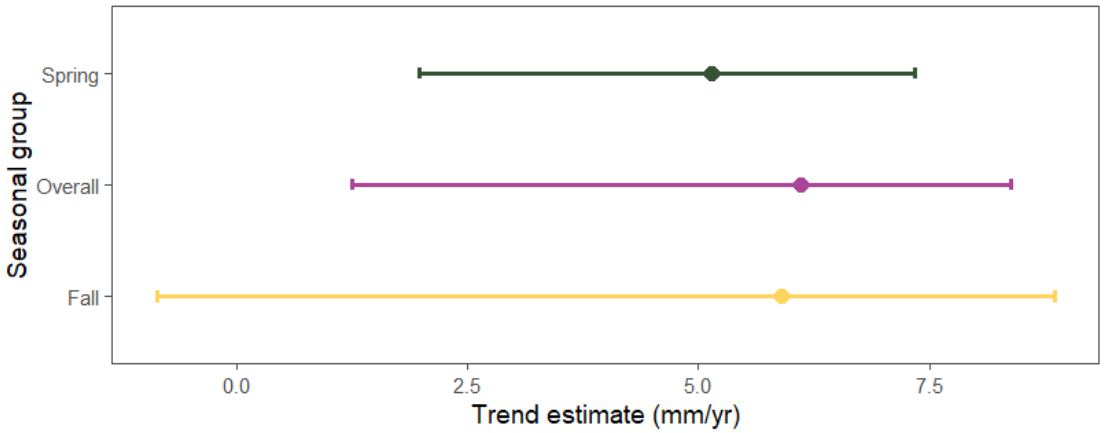


Figure E-160. Overall accretion trend estimates by season for the Marsh 19 site, Colonial National Historical Park. The trend was averaged over the stations to get an 'overall accretion' trend.

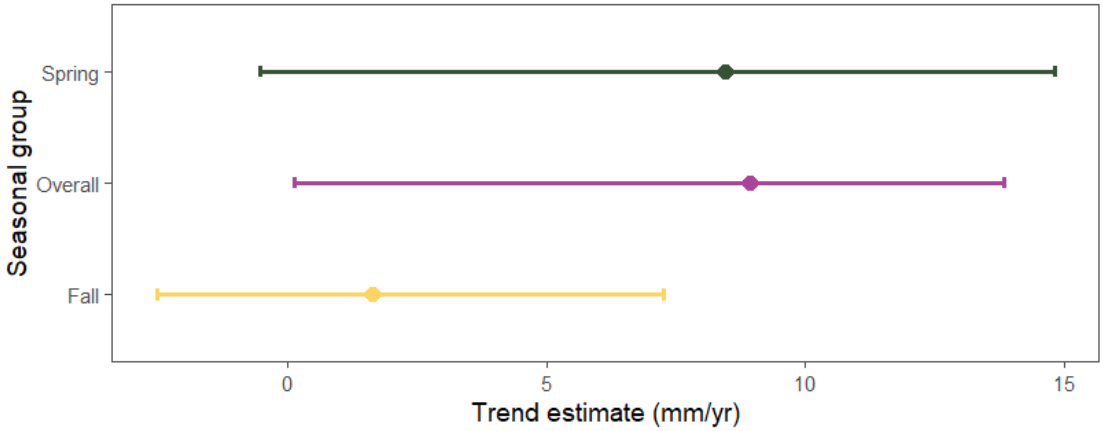


Figure E-161. Overall accretion trend estimates by season for the Marsh 30 site, Colonial National Historical Park. The trend was averaged over the stations to get an 'overall accretion' trend.

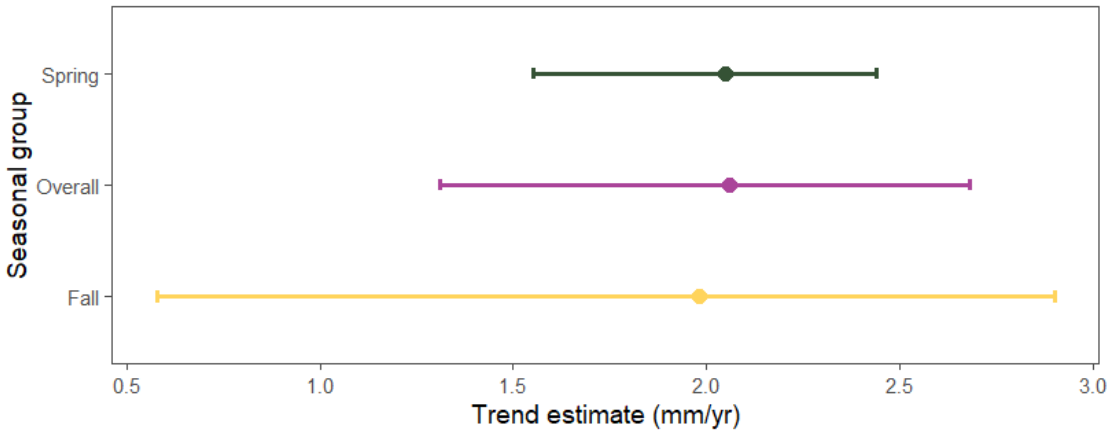


Figure E-162. Overall accretion trend estimates by season for the Great Gun site, Fire Island National Seashore. The trend was averaged over the stations to get an 'overall accretion' trend.

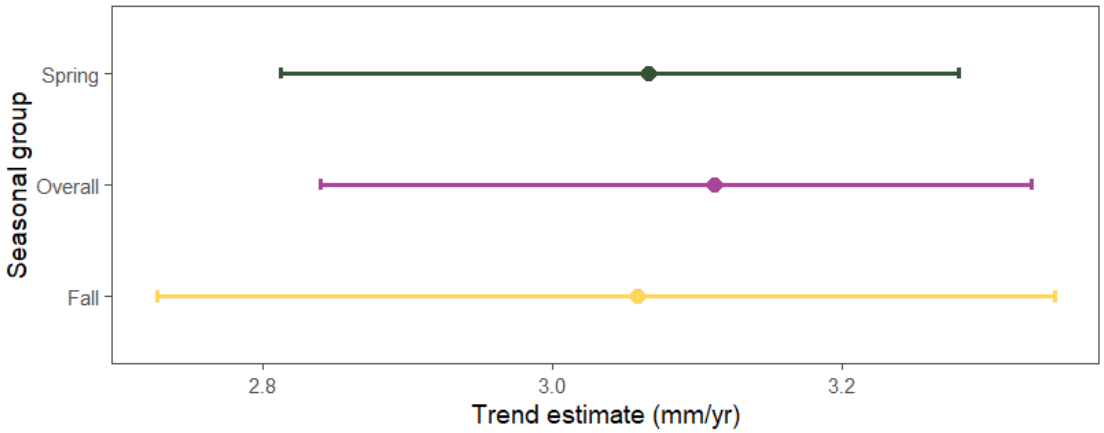


Figure E-163. Overall accretion trend estimates by season for the Hospital Point site, Fire Island National Seashore. The trend was averaged over the stations to get an 'overall accretion' trend.

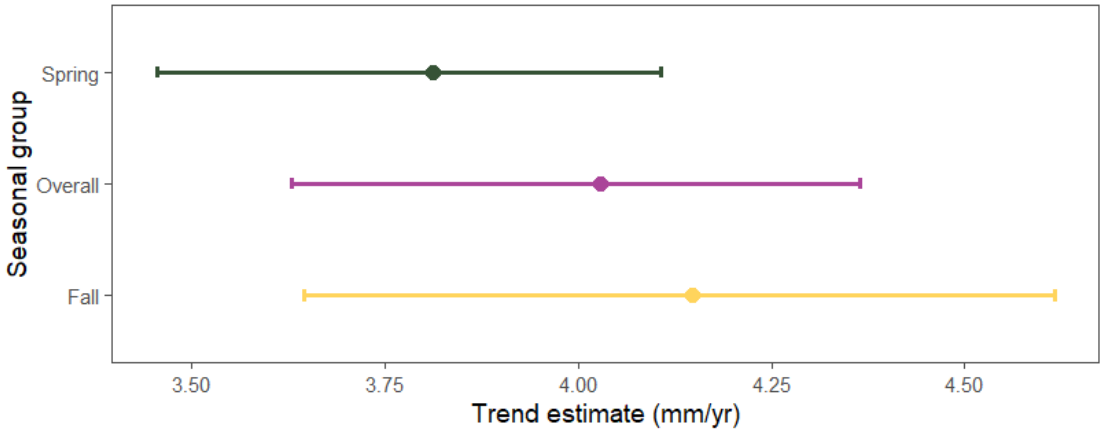


Figure E-164. Overall accretion trend estimates by season for the Watch Hill site, Fire Island National Seashore. The trend was averaged over the stations to get an 'overall accretion' trend.

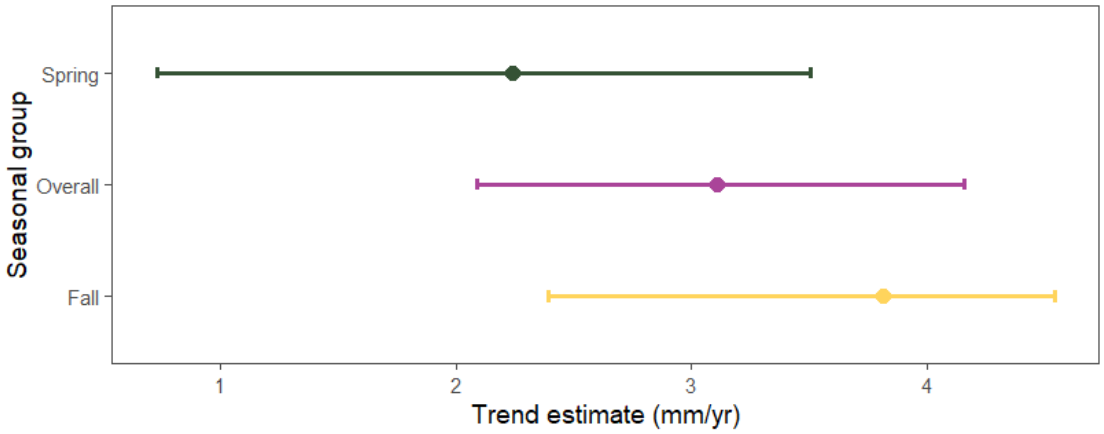


Figure E-165. Overall accretion trend estimates by season for the Big Egg Control site, Gateway National Recreation Area. The trend was averaged over the stations to get an 'overall accretion' trend.

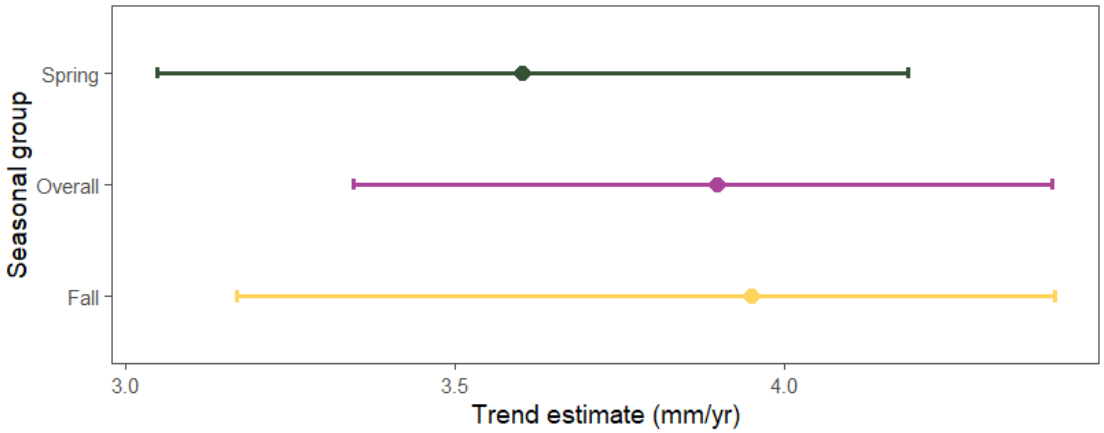


Figure E-166. Overall accretion trend estimates by season for the Big Egg Spray site, Gateway National Recreation Area. The trend was averaged over the stations to get an 'overall accretion' trend.

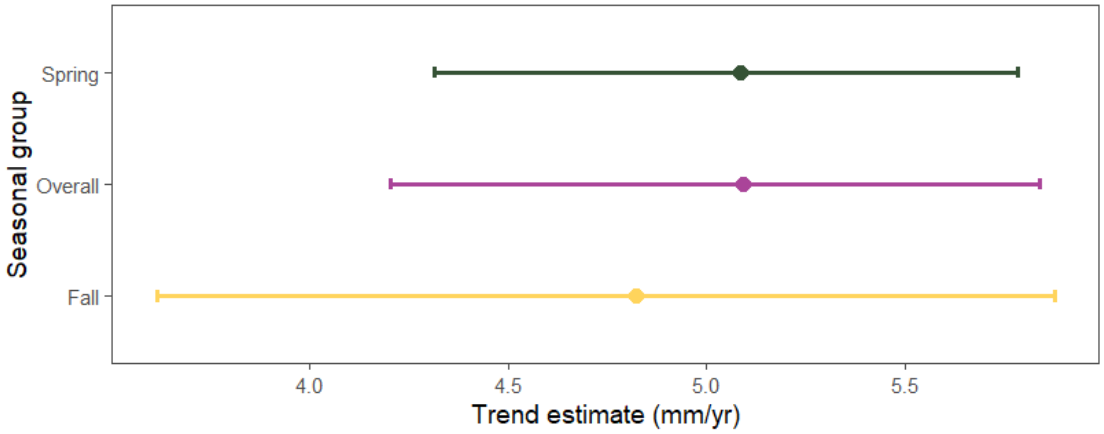


Figure E-167. Overall accretion trend estimates by season for the Black Bank site, Gateway National Recreation Area. The trend was averaged over the stations to get an 'overall accretion' trend.

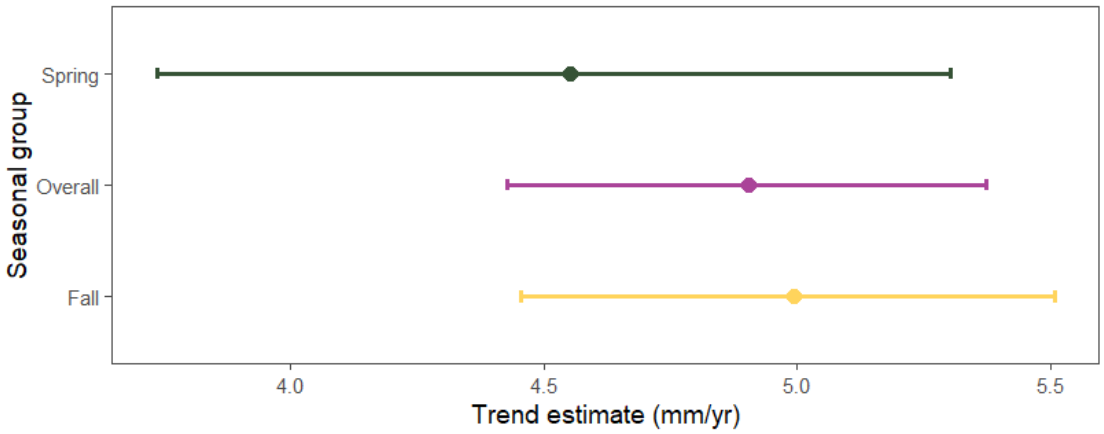


Figure E-168. Overall accretion trend estimates by season for the Elders East site, Gateway National Recreation Area. The trend was averaged over the stations to get an 'overall accretion' trend.

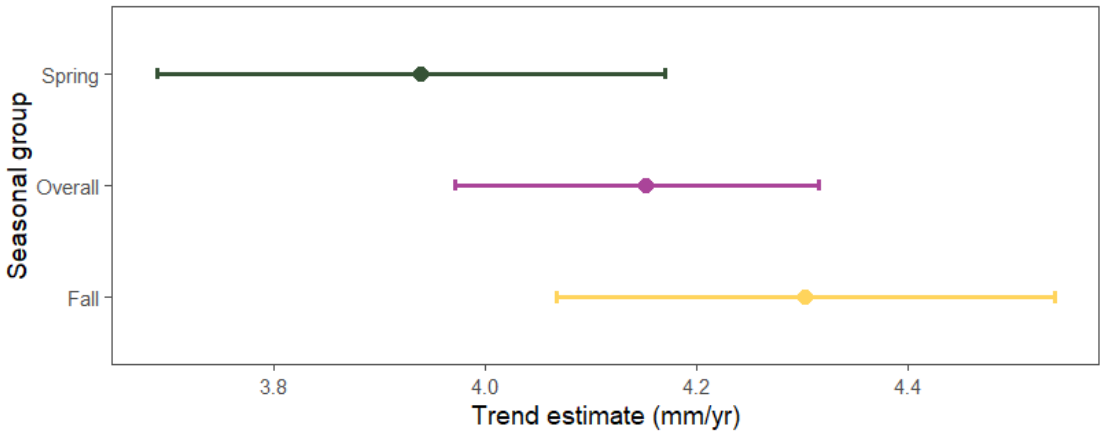


Figure E-169. Overall accretion trend estimates by season for the JOCO site, Gateway National Recreation Area. The trend was averaged over the stations to get an 'overall accretion' trend.

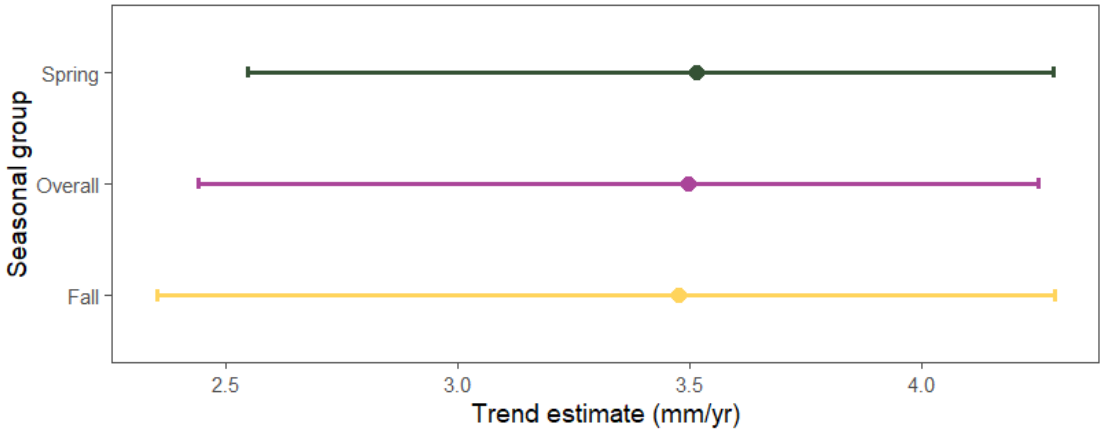


Figure E-170. Overall accretion trend estimates by season for the JOCO REF site, Gateway National Recreation Area. The trend was averaged over the stations to get an 'overall accretion' trend.

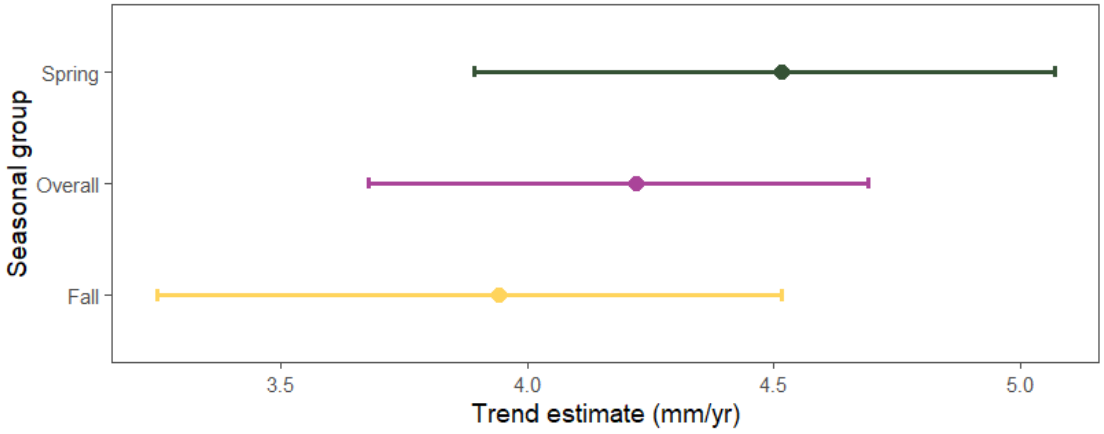


Figure E-171. Overall accretion trend estimates by season for the Sandy Hook site, Gateway National Recreation Area. The trend was averaged over the stations to get an 'overall accretion' trend.

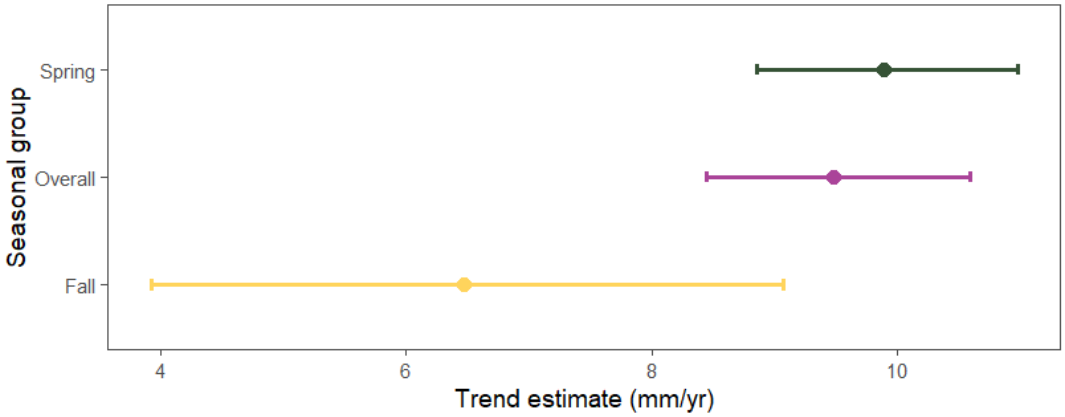


Figure E-172. Overall accretion trend estimates by season for the Dyke Marsh Creek site, George Washington Memorial Parkway. The trend was averaged over the stations to get an 'overall accretion' trend.

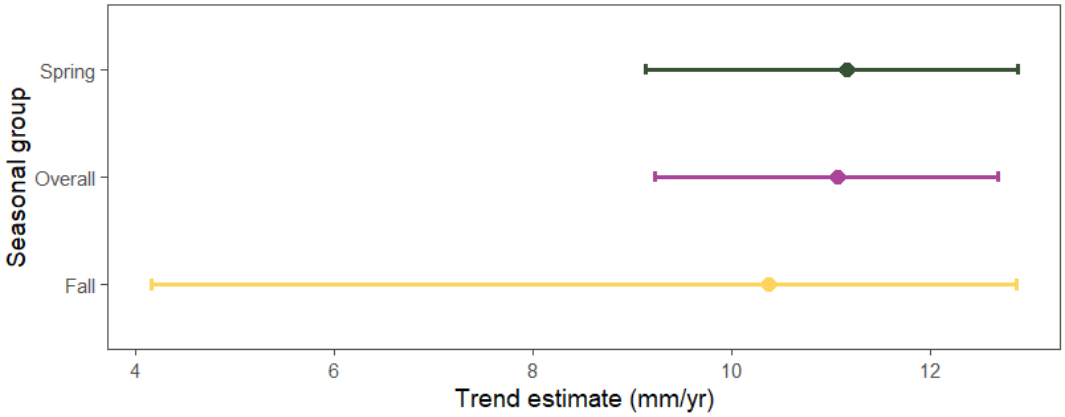


Figure E-173. Overall accretion trend estimates by season for the Dyke Marsh Interior site, George Washington Memorial Parkway. The trend was averaged over the stations to get an 'overall accretion' trend.

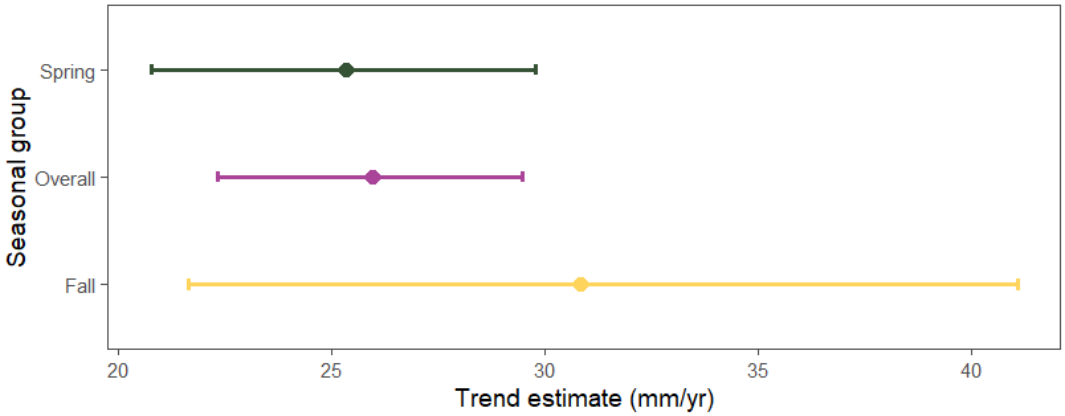


Figure E-174. Overall accretion trend estimates by season for the Dyke Marsh River site, George Washington Memorial Parkway. The trend was averaged over the stations to get an 'overall accretion' trend.

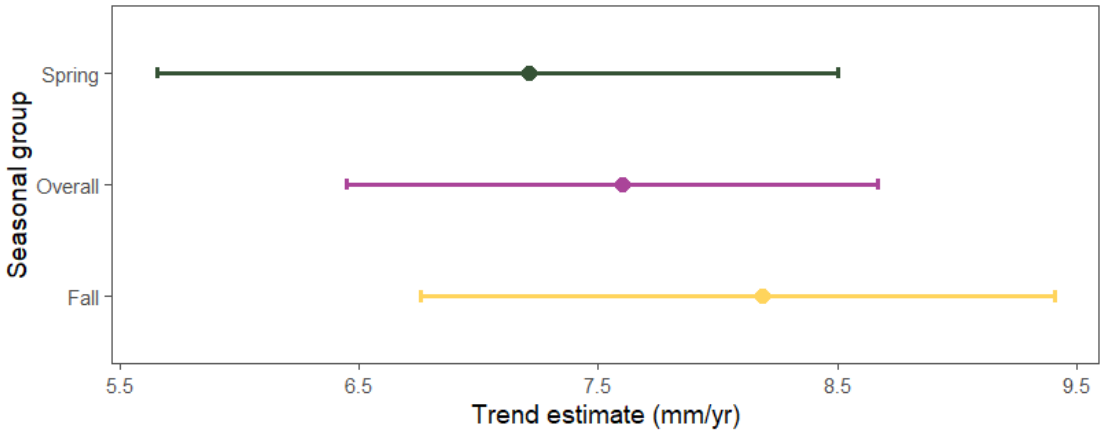


Figure E-175. Overall accretion trend estimates by season for the Kenilworth Marsh River site, National Capital Parks-East. The trend was averaged over the stations to get an 'overall accretion' trend.

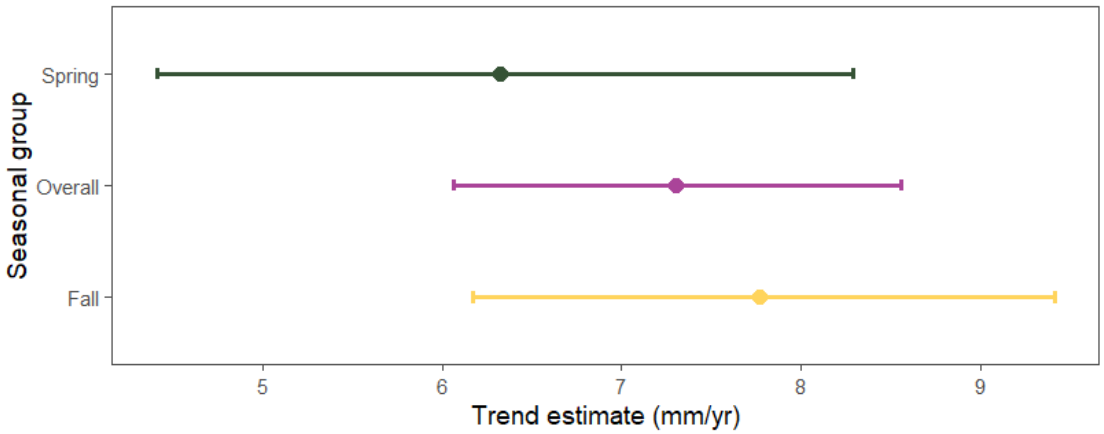


Figure E-176. Overall accretion trend estimates by season for the Kingman Lake site, National Capital Parks-East. The trend was averaged over the stations to get an 'overall accretion' trend.